



**Calhoun: The NPS Institutional Archive**  
**DSpace Repository**

---

Theses and Dissertations

Thesis and Dissertation Collection

---

1986

Vortex motion in a stratified medium.

Miller, Brian S. L.

---

<http://hdl.handle.net/10945/22181>

*Downloaded from NPS Archive: Calhoun*



Calhoun is a project of the Dudley Knox Library at NPS, furthering the precepts and goals of open government and government transparency. All information contained herein has been approved for release by the NPS Public Affairs Officer.

**Dudley Knox Library / Naval Postgraduate School**  
**411 Dyer Road / 1 University Circle**  
**Monterey, California USA 93943**

<http://www.nps.edu/library>

NAVAL POSTGRADUATE SCHOOL  
Monterey, California



THESIS

VORTEX MOTION IN A STRATIFIED MEDIUM

by

Brian S. L. Miller

December 1986

Thesis Advisor

T. Sarpkaya

Approved for public release; distribution is unlimited.

T230803



## REPORT DOCUMENTATION PAGE

1a REPORT SECURITY CLASSIFICATION UNCLASSIFIED		1b RESTRICTIVE MARKINGS	
2a SECURITY CLASSIFICATION AUTHORITY		3 DISTRIBUTION/AVAILABILITY OF REPORT Approved for public release; distribution is unlimited.	
2b DECLASSIFICATION/DOWNGRADING SCHEDULE		4 PERFORMING ORGANIZATION REPORT NUMBER(S)	
4 PERFORMING ORGANIZATION REPORT NUMBER(S)		5 MONITORING ORGANIZATION REPORT NUMBER(S)	
6a NAME OF PERFORMING ORGANIZATION Naval Postgraduate School	6b OFFICE SYMBOL (If applicable) Code 69	7a NAME OF MONITORING ORGANIZATION Naval Postgraduate School	
6c ADDRESS (City, State, and ZIP Code) Monterey, California 93943-5000		7b ADDRESS (City, State, and ZIP Code) Monterey, California 93943-5000	
8a NAME OF FUNDING/SPONSORING ORGANIZATION	8b OFFICE SYMBOL (If applicable)	9 PROCUREMENT INSTRUMENT IDENTIFICATION NUMBER	
8c ADDRESS (City, State, and ZIP Code)		10 SOURCE OF FUNDING NUMBERS	
		PROGRAM ELEMENT NO	PROJECT NO
		TASK NO	WORK UNIT ACCESSION NO
11 TITLE (Include Security Classification) VORTEX MOTION IN A STRATIFIED MEDIUM			
12 PERSONAL AUTHOR(S) Miller, Brian S. L.			
13a TYPE OF REPORT Master's Thesis	13b TIME COVERED FROM _____ TO _____	14 DATE OF REPORT (Year Month Day) 1986, December	15 PAGE COUNT 235
16 SUPPLEMENTARY NOTATION			
17 COSATI CODES		18 SUBJECT TERMS (Continue on reverse if necessary and identify by block number)	
FIELD	GROUP	Trailing Vortices Stratification	
19 ABSTRACT (Continue on reverse if necessary and identify by block number)			
<p>A comprehensive computer code has been developed through the use of the governing equations of motion and the Boussinesq hypothesis and the rise of a vortex pair in a linearly density-stratified medium has been calculated through the use of the Biot-Savart law and a finite difference scheme. The results have shown that the code is capable of predicting the behavior of the vortices and the propagation of the internal waves resulting from the vortex motion. The reasons for the finite rise of the vortices in a stratified medium is clearly explained in terms of the counter-rotating vortices induced by the stratification.</p>			
20 DISTRIBUTION/AVAILABILITY OF ABSTRACT <input checked="" type="checkbox"/> UNCLASSIFIED/UNLIMITED <input type="checkbox"/> SAME AS RPT <input type="checkbox"/> DTIC USERS		21 ABSTRACT SECURITY CLASSIFICATION Unclassified	
22a NAME OF RESPONSIBLE INDIVIDUAL Prof. T. Sarpkaya		22b TELEPHONE (Include Area Code) (408) 646-3425	22c OFFICE SYMBOL Code 69SL

Approved for public release; distribution is unlimited.

Vortex Motion in a Stratified Medium

by

Brian S. L. Miller  
Lieutenant, United States Navy  
B.S., Purdue University, 1980

Submitted in partial fulfillment of the  
requirements for the degree of

MASTER OF SCIENCE IN MECHANICAL ENGINEERING

from the

NAVAL POSTGRADUATE SCHOOL  
December 1986

## ABSTRACT

A comprehensive computer code has been developed through the use of the governing equations of motion and the Boussinesq hypothesis and the rise of a vortex pair in a linearly density-stratified medium has been calculated through the use of the Biot-Savart law and a finite difference scheme. The results have shown that the code is capable of predicting the behavior of the vortices and the propagation of the internal waves resulting from the vortex motion. The reasons for the finite rise of the vortices in a stratified medium is clearly explained in terms of the counter-rotating vortices induced by the stratification.

## TABLE OF CONTENTS

I.	INTRODUCTION .....	13
II.	EXPERIMENTAL EQUIPMENT AND PROCEDURES .....	15
	A. EQUIPMENT .....	15
	B. MODEL .....	15
	C. TEST PROCEDURES .....	16
	D. COMPUTER MODEL .....	17
III.	ANALYSIS .....	18
	A. NUMERICAL ANALYSIS OF THE VORTEX MOTIONS .....	18
	B. COMPUTER AIDED MODELING OF VORTEX MOTION .....	22
IV.	DISCUSSION OF RESULTS .....	24
V.	CONCLUSIONS .....	27
	APPENDIX A: VORTEX MOTION COMPUTER MODEL .....	28
	APPENDIX B: FIGURES .....	59
	LIST OF REFERENCES .....	232
	INITIAL DISTRIBUTION LIST .....	234

## LIST OF FIGURES

B.1a	Velocity Field: $SP = 0.00$ , $T^* = 0.05952$ .....	59
B.1b	Vorticity Field: $SP = 0.00$ .....	60
B.2a	Velocity Field: $SP = 0.00$ .....	61
B.2b	Vorticity Field: $SP = 0.00$ .....	62
B.3a	Velocity Field: $SP = 0.00$ .....	63
B.3b	Vorticity Field: $SP = 0.00$ .....	64
B.4a	Velocity Field: $SP = 0.00$ .....	65
B.4b	Vorticity Field: $SP = 0.00$ .....	66
B.5a	Velocity Field: $SP = 0.00$ .....	67
B.5b	Vorticity Field: $SP = 0.00$ .....	68
B.6a	Velocity Field: $SP = 0.00$ .....	69
B.6b	Vorticity Field: $SP = 0.00$ .....	70
B.7a	Velocity Field: $SP = 0.00$ .....	71
B.7b	Vorticity Field: $SP = 0.00$ .....	72
B.8a	Velocity Field: $SP = 0.00$ .....	73
B.8b	Vorticity Field: $SP = 0.00$ .....	74
B.9a	Velocity Field: $SP = 0.00$ .....	75
B.9b	Vorticity Field: $SP = 0.00$ .....	76
B.10a	Velocity Field: $SP = 0.00$ .....	77
B.10b	Vorticity Field: $SP = 0.00$ .....	78
B.11a	Velocity Field: $SP = 0.00$ .....	79
B.11b	Vorticity Field: $SP = 0.00$ .....	80
B.12a	Velocity Field: $SP = 0.00$ .....	81
B.12b	Vorticity Field: $SP = 0.00$ .....	82
B.13a	Velocity Field: $SP = 0.00$ .....	83
B.13b	Vorticity Field: $SP = 0.00$ .....	84
B.14	Experimental and Numerical Results for Various Initial Core Radii .....	85
B.15a	Constant Density Contours: $SP = 1.00$ .....	86

B.15b	Velocity Field: SP = 1.00	87
B.15c	Density Perturbation Contours: SP = 1.00	88
B.15d	Vorticity Field: SP = 1.00	89
B.16a	Constant Density Contours: SP = 1.00	90
B.16b	Velocity Field: SP = 1.00	91
B.16c	Density Perturbation Contours: SP = 1.00	92
B.16d	Vorticity Field: SP = 1.00	93
B.17a	Constant Density Contours: SP = 1.00	94
B.17b	Velocity Field: SP = 1.00	95
B.17c	Density Perturbation Contours: SP = 1.00	96
B.17d	Vorticity Field: SP = 1.00	97
B.18a	Constant Density Contours: SP = 1.00	98
B.18b	Velocity Field: SP = 1.00	99
B.18c	Density Perturbation Contours: SP = 1.00	100
B.18d	Vorticity Field: SP = 1.00	101
B.19a	Constant Density Contours: SP = 1.00	102
B.19b	Velocity Field: SP = 1.00	103
B.19c	Density Perturbation Contours: SP = 1.00	104
B.19d	Vorticity Field: SP = 1.00	105
B.20a	Constant Density Contours: SP = 1.00	106
B.20b	Velocity Field: SP = 1.00	107
B.20c	Density Perturbation Contours: SP = 1.00	108
B.20d	Vorticity Field: SP = 1.00	109
B.21a	Constant Density Contours: SP = 1.00	110
B.21b	Velocity Field: SP = 1.00	111
B.21c	Density Perturbation Contours: SP = 1.00	112
B.21d	Vorticity Field: SP = 1.00	113
B.22a	Constant Density Contours: SP = 1.00	114
B.22b	Velocity Field: SP = 1.00	115
B.22c	Density Perturbation Contours: SP = 1.00	116
B.22d	Vorticity Field: SP = 1.00	117
B.23a	Constant Density Contours: SP = 1.00	118
B.23b	Velocity Field: SP = 1.00	119

B.23c	Density Perturbation Contours: SP = 1.00	120
B.23d	Vorticity Field: SP = 1.00	121
B.24a	Constant Density Contours: SP = 1.00	122
B.24b	Velocity Field: SP = 1.00	123
B.24c	Density Perturbation Contours: SP = 1.00	124
B.24d	Vorticity Field: SP = 1.00	125
B.25a	Constant Density Contours: SP = 1.00	126
B.25b	Velocity Field: SP = 1.00	127
B.25c	Density Perturbation Contours: SP = 1.00	128
B.25d	Vorticity Field: SP = 1.00	129
B.26a	Constant Density Contours: SP = 1.00	130
B.26b	Velocity Field: SP = 1.00	131
B.26c	Density Perturbation Contours: SP = 1.00	132
B.26d	Vorticity Field: SP = 1.00	133
B.27a	Constant Density Contours: SP = 1.00	134
B.27b	Velocity Field: SP = 1.00	135
B.27c	Density Perturbation Contours: SP = 1.00	136
B.27d	Vorticity Field: SP = 1.00	137
B.28a	Constant Density Contours: SP = 1.00	138
B.28b	Velocity Field: SP = 1.00	139
B.28c	Density Perturbation Contours: SP = 1.00	140
B.28d	Vorticity Field: SP = 1.00	141
B.29a	Constant Density Contours: SP = 1.00	142
B.29b	Velocity Field: SP = 1.00	143
B.29c	Density Perturbation Contours: SP = 1.00	144
B.29d	Vorticity Field: SP = 1.00	145
B.30a	Constant Density Contours: SP = 1.00	146
B.30b	Velocity Field: SP = 1.00	147
B.30c	Density Perturbation Contours: SP = 1.00	148
B.30d	Vorticity Field: SP = 1.00	149
B.31a	Constant Density Contours: SP = 1.00	150
B.31b	Velocity Field: SP = 1.00	151
B.31c	Density Perturbation Contours: SP = 1.00	152

B.31d	Vorticity Field: SP = 1.00	153
B.32	Experimental and Numerical Results for SP = 1.00	154
B.33a	Constant Density Contours: SP = 0.50	155
B.33b	Velocity Field: SP = 0.50	156
B.33c	Density Perturbation Contours: SP = 0.50	157
B.33d	Vorticity Field: SP = 0.50	158
B.34a	Constant Density Contours: SP = 0.50	159
B.34b	Velocity Field: SP = 0.50	160
B.34c	Density Perturbation Contours: SP = 0.50	161
B.34d	Vorticity Field: SP = 0.50	162
B.35a	Constant Density Contours: SP = 0.50	163
B.35b	Velocity Field: SP = 0.50	164
B.35c	Density Perturbation Contours: SP = 0.50	165
B.35d	Vorticity Field: SP = 0.50	166
B.36a	Constant Density Contours: SP = 0.50	167
B.36b	Velocity Field: SP = 0.50	168
B.36c	Density Perturbation Contours: SP = 0.50	169
B.36d	Vorticity Field: SP = 0.50	170
B.37a	Constant Density Contours: SP = 0.50	171
B.37b	Velocity Field: SP = 0.50	172
B.37c	Density Perturbation Contours: SP = 0.50	173
B.37d	Vorticity Field: SP = 0.50	174
B.38a	Constant Density Contours: SP = 0.50	175
B.38b	Velocity Field: SP = 0.50	176
B.38c	Density Perturbation Contours: SP = 0.50	177
B.38d	Vorticity Field: SP = 0.50	178
B.39a	Constant Density Contours: SP = 0.50	179
B.39b	Velocity Field: SP = 0.50	180
B.39c	Density Perturbation Contours: SP = 0.50	181
B.39d	Vorticity Field: SP = 0.50	182
B.40a	Constant Density Contours: SP = 0.50	183
B.40b	Velocity Field: SP = 0.50	184
B.40c	Density Perturbation Contours: SP = 0.50	185

B.40d	Vorticity Field: $SP = 0.50$ .....	186
B.41a	Constant Density Contours: $SP = 0.50$ .....	187
B.41b	Velocity Field: $SP = 0.50$ .....	188
B.41c	Density Perturbation Contours: $SP = 0.50$ .....	189
B.41d	Vorticity Field: $SP = 0.50$ .....	190
B.42a	Constant Density Contours: $SP = 0.50$ .....	191
B.42b	Velocity Field: $SP = 0.50$ .....	192
B.42c	Density Perturbation Contours: $SP = 0.50$ .....	193
B.42d	Vorticity Field: $SP = 0.50$ .....	194
B.43a	Constant Density Contours: $SP = 0.50$ .....	195
B.43b	Velocity Field: $SP = 0.50$ .....	196
B.43c	Density Perturbation Contours: $SP = 0.50$ .....	197
B.43d	Vorticity Field: $SP = 0.50$ .....	198
B.44	Experimental and Numerical Results for Various Initial Core Radii .....	199
B.45a	Constant Density Contours: $SP = 0.50$ .....	200
B.45b	Velocity Field: $SP = 0.50$ .....	201
B.45c	Density Perturbation Contours: $SP = 0.50$ .....	202
B.45d	Vorticity Field: $SP = 0.50$ .....	203
B.46a	Constant Density Contours: $SP = 0.50$ .....	204
B.46b	Velocity Field: $SP = 0.50$ .....	205
B.46c	Density Perturbation Contours: $SP = 0.50$ .....	206
B.46d	Vorticity Field: $SP = 0.50$ .....	207
B.47a	Constant Density Contours: $SP = 0.50$ .....	208
B.47b	Velocity Field: $SP = 0.50$ .....	209
B.47c	Density Perturbation Contours: $SP = 0.50$ .....	210
B.47d	Vorticity Field: $SP = 0.50$ .....	211
B.48a	Constant Density Contours: $SP = 0.50$ .....	212
B.48b	Velocity Field: $SP = 0.50$ .....	213
B.48c	Density Perturbation Contours: $SP = 0.50$ .....	214
B.48d	Vorticity Field: $SP = 0.50$ .....	215
B.49a	Constant Density Contours: $SP = 0.50$ .....	216
B.49b	Velocity Field: $SP = 0.50$ .....	217
B.49c	Density Perturbation Contours: $SP = 0.50$ .....	218

B.49d	Vorticity Field: SP = 0.50 .....	219
B.50a	Constant Density Contours: SP = 0.50 .....	220
B.50b	Velocity Field: SP = 0.50 .....	221
B.50c	Density Perturbation Contours: SP = 0.50 .....	222
B.50d	Vorticity Field: SP = 0.50 .....	223
B.51a	Constant Density Contours: SP = 0.50 .....	224
B.51b	Velocity Field: SP = 0.50 .....	225
B.51c	Density Perturbation Contours: SP = 0.50 .....	226
B.51d	Vorticity Field: SP = 0.50 .....	227
B.52a	Constant Density Contours: SP = 0.50 .....	228
B.52b	Velocity Field: SP = 0.50 .....	229
B.52c	Density Perturbation Contours: SP = 0.50 .....	230
B.52d	Vorticity Field: SP = 0.50 .....	231

## TABLE OF SYMBOLS AND ABBREVIATIONS

$b_o$	Initial Vortex Core Spacing
$d_o$	Initial Depth of the Vortex Pair
$F_v$	Froude Number
$g$	Gravitational Acceleration
$H$	Vortex Rise Height
$H^*$	Normalized Migration Height, $H/b_o$
$N_c$	$(g/b_o)^{1/2}$
$N_o$	Brunt-Vaisala Frequency
$n$	$N_o/N_c$
$Re$	Reynolds Number
$r$	Radial Distance
$T^*$	Normalized Time, $\dot{V}_o t/b_o$
$t$	Time
$U$	Model Velocity
$U_c$	Characteristic Velocity
$u$	x-Component of Velocity
$v$	y-Component of Velocity
$V_o$	Initial Mutual Induction Velocity
$x$	Horizontal Component of the Coordinate Axis (Parallel to the Line Joining the Vortex Cores)
$y$	Vertical Component of the Coordinate Axis
$\alpha$	Model Angle of Attack
$\Gamma$	Circulation of the Vortex
$\Gamma_o$	Initial Circulation of the Vortex
$\nu$	Kinematic Viscosity of Water
$\rho$	Density of Water
$\rho_o$	Reference Density of Water in Stratified Medium
$\rho'$	Density Fluctuations
$\bar{\rho}(y)$	Density of $y$ at $t = 0$
$\zeta$	Vorticity

## ACKNOWLEDGEMENTS

The author wishes to express his sincere thanks to Distinguished Professor Turgut Sarpkaya for providing his invaluable knowledge, insights, wit and his everpresent guidance throughout the entire thesis process. It is a rare occasion that one is allowed the opportunity to work with a man with such dedication and I consider it a true privilege. This experience will be looked fondly upon for years to come.

Finally, my loving appreciation goes to my wife, Sue Miller, for her infinite understanding and patience when things weren't going right and her excitement when they were right.

## I. INTRODUCTION

Vortices and vortex wakes have become a major theme of aerodynamics research since the advent of the large aircraft and the understanding of their evolution required an examination of many fundamental problems in fluid mechanics. Much of the progress made during the past two decades was discussed at the Symposium on Aircraft Wake Turbulence and Its Detection [Ref. 1] and at the Aircraft Wake Vortices Conference [Ref. 2]. Comprehensive reviews of the entire subject have been given by Donaldson and Bilanin [Ref. 3], Widnall [Ref. 4] and Hallock and Eberle [Ref. 5].

These studies, as well as numerous others carried out since 1977, have uncovered a number of complex problems which must be resolved in order to achieve a better understanding of the important features of trailing vortices in homogeneous and stratified media. The principal ones are as follows [Ref. 6]:

- (a) Roll-up process: The velocity and turbulence distribution at any station behind the wing depend on the wing section, wing-tip shape, Reynolds number, wing incidence, and the distance of the station from the wing [Ref. 7]. The distributions of the initial velocity and turbulence, which influence the roll-up and the decay process, cannot be changed independently. For example, a change in tip shape changes the core size, as well as the velocity and turbulence distributions. High levels of turbulence result in an increased diffusion of vorticity, which in turn increases the core size.
- (b) Probe sensitivity of the vortices: Flow visualization studies suggest that trailing vortices are extremely sensitive to disturbances created by even very small probes or bubbles. This forces one to use non-intrusive means of measurements such as an LDV. Even then, 'vortex wandering' [Ref. 8], which makes the vortices appear larger than normal in time-averaged velocity measurements (for vortices generated by a wing in a wind tunnel), or the unsteady nature of the flow (for vortices generated by a wing in a tow basin) makes the mean velocity profiles in the vortices difficult to determine.
- (c) Large-scale instabilities: The vortices are seldom observed to decay away owing to viscous and turbulent dissipation, but are almost always destroyed by either mutual induction instability (Crow instability [Ref. 9]) and/or vortex breakdown. The Crow instability grows exponentially, and results either in a linking of the vortex pair into a series of crude vortex rings or in a highly disorganized intermingling of the vortices. Vortex breakdown, whose mathematical details have not yet been adequately treated, rearranges the vortex structure and increases the core size, turbulence, and energy dissipation. Thus, it is very difficult to measure accurately the trajectories of the three-dimensional vortices from their creation to their ultimate demise.
- (d) Reynolds number: Even the highest Reynolds numbers, based on wing chord, reached in wind tunnels or towing basins, are in order of magnitude lower than what is possible for an aircraft. Thus, the scale effects are not easy to assess.
- (e) Ambient conditions such as turbulence and stratification play major roles in the evolution of vortices. The quantification of these effects requires numerical analysis and extremely careful experiments.

- (f) Ground or free-surface effects: The vortex pair may move towards a rigid boundary at which the no-slip condition must be satisfied or towards a free surface at which the zero-shear condition must be satisfied. In either case, the vortices come under the influence of their images and move accordingly.

The phenomenon is further complicated by several additional facts. When the vortices are propelled towards a rigid surface, vorticity of opposite sign is generated on the no-slip boundary and swept towards the vortex pair. The total vorticity diminishes very quickly as vorticity from the two regions diffuses, the wall region serving as a strong sink for the vorticity associated with the original vortex [Ref. 10]. The development of a boundary layer along the rigid wall may give rise to flow separation for sufficiently high Reynolds numbers. With or without such a separation, however, the center of the vortex pair eventually moves away, or 'rebounds', from the wall [Refs. 10-12].

For the case of a zero-stress boundary, the free surface still acts as a vorticity sink, but this is relatively weak due to the absence of intense oppositely-signed vorticity. Thus, in the absence of other impeding phenomena, one expects a mild interaction between the vortices and the free surface and a small rebound of the vortex center from the free surface. However, the ability of the free surface to deform under the influence of strain fields leads to a strong interaction between the vortices and the free surface.

It is evident from the foregoing that the motion and the life-span of trailing vortices are governed by a number of nonlinearly-dependent complex phenomena. A number of experimental and analytical studies have been carried out at the Naval Postgraduate School by Sarpkaya and his students [Refs. 6,13-17] in order to investigate the effects of these parameters on the rise and demise of the trailing vortices in homogeneous and density stratified media. These studies have clearly identified the various demise mechanisms in both media and established basic relationships between the rise of vortices and the governing parameters in a finite as well as effectively infinite medium [Ref. 18], free from ambient turbulence. The present investigation is a continuation of the foregoing studies and is confined to the computer modeling, via a finite differencing technique, of the rise and demise of trailing vortices in stratified media.

## II. EXPERIMENTAL EQUIPMENT AND PROCEDURES

### A. EQUIPMENT

The equipment used to generate the trailing vortices has been extensively used at this facility over the past three years [Refs. 6,14-19]. Only the salient features, most recent modifications and the adaptation for this work are briefly described in the following.

The system consists essentially of a towing basin. The auxiliary components consist of the brine fill system, turbulence management system, top and bottom carriages, velocity measuring system, lighting system, and the model [Refs. 14-19]. The brine fill system is controlled by a computer to provide a consistently repeatable density stratified media [Ref. 19].

Drains are provided at the bottom of each end of the basin. Two parallel rails are mounted along the bottom of the tank. A carriage rides smoothly on these rails and provides the test body with a constant velocity through the use of an endless cable and a DC motor. The velocity of the model is measured and continuously monitored through the use of a magnetic linear displacement transducer. It yields a signal proportional to the velocity of the model with an error of less than one percent.

The two rails, the carriage and the filling pipes are located on or near the bottom of the basin and under a turbulence management system. This system consists of one inch thick polyurethane foam sandwiched between two perforated aluminum plates.

### B. MODEL

A rectangular foil (NACA 0012) was used in the present study. The foil had the following dimensions:  $B = 4.50$  in.,  $b_o = 3.53$  in., and  $c = 2.32$  in. The interior of this model was hollowed and used as dye reservoir to seed the vortex cores. The model was mounted on its base by means of a thin streamlined aluminum bar with a cross section of a NACA 0006 foil and set at the desired angle of attack. As noted earlier, the model was pulled by means of a DC motor, pulley, and cable system at the desired speed. Additional details of the model construction and mounting are discussed by Johnson [Ref. 15].

### C. TEST PROCEDURES

A model is placed in the basin and the basin is filled gradually with a brine solution [Ref. 19] to the desired level. In the cases where dye was used to seed the vortex pair, the model was filled with dye prior to filling the basin. After removal of trapped air and after sufficient time to allow for the escape of dissolved air in the water and the elimination of any internal currents in the basin, the model was set in motion. Most of the experiments were repeated at least three times.

The motion of the trailing vortices were recorded on highspeed Polaroid film at the test section (one of the plexiglass panels near the middle of the basin). Each picture included two clocks accurate to 0.1 seconds, the vertical and horizontal scales on the plexiglass window and, of course, the side view of the trailing vortices as they rose from the model after formation. The time interval between successive pictures is determined from the two clocks. The first picture always captured the model the instant it passed through the test section. The subsequent pictures (taken at about 0.75 second intervals) captured the rise and demise of the vortices. The vertical rise of the vortices is determined from the vertical scale. Attention has been paid to the fact that the vortices are farther away from the scale on the window and that the scale placed vertically in the middle of the test section does not exactly correspond to the scale marked on the window due to refraction and parallax. The necessary correction was made by photographing a scale placed in water in the middle of the test section together with a scale marked on the window. This resulted in a simple conversion table which enabled the determination of the actual position of the vortex from the scale reading on the photograph.

The results are normalized and plotted in various forms and compared with those obtained in the previous runs. Each experiment was repeated three times for most of the data presented herein. All trailing vortices were recorded on film until the time they have completely dissipated either due to aging (diffusion of vorticity due to viscosity, turbulence, entrainment, and detrainment), or due to Crow instability (sinusoidal instability and linking of vortices), and or due to vortex breakdown (core bursting). It was thus possible to determine the life span of vortex cores from their formation to their final demise.

#### D. COMPUTER MODEL

The computer model (Appendix A) is run on the IBM 3300 main-frame computer at the Naval Postgraduate School. The computer code was written to run on either the MVS Batch Processing system or the VM/CMS system. The stratification parameter specified for the experimental runs is used to determine other parameters [Ref. 17] used by the program. The code is compiled under VS Fortran and is loaded and executed using DISSPLA version 10.0. The code was written such that the user has the capacity to stipulate the number of time step iterations that are executed. Also, the time steps at which a constant density contour, complex velocity profile, density perturbation contour and the vorticity contour are plotted, are designated by the user prior to compilation. These plots are analyzed to determine the normalized rise height of the initial vortex pair until its demise. These are then compared with those obtained experimentally.

The computer model is an intense computational algorithm that requires approximately 12.5 minutes of Central Processing Unit (CPU) time per iteration. Due to this high use of CPU time, the code has been designed to be executed until stopped at a user defined step iteration and then save all necessary data required to restart the model. The code can then be restarted at that step iteration at a later time. The program VORRS (VORtex ReStart) has been specifically written to accomplish this task.

### III. ANALYSIS

#### A. NUMERICAL ANALYSIS OF THE VORTEX MOTIONS

The generation of the internal waves and the rise and demise of the vortices in a stratified medium may well be analyzed through the use of the equations of motion for an incompressible fluid for both laminar and turbulent motions provided that a suitable turbulence closure model is adopted and the usual Boussinesq approximation (gravitational acceleration is much larger than the fluid accelerations) is made. For the type of motions considered herein the Boussinesq approximation is quite valid and has been used in the investigation of all types of internal waves in stratified fluids.

For a two-dimensional flow, with  $y$  vertical and  $x$  horizontal, the equations of motion are

$$\frac{\partial u}{\partial t} + u \frac{\partial u}{\partial x} + v \frac{\partial u}{\partial y} = - \frac{1}{\rho} \frac{\partial p}{\partial x} + \nu \nabla^2 u \quad (3.1)$$

and

$$\frac{\partial v}{\partial t} + u \frac{\partial v}{\partial x} + v \frac{\partial v}{\partial y} = - g - \frac{1}{\rho} \frac{\partial p}{\partial y} + \nu \nabla^2 v \quad (3.2)$$

and the equation of continuity

$$\frac{\partial u}{\partial x} + \frac{\partial v}{\partial y} = 0. \quad (3.3)$$

Defining vorticity as usual by

$$\zeta = \frac{\partial u}{\partial y} - \frac{\partial v}{\partial x} \quad (3.4)$$

and eliminating pressure between Eq. 3.1 and Eq. 3.2, one has

$$\frac{\partial \zeta}{\partial t} + \frac{\partial u \zeta}{\partial x} + \frac{\partial v \zeta}{\partial y} = v \nabla^2 \zeta + \frac{g}{\rho_o} \frac{\partial \rho'}{\partial x} \quad (3.5)$$

in which  $\rho'$  is the fluctuating part of the density  $\rho$  given by

$$\rho = \rho_o + \bar{\rho}(y) + \rho'(x,y,t) \quad (3.6)$$

where  $\rho_o$  is the reference density, and  $\bar{\rho}(y)$  the initial density at elevation  $y$  at  $t = 0$ .

The diffusion of density is given by

$$\left( \frac{\partial}{\partial t} + u \frac{\partial}{\partial x} + v \frac{\partial}{\partial y} - v \nabla^2 \right) \rho = 0 \quad (3.7)$$

Combining Eqs. 3.3, 3.6 and 3.7, and simplifying, one has

$$\frac{\partial \rho'}{\partial t} + \frac{\partial u \rho'}{\partial x} + \frac{\partial v \rho'}{\partial y} = -v \frac{\partial \bar{\rho}}{\partial y} + v \nabla^2 \rho' + v \frac{\partial^2 \bar{\rho}}{\partial y^2} \quad (3.8)$$

It is convenient to cast the foregoing equations into nondimensional forms, scaling each variable by a quantity characteristic of its expected magnitude. Two possible time scales exist. There is the dynamic time scale, which is the time a characteristic length would be traversed by a fluid particle traveling at the characteristic velocity, and there is the buoyant time scale based on the natural buoyancy frequency of the stratified flow, i.e., the Brunt-Vaisala frequency  $N$ , as defined by Daly [Ref. 17]. Each of the scales gives a slightly different form of the normalized governing equations.

Dynamic Scale:

Introducing  $U_c$  and  $L_c$  as the characteristic velocity and length, one has

$$\zeta_m = \frac{\zeta L_c}{U_c}, \quad t_m = \frac{U_c t}{L_c}, \quad Re = \frac{U_c L_c}{\nu}, \quad F_v = \frac{U_c}{(g L_c)^{1/2}} \quad (3.9)$$

Normalizing Eqs. 3.5 and 3.8

$$\frac{\partial \zeta_m}{\partial t_m} + \left( \frac{\partial u_m \zeta_m}{\partial x_m} + \frac{\partial v_m \zeta_m}{\partial y_m} \right) = \frac{1}{Re} \nabla^2 \zeta_m + \frac{1}{F_v^2} \frac{\partial \rho_m}{\partial x_m} \quad (3.10)$$

and

$$\frac{\partial \rho_m'}{\partial t_m} + \left( \frac{\partial u_m \rho_m'}{\partial x_m} + \frac{\partial v_m \rho_m'}{\partial y_m} \right) = n^2 v_m + \frac{1}{\text{Re}} (\nabla^2 \rho_m' + \frac{\partial^2 \bar{\rho}_m}{\partial y_m^2}) \quad (3.11)$$

in which

$$F_v^2 = \frac{U_c^2}{g L_c}, \quad \text{Re} = \frac{U_c L_c}{\nu}, \quad n = \frac{N_o}{N_c}$$

$$N_c^2 = \frac{g}{L_c}, \quad N_o^2 = - \frac{g}{\rho_o} \frac{\bar{\rho}(y)}{\partial y} = - \frac{g}{L} \frac{\partial \bar{\rho}_m}{\partial y_m} = \frac{g n^2}{L_c}$$

Equations 3.10 and 3.11 are valid when  $F_v \gg 1$ , i.e., when the buoyancy has very little influence on the nonlinear dynamics of the motion. In this case, the density perturbation acts as a passive scalar advected by the velocity field.

Bouyant scale:

Introducing the following dimensionless parameters:

$$\begin{aligned} \bar{\rho}_m &= \frac{\bar{\rho}}{\rho_o}, & u_m &= \frac{u}{U_c}, & v_m &= \frac{v}{U_c}, & x_m &= \frac{x}{L_c} \\ y_m &= \frac{y}{L_c}, & t_m &= t N_c, & \zeta_m &= \frac{\zeta}{N_c}, & N_c^2 &= \frac{g}{L_c} \end{aligned} \quad (3.12)$$

and normalizing Eqs. 3.5 and 3.8, one has

$$\frac{\partial \zeta_m}{\partial t_m} + F_v \left( \frac{\partial u_m \zeta_m}{\partial x_m} + \frac{\partial v_m \zeta_m}{\partial y_m} \right) = \frac{F_v}{\text{Re}} \nabla^2 \zeta_m + \frac{\partial \rho_m'}{\partial x_m} \quad (3.13)$$

and

$$\frac{\partial \rho_m'}{\partial t_m} + F_v \left( \frac{\partial u_m \rho_m'}{\partial x_m} + \frac{\partial v_m \rho_m'}{\partial y_m} \right) = F_v n^2 v_m \quad (3.14)$$

in which  $F_v$ ,  $\text{Re}$  and  $n^2$  are as defined in Eq. 3.11.

Equations 3.13 and 3.14 are valid when  $F_v \ll 1$  and buoyancy dominates the flow. When  $F_v$  approaches zero, the equations that result from Eqs-3.13 and 3.14 describe the propagation of linear internal waves. The  $F_v \ll 1$  regime is of interest in the present investigation because for submerged bodies of naval interest  $F_v$  (the Froude number) is about 0.01. The analysis will consider the full nonlinear equations given by Eqs. 3.13 and 3.14 rather than their linearized form (i.e., the case of  $F_v = 0$ ). However, the flow will be assumed to be inviscid, i.e., the viscous diffusion will be ignored to a first order approximation. Subsequent analysis will incorporate the effects of viscous and turbulent diffusion into the numerical calculations. The velocities  $u$  and  $v$  are given by the Biot-Savart law as

$$u(x,y) = \int \frac{(y' - y)\zeta(x',y')dx'dy'}{2\pi r^2} \quad (3.15)$$

and

$$v(x,y) = \int \frac{(x - x')\zeta(x',y')dx'dy'}{2\pi r^2} \quad (3.16)$$

in which  $(x,y)$  is the point at which the velocity is calculated and  $(x',y')$  is an arbitrary point at which the vorticity is  $\zeta(x',y')$ .

The radial distance  $r$  is given by:

$$r^2 = (x - x')^2 + (y - y')^2 \quad (3.17)$$

Normalizing Eqs. 3.15 - 3.17 through the use of the characteristic dimensions given in Eq. 3.12

$$F_v u_m = \int \frac{(y'_m - y_m)\zeta(x'_m, y'_m)dx'_m dy'_m}{2\pi r_m^2} \quad (3.18)$$

$$F_v v_m = \int \frac{(x_m - x'_m)\zeta(x'_m, y'_m)dx'_m dy'_m}{2\pi r_m^2} \quad (3.19)$$

and

$$r_m^2 = (x_m - x_m')^2 + (y_m - y_m')^2 \quad (3.20)$$

It is appropriate to take  $V_o$ , the initial mutual induction velocity of the vortex pair, as the characteristic velocity and the  $b_o$ , the initial separation of the vortices, as the characteristic length. Thus, one has:

$$L_c = b_o, \quad U_c = V_o = \frac{\Gamma_o}{2\pi b_o}, \quad F_v = \frac{V_o}{N_c b_o} = \frac{V_o}{(g b_o)^{1/2}} \quad (3.21)$$

In dimensionless forms, one has:

$$\Gamma_m = \frac{\Gamma_o}{N_c b_o} = 2\pi F_v, \quad n = F_v \frac{N_o b_o}{V_o}, \quad t_m = t N_c = \frac{V_o t}{b_o F_v} \quad (3.22)$$

in which  $N_o b_o / V_o$  is called the stratification parameter SP. The value of SP normally varies from zero to about 100. The larger the SP, the stronger the stratification. For example, for a model running at a speed of 5 ft/sec at an angle of attack ( $\alpha$ ) of  $10^\circ$ , a SP smaller than 1.0 represents weak stratification, a SP between 1 and 5 represents medium stratification, and a SP larger than 5 corresponds to strong stratification.

## B. COMPUTER AIDED MODELING OF VORTEX MOTION

The computer algorithm for the numerical solution of Eqs. 3.13 and 3.14 is provided in Appendix A. The solution is done assuming the case of inviscid flow and the initial vorticity distribution was assumed to be Gaussian, i.e.:

$$\zeta_m = \frac{F_v}{r_{om}^2} \exp\left(-\frac{r_m^2}{2r_{om}^2}\right) \quad (3.23)$$

A computational domain of  $5b_o$  by  $10b_o$  is used in the algorithm in order to mimic the physical features of the tow basin. The no-slip condition is satisfied on the walls corresponding to the channel walls. The zero normal velocity condition is assumed at the free surface and along the vertical line of flow symmetry. All computations are done in the fourth quadrant. The fields of velocity, vorticity, density, and the fluctuating components of the density are calculated at each time step and plotted at

regular intervals. The computer algorithm is quite robust and can be applied to any stratified and unstratified flow situation. As the velocity field is computed from analytic expressions (i.e., the Biot-Savart equations) vice an algorithm involving an iterative scheme, stability of the program is enhanced at a slight expense in execution time. An upwind finite differencing technique [Ref. 20] was used with an original grid dimension of 24 by 44 nodes with a spacing of  $0.25b_0$ . This grid size was subsequently increased to 34 by 64 and 44 by 84 in order to examine the dependency of the results on the grid size.

The mesh coordinates  $(x,y)$  covering the computational domain (of dimension  $m-4$  by  $n-4$ ) are:

$$\begin{aligned} X &\in \{2,3,4,\dots,m-2\} \\ Y &\in \{2,3,4,\dots,n-2\}. \end{aligned} \tag{3.24}$$

The necessity for the the overlap of two nodes on all sides of the computational domain is to facilitate satisfying the boundary condiditons. Eqs. 3.13 and 3.14 are solved over the original mesh which results in vorticity and density information.

The two complex velocity grids are derived by shifting the original mesh  $h/2$  in the  $x$  direction for the  $u$  velocity and  $h/2$  in the  $y$  direction for the  $v$  velocity. The values of these new nodes are determined using the vorticity derived for the original computational grid using the Biot-Savart law, Eqs. 3.15 and 3.16. The velocities at the shifted grid points are then averaged across the computational grid points for further use in the finite differencing scheme.

#### IV. DISCUSSION OF RESULTS

The computer code described in the previous section has been used to carry out calculations for four specific cases. The first of these dealt with the case of the rise of vortices in a homogeneous unstratified medium. The grid size as well as the core radius were varied within limits to explore the differences in the motion of the vortices. Figures B.1 through B.13 show the velocity and vorticity contours at various normalized times. Clearly, the initial vortex spacing increases with time and the vortices remain symmetrical due to the conditions imposed on the numerical analysis. In other words, these vortices cannot be subjected to sinusoidal instability or core bursting. Thus, the numerical results should agree more closely with the experimental cases where the vortices did not undergo such instabilities. Figure B.14 shows the experimental and numerical results. The experimental data are separated as 'HIGH' and 'LOW' because of the fact that the crests and troughs of the sinusoidal instability were separately evaluated. The numerical results for three normalized core sizes are also shown in Figure B.14. It is clear that the core size has a pronounced effect on the numerical predictions and that the results obtained with  $r_0 = 0.08$  agree more closely with the experimental data. As noted earlier, the numerical results should be compared with the average instantaneous height rather than with the 'HIGH' and 'LOW' of the vortices. There is no conclusive analysis or data in the literature regarding the vortex core radius. It has been shown previously [Ref. 16] that the core radius depends strongly on the shape of the trailing edges of the lifting surface. The better rounded the edges of the control surface the tighter the winding of the vortex sheets and thus the smaller the vortex core. It appears that a vortex core of 0.07 or 0.08 should be used in future calculations.

Figures B.15 through B.31 show lines of constant density, velocity, density perturbations, and vorticity contours for the stratification parameter of 1.0,  $F_v = 0.02976$ ,  $r_0 = 0.09$ ,  $Y/b_0 = -8.0$  and  $X/b_0 = 0.5$ . The grid used was 44 by 84. These figures show that at small times the vortices rise vertically and the circulation in the flow field is primarily due to the initial vortices. As time increases (see e.g., Figure B.21b), the regions of circulation with countersigned vorticity develop in the upper right and lower left regions of the vortex. It is easy to show that this counter vorticity

not only reduces the rise velocity of the original vortex pair but pushed the pair against each other. Consequently, the countersigned vorticity begins to dominate the flow (see e.g., Figure B.28b) and the vortex pair migration stops. With further increases in time the vortex pair begins to migrate downward.

The density contours reveal the same phenomenon in a different context. As the vortices rise, fluid of greater density is pushed upwards (see e.g., Figure B.25a) into regions of lesser density. Since such a migration cannot go on indefinitely, the vortices rise to a maximum height and then begin to sink downwards. The calculations do not take into account the sinusoidal instability and the vortex breakdown. Consequently, the vortices in the numerical calculations continue to exist unimpeded by the instability mechanisms. In reality, the vortices begin to break up as they near the end of their maximum migration and eventually disappear.

The experimental and calculated values are compared in Figure B.32. The correspondence between the measured and calculated values is surprisingly good up to the time of maximum rise. This is partly because of the experimental fact that the rise of vortices in a highly stratified medium ( $N_o b_o / V_o = 1.00$ ,  $F_v = 0.02976$ ) is not strongly dominated by sinusoidal instability or vortex breakdown. The migration of vortices is inhibited primarily due to the reduction of vorticity of the initial vortices and the creation of countersigned vorticity.

The numerical calculations were also applied to a medium with a relatively smaller stratification for which the rise of vortices are closer to that of the homogeneous case and thus the effect of the core radius is more pronounced. The results obtained with  $N_o b_o / V_o = 0.50$ ,  $F_v = 0.02976$  and with  $r_o = 0.08$  are shown in Figures B.33 through B.43. The observations made earlier regarding the velocity, vorticity, and density contours may be made with this particular stratification also. Obviously, the vortices rise to a greater height and the countersigned vorticity is relatively weaker and develops at a later stage. The calculations with this particular stratification have been repeated by varying only the initial core radius. Figure B.44 shows the representative experimental data and the numerical results obtained with initial core radii of 0.07, 0.08, and 0.09. Evidently and as anticipated on the basis of the previous calculations the initial core radius of 0.07 yields results which are in excellent agreement with those obtained experimentally. Figure B.44 also shows that the rise and demise of vortices must be a strong function of their initial core radii. Experiments in both the laboratory and the field have shown that to be true and

pointed out the fact that the life of a vortex is dictated partly by the conditions prevailing at its creation and partly by the conditions surrounding the vortex at later stages of its motion.

The results presented so far have dealt with vortex pairs released at relatively large depths of submergence and have shown that the computer code predicts results which are in good agreement with those obtained experimentally provided that a core radius of about  $r_0 = 0.07$  is used in the calculations. It has further been shown that the smaller the stratification parameter the more dependent the results become on the initial core radius. Thus, the numerical analysis has not only provided a power of prediction for the motion of the vortices but also helped to delineate the proper value of the initial core radius.

Having ascertained the characteristics of the model and the features of the velocity, vorticity, and density variations it was deemed necessary to explore problems of greater practical and operational concern. It is because of this reason that the depth at which the vortices are generated was chosen to be  $Y/b_0 = -2.0$  and the subsequent motion of the vortices was explored. Figures B.45 through B.52 show the density, velocity, density fluctuations and vorticity contours at suitable time intervals. As the vortices approach the free surface and begin to move sideways under the influence of their images, the constant density contours begin to intersect with the free surface (see e.g., Figure B.49a) and move sideways also. The intersection of these density contours is expected to give rise to internal-wave-generated surface scars. The prediction of the characteristics of these scars in terms of the vortices is of importance and requires that the free surface condition be changed. This change is to allow for free surface deformation under the influence of the tangential as well as normal velocities induced at the free surface by the vortices.

Additional calculations are underway to examine the effects of free surface deformation, viscous diffusion and ambient turbulence for various degrees of initial stratification. The results presented herein and the initial comparisons are extremely encouraging and are expected to lead to a better understanding of this extremely complex and challenging phenomenon.

## V. CONCLUSIONS

The investigation reported herein warranted the following conclusions:

- (1) The motion of trailing vortices generated by submerged bodies in a stratified or unstratified medium can be effectively modeled by the developed computer algorithm;
- (2) The computer model has aided in the delineation of the proper value for the initial vortex core radius;
- (3) The initial vortex core radius and vorticity strength are the primary factors governing the stability of the numerical results;
- (4) The migration of vortices is inhibited primarily due to the reduction of the vorticity of the initial vortices and the creation of countersigned vorticity;
- (5) The computer model could be made more realistic through the inclusion of a deformable free surface in the computations.

APPENDIX A  
VORTEX MOTION COMPUTER MODEL

C\*\*\*\*\*

C

C

PROGRAM VORTEX

C

C

C

20 NOVEMBER 86

PROGRAMMER : BRIAN S. MILLER

C

C\*\*\*\*\*

C

C

PURPOSE:

C

C

C

THIS PROGRAM NUMERICALLY SIMULATES THE RISE OF A TRAILING  
VORTEX PAIR SHED OFF A LIFTING SURFACE SUBMERGED IN A  
DENSITY STRATIFIED MEDIUM.

C

C

C

TO RUN THIS PROGRAM:

C

C

1) GO TO "INPUT PARAMETERS" SECTION OF CODE AND CHANGE ANY PROBLEM  
PARAMETERS ( SP, FV, DT, ZTMAX, RO, MP, NP, ISAVE) AS DESIRED.

C

C

2) SET MAXIMUM TIME IN DATA STATEMENT MAXSTP;

C

EX: DATA MAXSTP /N/

C

( WHERE N= MAXIMUM NUMBER OF TIME STEPS)

C

C

3) SET INTERVALS FOR PLOTTING BY ENTRIES IN DATA STATEMENT NPLOT;

C

EX: DATA NPLOT/ 1,2,8,12,20,40,50,75/

C

( THIS PLOTS OUTPUT AT THE 1ST,2ND,8TH,12TH,40TH,50TH,AND  
75TH PROGRAM TIME STEP)

C

C

4) CHOOSE WHAT OUTPUT DEVICE TO USE, EITHER TEK 618 OR COMPRES

C (METAFILE OUTPUT) BY GOING TO GRAPHIC DEVICE SECTION OF PROGRAM  
C AND COMMENTING OUT WHICH OF TWO DEVICES YOU DONT WANT TO USE.

C 5) COMPILE PROGRAM UNDER VS FORTRAN USING THIS COMMAND;

C FORTVS VORTEX (OPT(3))

C ( NOTE: THIS OPTIMIZES CODE AT LEVEL 3 )

C 6) GO TO APPROPRIATE TERMINAL AND RUN UNDER DISSPLA.

C A. WHEN THE DISSPLA EXEC PROMPTS YOU ASK FOR 5 CYLINDERS OF  
C TEMPORARY DISK STORAGE AND ALSO YOU MAY WISH TO ISSUE

C B. WHEN THE EXEC PROMPTS YOU YOU MAY WISH TO ISSUE:

C FILEDEF 06 DISK VOR1OUT LISTING (PERM  
C IN ORDER TO REROUTE THE PRINTED OUTPUT TO A DISK FILE  
C NAMED: VOR1OUT LISTING A1 .

C C. PROGRAM WILL NOW RUN SENDING OUTPUT TO YOUR DESIGNATED  
C DEVICES.

C -----  
C  
C ADDITIONAL PROGRAM NOTES:

C 1) THIS PROGRAM COMPUTES DENSITY AND VORTICITY IN A (M-2 X N-2) GRID  
C BY SOLVING THE BOUYANTLY SCALED FORM OF THE NAVIER-STOKES  
C EQUATIONS VIA AN "UPWIND DIFFERENCING" FINITE DIFFERENCE METHOD.

C 2) THE VELOCITY FIELD IS COMPUTED USING A FORM OF THE BIOT-SAVART  
C LAW AT EACH NODAL POINT INCLUDING THE CONTRIBUTION OF THE  
C "IMAGE VORTICIES " ADDED TO INCLUDE THE FREE SURFACE EFFECT.

C 3) THIS VERSION OF THE PROGRAM INCLUDES A DISSPLA ROUTINE  
C TO PLOT THE DENSITY PERTUBATIONS ,CONSTANT DENSITY,  
C VORTICITY, AND VELOCITY FIELD AT EACH SELECTED TIME STEP.  
C THESE SELECTIONS FOR PLOTTING ARE INDICATED BY ENTRIES  
C IN THE ARRAY NSTEP. MAXIMUM NUMBER OF TIME STEPS IS INDICATED  
C BY AN ENTRY IN THE ARRAY MAXSTEP.

C

C

C 4) THE COMPUTATIONAL GRID  $(M-2) \times (N-2)$  IS USED FOR ALL COMPUTATIONS  
C EXCEPT FOR VELOCITY CALLS TO THE BIOT-SAVART SUBROUTINES.  
C TWO ADDITIONAL GRIDS, ONE FOR U AND ONE FOR V, ARE SHIFTED  $H/2$   
C UNITS IN THE X AND Y DIRECTION RESPECTIVELY. THE SUBROUTINES  
C COMPUTE U AND V VELOCITIES ON THESE GRIDS USING VORTICITY FROM  
C COMPUTATIONAL GRID. THE VELOCITIES ARE THEN AVERAGED ACROSS THE  
C COMPUTATIONAL GRID POINTS TO BE USED FOR THE FINITE DIFFERENCING.

C

C 5) THIS VERSION OF THIS PROGRAM WILL BE WRITTEN IN SINGLE PRECISION  
C AND IN AN OPTIMIZED FORM OF THE ORIGINAL CODE.

C

C 6) THIS PROGRAM HAS THE OPTION OF SAVING THE RHO AND ZETA ARRAYS  
C AND OTHER PROGRAM CONSTANTS IN ORDER TO RESTART THIS SIMULATION  
C AT THE TIME A PREVIOUS RUN HAD FINISHED. PROGRAM VORRS IS  
C SPECIFICALLY WRITTEN TO INPUT THE DATAFILE WRITTEN BY THIS  
C PROGRAM AND RESTART THE SIMULATION WITH THE SAME PARAMETERS.

C

C TO ACCESS THIS SAVE FEATURE SET VARIABLE ISAVE =1 . A FILEDEF  
C OF FORM ... FILEDEF 08 DISK <FN> <FT> <FM> ... MUST BE ISSUED  
C AT THE APPROPRIATE TIME IN EXECUTION.

C (NOTE: TO DISABLE THIS SAVE FEATURE SET ISAVE =0 )

C

C

C 7) TO CHANGE THE MESH DENSITY OF THE COMPUTATIONAL DOMAIN THE  
C USER SHOULD DO THE FOLLOWING:

C

A. ADJUST M AND N

C

B. ADJUST INITIAL VORTEX POSITION: MP, NP

C

C. ADJUST THE DIMENSIONS OF THE W ARRAY IN SUBROUTINES

C

CPLLOT, ZPLOT, AND DRPLOT TO BE (MW,NW)

C

D. IF THE GRID IS LARGER THAN 50 X 100 THEN ADJUST THE

C

DIMENSION STATEMENTS IN THE MAIN PROGRAM AND IN

C

SUBROUTINES ZPL, VPLOT AND V2PLOT TO THE NEW GRID

C

DIMENSION.

```

C
C
C
C*****
C
C   MAJOR VARIABLES USED IN THIS PROGRAM;
C
C   REAL VARIABLES;
C   T       = NONDIMENSIONAL TIME
C   DT      = TIME STEP
C   H       = NONDIMENSIONAL GRID LENGTH PARAMETER= DX = DY
C   RO      = NONDIMENSIONAL VORTEX CORE RADIUS
C   XWIDTH  = NONDIMENSIONAL WIDTH OF COMPUTATIONAL AREA
C   ZTMAX   = MAXIMUM VORTEX STRENGTH
C   SP      = NONDIMENSIONAL STRATIFICATION PARAMETER
C   FV      = NONDIMENSIONAL FROUDE NUMBER
C   BVND    = NONDIMENSIONAL BRUNT-VALSA FREQUENCY
C
C   INTEGER VARIABLES;
C   M       = NUMBER OF NODES IN X DIRECTION
C   N       = NUMBER OF NODES IN Y DIRECTION
C   MP      = X NODAL POINT OF VORTEX START POSITION
C   NP      = Y NODAL POINT OF VORTEX START POSITION
C   MM      = X ARRAY DIMENSION
C   NN      = Y ARRAY DIMENSION
C   NFIG    = PLOT NUMBER
C   NSTEP   = ITERATION NUMBER
C
C   ARRAY VARIABLES;
C   RHO     = DENSITY PERTUBATIONS AT EACH NODE DUE TO DYNAMICS
C   RHOI    = INITIAL VALUES OF DENSITY AT EACH NODE DUE TO GRADIENT
C   RHOT    = SUM OF BOTH DENSITY EFFECTS AT EACH NODE
C   RHNEW   = NEW VALUE OF RHO AT NEXT TIME STEP
C   ZETA    = VORTICITY AT EACH NODE
C   ZTNEW   = NEW VALUE OF VORTICITY AT NEXT TIME STEP

```

C U = X COMPONENT OF VELOCITY AT EACH NODAL POINT  
C V = Y COMPONENT OF VELOCITY AT EACH NODAL POINT  
C U2 = U VELOCITYS COMPUTED AT BIOT-SAVART NODAL POINTS  
C V2 = V VELOCITYS COMPUTED AT BIOT-SAVART NODAL POINTS  
C X = X COORDINATES AT EACH NODAL POINT  
C Y = Y COORDINATES AT EACH NODAL POINT  
C XU = X COORDINATE AT EACH U B. S. NODAL POINT  
C YU = Y COORDINATE AT EACH U B. S. NODAL POINT  
C XV = X COORDINATE AT EACH V B. S. NODAL POINT  
C YV = Y COORDINATE AT EACH V B. S. NODAL POINT

C

C-----

C

C SUBROUTINES USED IN THIS PROGRAM:

C

C SUBROUTINE COUÏ - OUTPUTS NODE COORDINATES

C

C SUBROUTINE OUTPT - OUTPUTS VARIOUS PROGRAM ARRAYS WHEN CALLED

C

C SUBROUTINE CPLÔT - CREATES ARRAY OF DENSITY AT EACH POINT  
C AND CALLS DISSPLA CONTOURING ROUTINE TO PLOT.

C

C SUBROUTINE ZPLOT - CREATES ARRAY OF VORTICITY AT EACH POINT AND  
C CALLS DISSPLA COUTOURING ROUTINE TO PLOT.

C

C SUBROUTINE DRPLOT- CREATES ARRAY OF DENSITY PERTUBATIONS AT EACH  
C POINT AND CALLS DISSPLA CONTOURING ROUTINE  
C TO PLOT.

C

C SUBROUTINE ZPL - OUTPUTS VORTICITY CONTOURS AS A PRINTER PLOT.

C

C SUBROUTINE VPLOT - CREATES COMPLEX VELOCITY VECTORS AT EACH  
C NODAL POINT AND THEN CALLS THE FOLLOWING  
C SUBROUTINES TO PLOT THEM ON DISSPLA:

C

A) V2PLOT

```

C          B)    AMIN
C          C)    AMAX
C
C    SUBROUTINE CON  - CALLED BY ZPL TO CONTOUR VORTICITY ON PRINTER.

```

```

C
C
C    FUNCTIONS USED IN THIS PROGRAM:

```

```

C
C    FUNCTION VBS - COMPUTES THE V COMPONENT OF VELOCITY USING
C                  THE BIOT-SAVART LAW.

```

```

C
C    FUNCTION UBS - COMPUTES THE U COMPONENT OF VELOCITY USING
C                  THE BIOT- SAVART LAW.

```

```

C
C    FUNCTION PNEW - TAKES THE FINITE DIFFERENCE TO STEP THE
C                  EQUATIONS IN TIME.

```

```

C
C *****

```

```

    DIMENSION RHOI(50,100),U(50,100),V(50,100),ZETA(50,100)
* ,ZTNEW(50,100),RHNEW(50,100),NPLOT(8),X(50),Y(100),RHO(50,100)
* ,XU(50),YU(100),XV(50),YV(100),U2(50,100),V2(50,100)
    CHARACTER*8 LABEL
    COMMON WK(15000)
    COMMON /PN/ DT,I,J,UF,UFA,UB,UBA,VF,VFA,VB,VBA,VPT,FV
    COMMON /PARM/ H;M;N,PI
    DATA MAXSTP/40 /
    DATA NPLOT/1,10,20,30,40,50,60,70/

```

```

C
C -----( CALL GRAPHIC OUTPUT DEVICE )-----

```

```

    CALL COMPRS
    CALL TEK618

```

```

C-----
C

```

```

    MM= 50
    NN= 100

```

C

C ----- INPUT PROGRAM PARAMETERS -----

C

DT= 2.000E0

T=0.0

XWIDTH = 5.0

RO= 0.09E0

SP= 1.20

FV=0.029765

ZTMIN= 1.0E-8

M= 44

N= 84

ISAVE= 1

C..... DESIGNATE NODAL POINTS TO PLACE INITIAL VORTEX AT (MP,NP)

MP=6

NP=66

C----- COMPUTE ADDITIONAL PARAMETERS-----

C

C..... DENSITY GRADIENT IN Y DIRECTION INITIALLY = DRHO

DRHOI=-SP\*SP\*FV\*FV

C..... NONDIMENSIONAL B. V. FREQUENCY = BVND

BVND= SP\*SP\*FV\*FV

C..... MAXIMUM VORTICITY AT ANY POINT = ZTMAX

ZTMAX=-(FV/(RO\*RO))

C..... GEOMETRIC CONSTANT PI

PI= 4.0E0\*ATAN(1.0E0)

C..... GRID LENGTH PARAMETER = H

H= XWIDTH/(M-4)

C

C..... COMPUTE MISC M AND N PARAMETERS

MM1= M-1

MP1= M+1

MM2= M-2

NP1=N+1

NM1=N-1

```
NM2= N-2
MW = (2*M) - 7
NW = NM2 - 1
```

C

C-----INITALIZE COORDINATE SYSTEM ORIGINS -----

C

```
X(1)= -H
Y(1)=  H
XU(1)= -1.5E0*H
YU(1)=  H
XV(1)= -H
YV(1)=  1.5E0*H
```

C

C ----- COMPUTE COORDINATES -----

C ( NOTE: COMPUTATIONAL GRID IS IN 4TH QUADRANT +X -Y )

C

```
DO 10 I= 2,MP1
    XU(I)= XU(I-1)+H
    XV(I)=XV(I-1)+ H
10  X(I) = X(I-1) + H
DO 11 J = 2,NP1
    YU(J) = YU(J-1) - H
    YV(J) = YV(J-1) - H
11  Y(J) = Y(J-1) - H
    YHT = ABS(Y(N-2))
```

C..... OUTPUT INITAL PARAMETERS OF THIS RUN OF PROGRAM.....

C

```
WRITE(6,1275)
WRITE(6,1500)
WRITE(6,1535) DT,H
WRITE(6,1540) XWIDTH,YHT
WRITE(6,1550) SP,FV
WRITE(6,1560) M,N
WRITE(6,1570) BVND
```

C

```

C..... OUTPUT COORDINATES OF NODES.....
      WRITE(6,1580) X(MP),Y(NP)
      WRITE(6,1590)
      CALL COUT(X,Y,MM,NN)

C
C ----- SPECIFY INITIAL VORTICITY AND DENSITY FIELDS -----
C
C ( FOR GRID SYSTEM X,Y COMPUTATIONAL GRID IN THE 4TH QUADRANT )
C ( TERMS ARG1 - ARG4 ARE IN QUADRANTS 1 - 4 )
C
      ARGMN= 30.0
      XCENT= X(MP)
      YCENT= Y(NP)
      DEN= 2.0E0*R0*R0
      ZETA(MP,NP)= ZTMAX
DO 30 J=1,N
      DO 30 I=1,M
          TRM1=0.0E0
          TRM2=0.0E0
          TRM3=0.0E0
          TRM4=0.0E0
          ARG1= ((X(I)-XCENT)**2 + (Y(J)+YCENT)**2)/DEN
          IF (ARG1 .GT. ARGMN) GO TO 12
          TRM1= EXP(-ARG1)
12      ARG2= ((X(I)+XCENT)**2 + (Y(J)+YCENT)**2)/DEN
          IF(ARG2 .GT. ARGMN) GO TO 14
          TRM2= EXP(-ARG2)
14      ARG3= ((X(I)+XCENT)**2 + (Y(J)-YCENT)**2)/DEN
          IF(ARG3 .GT. ARGMN) GO TO 16
          TRM3= EXP(-ARG3)
16      ARG4= ((X(I)-XCENT)**2 + (Y(J)-YCENT)**2)/DEN
          IF(ARG4 .GT. ARGMN) GO TO 18
          TRM4= EXP(-ARG4)
18      IF((J.EQ.NP) .AND. (I .EQ.MP)) GO TO 20
      ZETA(I,J)=ZTMAX*(-TRM1 +TRM2 -TRM3 +TRM4)

```

```

        IF(ABS(ZETA(I,J)) .LT. ZTMIN) ZETA(I,J)=0.0E0
20      RHOI(I,J)= DRHOI*Y(J)
        RHO(I,J)= 0.0E0
30      CONTINUE
        WRITE(6,1250)
C      CALL OUTPT(ZETA,'ZTA(I,J)',MM,NN,0)
C      CALL OUTPT(RHOI,'ROI(I,J)',MM,NN,0)
C
C..... INITIALIZE TIME STEP COUNTERS.....
        NFIG=0
        NSTEP=0
C
C***** ENTRY POINT OF TIME LOOP *****
        60      CONTINUE
C
C..... COMPUTE U VELOCITY FOR ALL NODES IN U VELOCITY GRID.....
C
        DO 70 I= 1,MP1
            DO 70 J= 1,N
70      U2(I,J)= UBS(XU(I),YU(J),MM,NN,X,Y,ZETA)
C
C..... COMPUTE V VELOCITY FOR ALL NODES IN V VELOCITY GRID.....
C
        DO 100 I= 1,M
            DO 100 J= 1,NP1
100     V2(I,J)= VBS(XV(I),YV(J),MM,NN,X,Y,ZETA)
C
C..... INTERPOLATE VELOCITIES FROM VELOCITY GRIDS TO NODAL
C                                     POINTS ON COMPUTATIONAL GRID.
        VMIN= 1.0E-08
        DO 120 I= 1,M
            DO 120 J= 1,N
                U(I,J)= (U2(I,J) + U2(I+1,J))/2.0E0
                V(I,J)= (V2(I,J)+ V2(I,J+1))/2.0E0
                IF (ABS(U(I,J)) .LT. VMIN) U(I,J)= 0.0E0

```

```

        IF (ABS(V(I,J)) .LT. VMIN) V(I,J)= 0.0E0
120    CONTINUE
C     IF (NSTEP .EQ. 0) CALL OUTPT(V,'V(I,J) ',MM,NN,1)
C     IF (NSTEP .EQ. 0) CALL OUTPT(U,'U(I,J) ',MM,NN,1)
C
C
C .....
C             INCREASE TIME COUNTER BY ONE.
C     CHECK ITERATION COUNTER AND TERMINATE IF NSTEP IS MORE THAN MAX
C     COMPUTE VORTICITY AND DENSITY AT ALL INTERIOR POINTS
C         ( STORED AS ELEMENTS OF ZTNEW AND RHNEW )
C .....
C
        NSTEP=NSTEP+1
        IF (NSTEP .GT. MAXSTP) GO TO 1700
        T= T+DT
        DO 600 I=2,MM1
            DO 600 J=2,NM1
                VPT= V(I,J)
                UF= (U(I+1,J)+U(I,J))/2.0E0
                UFA=ABS(UF)
                UB= (U(I-1,J)+U(I,J))/2.0E0
                UBA=ABS(UB)
                VF= (V(I,J-1)+V(I,J))/2.0E0
                VFA=ABS(VF)
                VB= (V(I,J+1)+V(I,J))/2.0E0
                VBA=ABS(VB)
                ZTNEW(I,J)= PNEW(ZETA,RHO,MM,NN,-1.0E0,0.0E0,0.0E0)
600        RHNEW(I,J)= PNEW(RHO,RHO,MM,NN,0.0E0,0.0E0,BVND)
C
C
C ----- APPLY BOUNDRY CONDITIONS TO RHO AND ZETA -----
C
C ..... ASSIGN NEW VALUES OF RHO AND ZETA TO RHO AND ZETA ARRAYS ...
C

```

```

C
      DO 700 I = 2,MM1
        DO 700 J = 2,NM1
          ZETA(I,J)= ZTNEW(I,J)
700      RHO(I,J)=RHNEW(I,J)
C..... CALCULATE RHO AND ZETA VALUES AT I=M-2 AND J=N-2 BOUNDRIES ...
C
      DO 800 I= 2,MM2
        DO 800 J= 2,NM2
          ZETA(MM2,J)= (ZETA(MM1,J)+ ZETA(M-3,J))/2.0E0
          ZETA(I,NM2)= (ZETA(I,NM1)+ ZETA(I,N-3))/2.0E0
          RHO(MM2,J)= (RHO(MM1,J)+ RHO(M-3,J))/2.0E0
          RHO(I,NM2)= (RHO(I,NM1)+ RHO(I,N-3))/2.0E0
          IF(ABS(ZETA(I,J)).LT. ZTMIN) ZETA(I,J)=0.0E0
          IF(ABS(RHO(I,J)).LT. ZTMIN) RHO(I,J)= 0.0E0
800      CONTINUE
C
C.....
C      PLOT FLOW PATTERN WHEN NSTEP = VALUE SPECIFIED IN NPLOT
C
C      THEN RESTART ALGORITHM AT LINE 60 FOR A NEW TIME STEP
C.....
      DO 1100 K= 1,8
        IF (NSTEP-NPLOT(K)) 1100, 1200, 1100
1100 CONTINUE
        GO TO 60
1200 NFIG=NFIG+1
      TM= T*FV
      IF (NSTEP .EQ. MAXSTP ) CALL OUTPT(ZETA,'ZTA(I,J)',MM,NN,NSTEP)
      IF (NSTEP .EQ. MAXSTP) CALL OUTPT (RHO, 'RHO(I,J)',MM,NN,NSTEP)
      WRITE(6,1300)NSTEP,T,TM
      CALL CPLOT(RHO,RHOI,MM,NN,NSTEP,TM,MW,NW)
      CALL VPLOT(U,V,X,Y,MM,NN,TM)
      CALL DRPLOT(RHO,MM,NN,NSTEP,TM,MW,NW)
      CALL ZPL(ZETA,MM,NN,XWIDTH,YHT,ITER)

```

```

      CALL ZPLOT(ZETA,MM,NN,TM,MW,NW)
1250 FORMAT(// 10X,'INITIAL ZETA AND RHO VALUES : ')
1275 FORMAT('1')
1300 FORMAT(/10X,'ITERATION NUM:',I6,4X,'TIME=',F9.3,4X,'T* =',F10.6)
1400 WRITE(6,1500)
1500 FORMAT( ///)
1530 FORMAT(' ',5X,'INITIAL PROGRAM PARAMETERS:' )
1535 FORMAT('0',5X,'TIME STEP= ',F8.4,5X,'GRID SPACING H = ',F8.4)
1540 FORMAT('0',5X,'NON DIMENSIONAL CELL DIMENSIONS : XDIRECTION =',
      * F8.4,5X,'YDIRECTION =',F8.4)
1550 FORMAT('0',5X,'STRATIFICATION PARAMETER =',F8.4,5X,
      * 'FROUDE NUMBER =',F8.4)
1560 FORMAT('0',5X,'NUMBER OF NODES IN X DIRECTION =',I4,5X,
      * 'IN Y DIRECTION =',I4)
1570 FORMAT('0',5X,'NONDIMENSIONAL B. V. FREQUENCY =',F15.9)
1580 FORMAT('0',5X,'X COORDINATE OF VORTEX START POSITION =',F8.4,5X,
      * 'Y COORDINATE =',F8.4)
1590 FORMAT('0',5X,'OUTPUT COORDINATES OF ALL OTHER NODES:')
C
C      LOOP BACK TO STARTING POINT OF ITERATION
      GO TO 60
1700 CALL DONEPL
C1700 CONTINUE
C
C----- SAVE ARRAYS AND TIME DATA TO RESTART PROGRAM LATER -----
C
      IF (ISAVE .EQ. 0 ) GO TO 1900
      WRITE(8,*) SP,FV,DT,T
      WRITE(8,*) M,N,MP,NP
      WRITE(8,*) BVND,H,ZTMAX
      DO 1800 I= 1,M
          DO 1800 J= 1,N
1800      WRITE(8,*) ZETA(I,J), RHO(I,J)
1900 STOP
      END

```

```

C
C ++++++
C
C          SUBROUTINES :
C
C =====
C
C =====
C
C          REAL FUNCTION  PNEW(P,Q,MM,NN,A,B,C)
C
C THIS FUNCTION INTEGRATES THIS EQUATION WITH RESPECT TO TIME
C $$$ DP/DT= (-D(UP)/DX -D(VP)/DY + A*DQ/DX + B*DEL(P) +C*V ) $$$
C UTILIZING AN UPWIND DIFFERENCING SCHEME
C
C          DIMENSION P(MM,NN),Q(MM,NN)
C          COMMON /PN/ DT,I,J,UF,UFA,UB,UBA,VF,VFA,VB,VBA,VPT,FV
C          COMMON /PARM/ H,M,N,PI
C          P1= (UF-UFA)*P(I+1,J) +(UF+UFA-UB+UBA)*P(I,J) -(UB+UBA)*P(I-1,J)
C          P2= (VF-VFA)*P(I,J-1) +(VF+VFA-VB+VBA)*P(I,J) -(VB+VBA)*P(I,J+1)
C          P3= Q(I+1,J) -Q(I-1,J)
C          P4= P(I+1,J) +P(I-1,J)+P(I,J-1)+P(I,J+1)-4.0E0*P(I,J)
C          P5= 2.0E0*H*VPT
C          TEMP1=(DT/(2.0E0*H))*((-P1-P2) +A*P3+(2.0E0/H)*B*P4+C*P5)
C          PNEW=P(I,J)+TEMP1
C          RETURN
C          END
C
C =====
C
C          REAL FUNCTION  UBS(XU,YU,MM,NN,X,Y,ZETA)
C
C THIS SUBROUTINE FINDS BOUNDRY VALUES OF VELOCITY U
C UTILIZING THE BIOT-SAVART LAW
C
C (NOTE: TERMS IN EQUATION ARE EVALUATED CONSECUTIVELY IN EACH

```

```

C           QUADRANT FROM ONE TO FOUR )
C-----
      DIMENSION X(MM),Y(NN),ZETA(MM,NN)
      COMMON /PARM/ H,M,N,PI
C
      UMIN= 1.0E-08
      U1= 0.0E0
      U2= 0.0E0
      U3= 0.0E0
      U4= 0.0E0
C
      SIGNP=1.0E0
      SIGNM=-1.0E0
      DA= H*H
C
C ----- COMPUTE U COMPONENT OF VELOCITY USING THE B-S LAW-----
C
      DO 20 I= 1,M
        DO 20 J= 1,N
C -- QUADRANT ONE --
          RSQ1=((XU-X(I))**2 + (YU+Y(J))**2)
          U1= U1+ ((-Y(J)-YU)/(2.0E0*PI*RSQ1))*SIGNM*ZETA(I,J)*DA
C -- QUADRANT TWO --
          RSQ2= ((XU+X(I))**2 + (YU+Y(J))**2)
          U2= U2+ ((-Y(J)-YU)/(2.0E0*PI*RSQ2))*SIGNP*ZETA(I,J)*DA
C -- QUADRANT THREE --
          RSQ3= ((XU+X(I))**2 + (YU-Y(J))**2)
          U3= U3+ ((Y(J)-YU)/(2.0E0*PI*RSQ3))*SIGNM*ZETA(I,J)*DA
C -- QUADRANT FOUR --
          RSQ4= ((XU-X(I))**2 + (YU-Y(J))**2)
20      U4 = U4 + ((Y(J)-YU)/(2.0E0*PI*RSQ4))*SIGNP*ZETA(I,J)*DA
      UTEMP= U1+U2 +U3+ U4
      IF (ABS(UTEMP).LT.UMIN) UTEMP=0.0E0
      UBS= UTEMP
      RETURN

```

END

C  
C  
C=====

C  
REAL FUNCTION VBS(XV,YV,MM,NN,X,Y,ZETA)

C  
C THIS SUBROUTINE FINDS BOUNDRY VALUES OF VELOCITY V  
C UTILIZING THE BIOT-SAVART LAW

C  
C (NOTE : TERMS IN THE EQUATION ARE EVALUATED CONSECUTIVELY IN EACH  
C QUADRANT FROM ONE TO FOUR)

C-----  
DIMENSION X(MM),Y(NN),ZETA(MM,NN)

COMMON/PARM/ H,M,N,PI

C  
VMIN= 1.0E-08

V1= 0.0E0

V2= 0.0E0

V3= 0.0E0

V4= 0.0E0

C  
SIGNP=1.0E0

SIGNM=-1.0E0

DA= H\*H

C  
C ----- COMPUTE V COMPONENT OF VELOCITY USING THE B-S LAW-----

C  
DO 20 I= 1,M

DO 20 J= 1,N

C -- QUADRANT ONE --

RSQ1=((XV-X(I))\*\*2 + (YV+Y(J))\*\*2)

V1= V1+ ((XV-X(I))/(2.E0\*PI\*RSQ1))\*SIGNM\*ZETA(I,J)\*DA

C -- QUADRANT TWO --

RSQ2= ((XV+X(I))\*\*2 +(YV+Y(J))\*\*2)

```

      V2= V2+ ((XV+X(I))/(2.0E0*PI*RSQ2))*SIGNP*ZETA(I,J)*DA
C.  -- QUADRANT THREE --
      RSQ3= ((XV+X(I))**2 +(YV-Y(J))**2)
      V3= V3+((XV+X(I))/(2.0E0*PI*RSQ3))*SIGNM*ZETA(I,J)*DA
C   -- QUADRANT FOUR --
      RSQ4= ((XV-X(I))**2 + (YV-Y(J))**2)
20   V4 = V4 + ((XV-X(I))/(2.0E0*PI*RSQ4))*SIGNP*ZETA(I,J)*DA
      VTEMP = V1+V2 +V3+ V4
      IF(ABS(VTEMP).LT.VMIN) VTEMP=0.0E0
      VBS= VTEMP
      RETURN
      END

C
C
C-----
C
      SUBROUTINE COUT(X,Y,MM,NN)
C
C
C-----

      REAL X(MM),Y(NN),H,PI
      COMMON/PARM/H,M,N,PI
      WRITE(6,50)
      WRITE(6,*) '          ARRAY X'
      WRITE(6,*)
      WRITE(6,*) (X(I), I=1,M)
      WRITE(6,*)
      WRITE(6,*)
      WRITE(6,*) '          ARRAY Y'
      WRITE(6,*)
      WRITE(6,*) (Y(J), J=1,N)
      WRITE(6,*)
      WRITE(6,*)
50   FORMAT(////)
      RETURN

```

END

=====

SUBROUTINE OUTPT(A,LBL,MM,NN,KAL)

C  
C THIS SUBROUTINE PRINTS OUT AN (NKM) ARRAY WITH A LABEL  
C IN A RECTANGULAR ( 2,M-2)X(2,N-2) GRID  
C

DIMENSION A(MM,NN)

COMMON/PARM/ H,M,N,PI

CHARACTER\*8 LBL

NM2= N-2

MM2= M-2

WRITE(6,50)

WRITE(6,\*)

WRITE(6,\*) ' OUTPUT OF ARRAY: ',LBL,' ITER NUM:',KAL

WRITE(6,\*)

DO 10 J= 2,NM2

WRITE(6,\*)

WRITE(6,\*) (A(I,J), I=2,MM2)

10 CONTINUE

50 FORMAT('1')

RETURN

END

C  
C-----

SUBROUTINE CPLOT(RHO,RHOI,MM,NN,NSTEP,TM,MW,NW)

COMMON WK(15000)

COMMON /PARM/ H,M,N,PI

REAL W(81,81)

REAL RHO(MM,NN),RHOI(MM,NN),H,PI,RHOT(50,100)

DATA ISCALE/4HSCAL/

C  
C...CREATE ARRAY OF DENSITY CHANGES AT EACH NODE (DRHO) .....

C

```

MM2= M-2
NM2= N-2
DO 10 I= 2,MM2
    DO 10 J= 2,NM2
        JJ= (NM2+1)-J
        II= I+(M-5)
        RHOT(I,J)=RHO(I,J)+RHOI(I,J)
        W(II,JJ)= RHOT(I,J)
10    CONTINUE
        DO 20 I= 3,MM2
            II= (M-1)-I
                DO 20 J= 2,NM2
                    JJ= (NM2+1) -J
20                W(II,JJ)= RHOT(I,J)
C
C        CALL OUTPT(RHOT, 'RHT(I,J)',MM,NN,NSTEP)
C..... CALL SUBROUTINE CONTR TO PLOT THESE PERTUBATIONS.....
C
CALL RESET (3HALL)
CALL PAGE(8.7,11.2)
CALL PHYSOR(2.0,3.00)
CALL AREA2D (5.0,6.0)
CALL HEIGHT(.2 )
CALL INTAXS
CALL XNAME ('X/BO',4)
CALL YNAME ('Y/BO',4)
CALL XTICKS(2)
CALL YTICKS(2)
CALL GRAF (-5.0,1.,5.,10.,1.,0.)
CALL MIXALF('INSTRU')
CALL MESSAG('T(EH.5)*(EXHX) =$',100,1.5,6.5)
CALL REALNO(TM,106,'ABUT','ABUT')
CALL FRAME
CALL BCOMON (15000)
CALL CONMIN(2.0)

```

```

CALL CONANG (20.)
CALL CONMAK (W,MW,NW,ISCALE)
CALL HEIGHT(.08)
CALL CONLIN (0,5HSOLID,'LABELS',2,5)
CALL CONLIN (1,4HDASH,3HNOLABELS,1,3)
CALL RASPLN(0.25)
CALL CONTUR (2,6HLABELS,4HDRAW)
CALL HEIGHT(.2)
CALL COMPLX
CALL RESET('HEIGHT')
CALL RESET('COMPLX')
CALL ENDPL (0)
RETURN
END

```

C

C-----

C

```

SUBROUTINE ZPLOT(ZETA,MM,NN, TM,MW,NW)
REAL ZETA(MM,NN),H,PI
COMMON WK(15000)
COMMON /PARM/ H,M,N,PI
DIMENSION W(81,81)
DATA ISCALE/4HSCAL/

```

C

C...CREATE ARRAY FOR PLOTTING OF ZETA IN ACTUAL COMPUTATIONAL AREA..

C

```

MM2= M-2
NM2=N-2
DO 10 I= 2,MM2
  II= I+(M-5)
  DO 10 J= 2,NM2
    JJ= (NM2+1)-J
10  W(II,JJ)=ZETA(I,J)
  DO 20 I= 3,MM2
    II= (M-1)-I

```

```

                DO 20 J= 2,NM2
                JJ= (NM2+1) - J
20              W(II,JJ) = -ZETA(I,J)
C
C..... CALL SUBROUTINE CONTR TO PLOT VORTICITY.....
C
C
                CALL RESET (3HALL)
                CALL PAGE(8.7,11.2)
                CALL PHYSOR(2.0,3.00)
                CALL AREA2D (5.0,6.0)
                CALL HEIGHT(.2 )
                CALL INTAXS
                CALL XNAME ('X/BO',4)
                CALL YNAME ('Y/BO',4)
                CALL XTICKS(2)
                CALL YTICKS(2)
                CALL GRAF (-5.0,1.,5.,10.,1.,0.)
                CALL MIXALF('INSTRU')
                CALL MESSAG('T(EH.5)*(EXHX) =$',100,1.5,6.5)
                CALL REALNO(TM,106,'ABUT','ABUT')
                CALL FRAME
                CALL BCOMON (15000)
                CALL CONANG (60.)
                CALL CONMIN(2.0)
                CALL CONMAK (W,MW,NW,ISCALE)
                CALL HEIGHT(.08)
                CALL CONLIN (0,5HSOLID,'LABELS',2,5)
                CALL CONLIN (1,4HDASH,'LABELS',1,3)
                CALL RASPLN(0.25)
                CALL CONTUR (2,6HLABELS,4HDRAW)
                CALL HEIGHT(.2)
                CALL COMPLX
                CALL RESET('HEIGHT')
                CALL RESET('COMPLX')

```

```
CALL ENDPL (0)
```

```
RETURN
```

```
END
```

```
C
```

```
C
```

```
C-----
```

```
C
```

```
      SUBROUTINE DRPLOT(RHO,MM,NN,NSTEP,TH,MW,NW)
```

```
      COMMON WK(15000)
```

```
      COMMON /PARM/ H,M,N,PI
```

```
      REAL W(81,81)
```

```
      REAL RHO(MM,NN),H,PI
```

```
      DATA ISCALE/4HSCAL/
```

```
C
```

```
C...CREATE ARRAY OF DENSITY CHANGES AT EACH NODE (DRHO) .....
```

```
C
```

```
      MM2= M-2
```

```
      NM2= N-2
```

```
      DO 10 I= 2,MM2
```

```
          DO 10 J= 2,NM2
```

```
            JJ= (NM2+1)-J
```

```
            II= I+(M-5)
```

```
            W(II,JJ)= RHO(I,J)
```

```
10      CONTINUE
```

```
          DO 20 I= 3,MM2
```

```
            II= (M-1)-I
```

```
              DO 20 J= 2,NM2
```

```
                JJ= (NM2+1) -J
```

```
20      W(II,JJ)= RHO(I,J)
```

```
C
```

```
C..... CALL SUBROUTINE CONTR TO PLOT THESE PERTUBATIONS.....
```

```
C
```

```
      CALL RESET (3HALL)
```

```
      CALL PAGE(8.7,11.2)
```

```
      CALL PHYSOR(2.0,3.00)
```

```

CALL AREA2D (5.0,6.0)
CALL HEIGHT(.2 )
CALL INTAXS
CALL XNAME ('X/BO',4)
CALL YNAME ('Y/BO',4)
CALL XTICKS(2)
CALL YTICKS(2)
CALL GRAF (-5.0,1.,5.,10.,1.,0.)
CALL MIXALF('INSTRU')
CALL MESSAG('T(EH.5)*(EXHX) =$',100,1.5,6.5)
CALL REALNO(TM,106,'ABUT','ABUT')
CALL FRAME
CALL BCOMON (15000) .
CALL CONMIN(2.0)
CALL CONANG (20.)
CALL CONMAK (W,MW,NW,ISCALE)
CALL HEIGHT(.08)
CALL CONLIN (0,5HSOLID,'LABELS',2,5)
CALL CONLIN (1,4HDASH,8HNOLABELS,1,3)
CALL RASPLN(0.25)
CALL CONTUR (2,6HLABELS,4HDRAW)
CALL HEIGHT(.2)
CALL COMPLX
CALL RESET('HEIGHT')
CALL RESET('COMPLX')
CALL ENDPL (0)
RETURN
END

```

C

C=====

C

```

SUBROUTINE CON(Z2,XRANGE,YRANGE,NX,H,MM,NN,ZMAX,ZMIN)

```

C

```

C THIS SUBROUTINE GENERATES A CONTOUR PLOT OF ZETA IN A RECTANGULAR
C DOMAIN OF SIZE: YRANGE * XRANGE ON THE PRINTER.

```

C

```
CHARACTER*1 SYMBOL(8),GRAPH(100)
REAL LX,LY
DIMENSION Z2(MM,NN),VALUE(7)
DATA SYMBOL / 'X','A','-',',',' ','+',',','1',' ' /
VALUE(1)= ZMIN
VALUE(2)= ZMIN*.75
VALUE(3)= ZMIN*.5
VALUE(4)= 0.0
VALUE(6)= ZMAX*.75
VALUE(7)= ZMAX
VALUE(5)=ZMAX*.45
NY= 0.8*NX*YRANGE/XRANGE
DELX= XRANGE/NX
DELY= YRANGE/NY
WRITE(6,50)
WRITE(6,*) 'NX=',NX, 'NY=',NY, 'XRANGE=',XRANGE,
*          'YRANGE=',YRANGE
WRITE(6,*)
  DO 11 I= 1,NX
11  GRAPH(I)= 'T'
    WRITE(6,6) (GRAPH(I), I= 1,NX)
    DO 5 JSYMBL = 1,NY
      Y= (JSYMBL-0.5)*DELY
      J= 1+Y/H
      LY= Y-(J-1)*H
      HMLY= H-LY
      DO 4 ISYMBL = 1,NX
        X= (ISYMBL-0.5)*DELX
        I=1+X/H
        LX= X-(I-1)*H
        HMLX= H- LX
        A1= HMLX*HMLY
        A2= HMLX*LY
        A3= LX*LY
```

```

      A4= LX*HMLY
      Z2C= (A1*Z2(I,J) +A2*Z2(I,J+1) +A3*Z2(I+1,J+1)
*         +A4*Z2(I+1,J))/H**2
C
C... DETERMINE THE VALUE OF NRANGE BASED ON Z2C.....
C
C.... PRINT OUT CHARACTERS IN ARRAY GRAPH BY ROW .....
C
      DO 2 K= 1,7
      IF (Z2C-VALUE(K)) 1, 1, 2
1      NRANGE = K
      GO TO 3
2      CONTINUE
      NRANGE= 8
3      GRAPH( ISYMBL)= SYMBOL(NRANGE)
4      CONTINUE
5      WRITE(6,6) (GRAPH(I), I=1,NX)
6      FORMAT(' ',10X,100A1 )
50     FORMAT('1!')
      DO 60 I= 1,NX
60     GRAPH(I)= 'B'
      WRITE(6,6) (GRAPH(I) ,I=1,NX)
      WRITE(6,*)
      WRITE(6,*) 'MAXIMUM VALUE OF NEGATIVE VORTICITY = SYMBOL (X) = '
*      ,ZMIN
      WRITE(6,*) ' 75% OF MAXIMUN NEGATIVE VORTICITY = SYMBOL (A) '
      WRITE(6,*) ' 50% OF MAXIMUM NEGATIVE VORTICITY = SYMBOL (-) '
      WRITE(6,*)
      WRITE(6,*) ' MAXIMUM VALUE OF POSITIVE VORTICITY = SYMBOL (1) = '
*      , ZMAX
      WRITE(6,*) ' 75% OF MAXIMUM POSITIVE VORTICITY = SYMBOL (+) '
      RETURN
      END
C-----
C

```

```
SUBROUTINE ZPL(ZETA,MM,NN,XWIDTH,YHT,ITER)
```

```
COMMON /PARM/ H,M,N,PI
```

```
DIMENSION Z2(50,100),ZETA(MM,NN)
```

```
C  
C...CREATE ARRAY FOR PLOTTING OF ZETA IN ACTUAL COMPUTATIONAL AREA..
```

```
C
```

```
MM3= M-3
```

```
NM3=N-3
```

```
ZMIN= 0.0
```

```
ZMAX= 0.0
```

```
DO 10 I= 1,MM3
```

```
DO 10 J= 1,NM3
```

```
Z2(I,J)= ZETA(I+1,J+1)
```

```
C.. FIND THE MAXIMUM POSITIVE VORTICITY IN ARRAY Z2(MM,NN).....
```

```
C
```

```
IF(Z2(I,J) .GT. ZMAX) ZMAX=Z2(I,J)
```

```
C.. FIND THE MAXIMUM NEGATIVE VORTICITY IN ARRAY Z2(MM,NN).....
```

```
C
```

```
IF( Z2(I,J) .LT. ZMIN) ZMIN= Z2(I,J)
```

```
10 CONTINUE
```

```
C
```

```
C
```

```
IF (ZMAX .LT. 1.0E-6 ) ZMAX=1.0
```

```
C..... CALL SUBROUTINE CON TO PLOT VORTICITY.....
```

```
C
```

```
CALL CON(Z2,XWIDTH,YHT,100,H,MM,NN,ZMAX,ZMIN)
```

```
RETURN
```

```
END
```

```
C-----
```

```
SUBROUTINE VPLOT(U,V,X,Y,MM,NN,TM)
```

```
COMMON /PARM/ H,M,N,PI
```

```
COMPLEX ZV(50,100), CV(50,100)
```

```
DIMENSION U(MM,NN), V(MM,NN), X(MM), Y(NN)
```

```
MM2= M-2
```

```
NM2= N-2
```

```

MM3 = M - 3
NM3 = N - 3

C
C..... FORM COMPLEX U, V, AND Z ARRAYS FOR QUADRANTS 3 AND 4 .....
C
DO 10 I= 2,MM2
  DO 10 J= 2,NM2
    II= I-1
    JJ= (NM2+1) -J
    ZV(II,JJ)= CMPLX(X(I),Y(J))
10  CV(II,JJ)= CMPLX(U(I,J),V(I,J))
C
C
C..... PLOT VECTORS USING SUBROUTINE V2PLOT .....
CALL V2PLOT(ZV,CV,MM3,NM3,TM)
C
RETURN
END

C
C-----
C
SUBROUTINE V2PLOT(Z,C,M,N,TM)
C
C *****
C * SUBROUTINE V2PLOT TO PLOT MXN COMPLX VELOCIT FIELD C(M,N) *
C * OVER A COMPLX DOMAIN Z(M,N) *
C * *
C *****
COMPLEX Z(50,100),C(50,100),CMAX
REAL X(100),Y(100),YX(100),YN(100),XX(100),
* XN(100),X2(100),Y2(100)
INTEGER PMAX,PMIN
EXTERNAL AMAX
EXTERNAL AMIN
C

```

```

DO 20 J =1,N
    DO 10 I =1,M
        X(I) =ABS(REAL(C(I,J)))
        Y(I) =ABS(AIMAG(C(I,J)))
10    CONTINUE
        CALL AMAX(Y,M,YMAX,PMAX)
        CALL AMAX(X,M,XMAX,PMAX)
        YX(J) = YMAX
        XX(J) = XMAX
        CALL AMIN(Y,M,YMIN,PMIN)
        CALL AMIN(X,M,XMIN,PMIN)
        YN(J) =YMIN
        XN(J) =XMIN
20    CONTINUE
        CALL AMAX(YX,N,YMAX,PMAX)
C    CALL AMIN(YN,N,YMIN,PMIN)
        CALL AMAX(XX,N,XMAX,PMAX)
C    CALL AMIN(XN,N,XMIN,PMIN)
C
        CMAX = CMPLX(XMAX,YMAX)
        UMAX =SQRT((XMAX)**2+(YMAX)**2)
        DO 24 I =1,M
            DO 22 J=1,N
                C(I,J) = C(I,J)/UMAX
22    CONTINUE
24    CONTINUE
C
        DO 40 J =1,N
            DO 30 I =1,M
                X(I) =REAL(Z(I,J))
                Y(I) =AIMAG(Z(I,J))
30    CONTINUE
        CALL AMAX(Y,M,YMAX,PMAX)
        CALL AMAX(X,M,XMAX,PMAX)
        YX(J) = YMAX

```

```
XX(J) = XMAX
CALL AMIN(Y,M,YMIN,PMIN)
CALL AMIN(X,M,XMIN,PMIN)
YN(J) =YMIN
XN(J) =XMIN
```

```
40 CONTINUE
CALL AMAX(YX,N,YMAX,PMAX)
CALL AMIN(YN,N,YMIN,PMIN)
CALL AMAX(XX,N,XMAX,PMAX)
CALL AMIN(XN,N,XMIN,PMIN)
```

C

```
CALL RESET(3HALL)
CALL PAGE(8.7,11.2)
CALL PHYSOR(2.0,3.0)
CALL AREA2D(5.,6.)
CALL HEIGHT(.2)
CALL INTAXS
CALL XNAME('X/BO',4)
CALL YNAME('Y/BO',4)
CALL XTICKS(2)
CALL YTICKS(2)
CALL GRAF(0.0,0.5,5.0,-10.0,1.0,0.0)
CALL MIXALF('INSTRU')
CALL MESSAG('T(EH.5)*(EXHX) =$',100,1.5,6.5)
CALL REALNO(TM,106,'ABUT','ABUT')
```

C

```
DO 60 J=1,N
DO 50 I=1,M
X(I) = REAL(Z(I,J))
X2(I) = X(I)+REAL(C(I,J))
Y(I)= AIMAG(Z(I,J))
Y2(I) = Y(I)+AIMAG(C(I,J))
50 CONTINUE
CALL MARKER (3)
CALL SCLPIC(.001)
```

```

        CALL CURVE(X,Y,M,-1)
    DO 54 I =1,M
        X11=X(I)
        X12=X2(I)
        Y11=Y(I)
        Y12=Y2(I)
        IF(X12.EQ.0..AND.Y12.EQ.0) GO TO 54
        CALL RLVEC (X11,Y11,X12,Y12,1121)
54      CONTINUE
60      CONTINUE
        CALL RESET('HEIGHT')
        CALL ENDPL(0)
RETURN
END

C
C
SUBROUTINE AMAX(Y,N,YMAX,PMAX)
C
C *****
C * SUBROUTINE TO COMPUTE THE LARGE ELELEMENT
C * IN A GIVEN ROW OR COLUMN IN ARRAY 'A'.
C *****
C
C *** VARIABLE DECLARATION ***
C REAL AMAX
C   INTEGER PMAX
C   DIMENSION Y(N)
C
C   YMAX=Y(1)
C   DO 5100 I=2,N
C       IF(Y(I).LE.YMAX) GO TO 5000
C       YMAX=Y(I)
C       PMAX=I
5000   CONTINUE
5100   CONTINUE

```

```

C      MAXROW=POS
      RETURN
      END

C
C
C
      SUBROUTINE AMIN(Y,N,YMIN,PMIN)

C
C      *****
C      * SUBROUTINE TO COMPUTE THE SMALL ELEMENT
C      * IN A GIVEN ROW OR COLUMN IN ARRAY 'A'.
C      *****

C      *** VARIABLE DECLARATION ***
C      REAL AMIN
C      INTEGER PMIN
C      DIMENSION Y(N)

C
C      YMIN=Y(1)
C      DO 6100 I=2,N
C          IF(Y(I).GE.YMIN) GO TO 6000
C          YMIN=Y(I)
C          PMIN=I
6000      CONTINUE
6100      CONTINUE
      RETURN
      END

```

APPENDIX B  
FIGURES

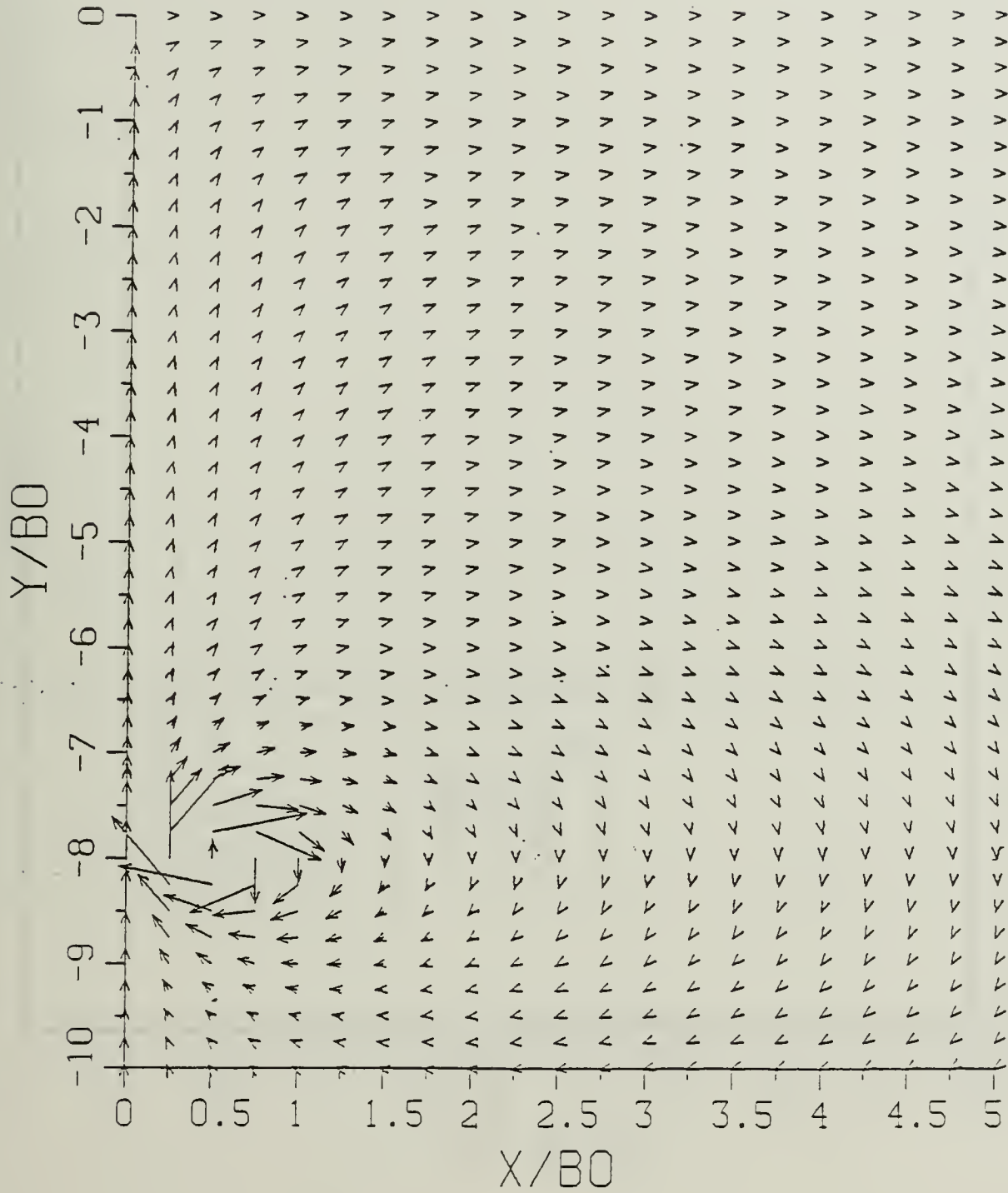


Figure B.1a Velocity Field:  $SP = 0.00$ ,  $T^* = 0.05952$ .

$$T^* = 0.05952$$

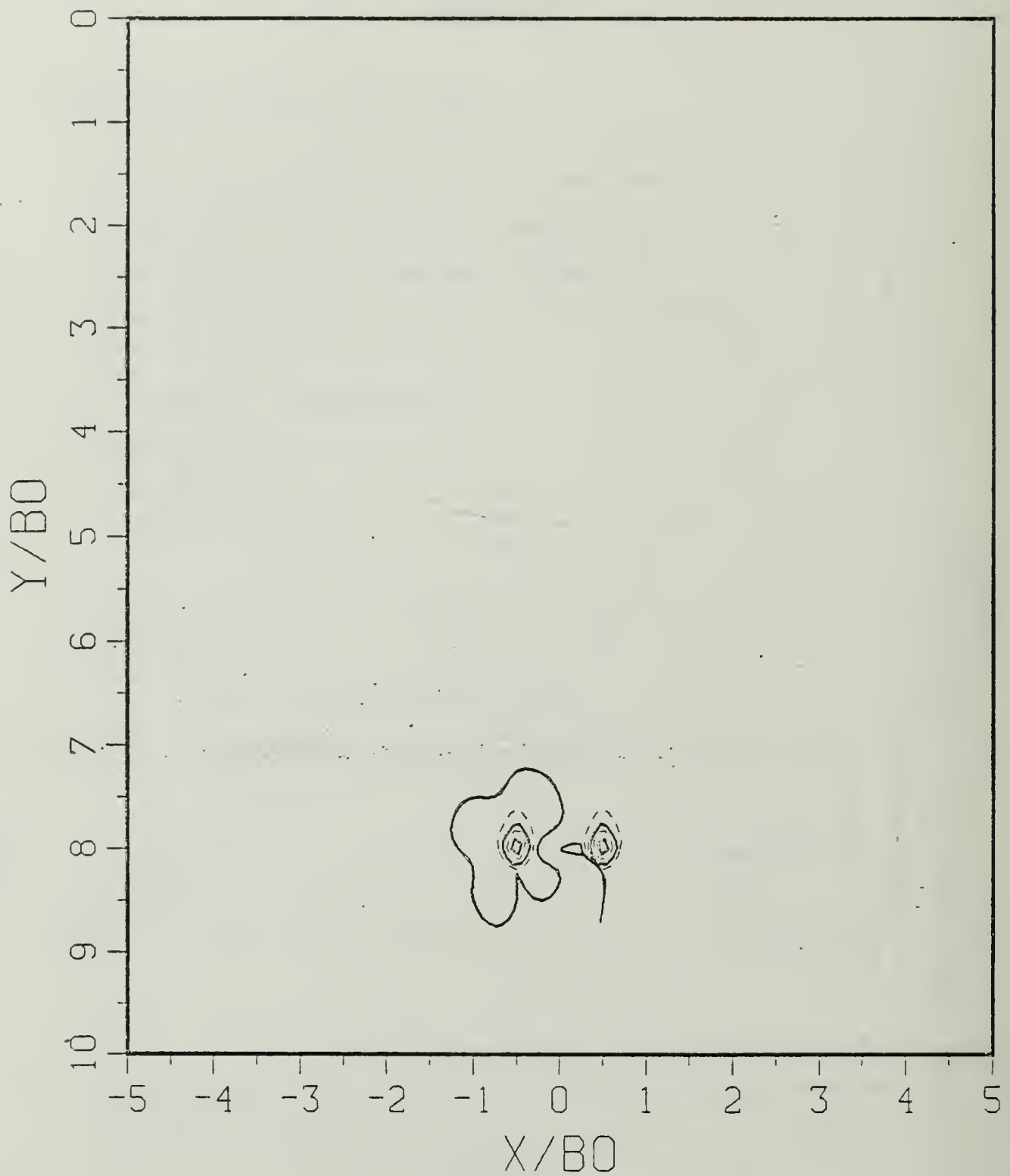


Figure B.1b Vorticity Field:  $SP = 0.00$ .

$$T^* = 0.59520$$

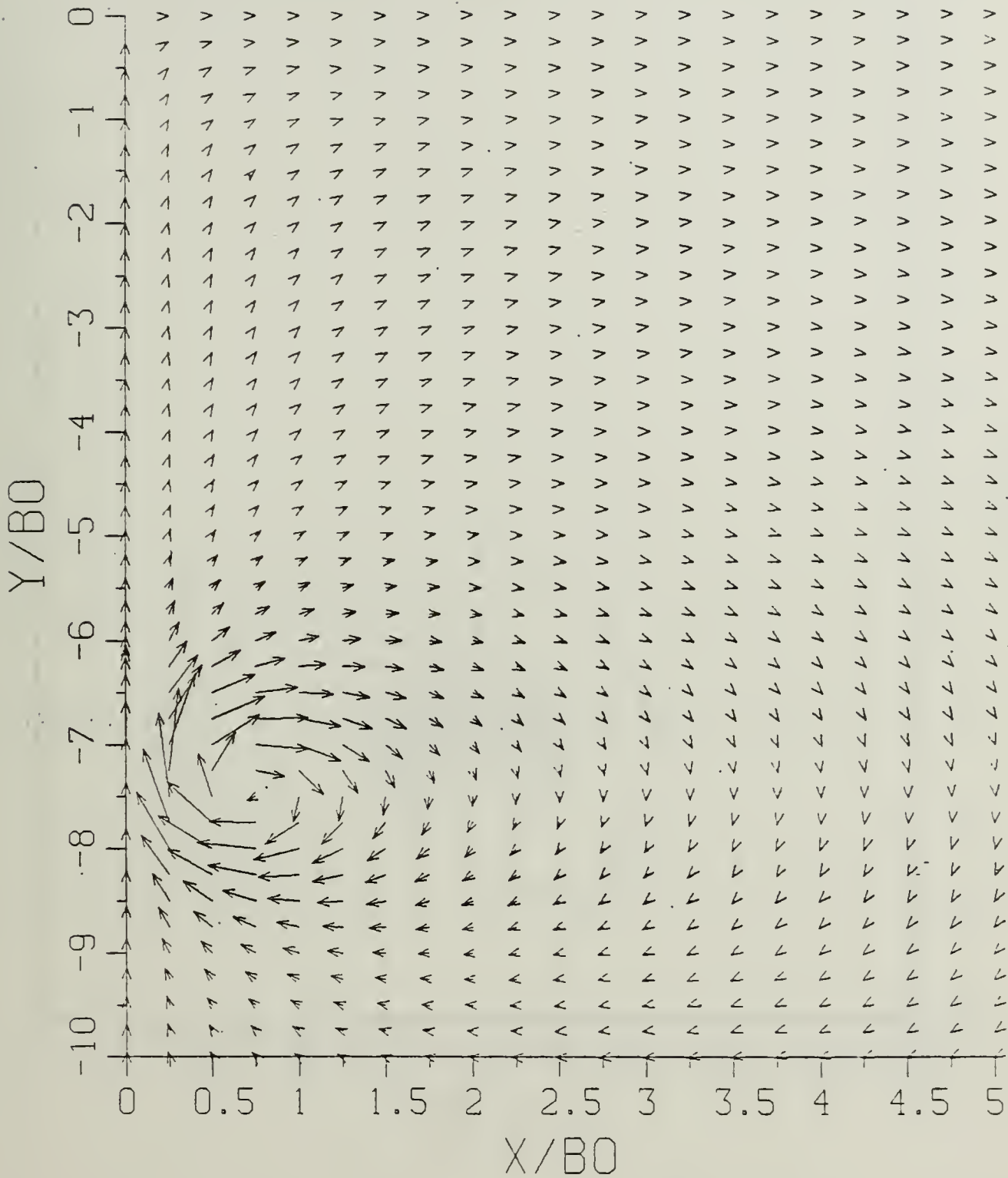


Figure B.2a Velocity Field: SP = 0.00.

$$T^* = 0.59520$$

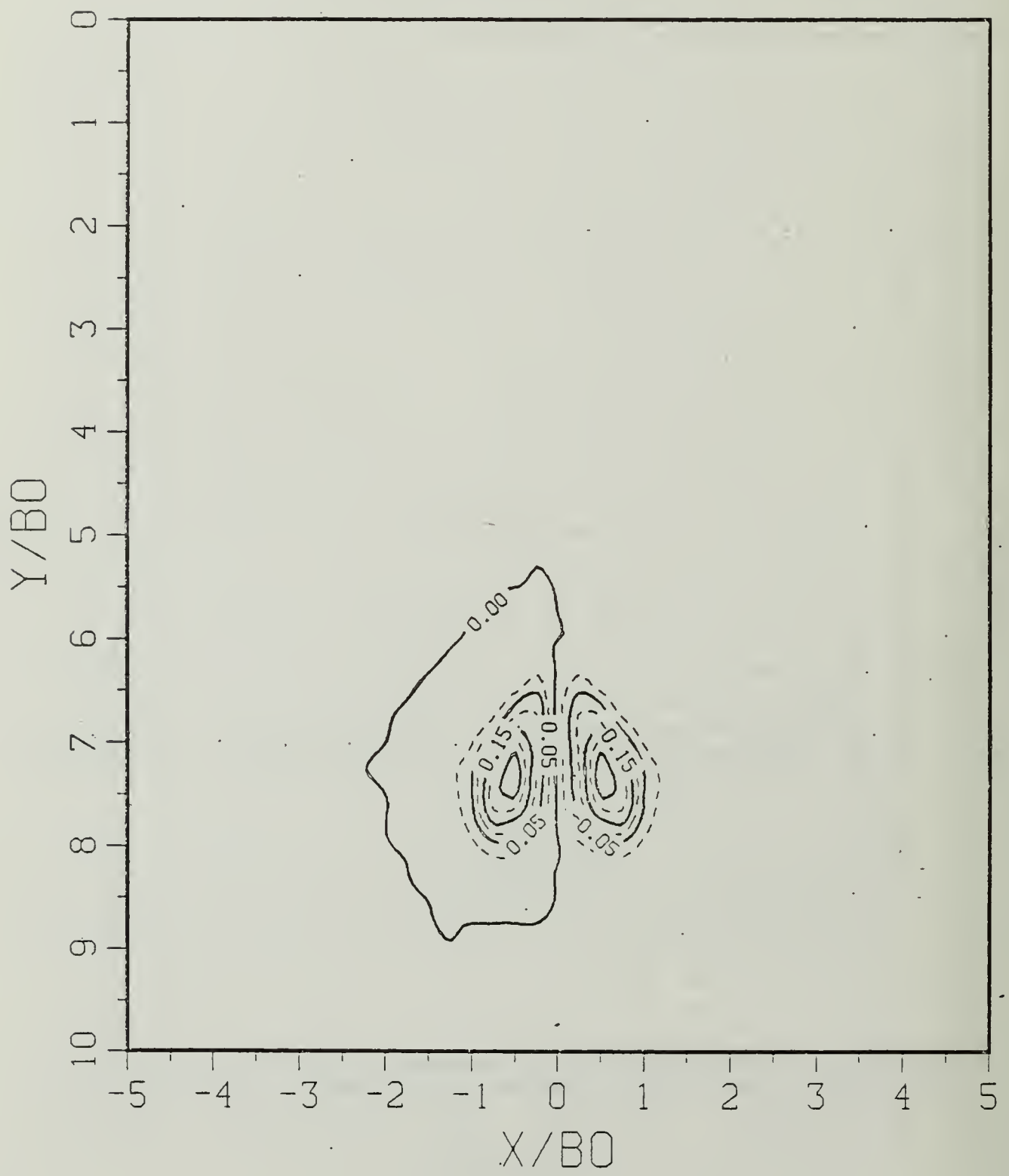


Figure B.2b Vorticity Field:  $SP = 0.00$ .

$$T^* = 1.19040$$

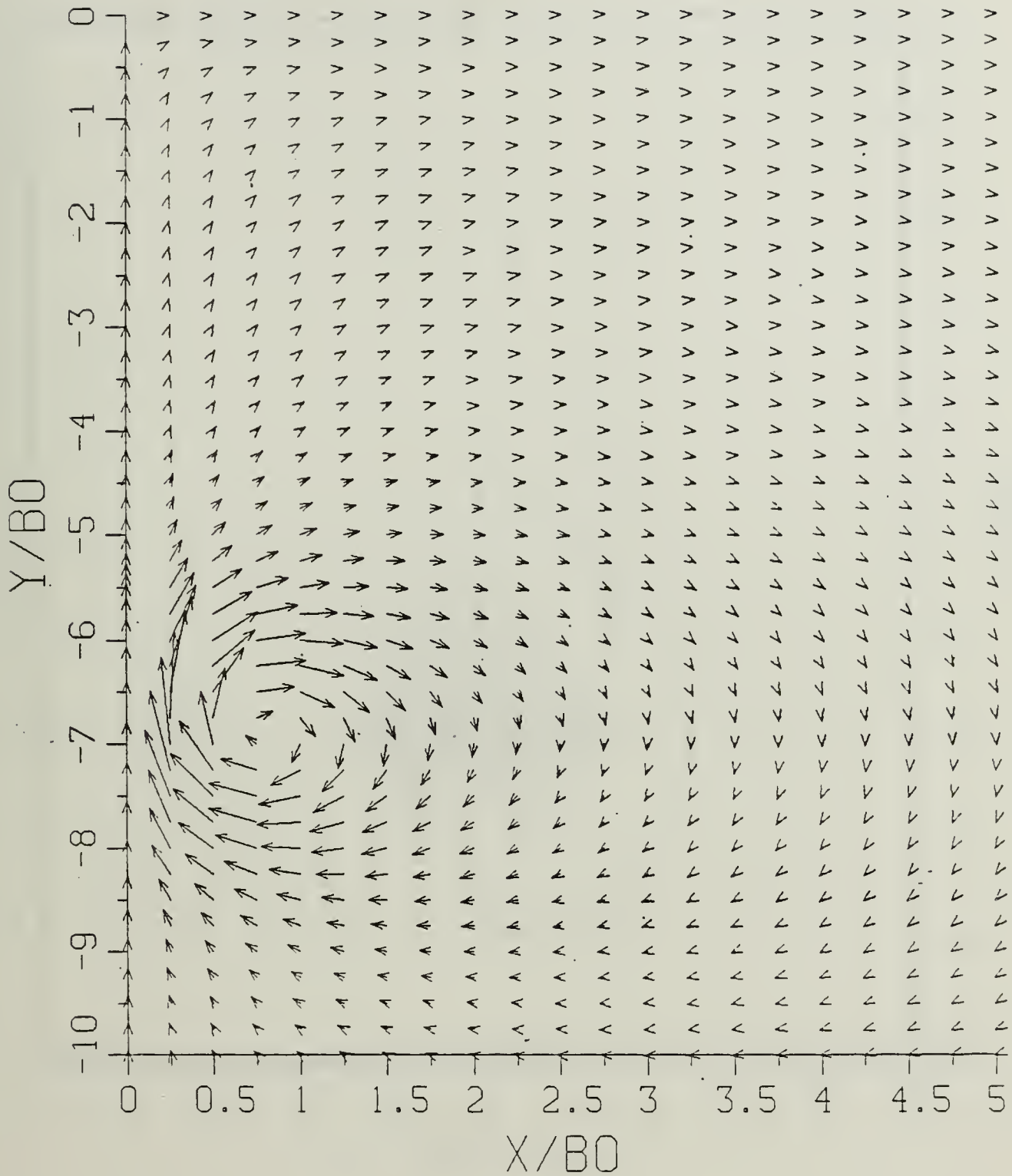


Figure B.3a Velocity Field: SP = 0.00.

$$\Gamma^* = 1.19040$$

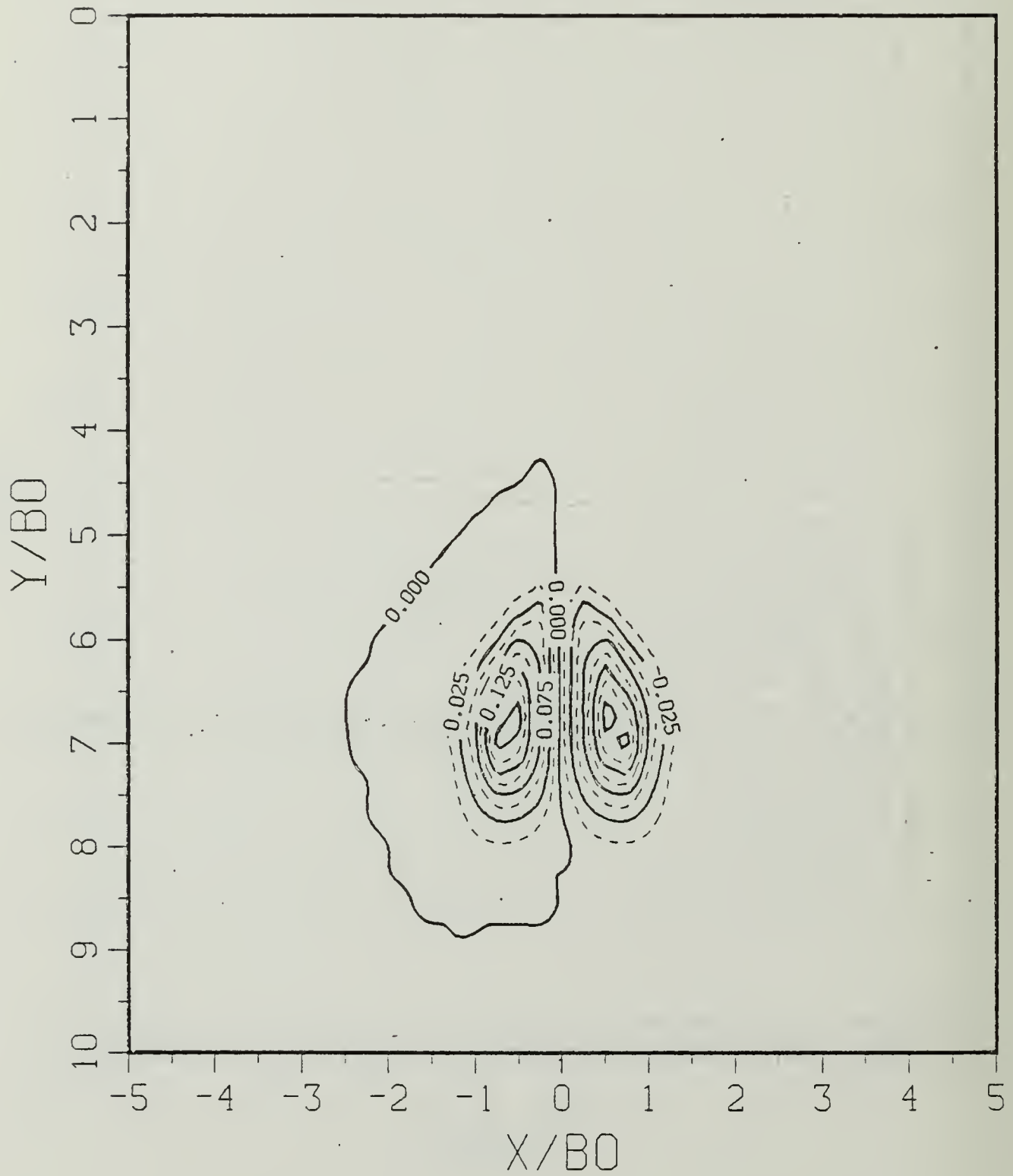


Figure B.3b Vorticity Field:  $SP = 0.00$ .

$$T^* = 1.78560$$

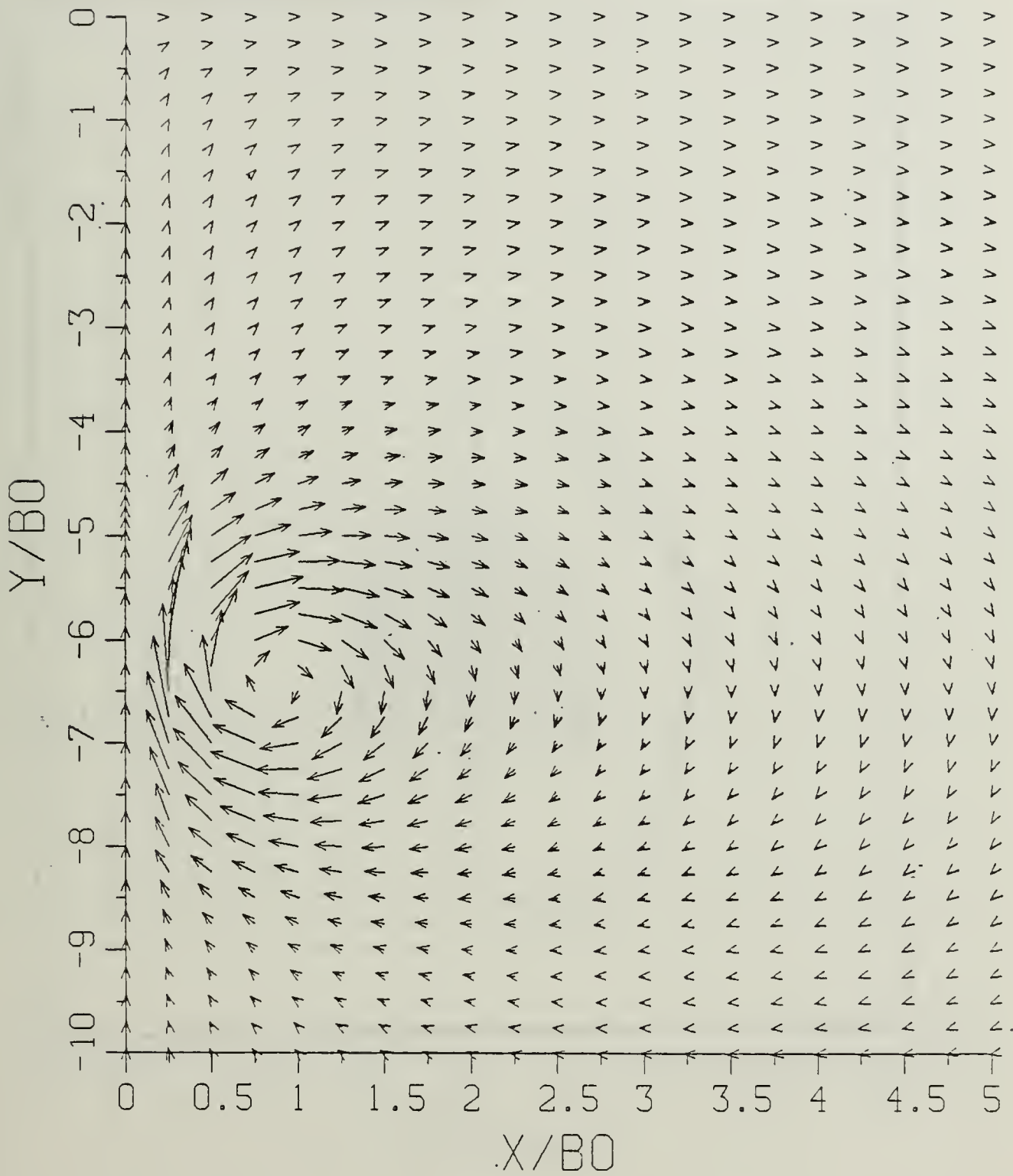


Figure B.4a Velocity Field: SP = 0.00.

$$T^* = 1.78560$$

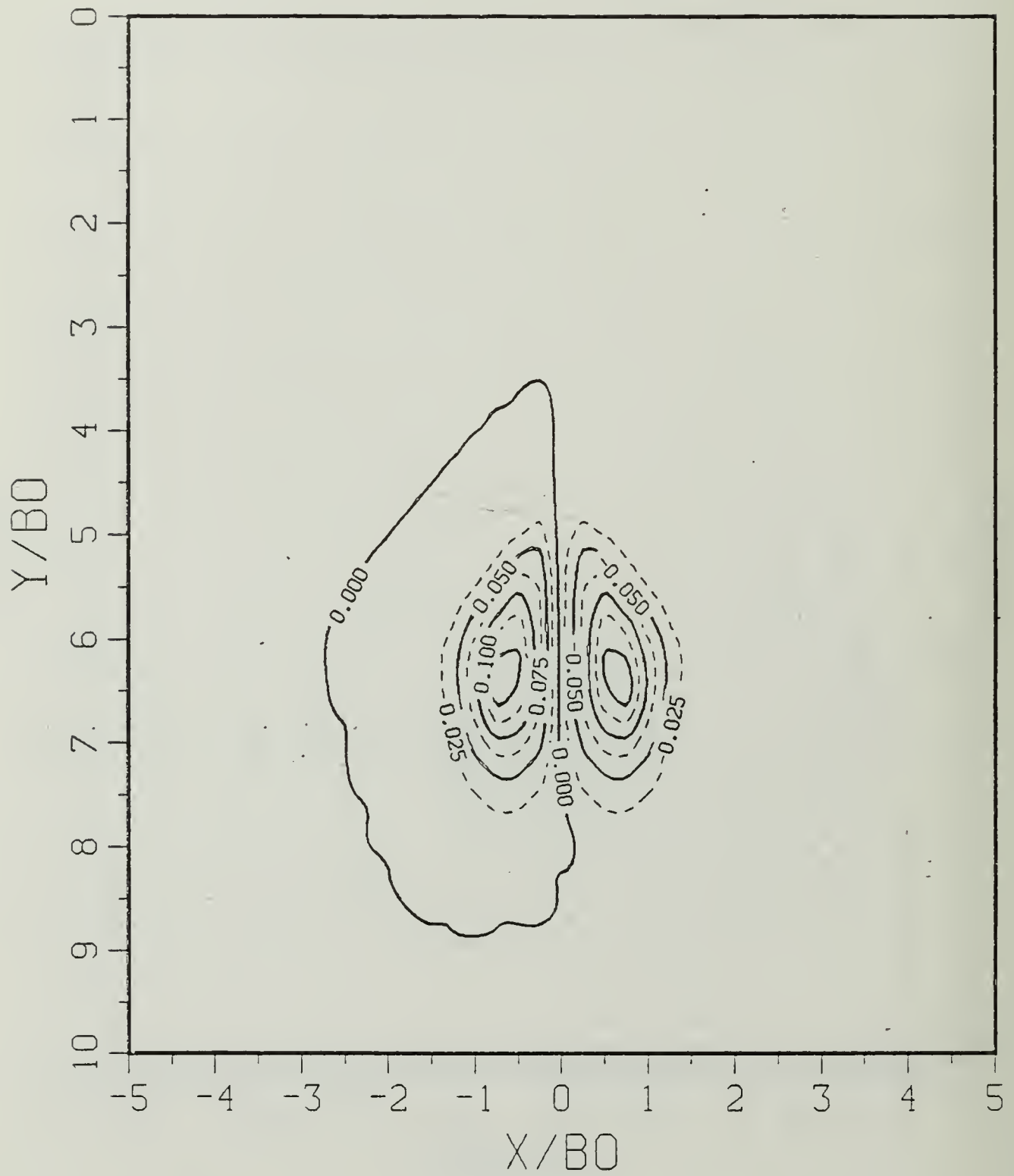


Figure B.4b Vorticity Field: SP = 0.00.

$$T^* = 2.38080$$

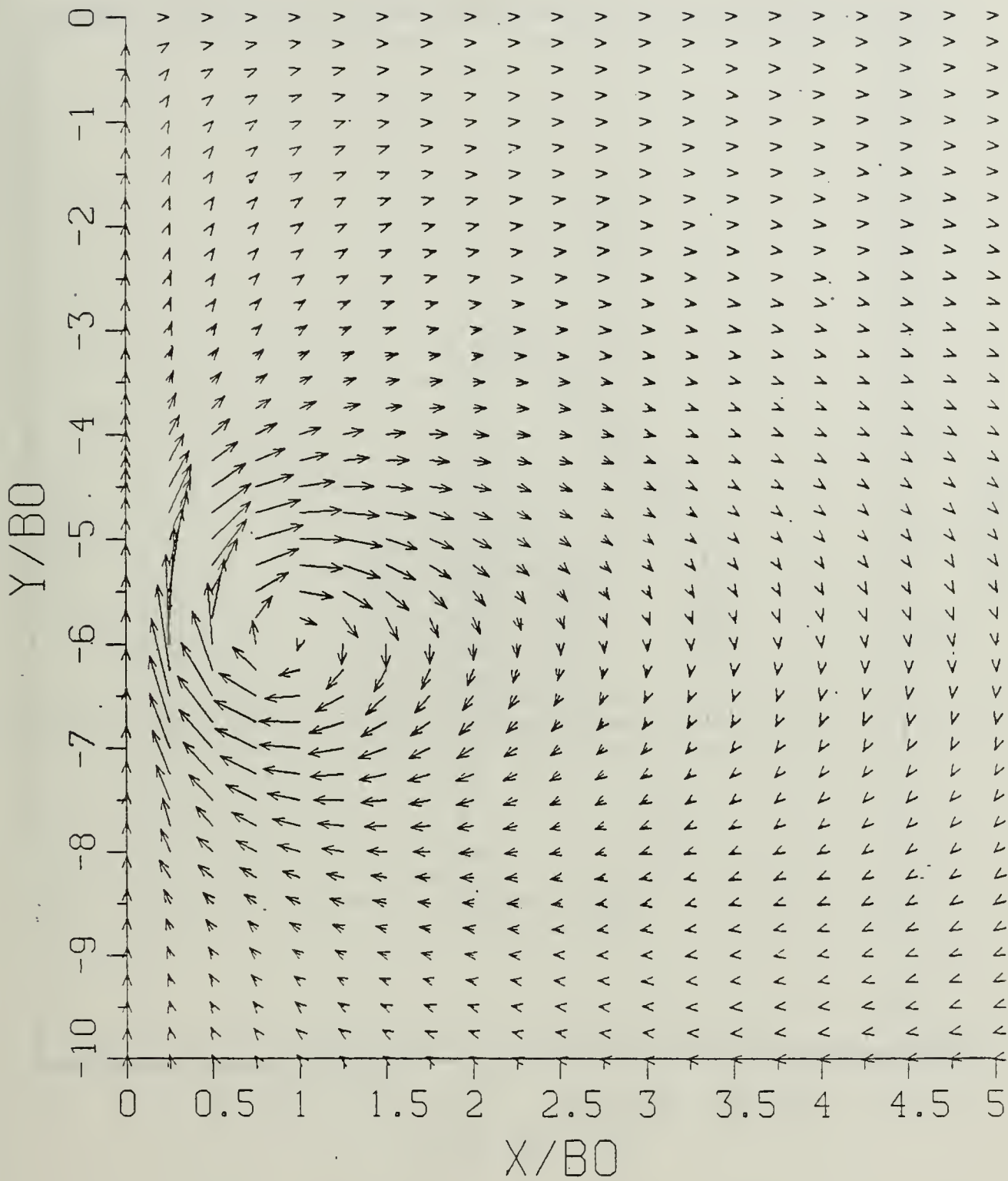


Figure B.5a Velocity Field: SP = 0.00.

$$T^* = 2.38080$$

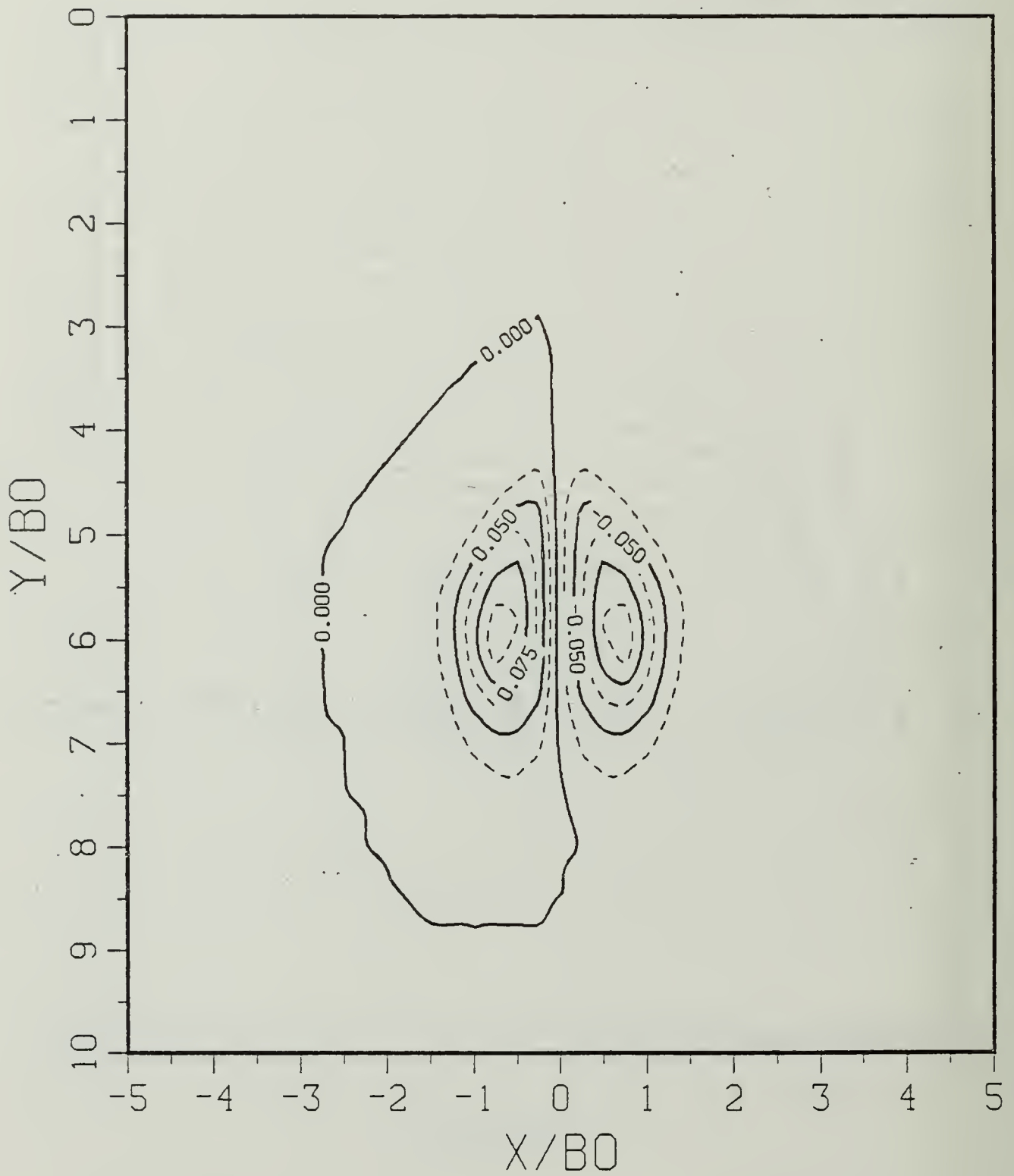


Figure B.5b Vorticity Field: SP = 0.00.

$$T^* = 2.97600$$

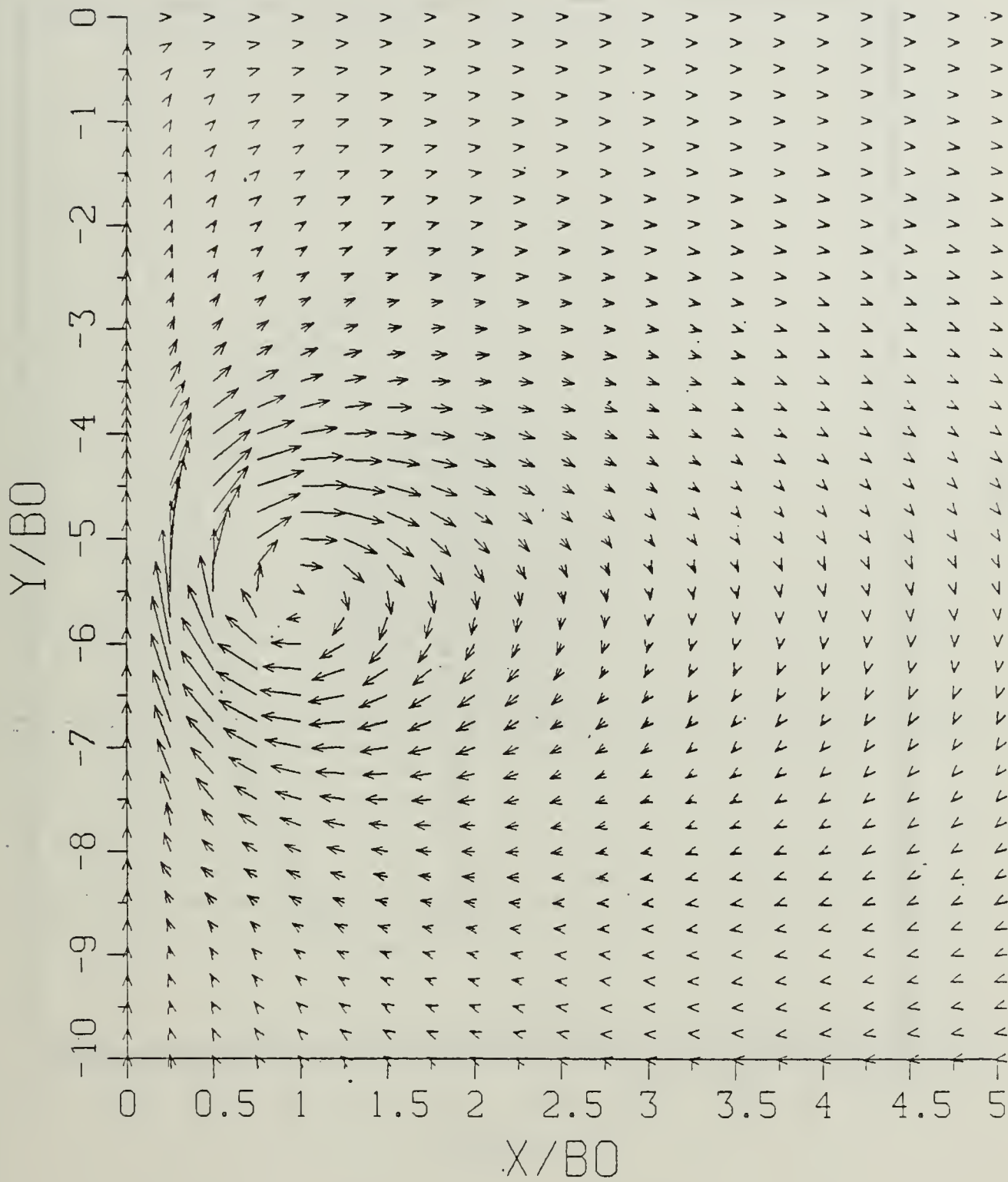


Figure B.6a Velocity Field:  $SP = 0.00$ .

$$T^* = 2.97600$$

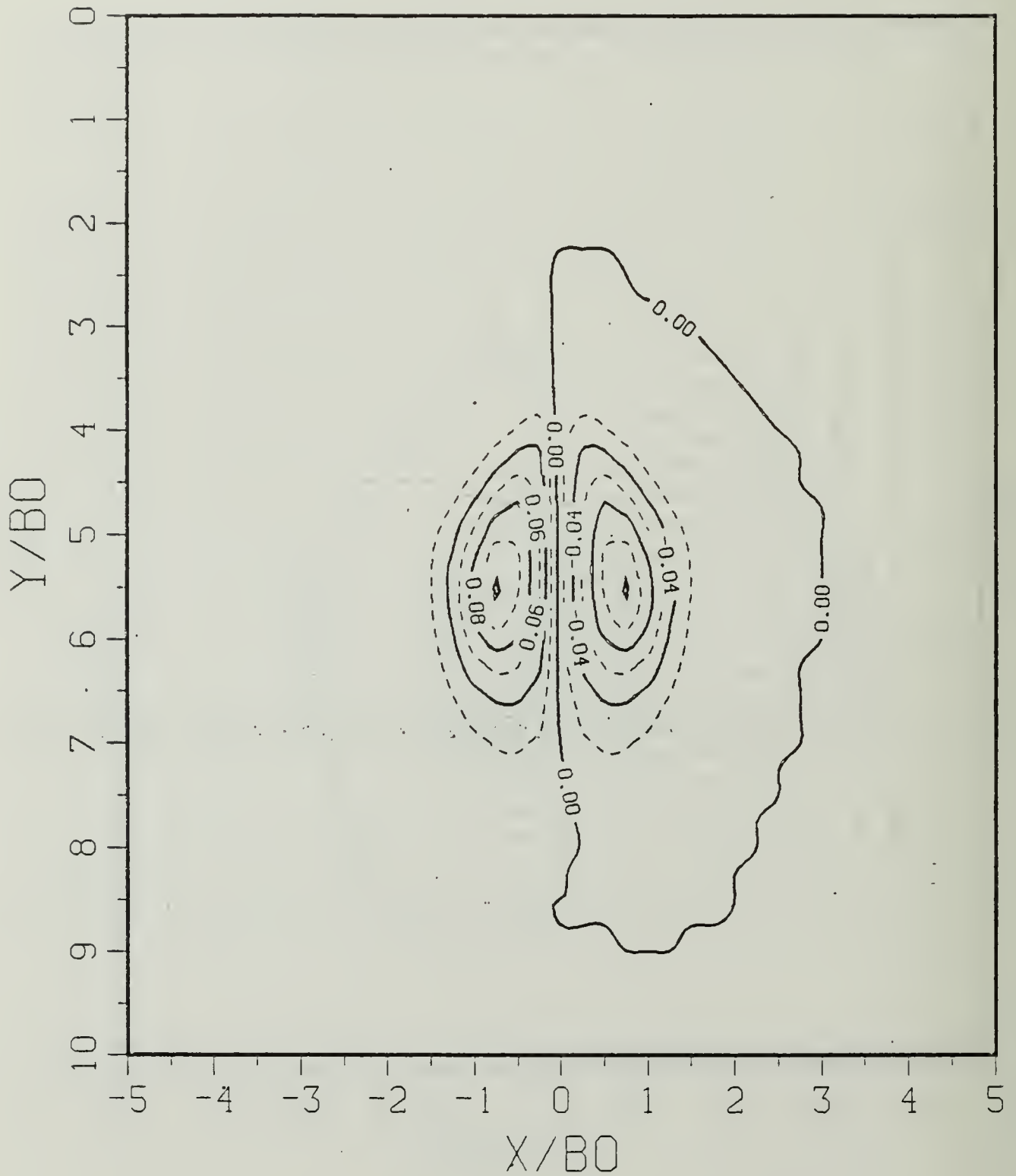


Figure B.6b Vorticity Field:  $SP = 0.00$ .

$$\Gamma^* = 3.57120$$

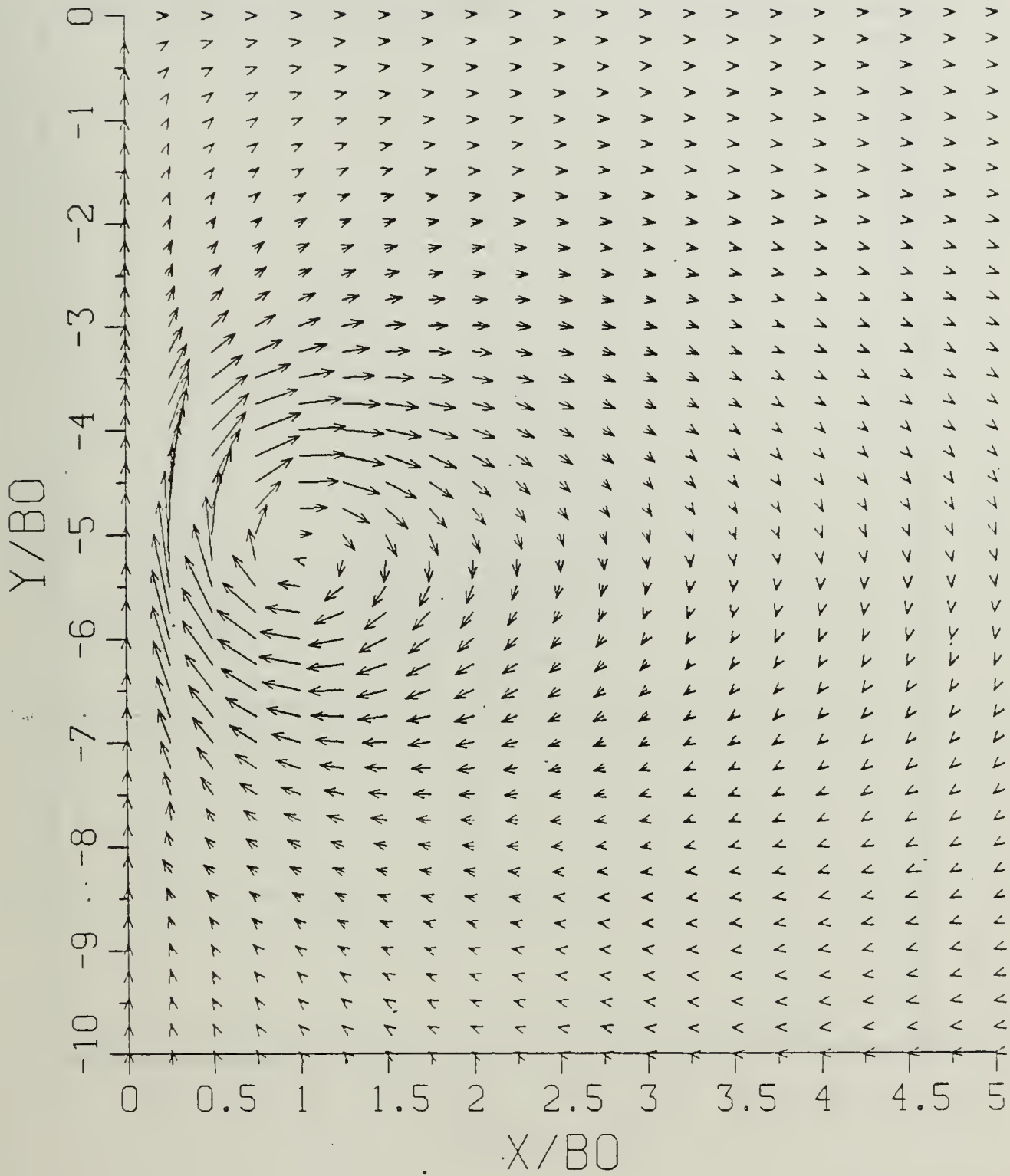


Figure B.7a Velocity Field:  $SP = 0.00$ .

$$T^* = 3.57120$$

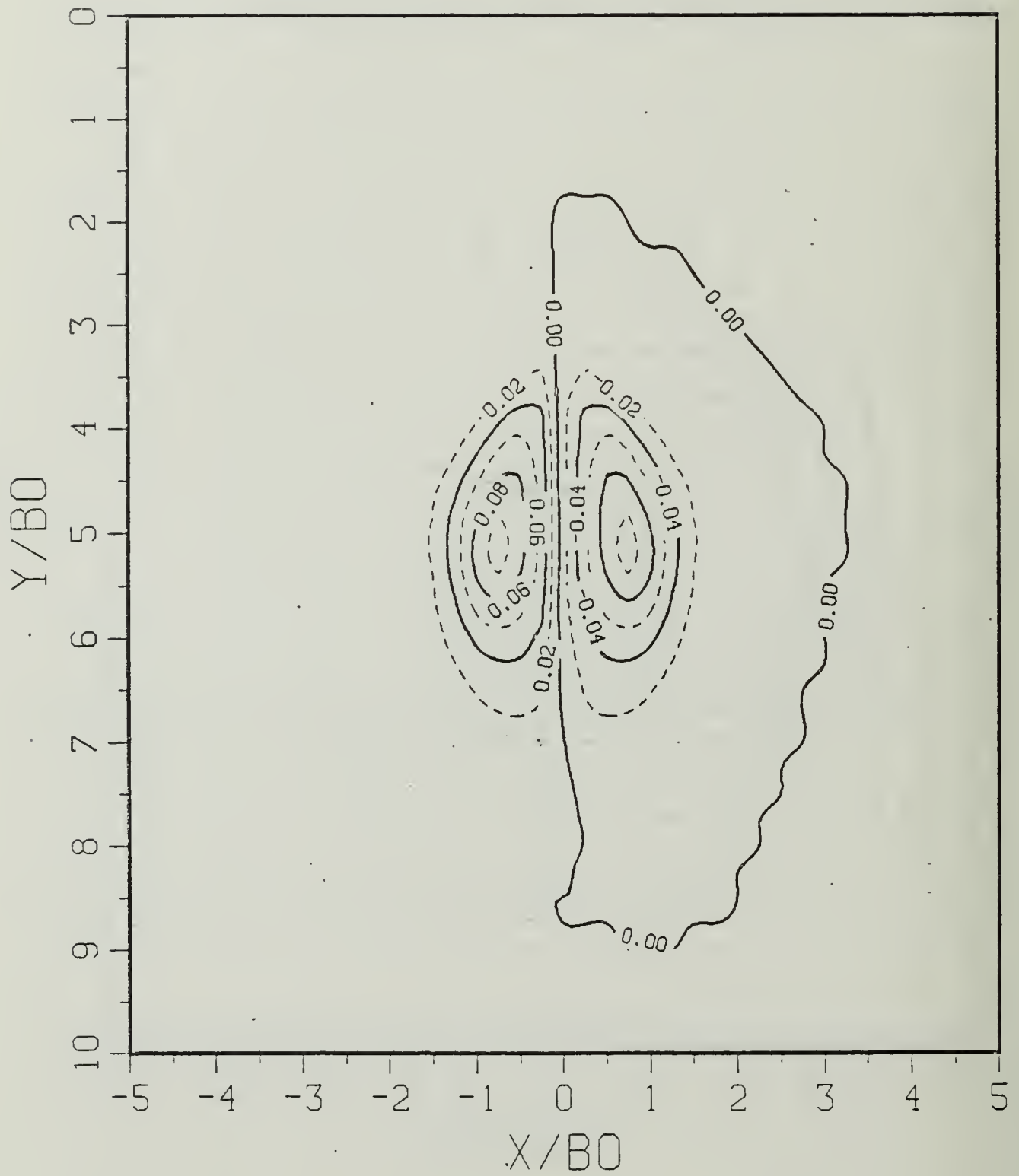


Figure B.7b Vorticity Field: SP = 0:00.

$$T^* = 4.16640$$

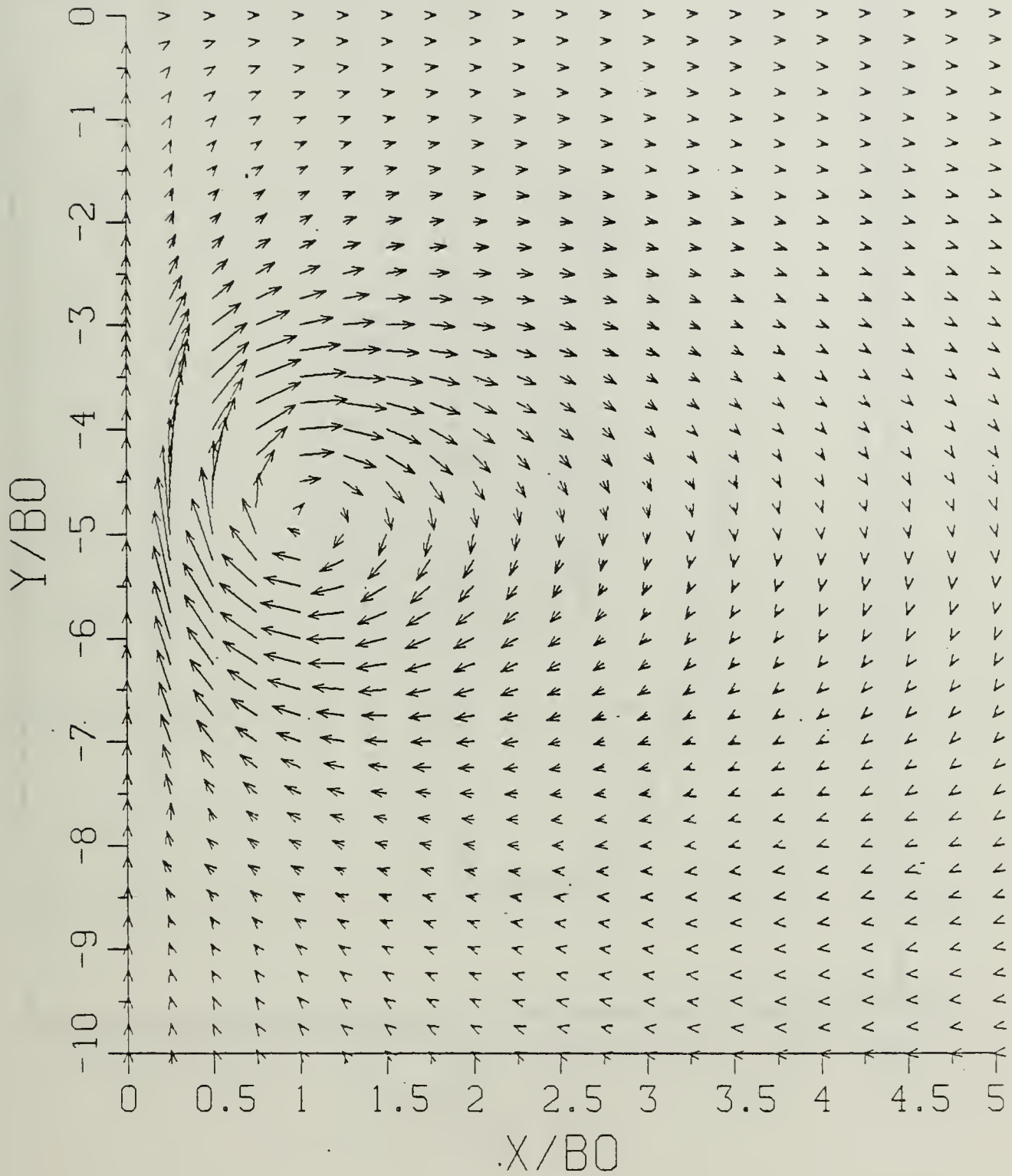


Figure B.8a Velocity Field:  $SP = 0.00$ .

$$T^* = 4.16640$$

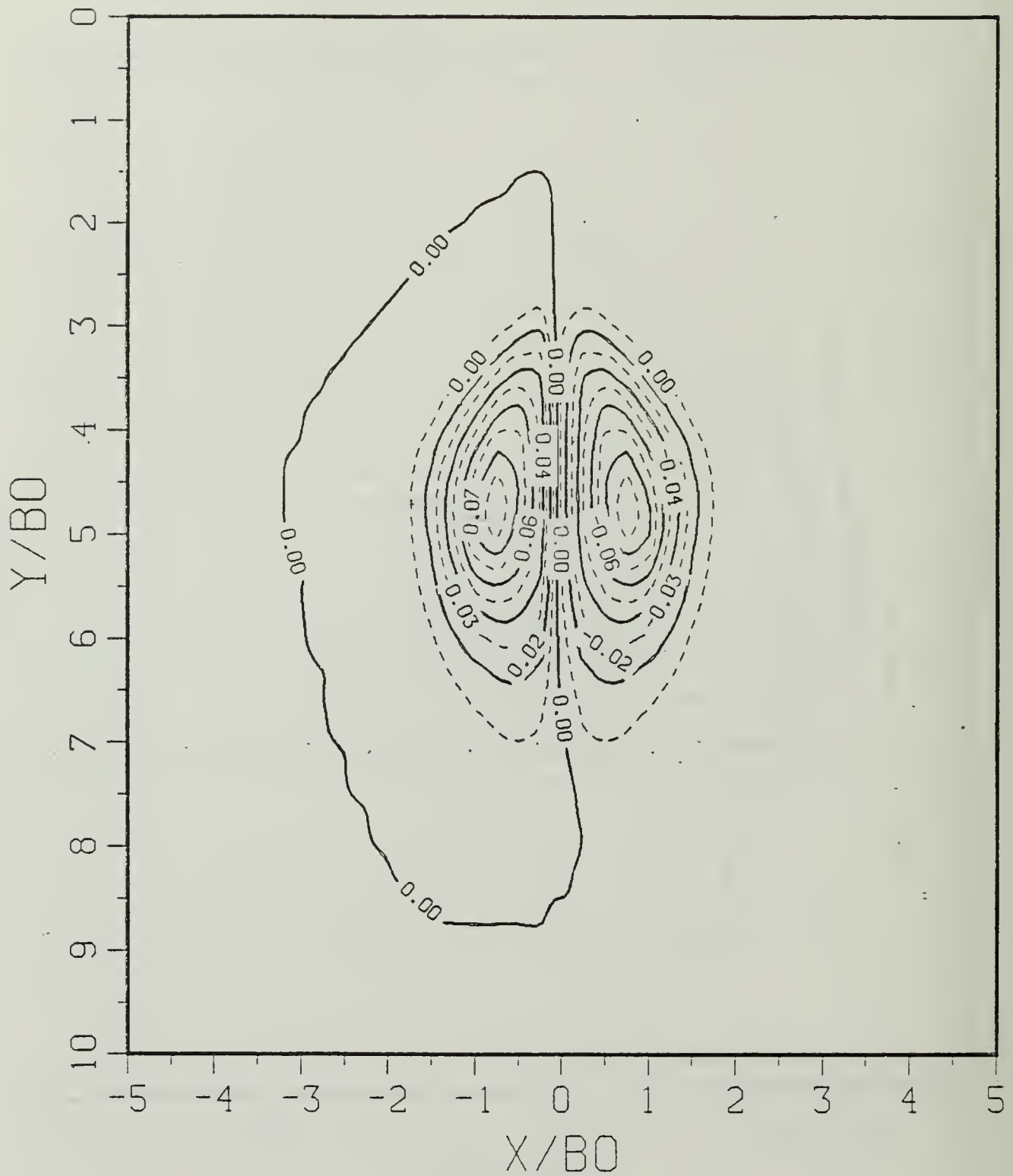


Figure B.8b Vorticity Field:  $SP = 0.00$ .

$$T^* = 4.76160$$

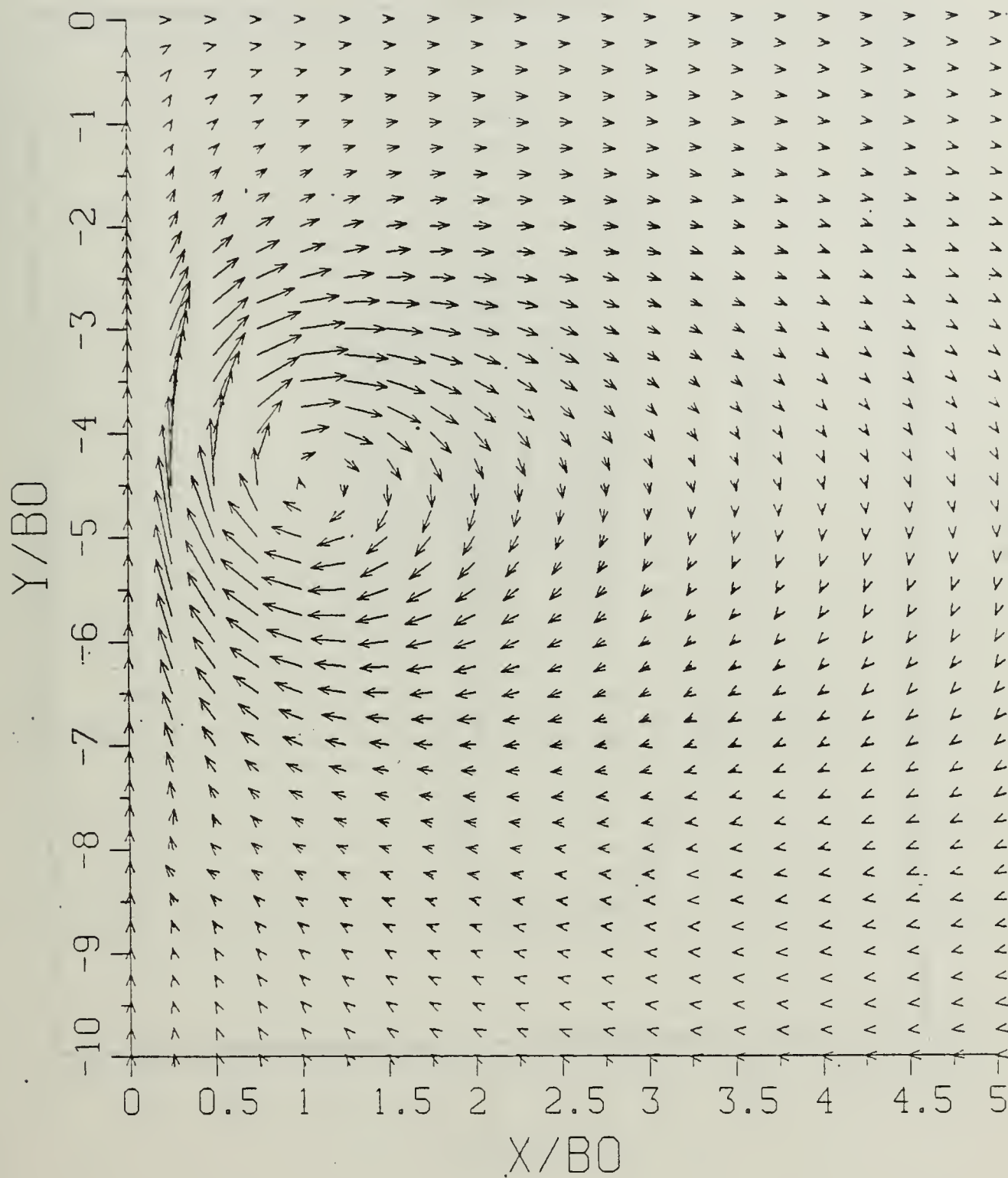


Figure B.9a Velocity Field: SP = 0.00.

$$\Gamma^* = 4.76160$$

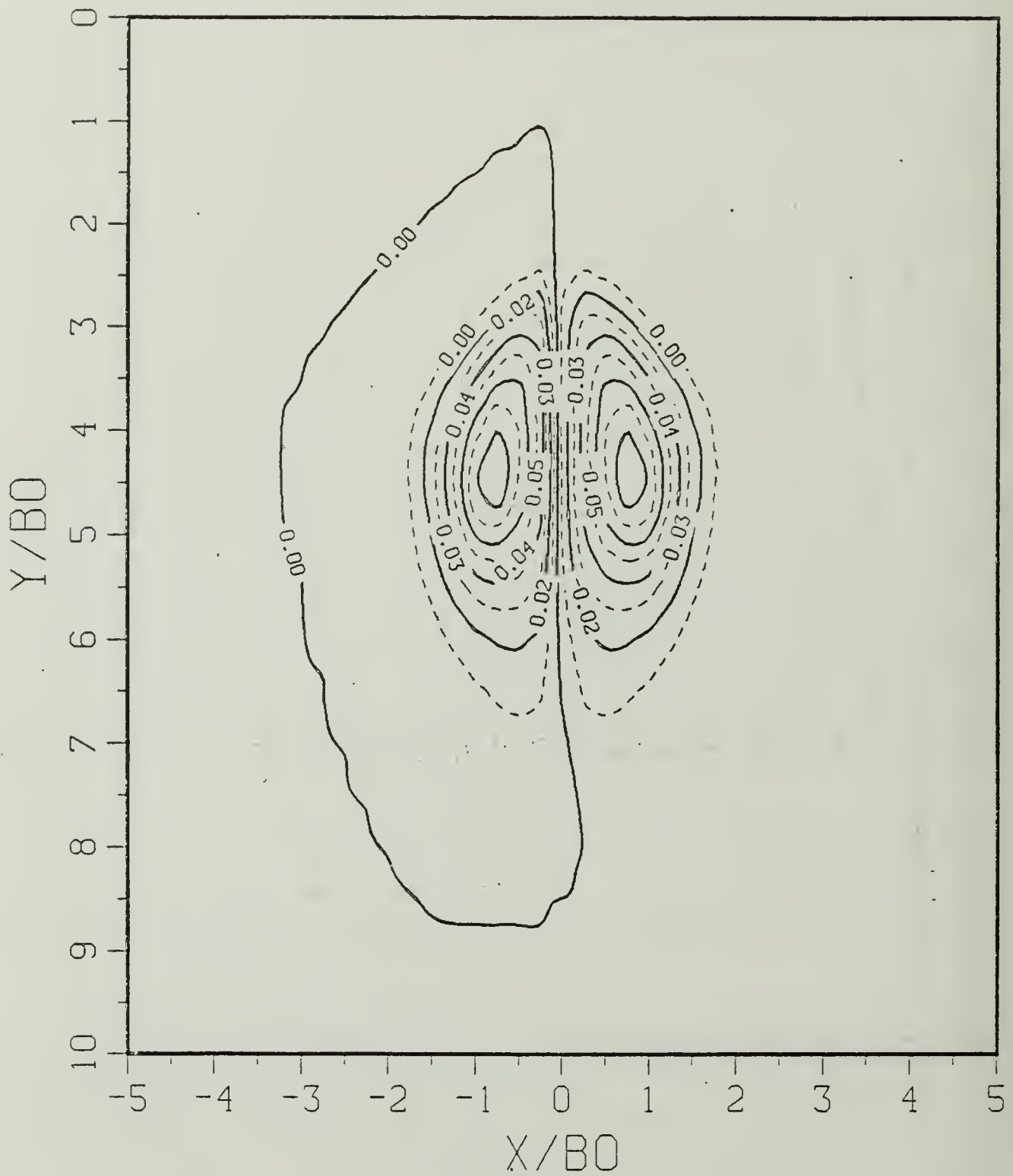


Figure B.9b Vorticity Field:  $SP = 0.00$ .

$$T^* = 5.35680$$

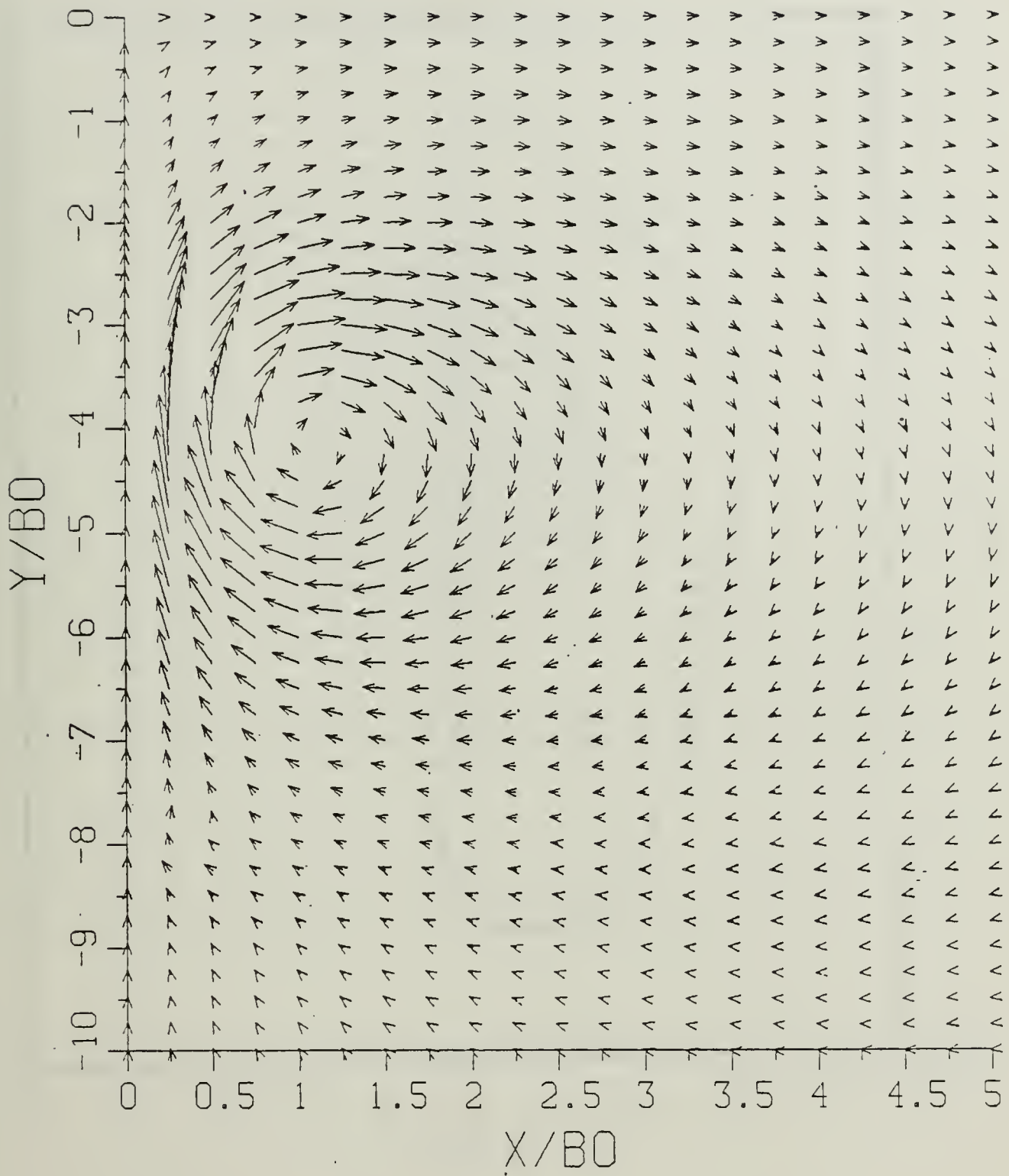


Figure B.10a Velocity Field: SP = 0.00.

$$\Gamma^* = 5.35680$$

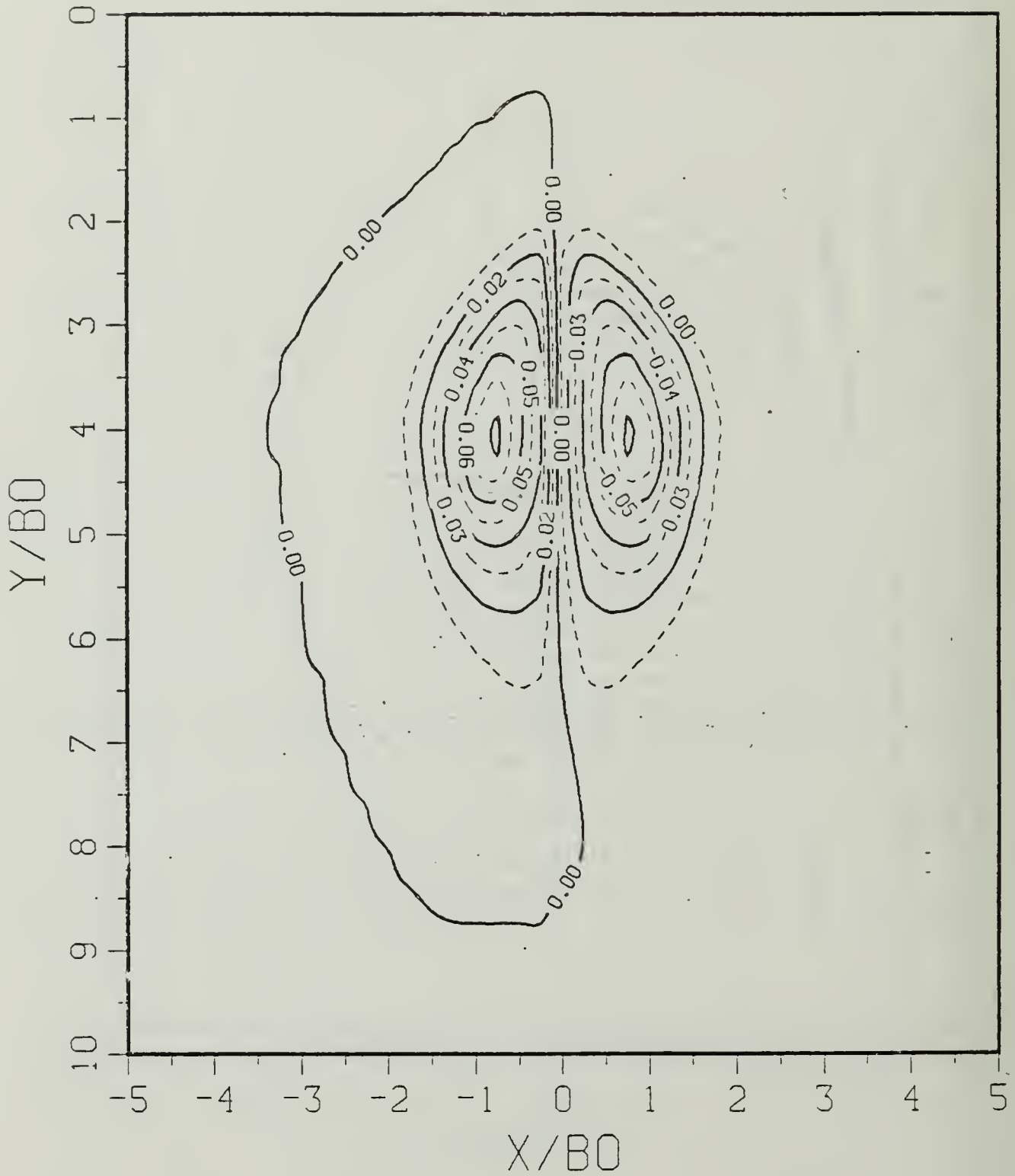


Figure B.10b Vorticity Field:  $SP = 0.00$ .

$$T^* = 5.95200$$

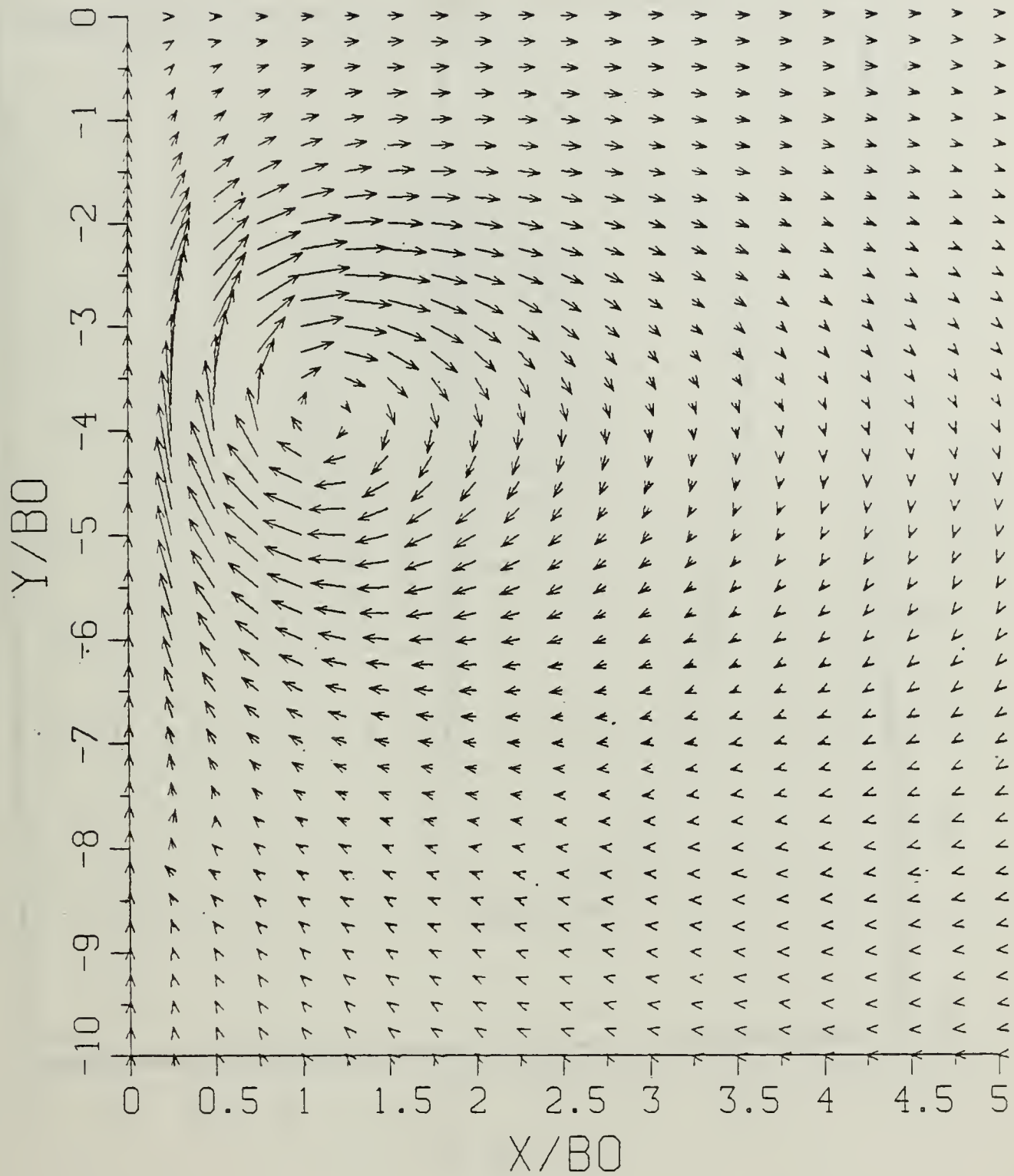


Figure B.11a Velocity Field:  $SP = 0.00$ .

$$T^* = 5.95200$$

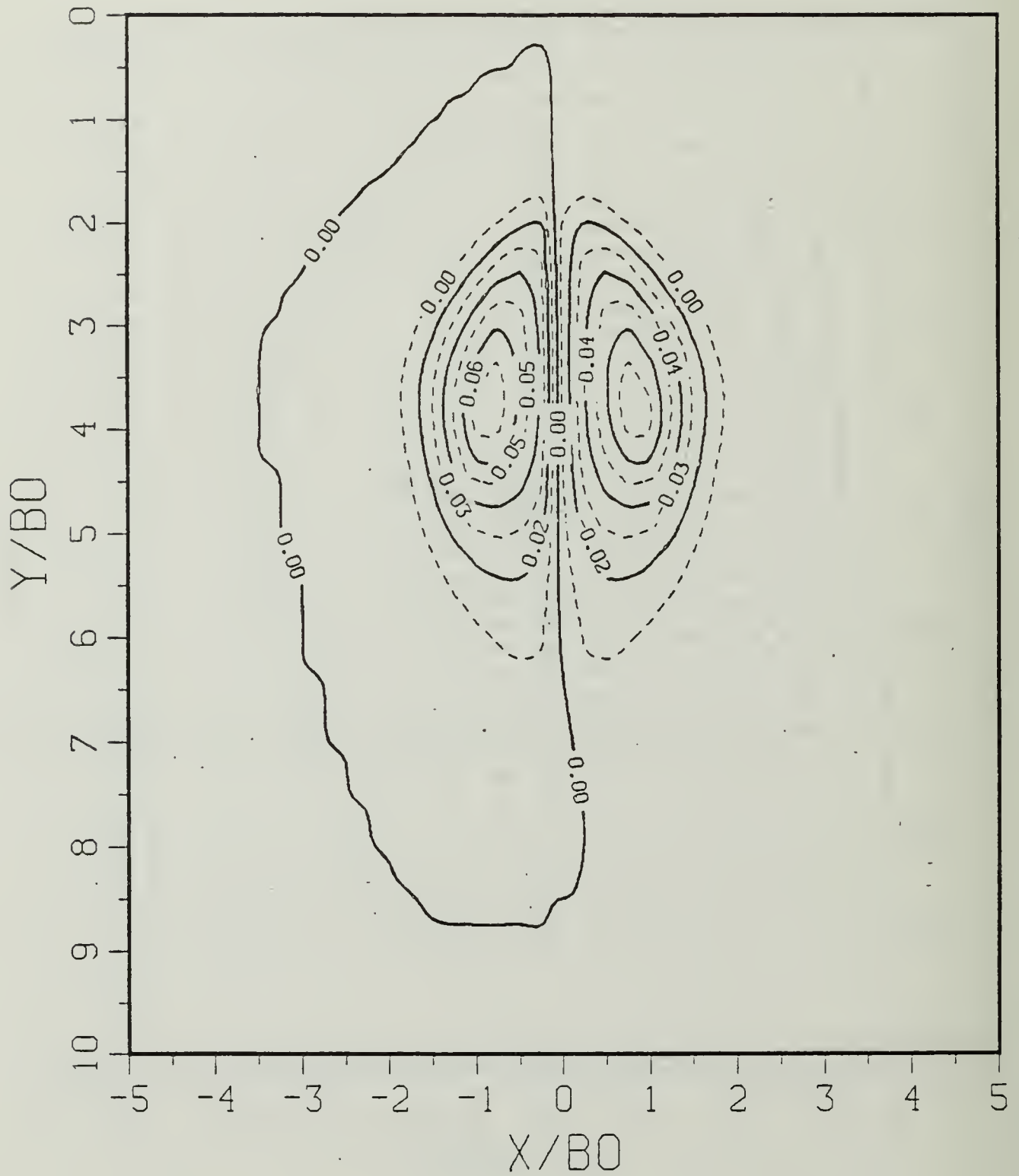


Figure B.11b Vorticity Field:  $SP = 0.00$ .

$$T^* = 6.54720$$

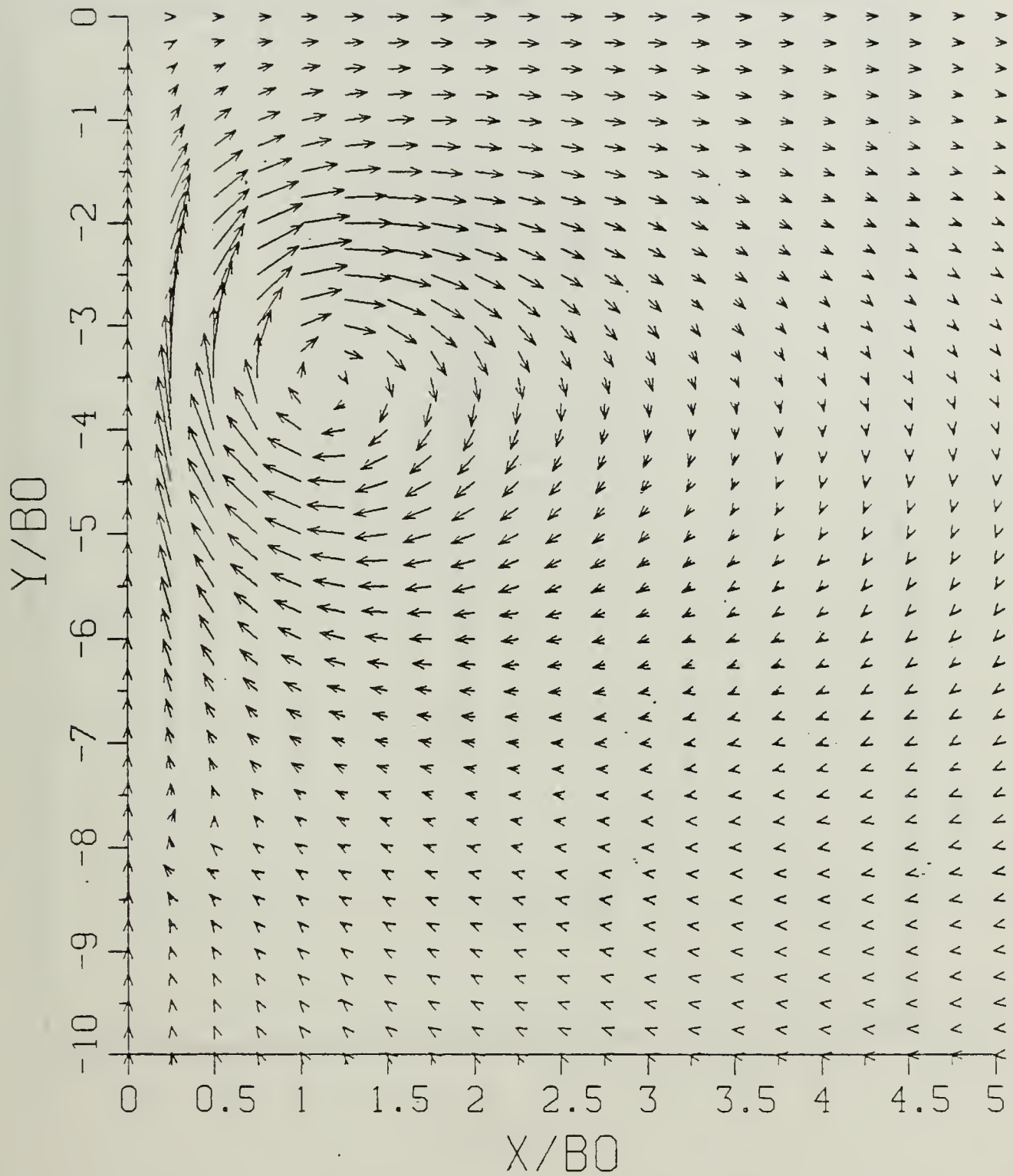


Figure B.12a Velocity Field: SP = 0.00.

$$T^* = 6.54720$$

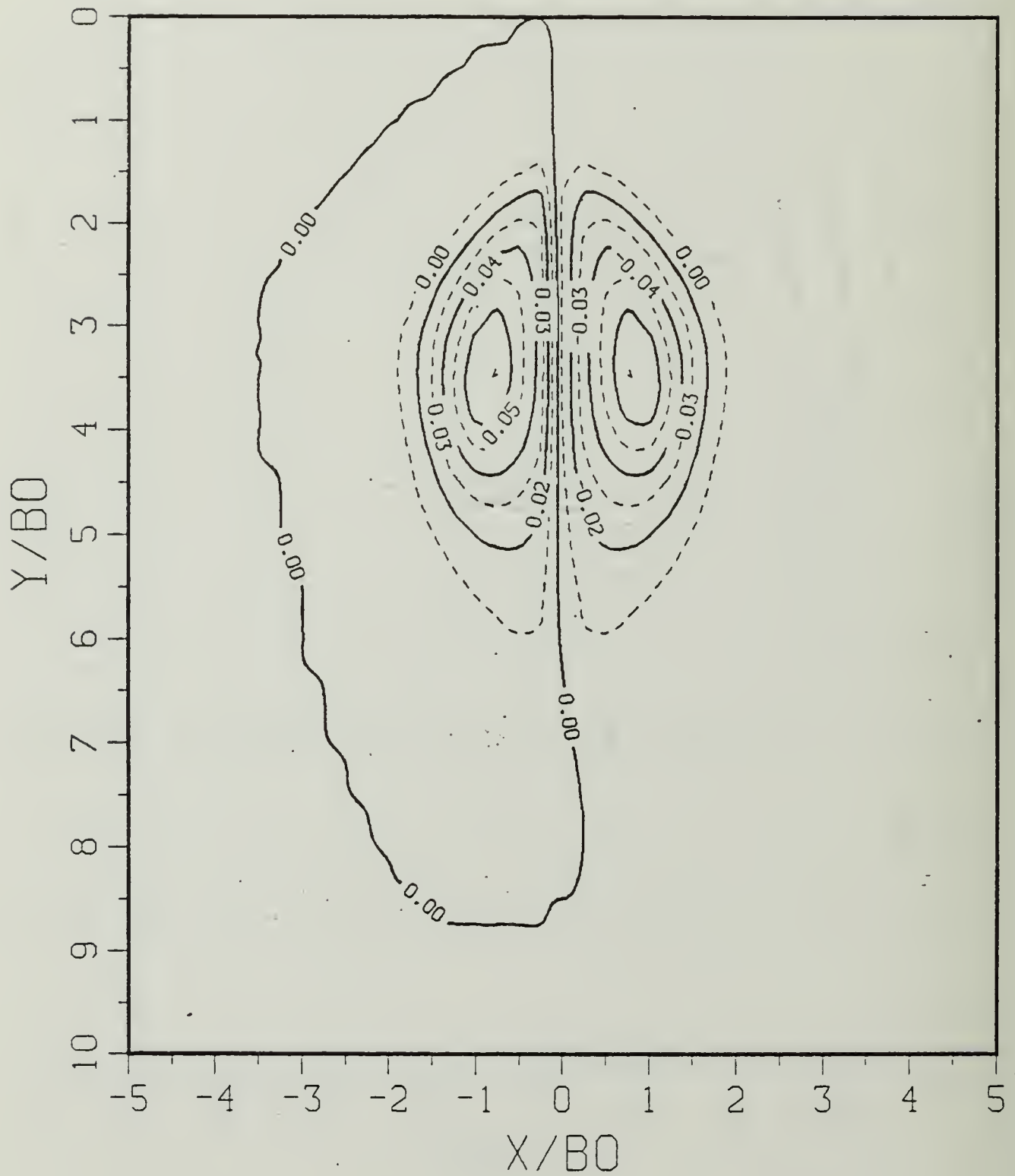


Figure B.12b Vorticity Field:  $SP = 0.00$ .

$$T^* = 7.14240$$

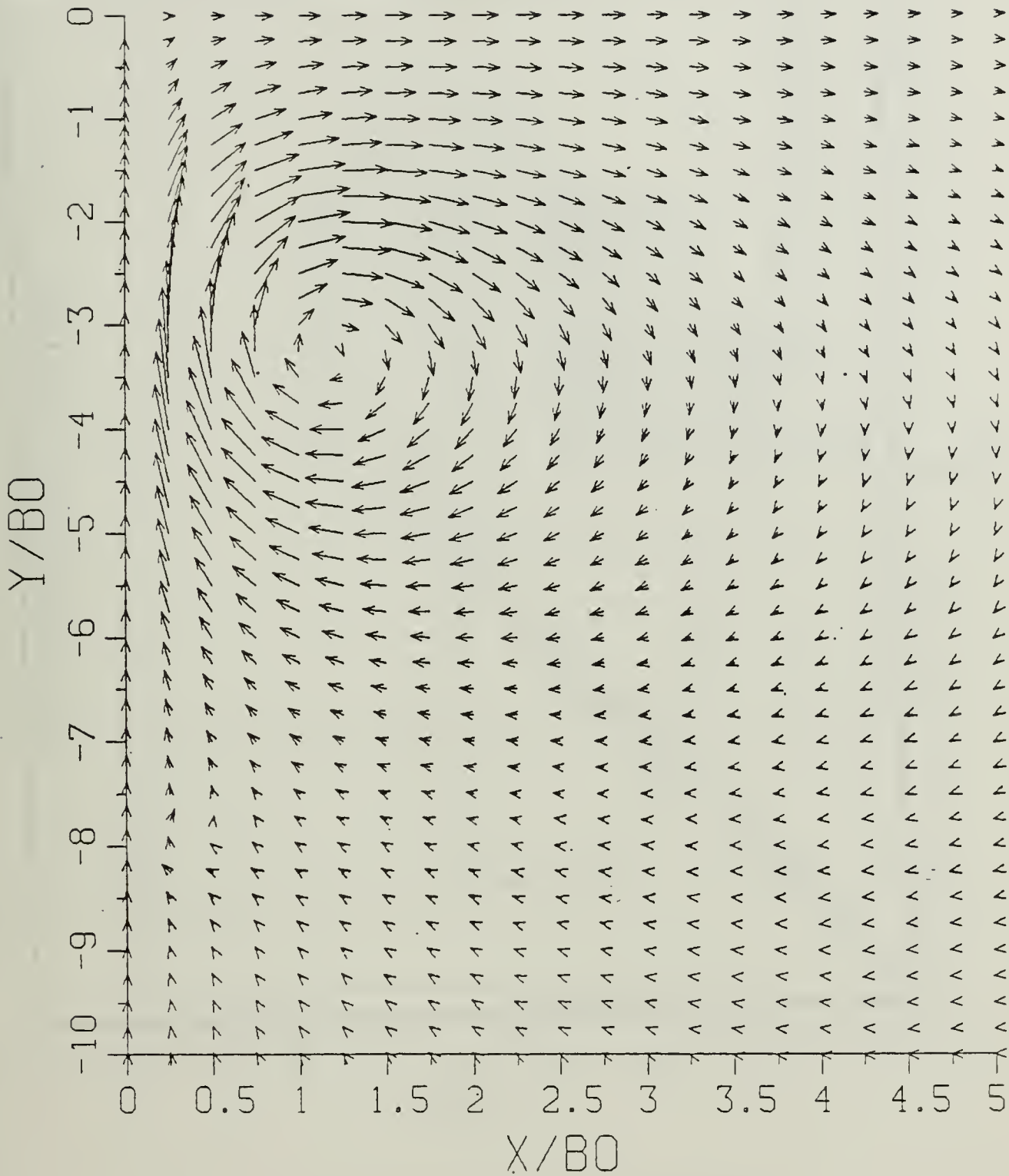


Figure B.13a Velocity Field:  $SP = 0.00$ .

$$T^* = 7.14240$$

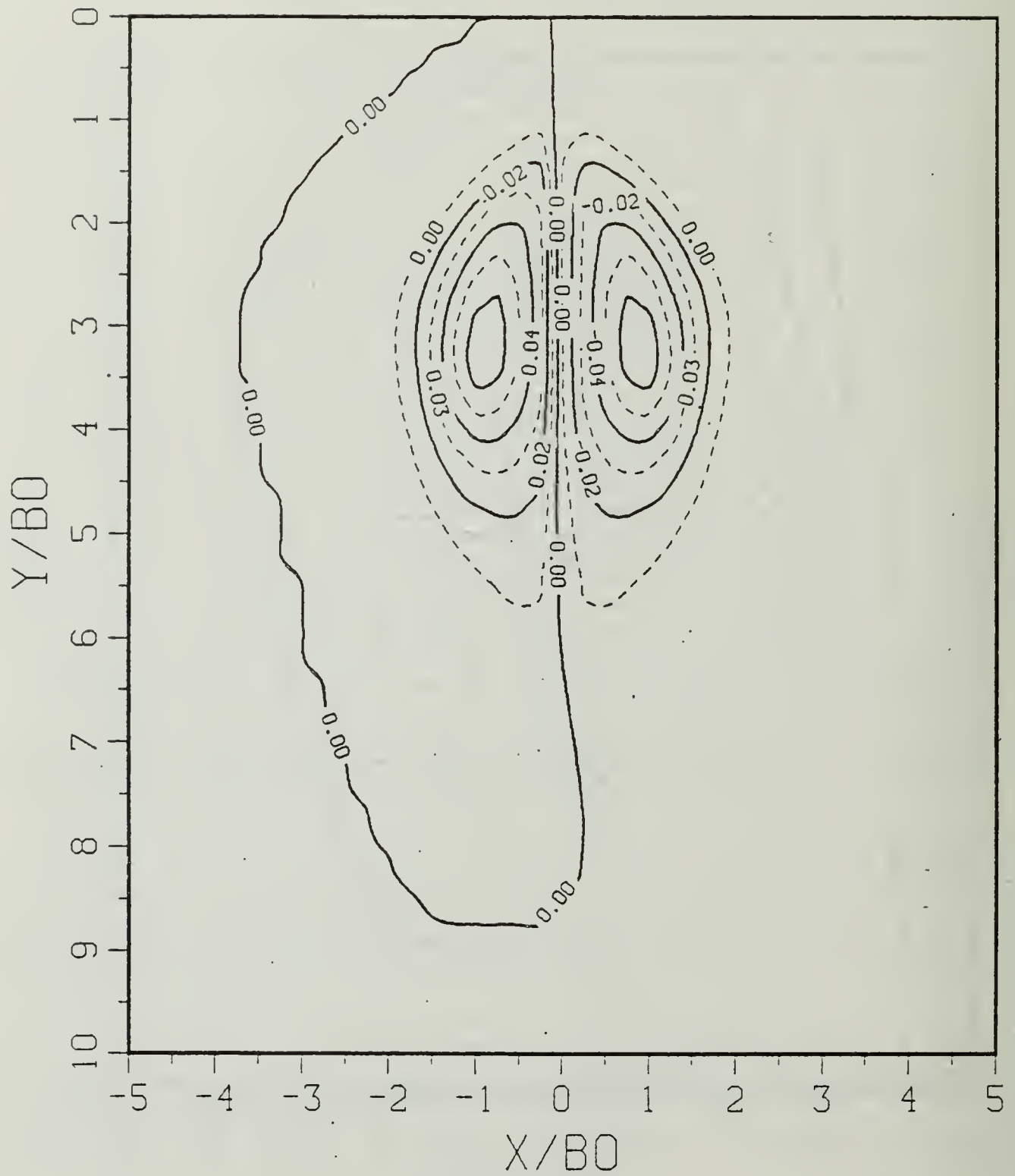


Figure B.13b Vorticity Field:  $SP = 0.00$ .

$T^*$  VS  $H/B_0$  ( $SP=0.00$ )

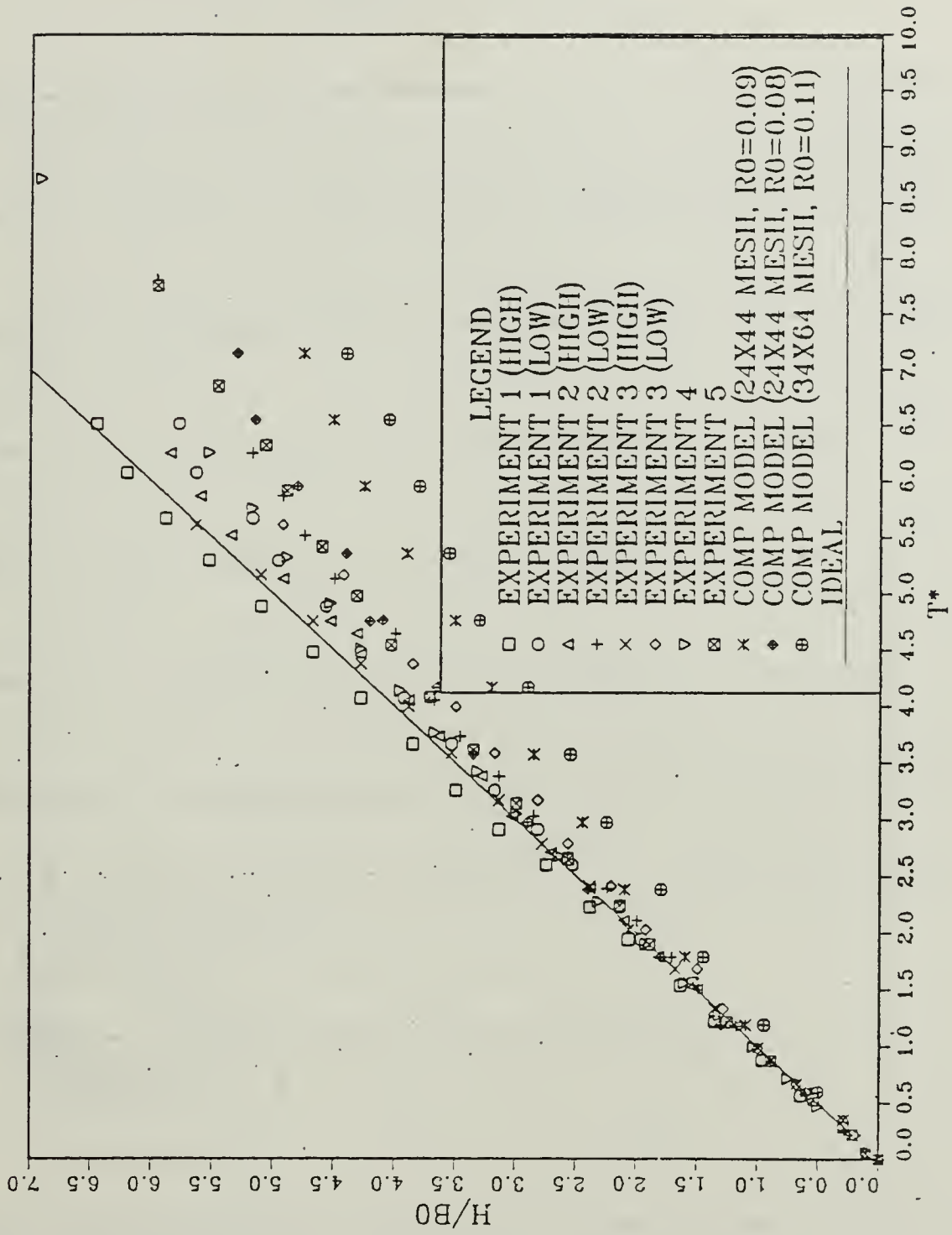


Figure B.14 Experimental and Numerical Results for Various Initial Core Radii.

$$T^* = 0.01719$$

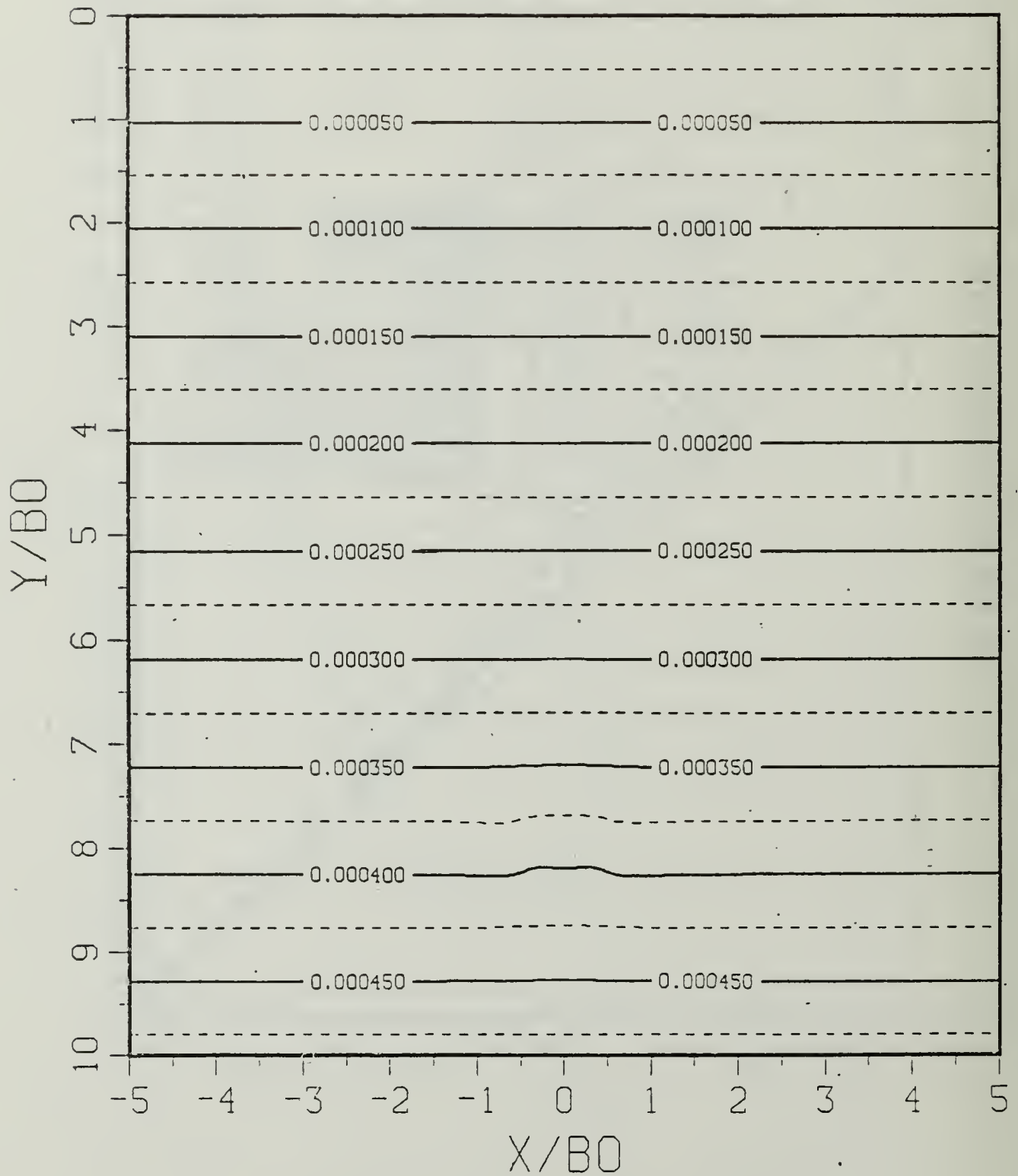


Figure B.15a Constant Density Contours:  $SP = 1.00$ .

$$T^* = 0.01719$$

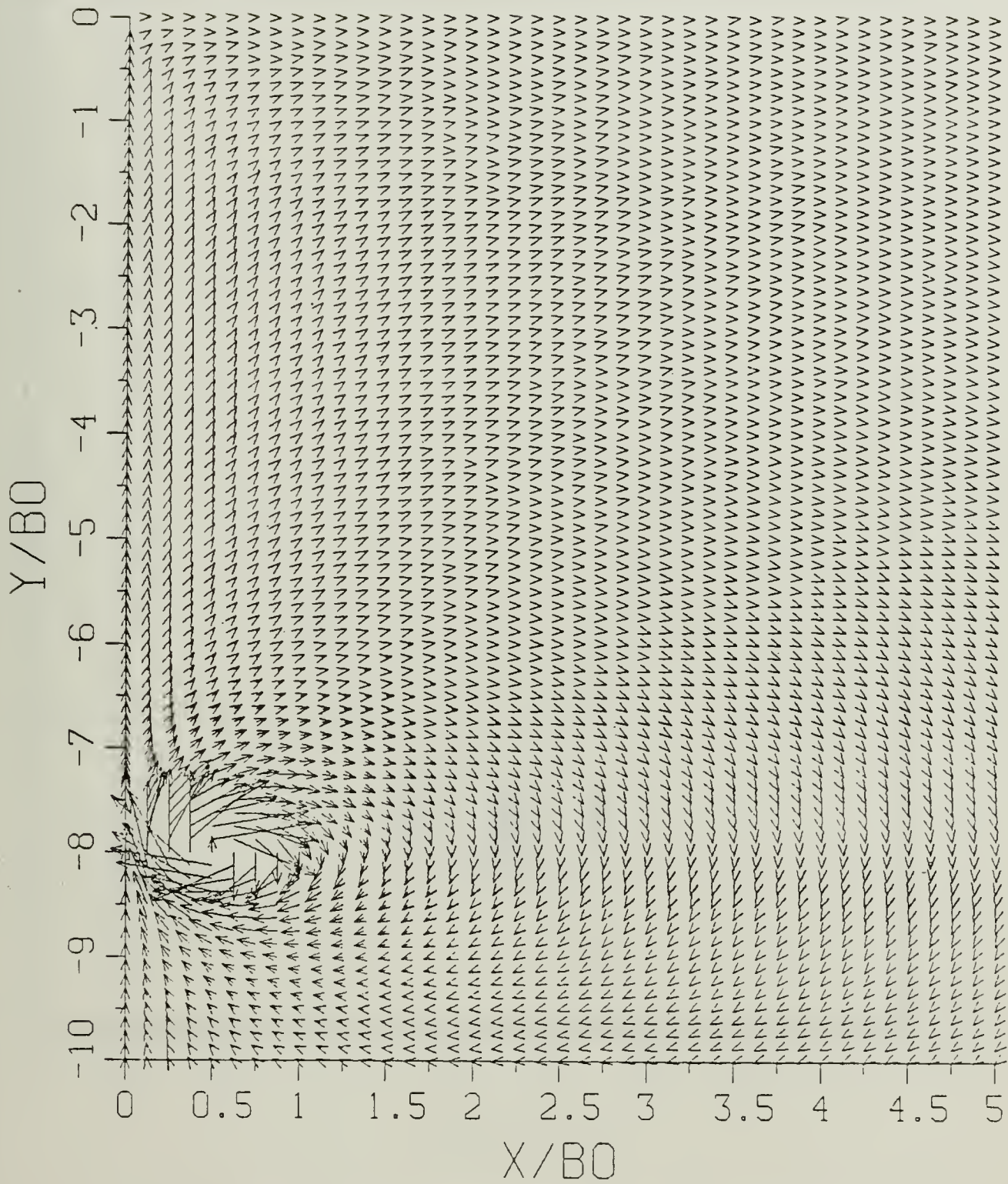


Figure B.15b Velocity Field:  $SP = 1.00$ .

$$T^* = 0.01719$$

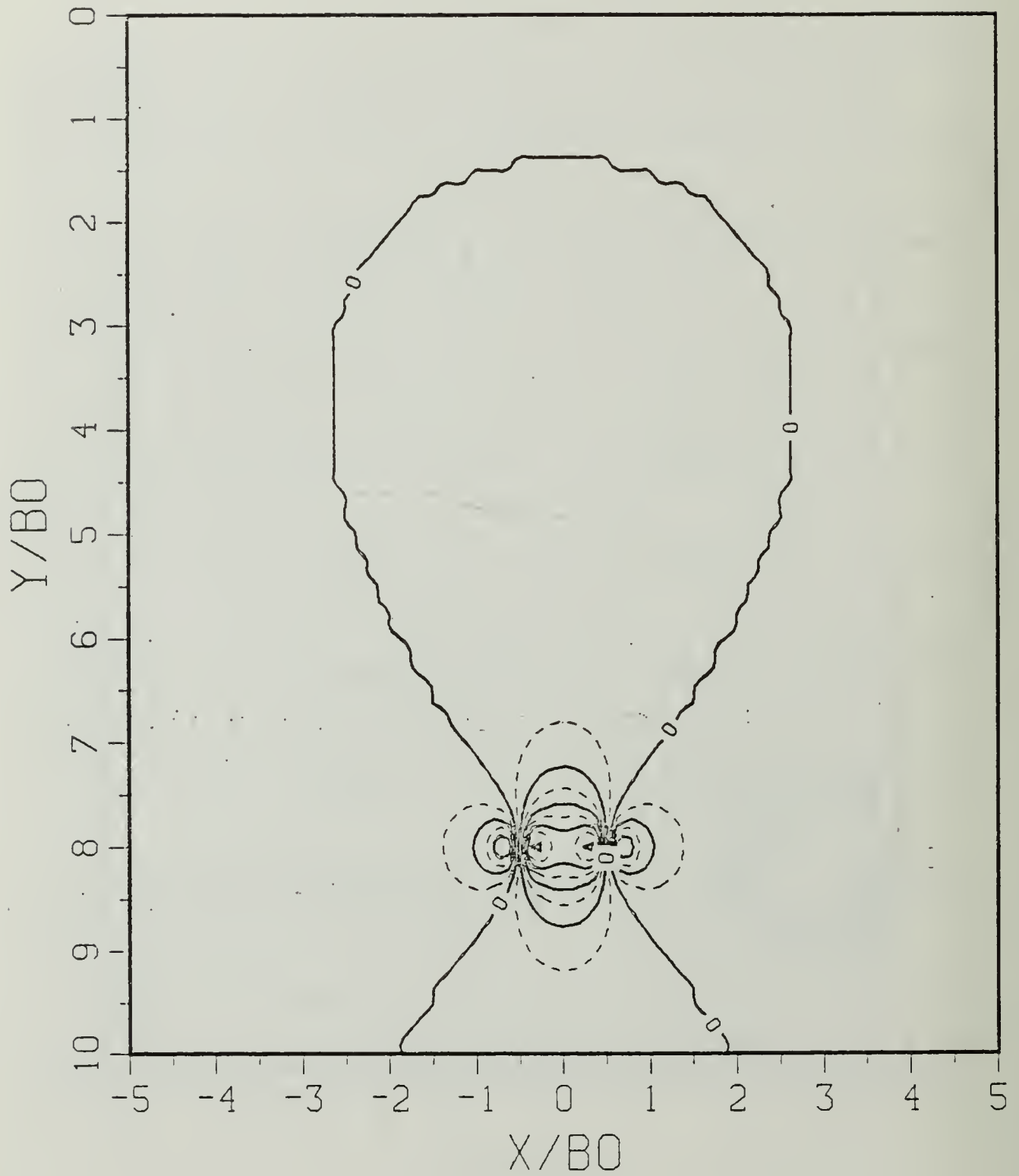


Figure B.15c Density Perturbation Contours:  $SP = 1.00$ .

$$\Gamma^* = 0.01719$$

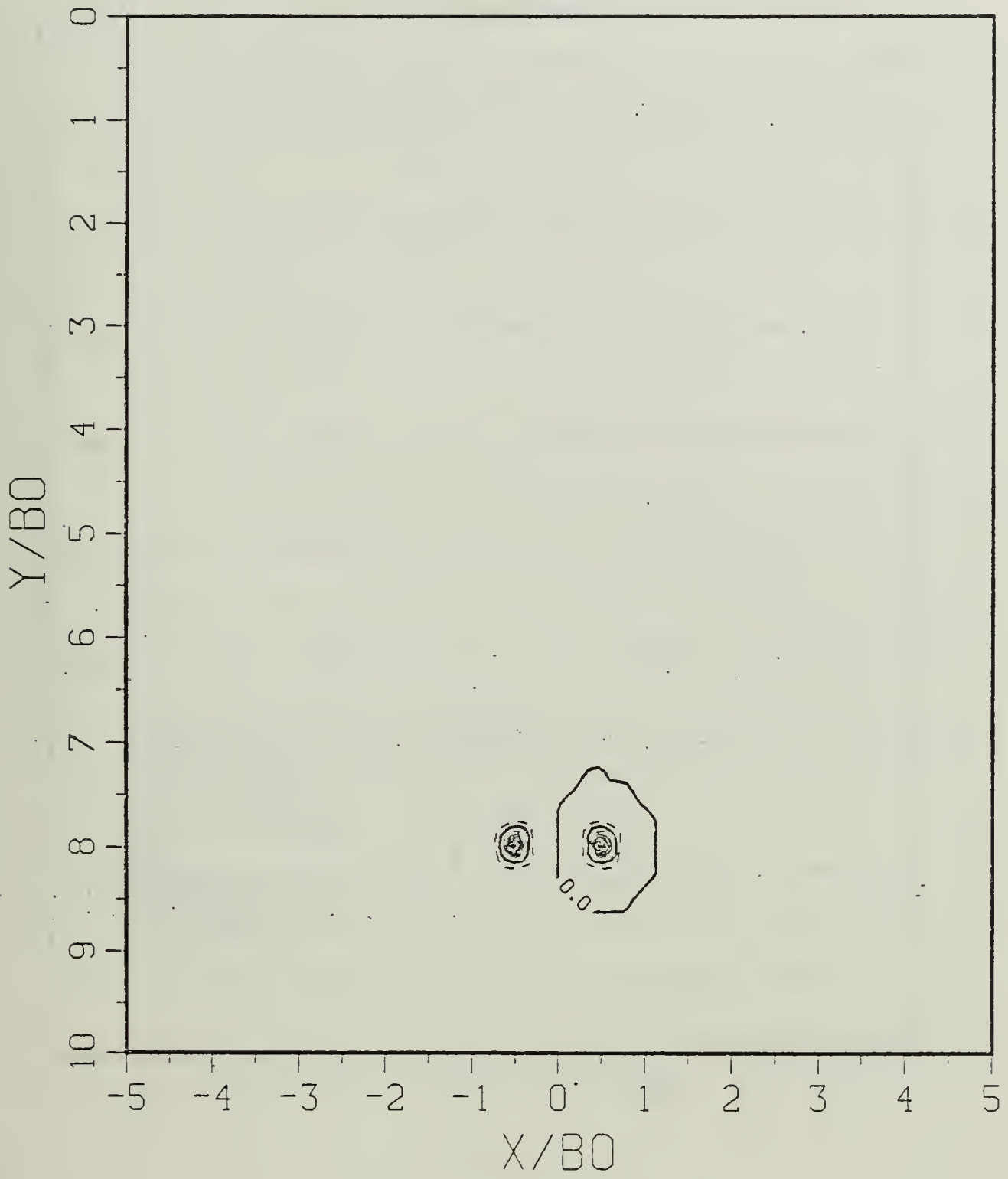


Figure B.15d Vorticity Field: SP = 1.00.

$$\Gamma^* = 0.34380$$

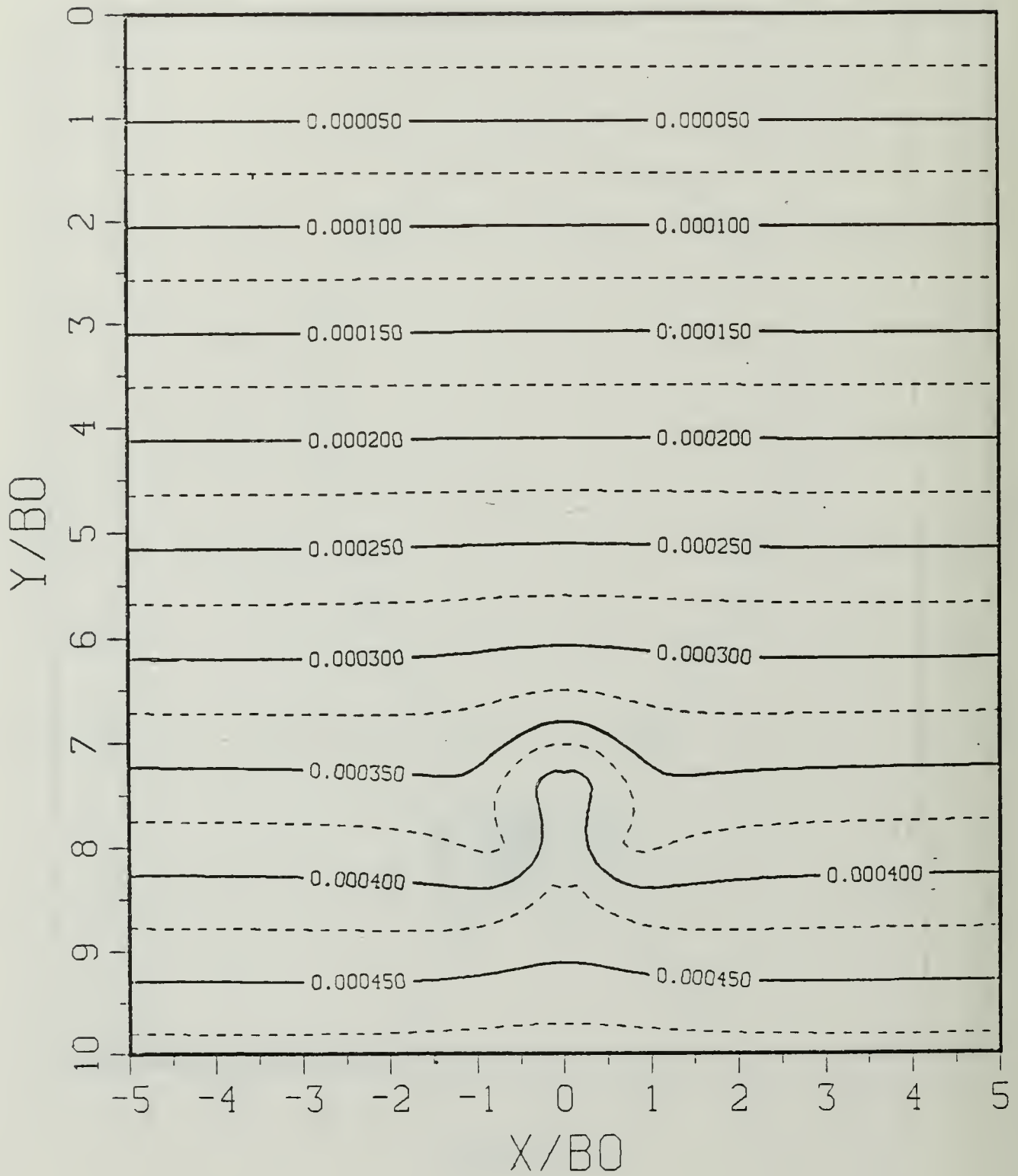


Figure B.16a Constant Density Contours:  $SP = 1.00$ .

$$T^* = 0.34380$$

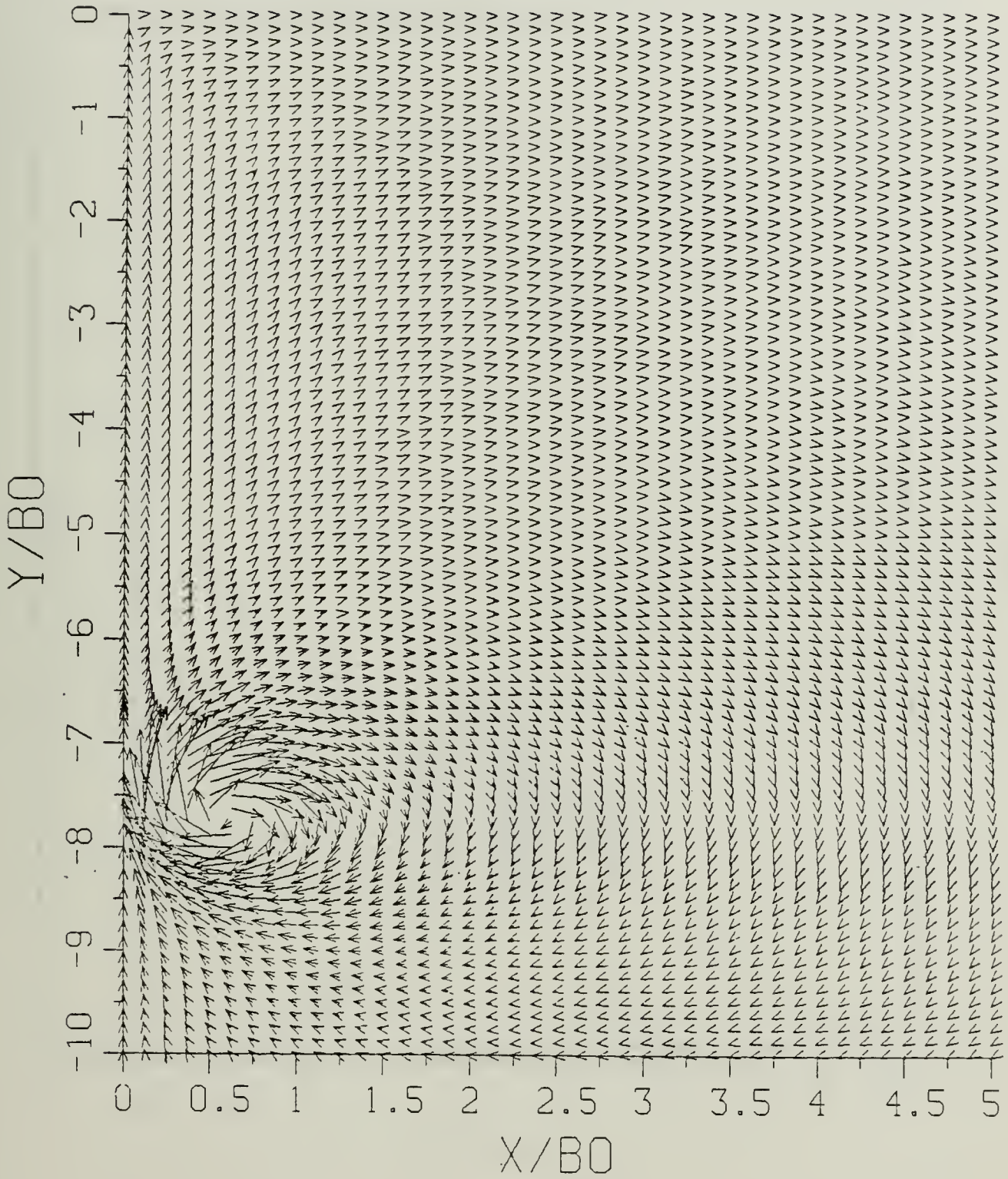


Figure B.16b Velocity Field: SP = 1.00.

$$T^* = 0.34380$$

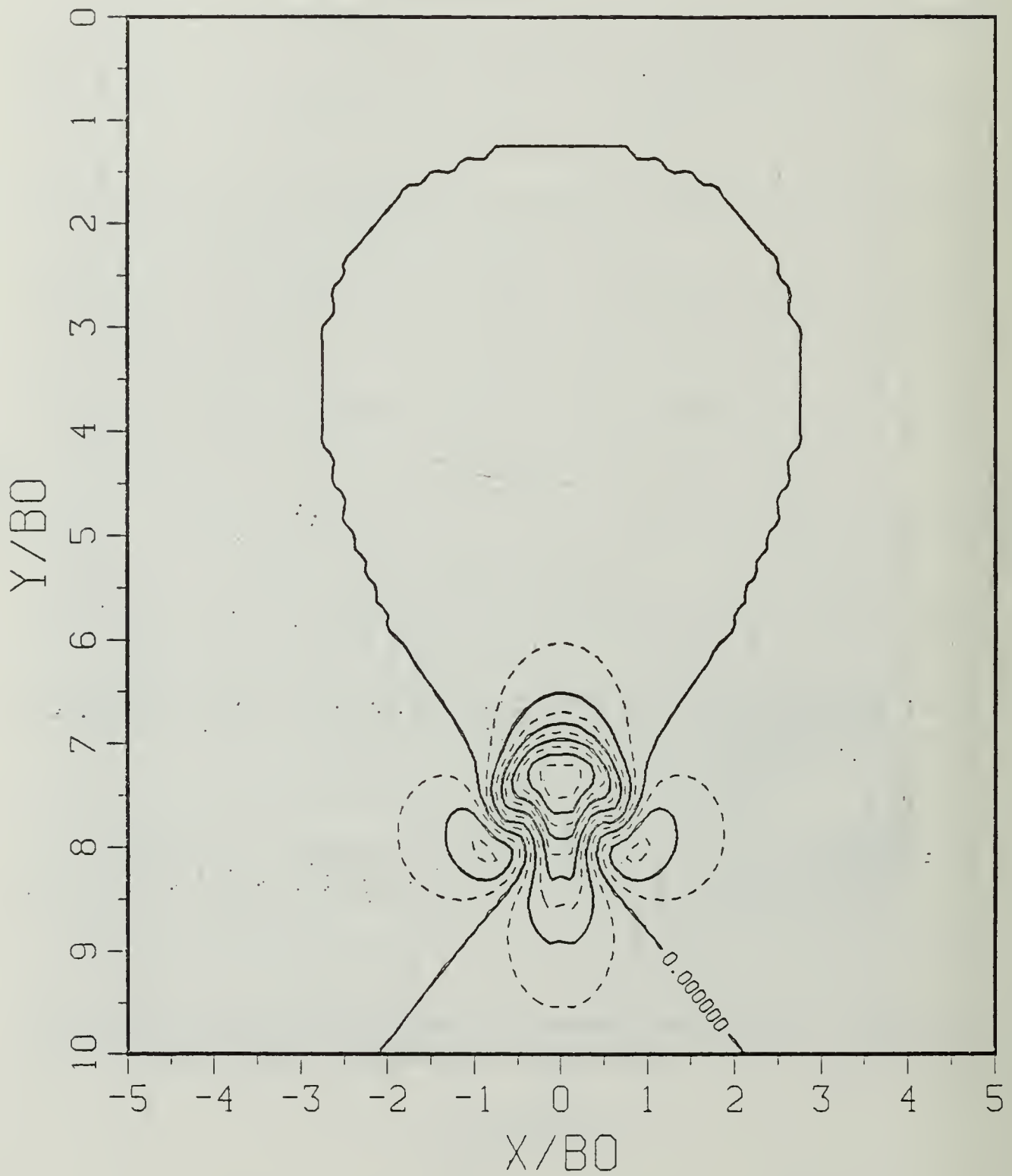


Figure B.16c Density Perturbation Contours:  $SP = 1.00$ .

$$T^* = 0.34380$$

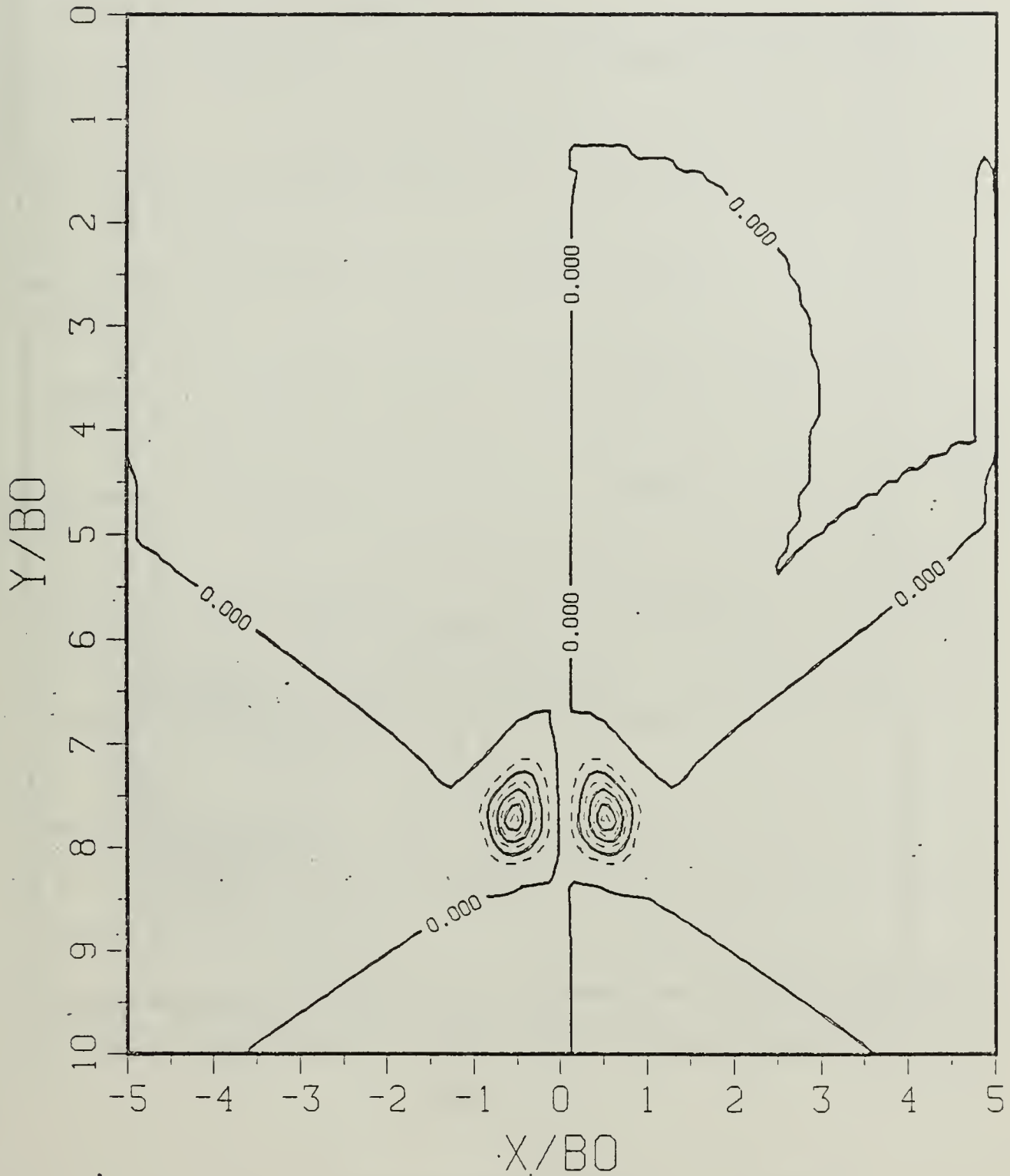


Figure B.16d Vorticity Field: SP = 1.00.

$$T^* = 0.68760$$

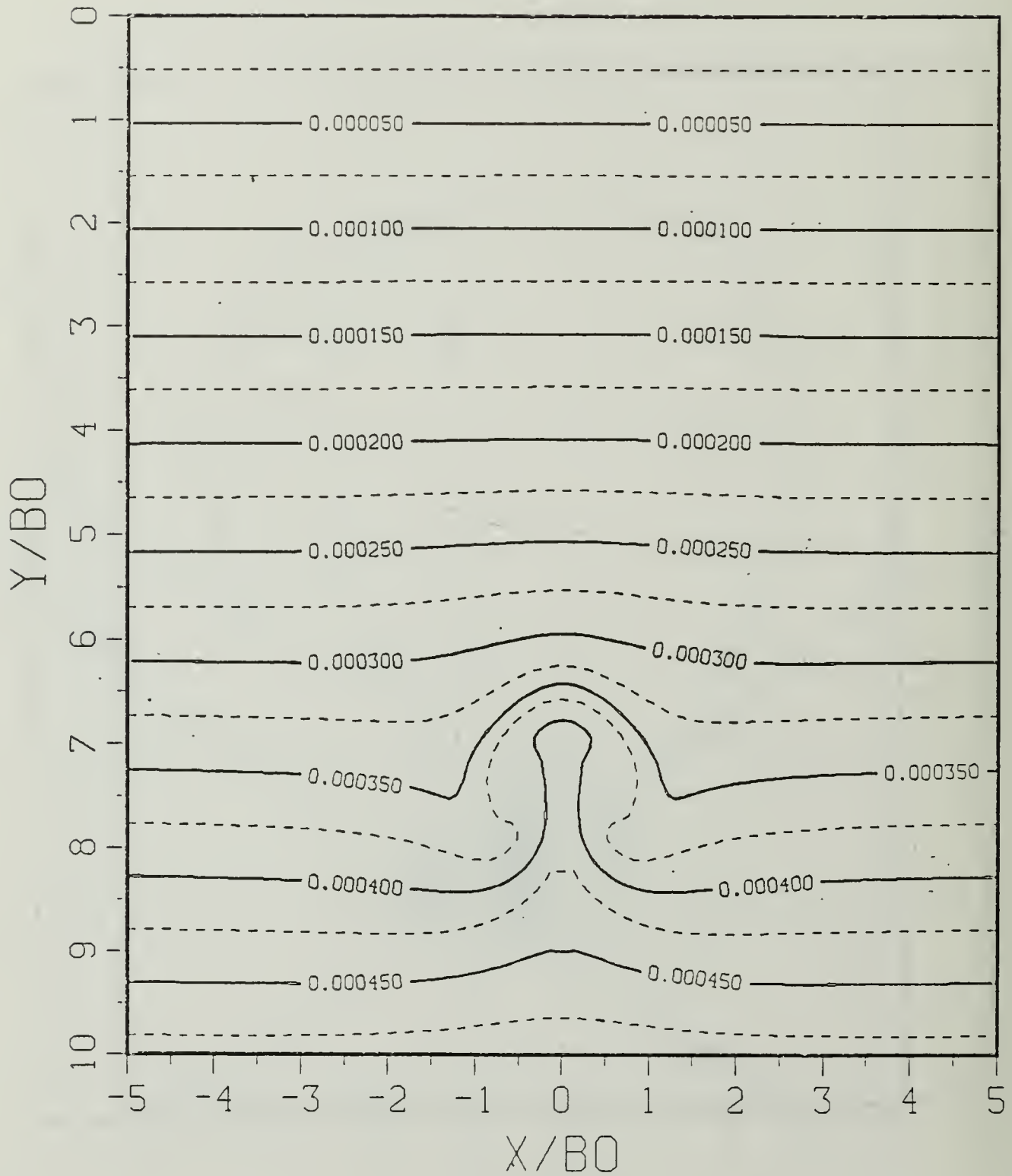


Figure B.17a Constant Density Contours:  $SP = 1.00$ .

$$\Gamma^* = 0.68760$$

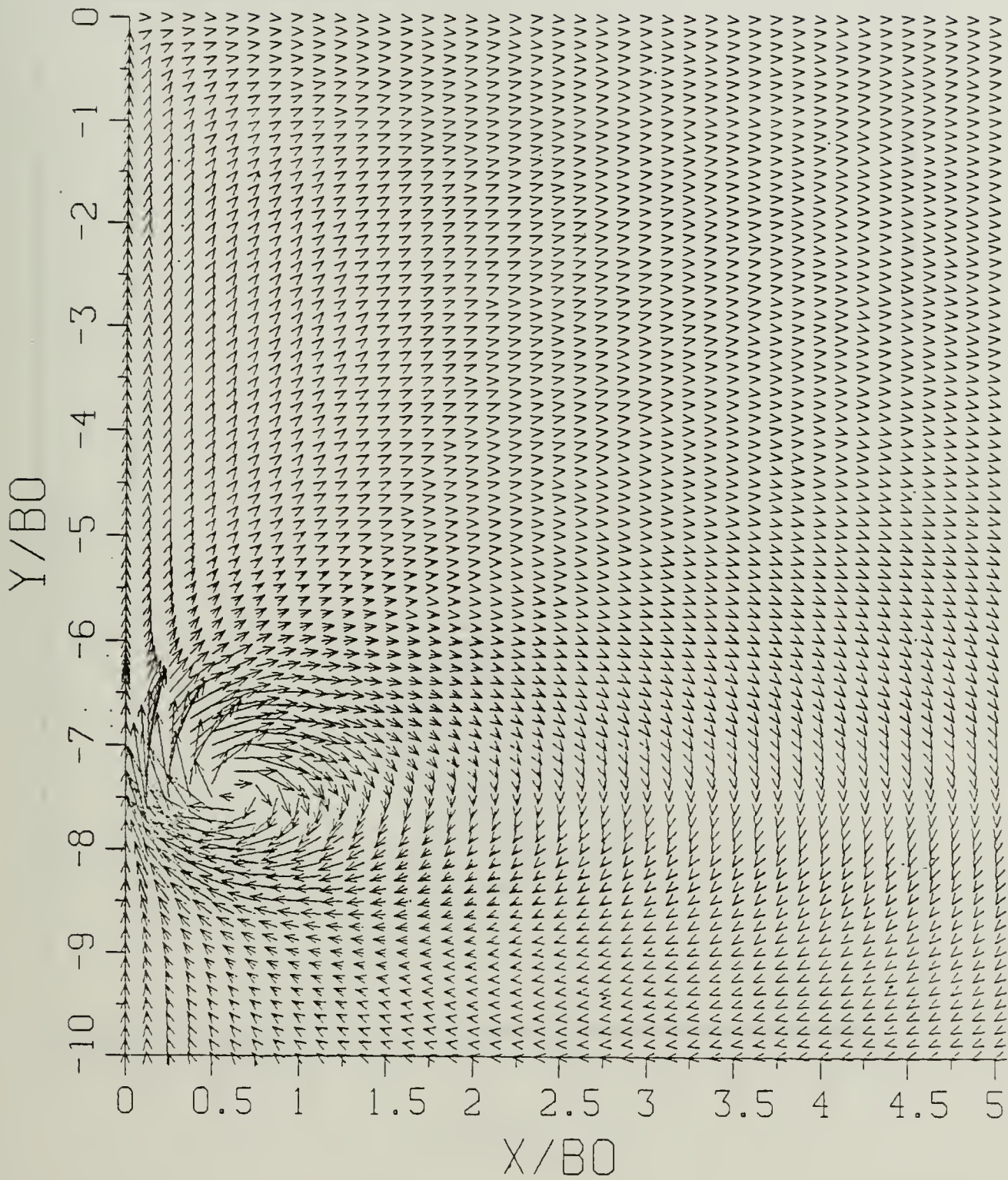


Figure B.17b Velocity Field: SP = 1.00.

$$T^* = 0.68760$$

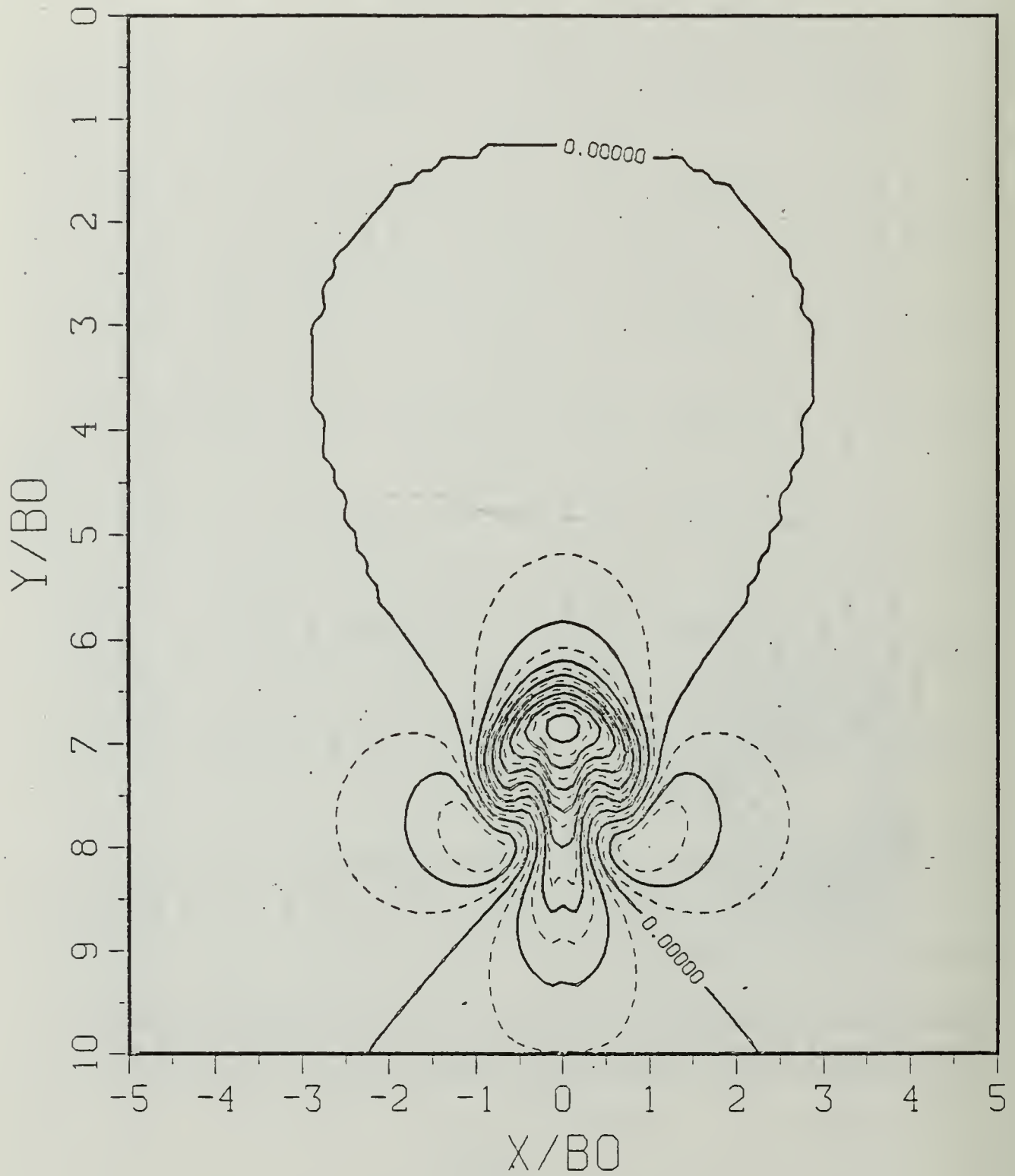


Figure B.17c Density Perturbation Contours: SP = 1.00.

$$T^* = 0.68760$$

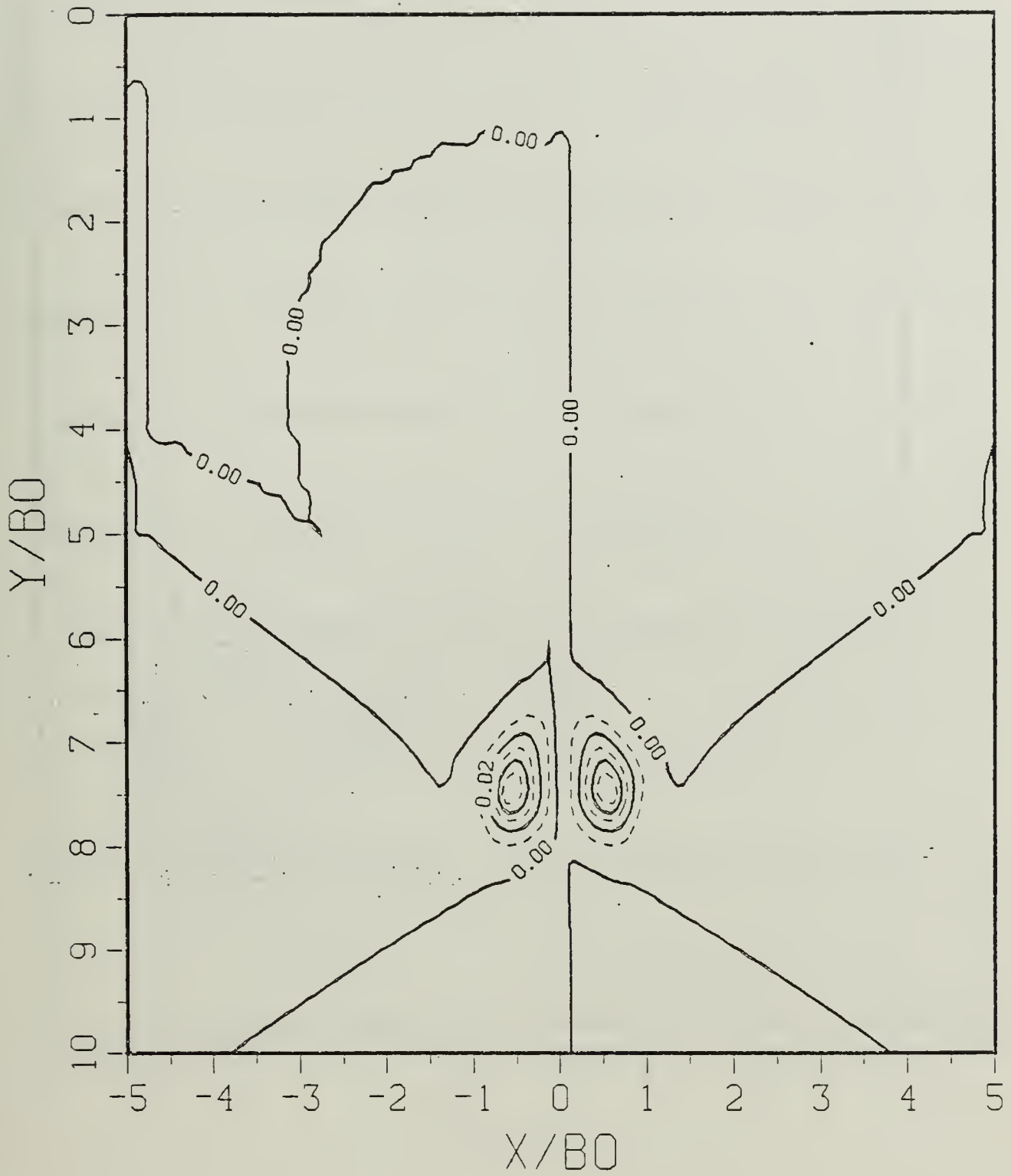


Figure B.17d Vorticity Field: SP = 1.00.

$$T^* = 1.03140$$

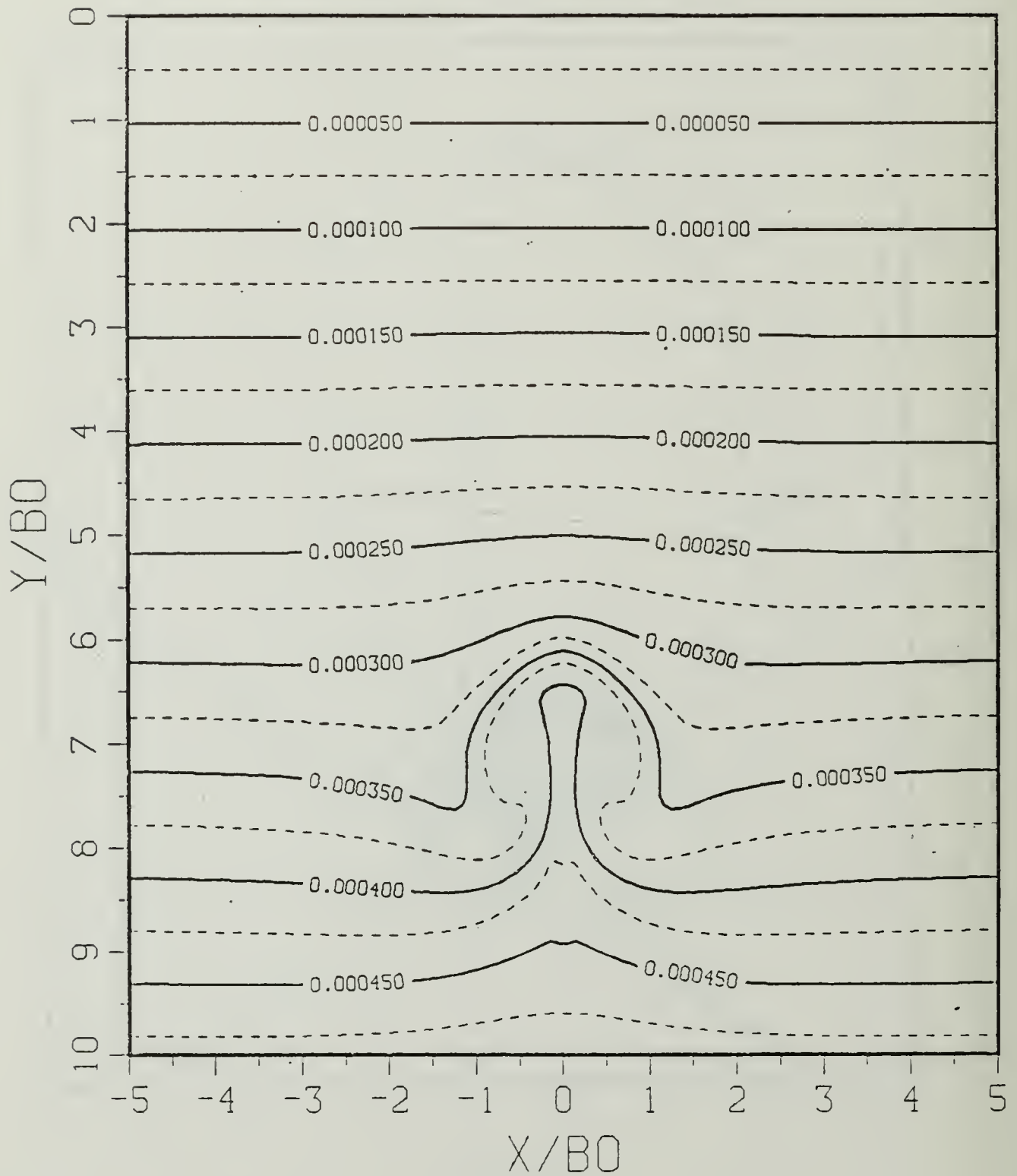


Figure B.18a Constant Density Contours:  $SP = 1.00$ .

$$T^* = 1.03140$$

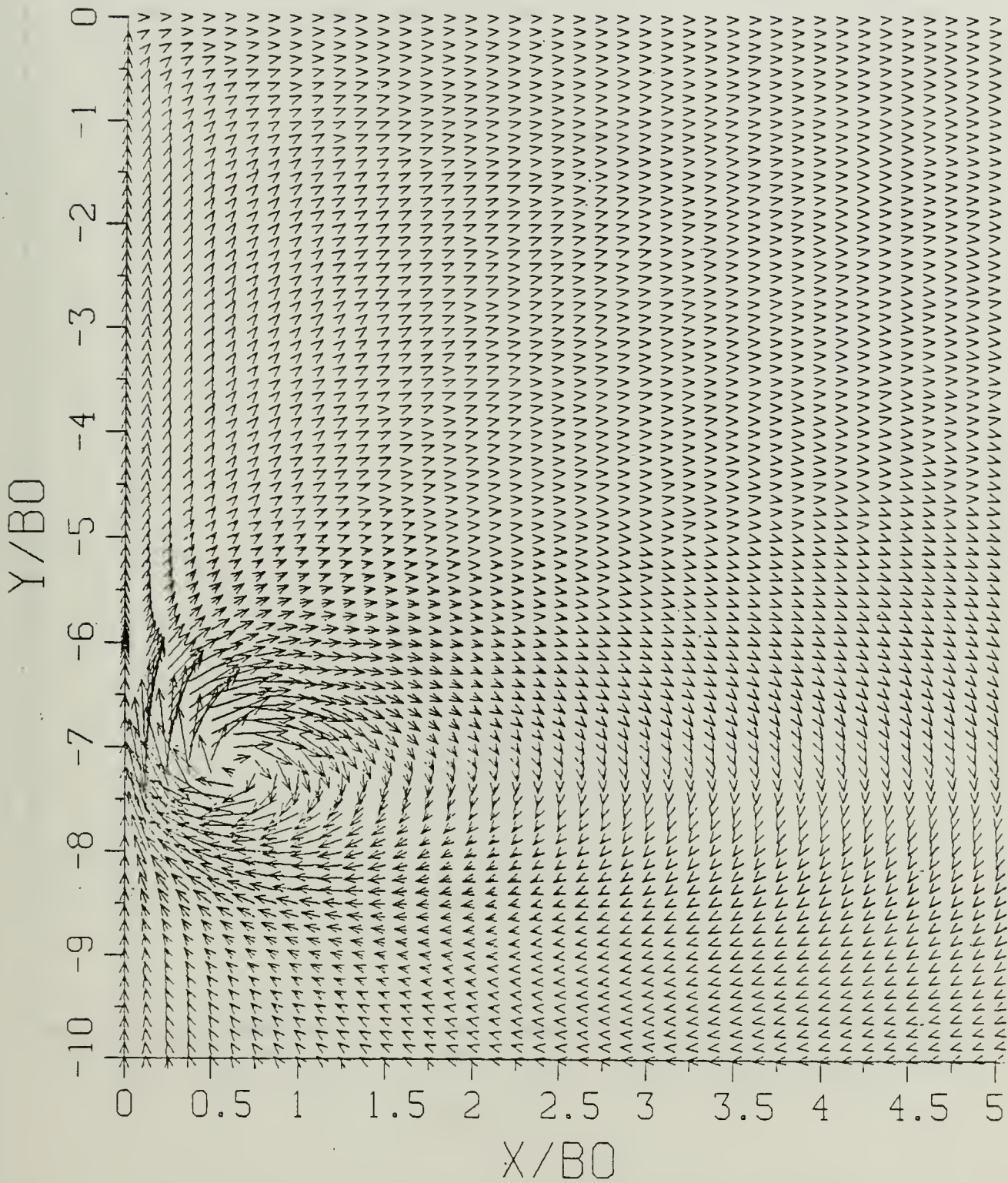


Figure B.18b Velocity Field: SP = 1.00.

$$T^* = 1.03140$$

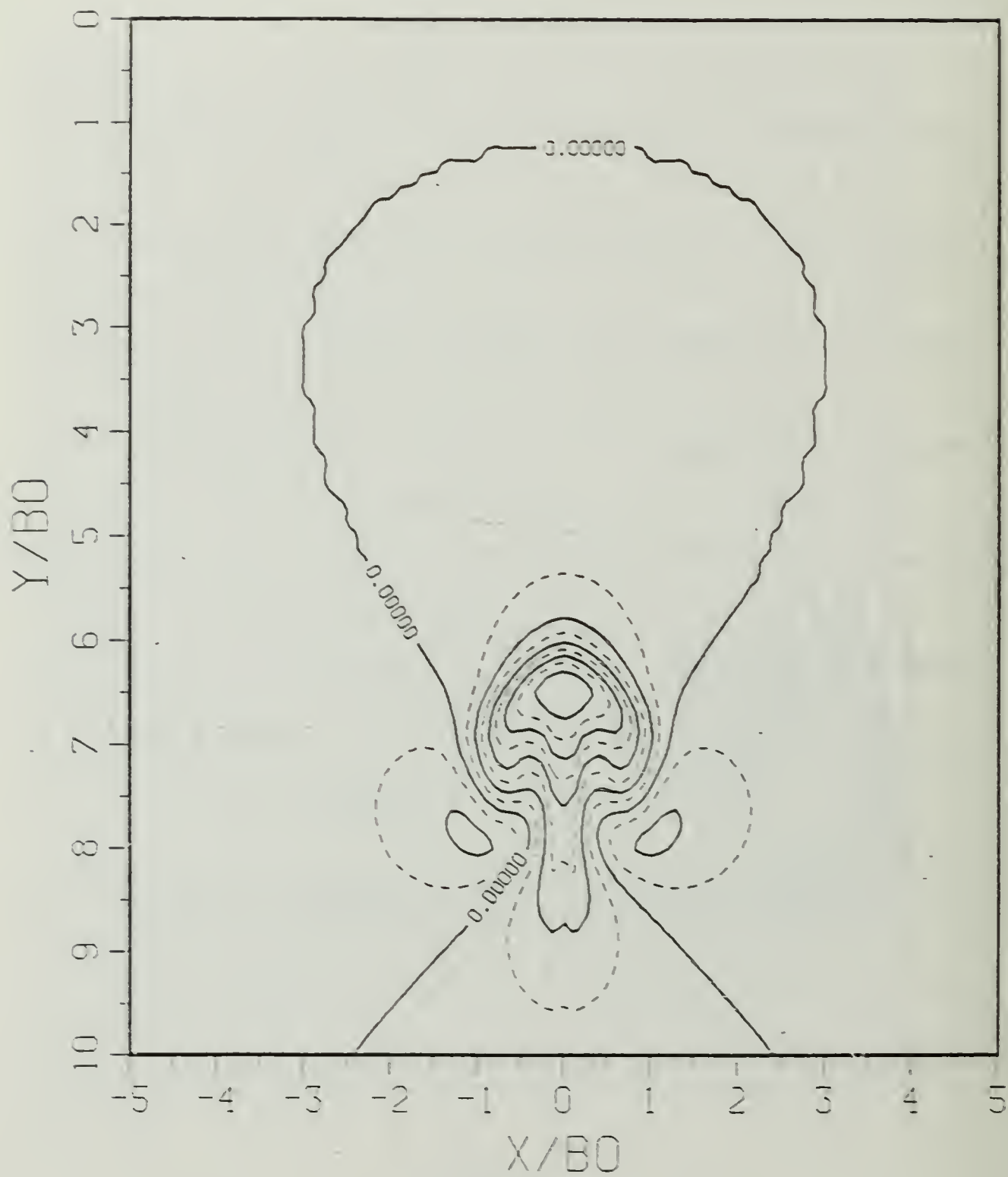


Figure B.18c Density Perturbation Contours:  $SP = 1.00$ .

$$\Gamma^* = 1.03140$$

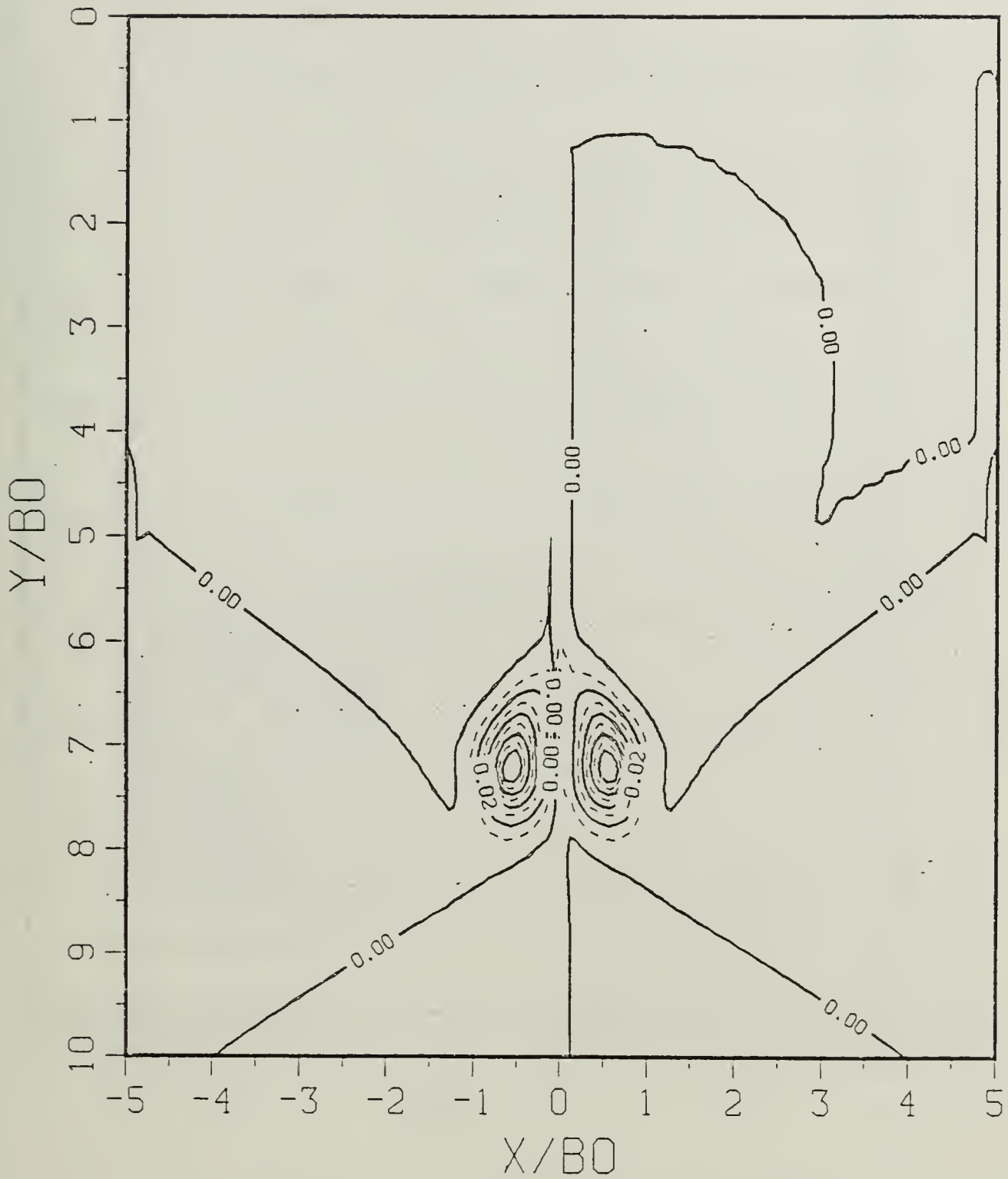


Figure B.18d Vorticity Field: SP = 1.00.

$$T^* = 1.37520$$

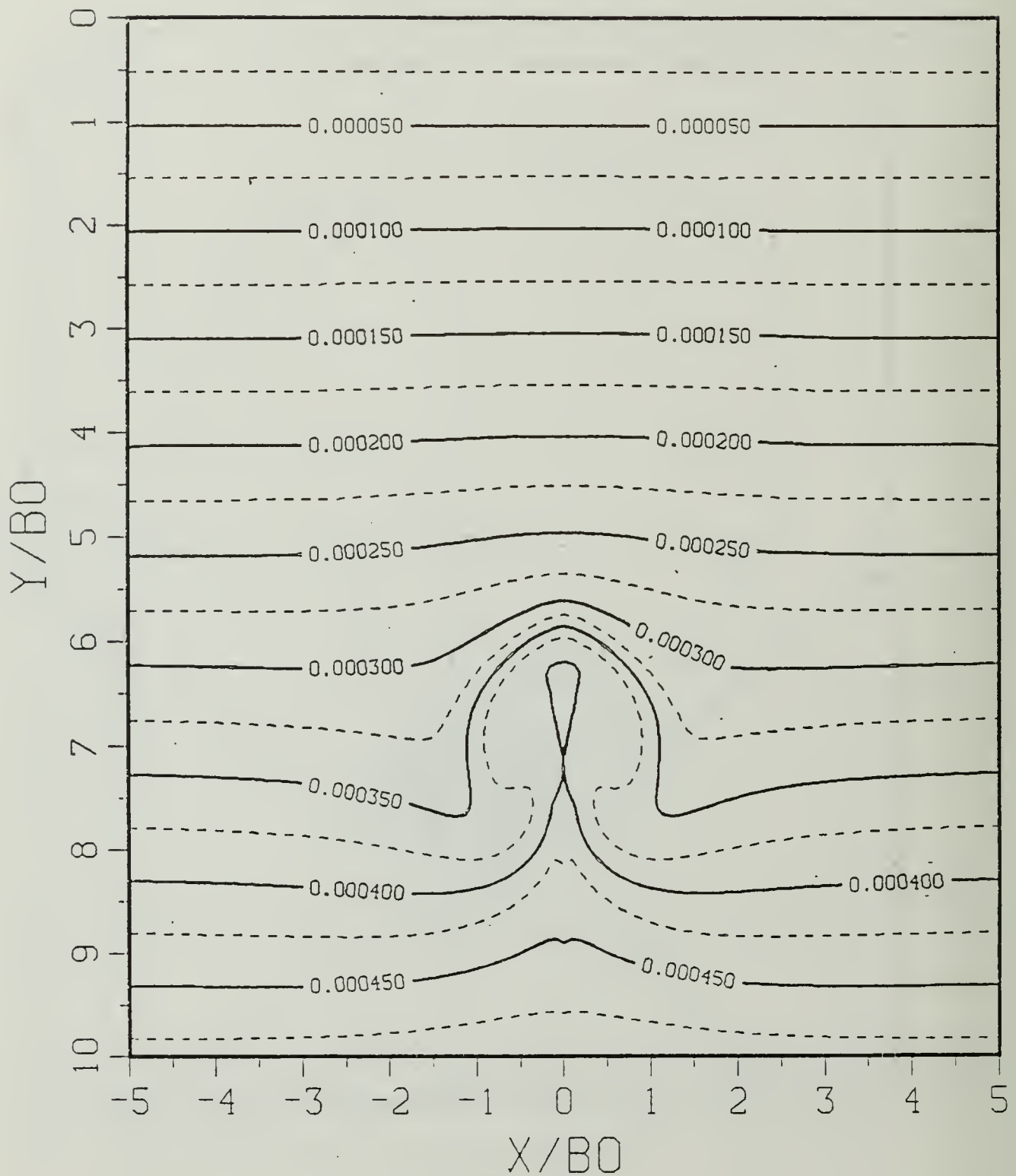


Figure B.19a Constant Density Contours:  $SP = 1.00$ .

$$T^* = 1.37520$$

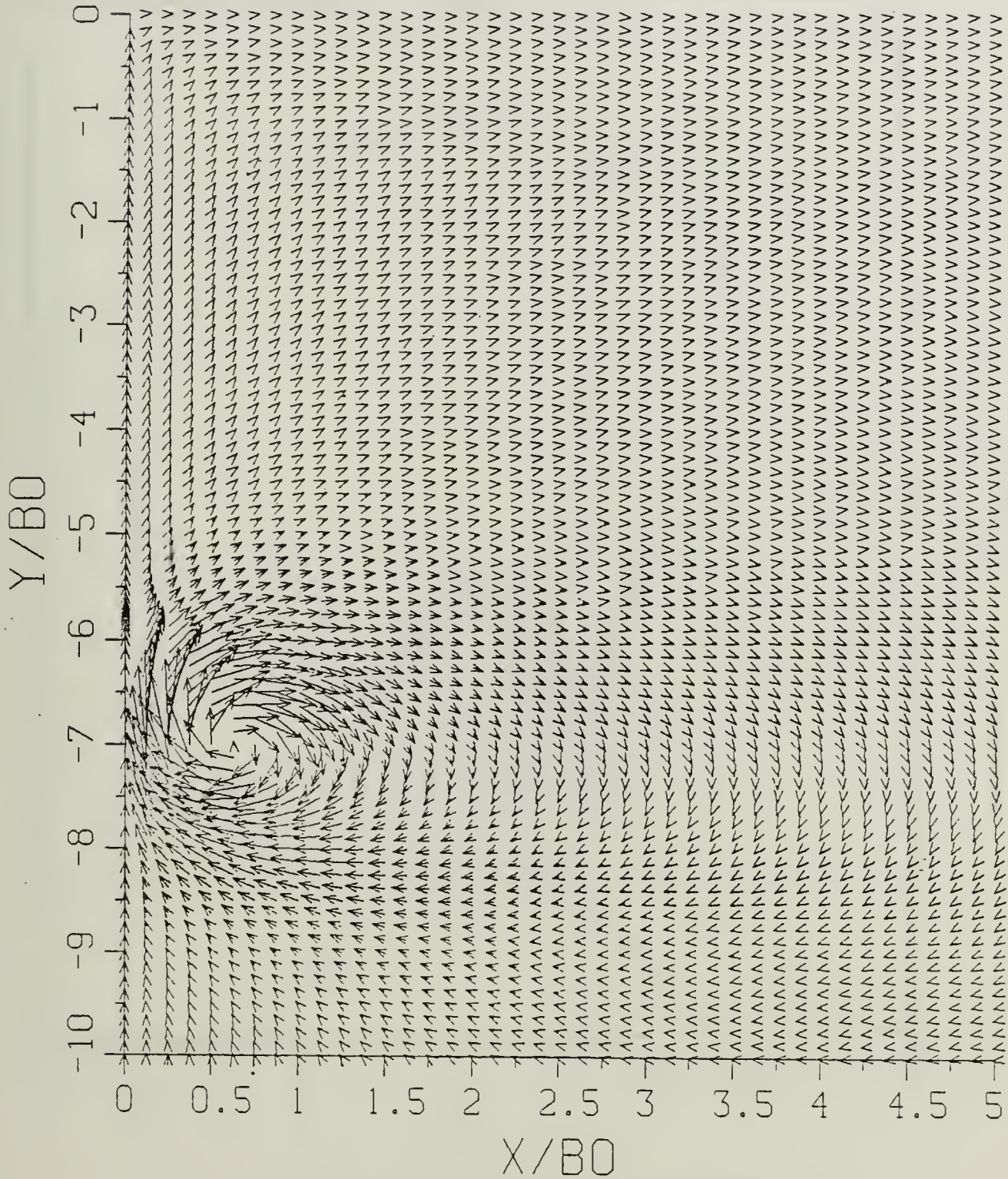


Figure B.19b Velocity Field:  $SP = 1.00$ .

$$T^* = 1.37520$$

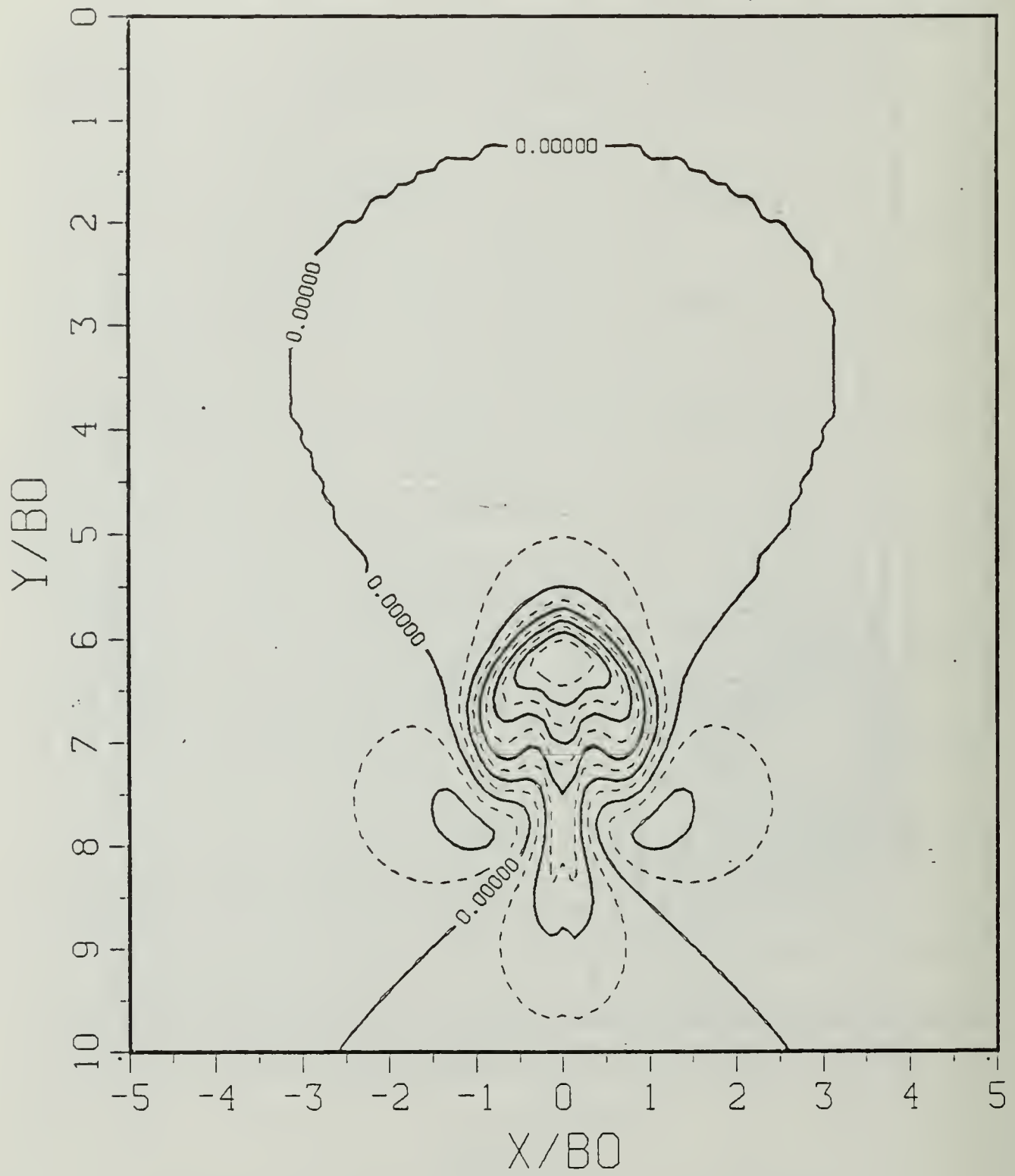


Figure B.19c Density Perturbation Contours:  $SP = 1.00$ .

$$T^* = 1.37520$$

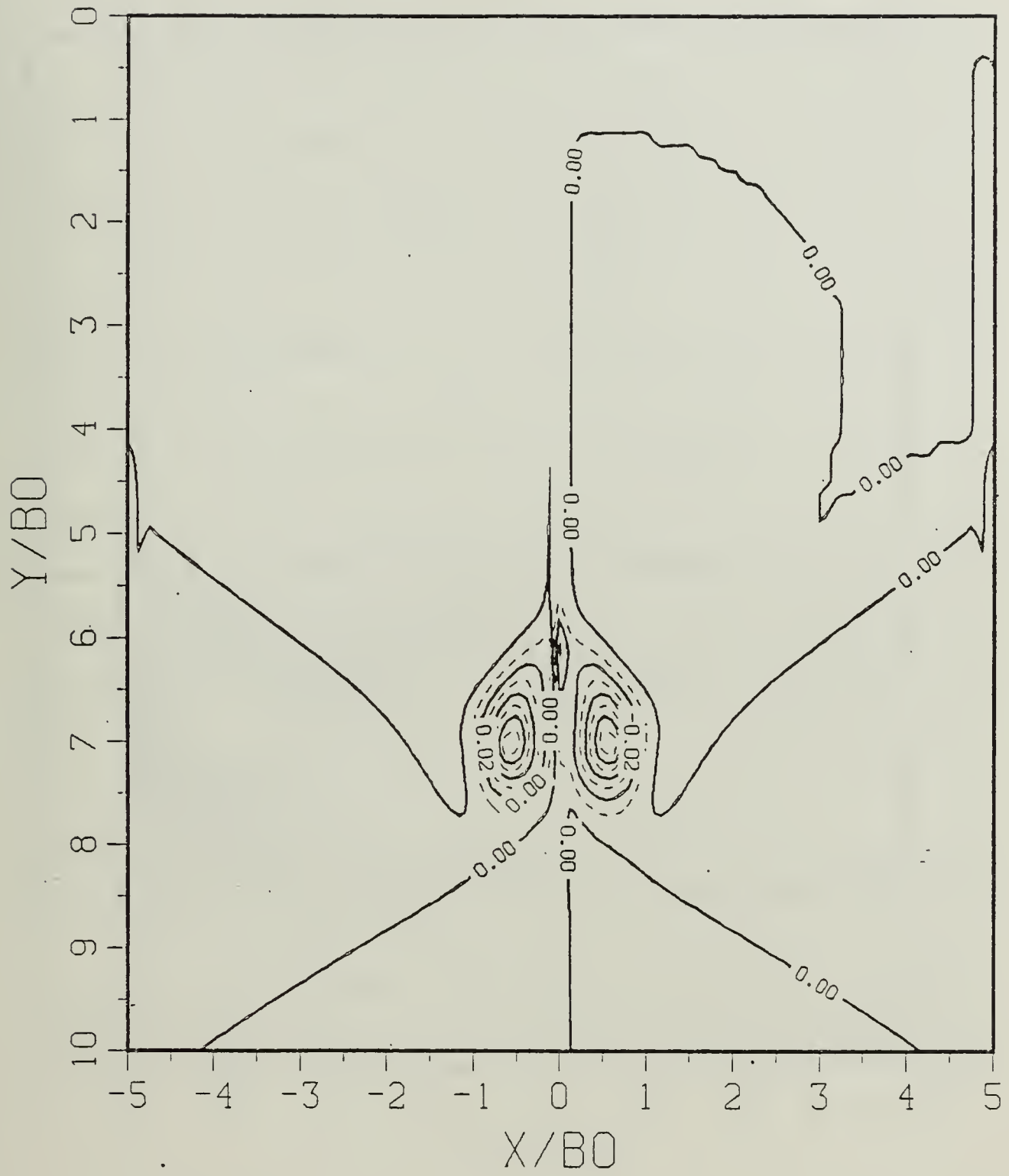


Figure B.19d Vorticity Field: SP = 1.00.

$$T^* = 1.71900$$

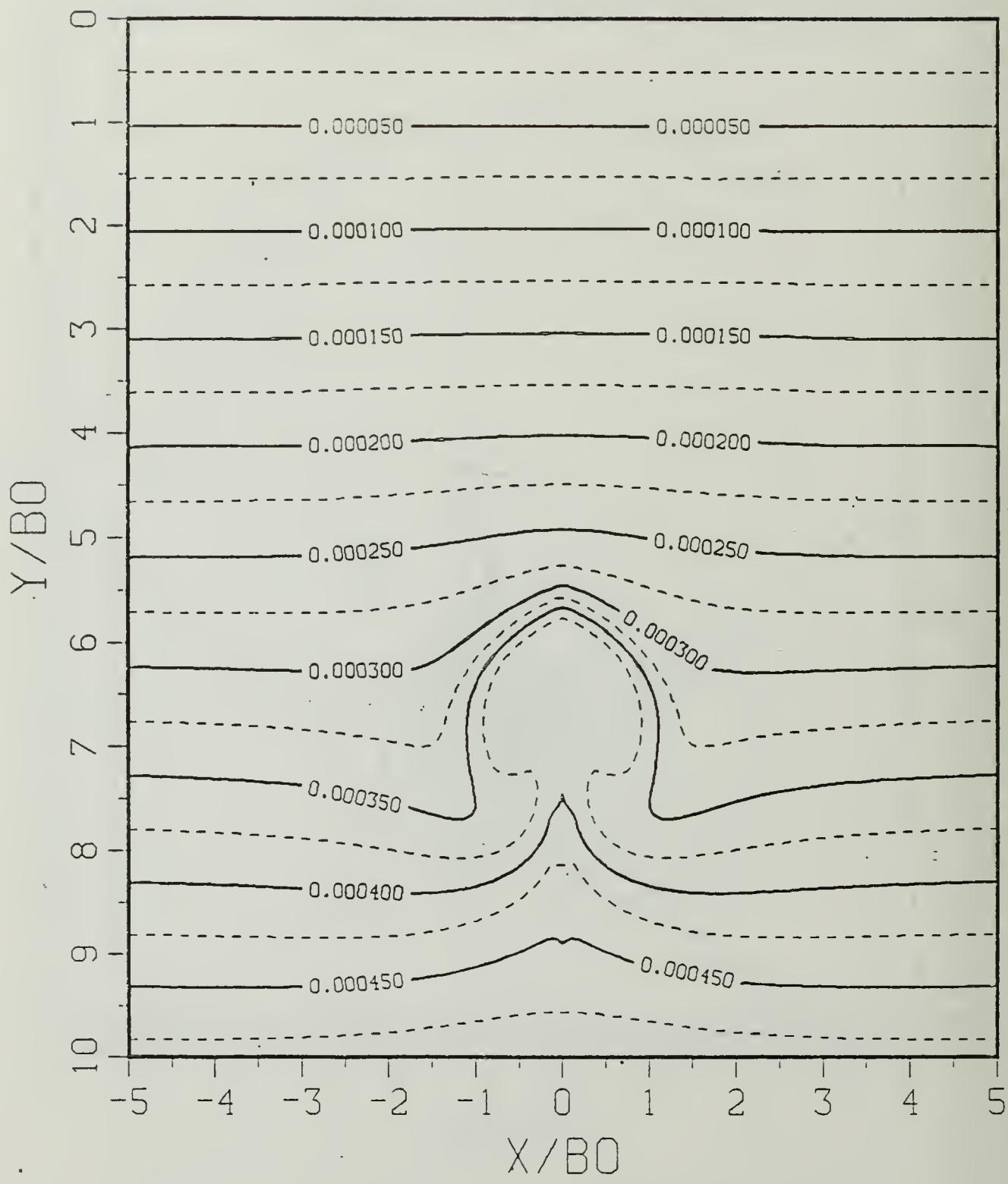


Figure B.20a Constant Density Contours:  $SP = 1.00$ .

$$\Gamma^* = 1.71900$$

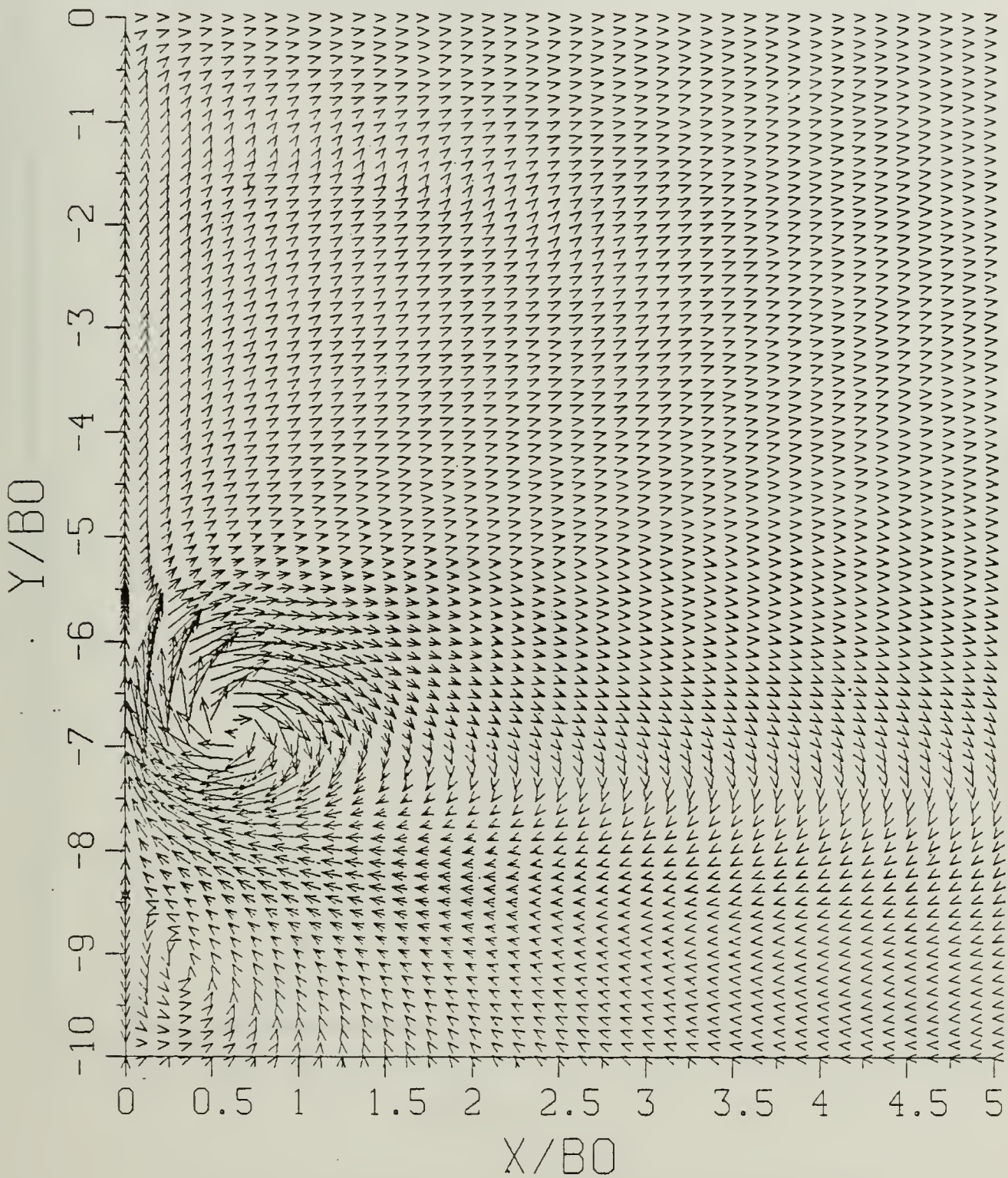


Figure B.20b Velocity Field: SP = 1.00.

$$T^* = 1.71900$$

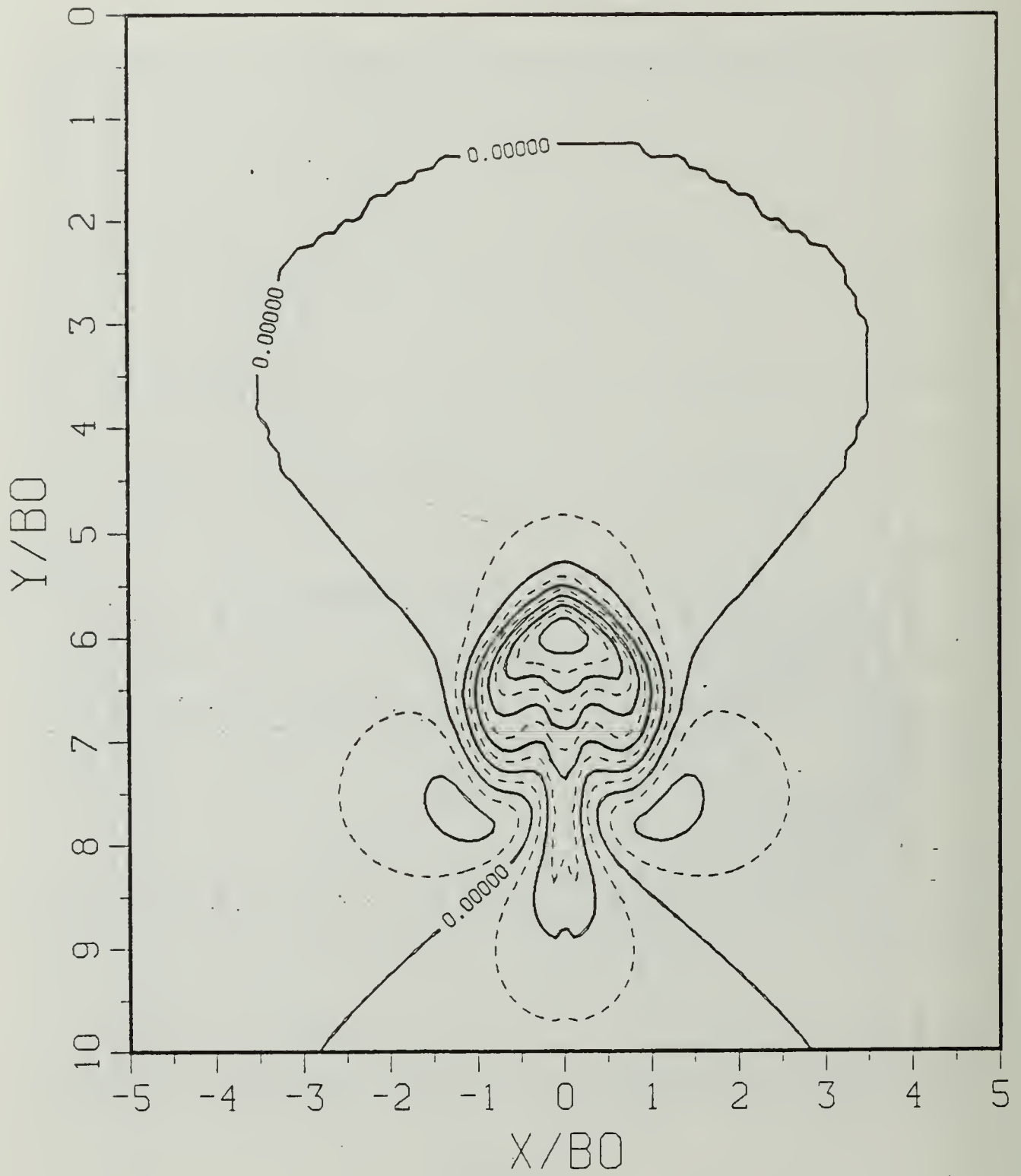


Figure B.20c Density Perturbation Contours:  $SP = 1.00$ .

$$T^* = 1.71900$$

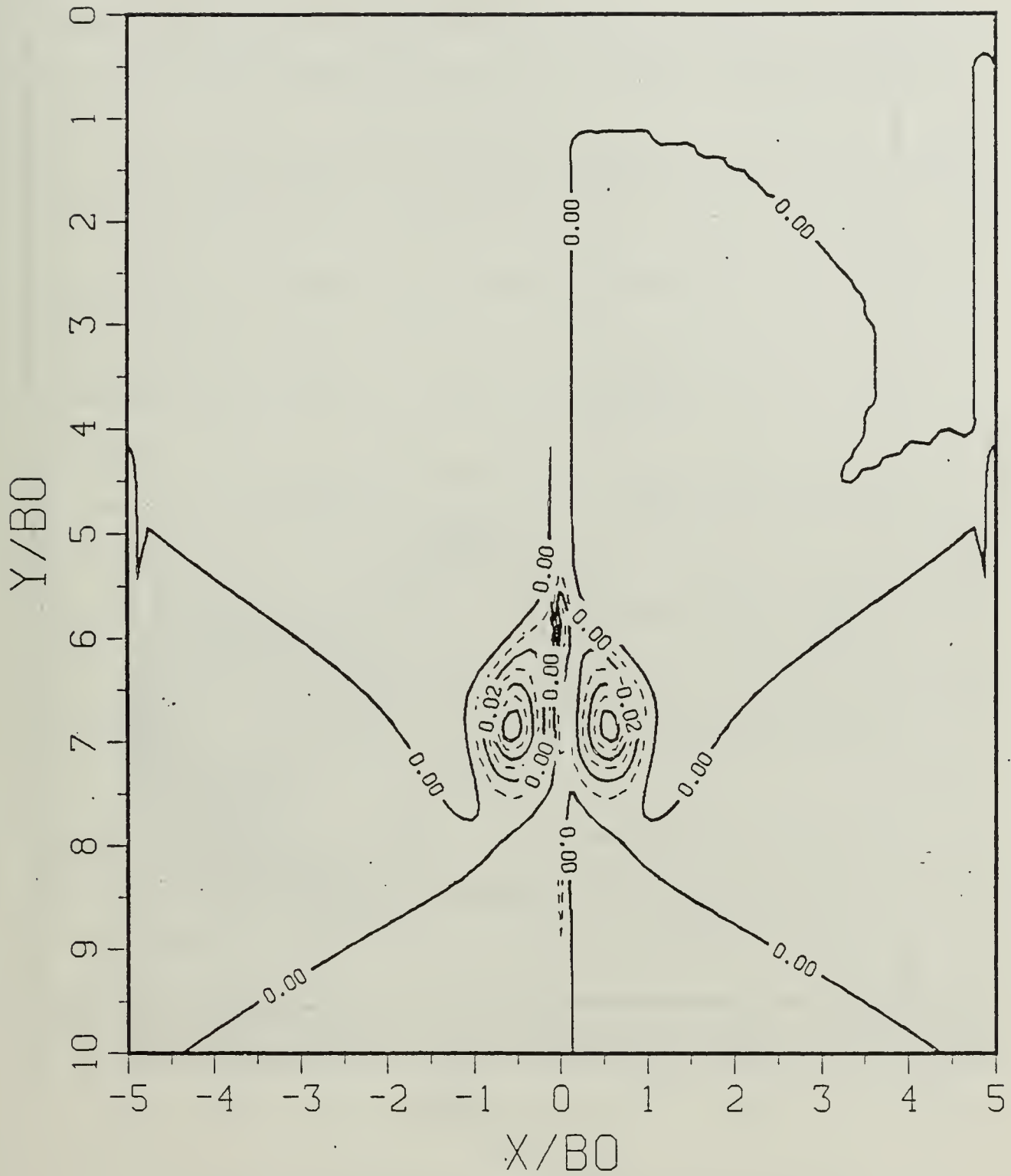


Figure B.20d Vorticity Field: SP = 1.00.

$$T^* = 2.06280$$

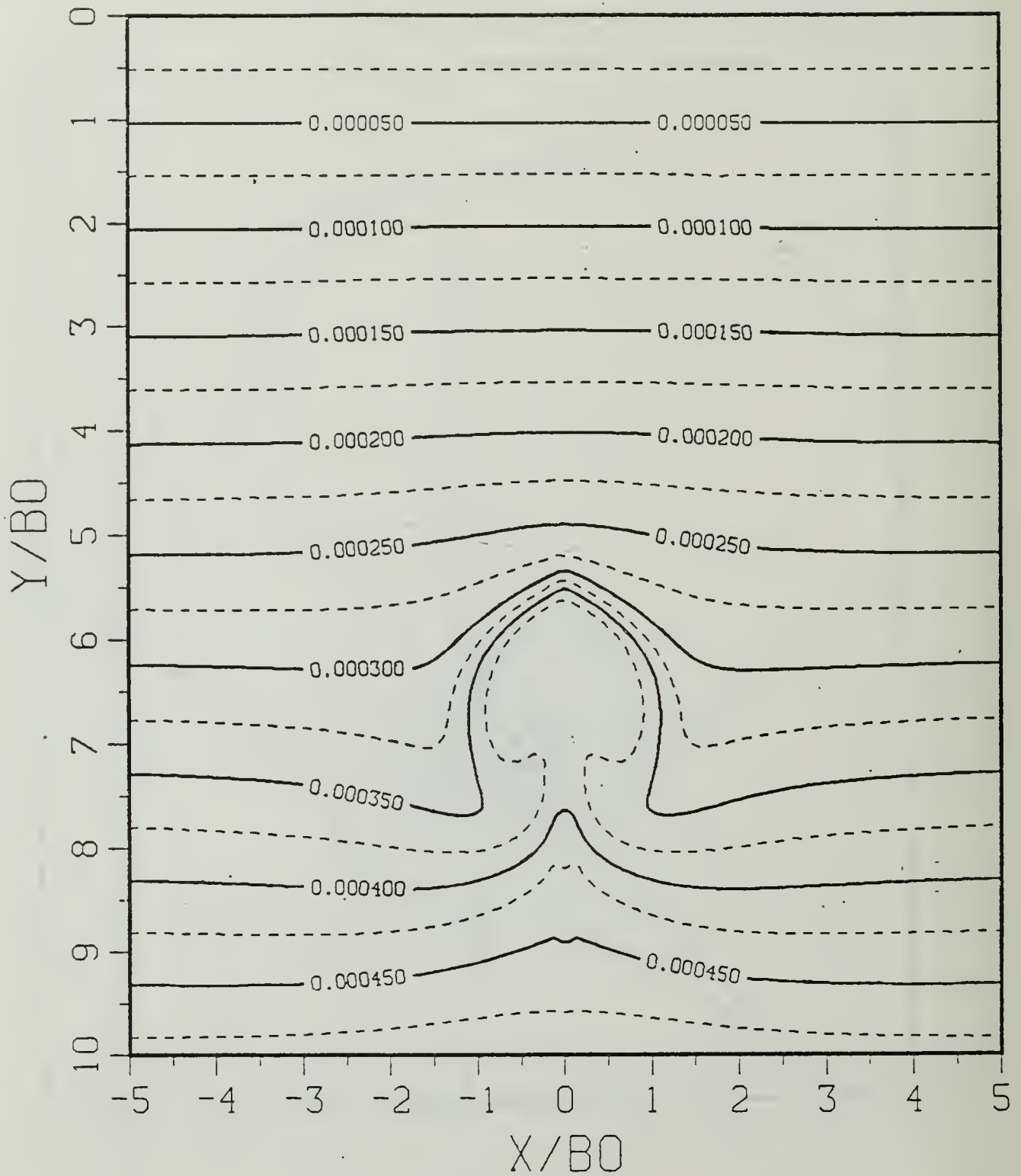


Figure B.21a Constant Density Contours:  $SP = 1.00$ .

$$T^* = 2.06280$$

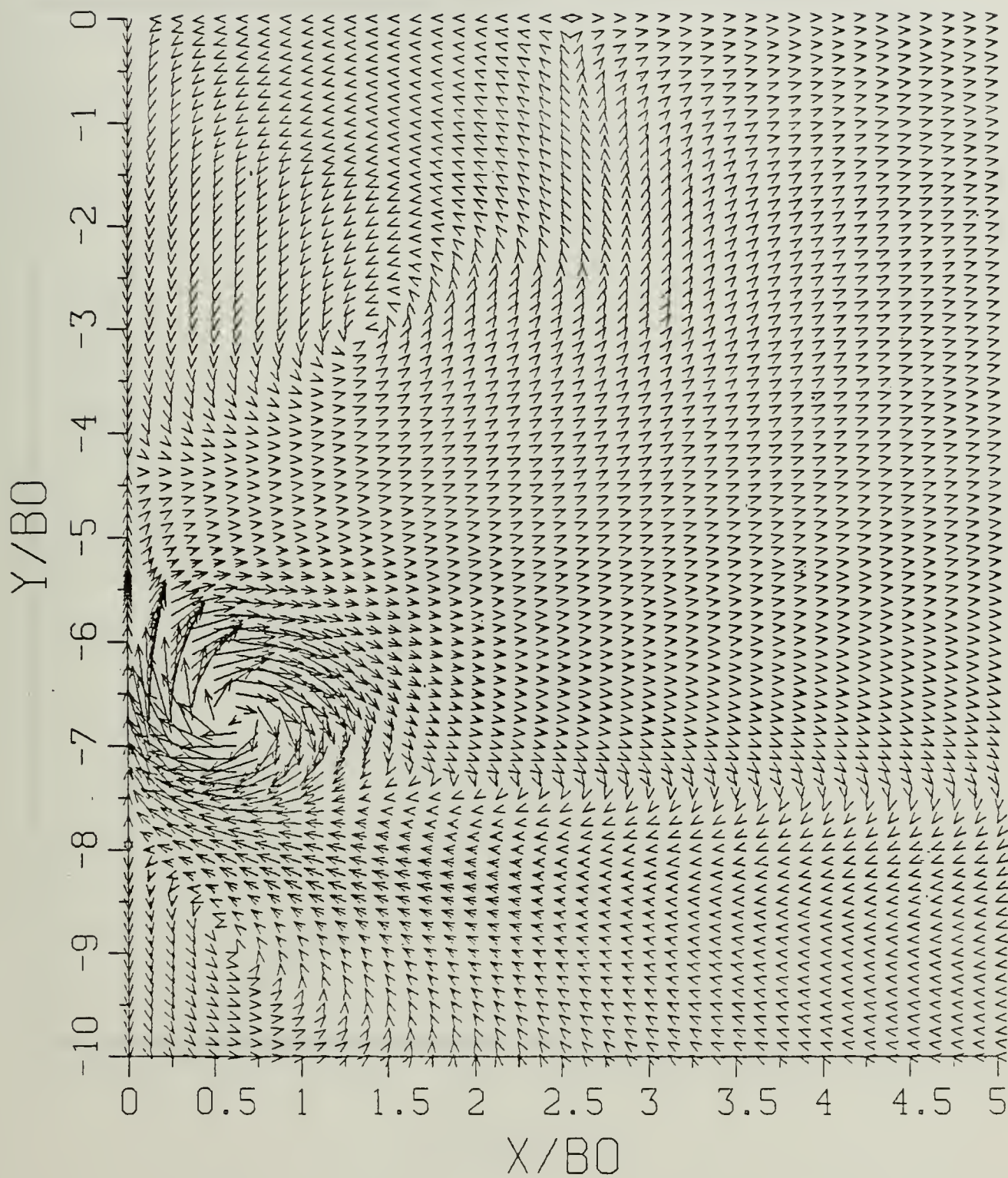


Figure B.21b Velocity Field: SP = 1.00.

$$T^* = 2.06280$$

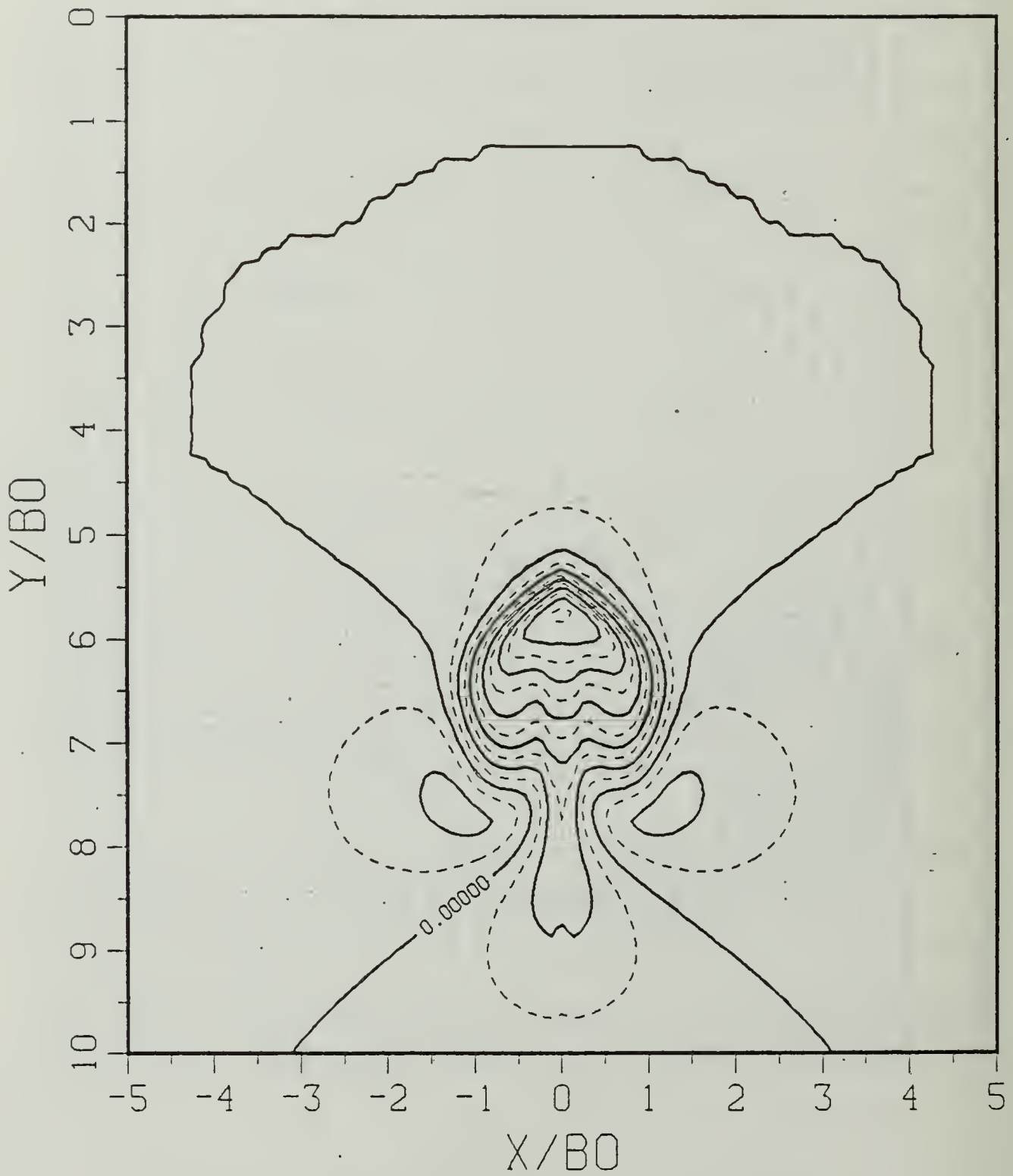


Figure B.21c Density Perturbation Contours: SP = 1.00.

$$T^* = 2.06280$$

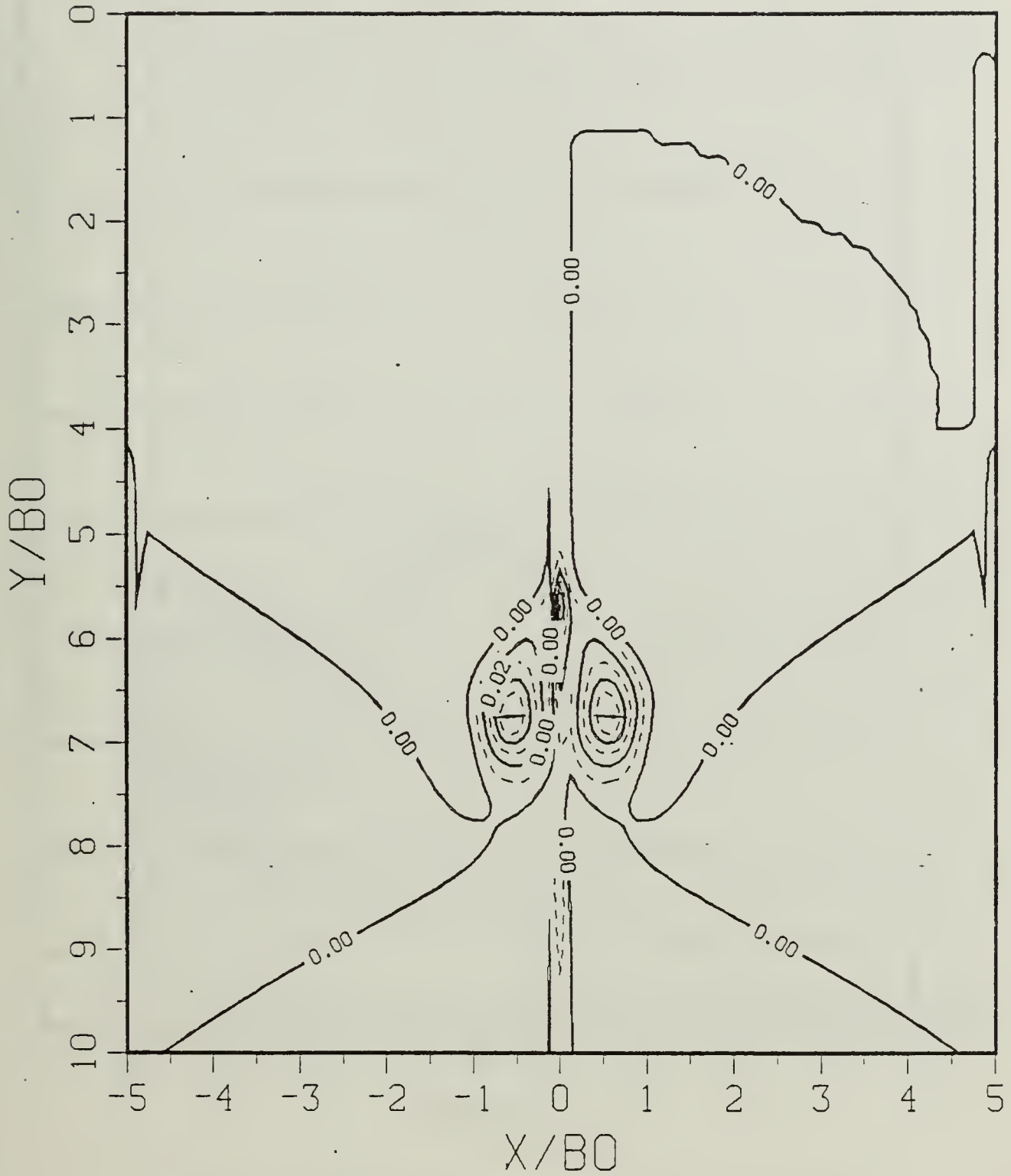


Figure B.21d Vorticity Field: SP = 1.00.

$$T^* = 2.40660$$

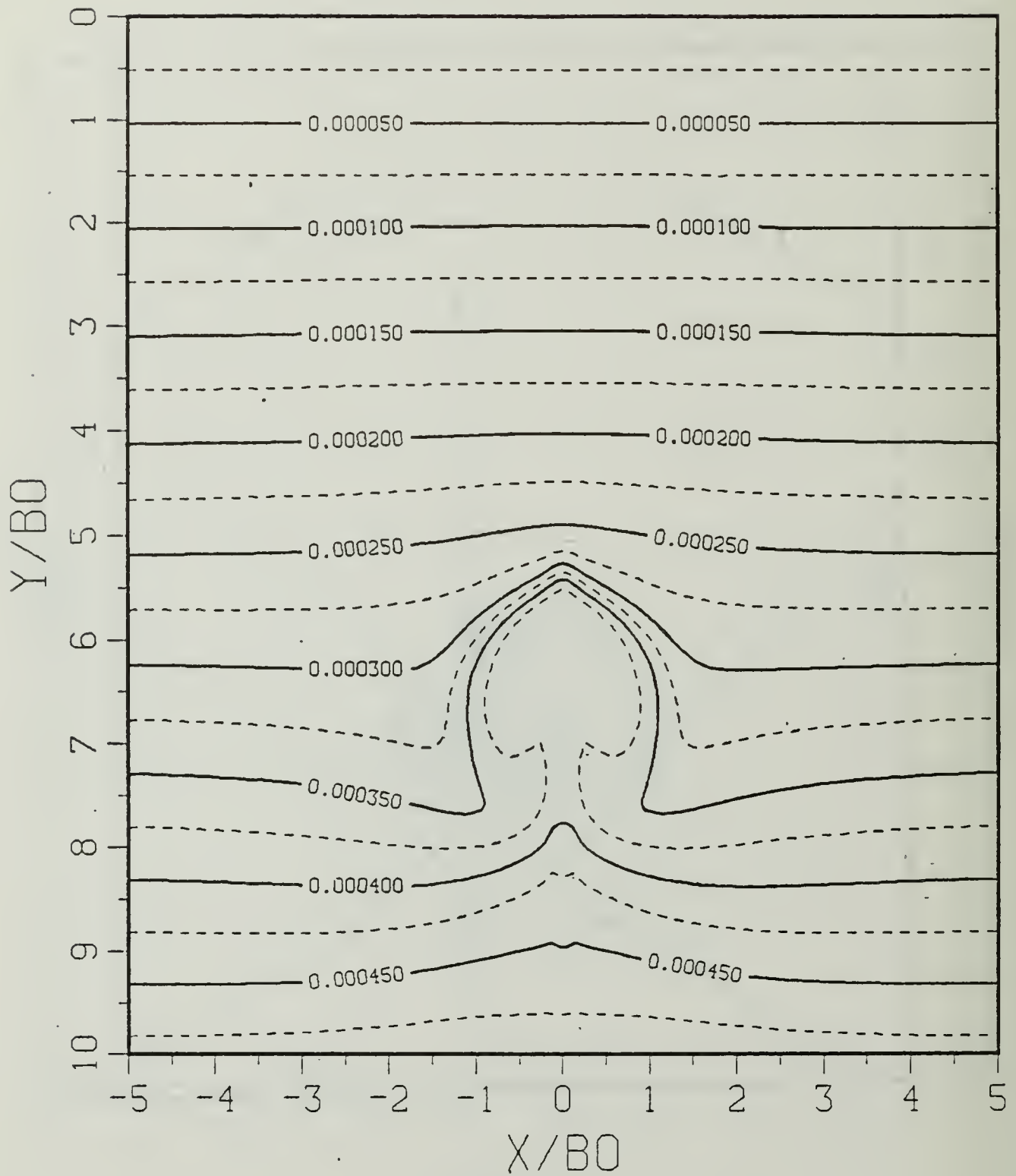


Figure B.22a Constant Density Contours:  $SP = 1.00$ .

$$\Gamma^* = 2.40660$$

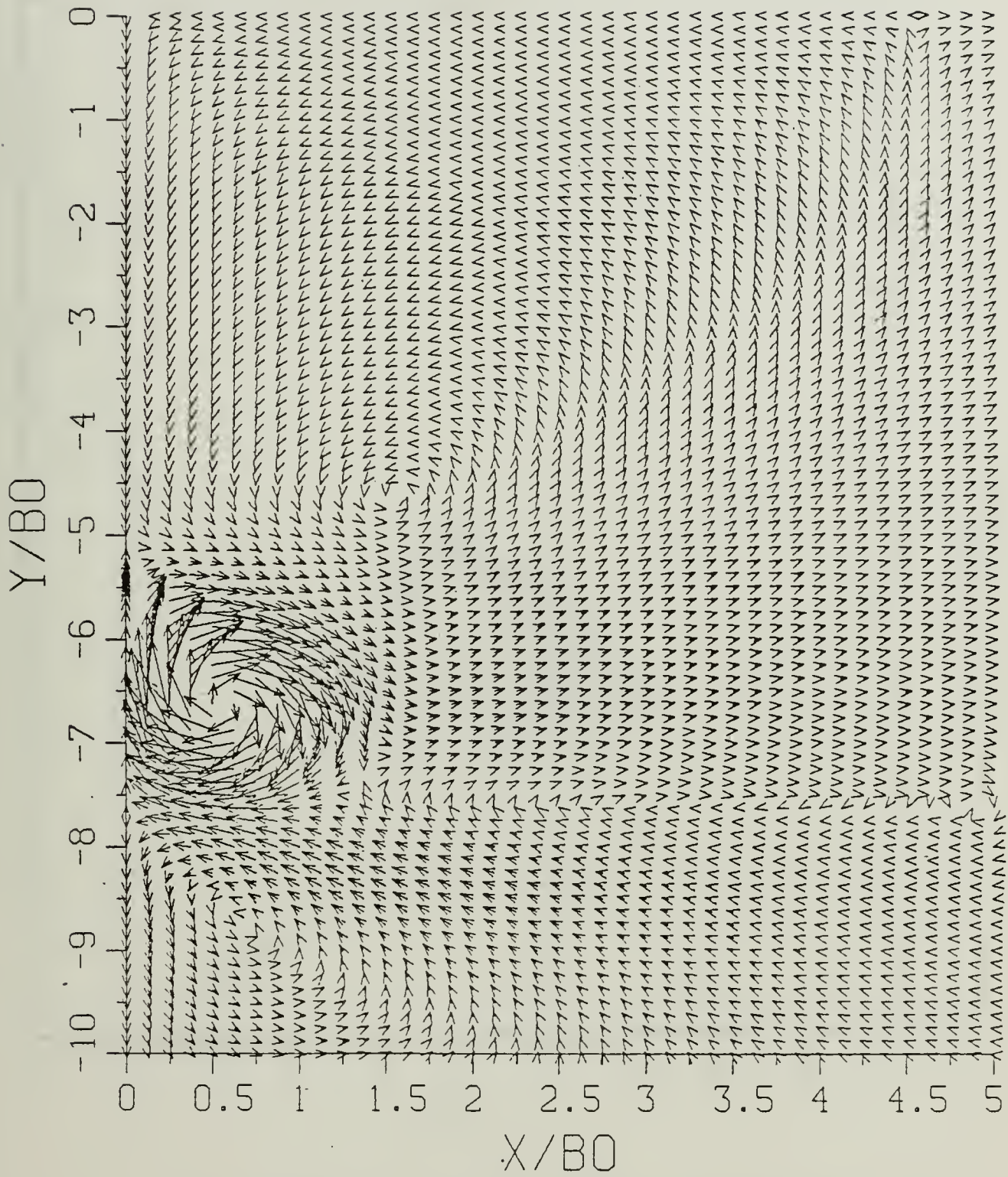


Figure B.22b Velocity Field: SP = 1.00.

$$T^* = 2.40660$$

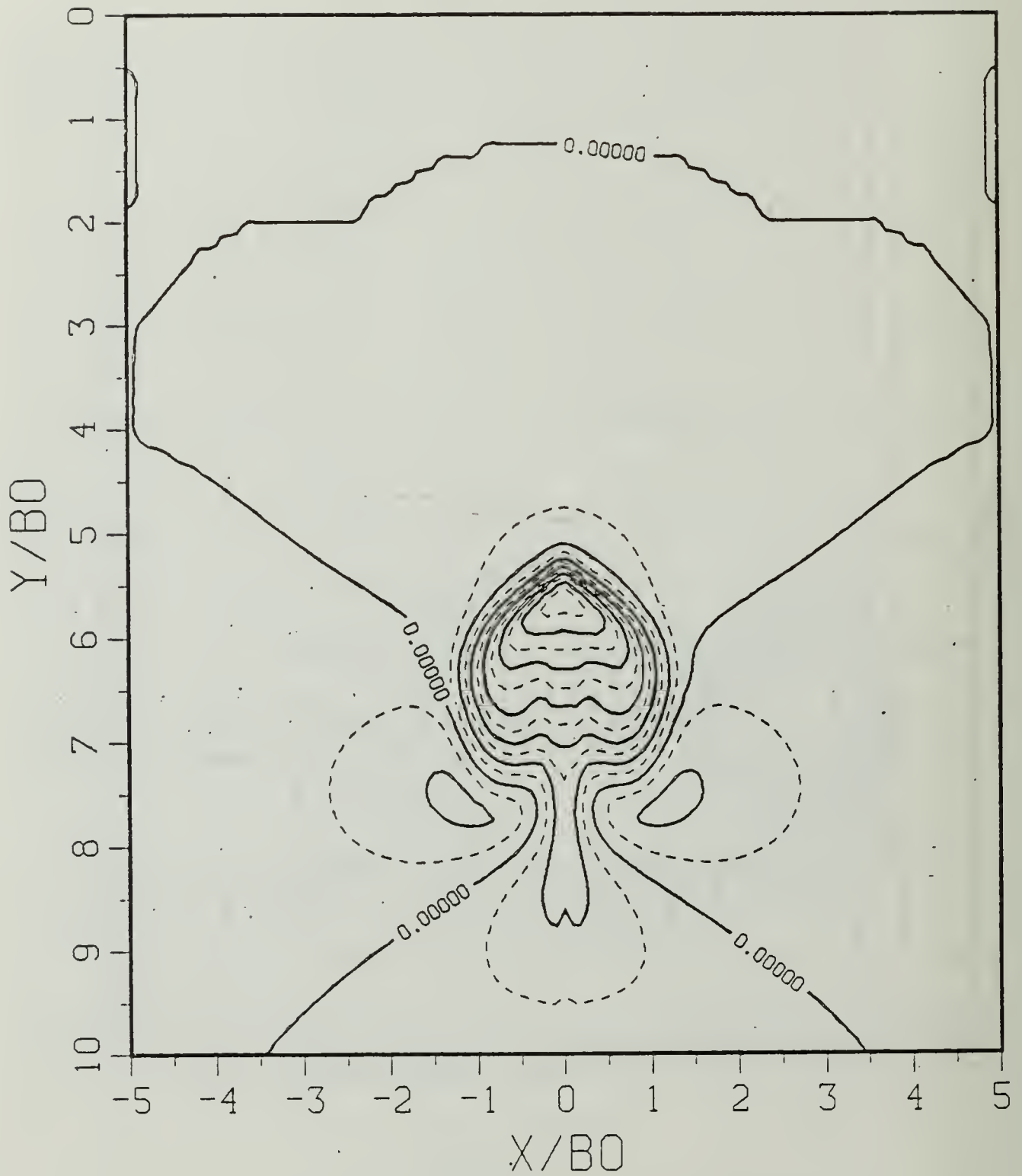


Figure B.22c Density Perturbation Contours:  $SP = 1.00$ .

$$T^* = 2.40660$$

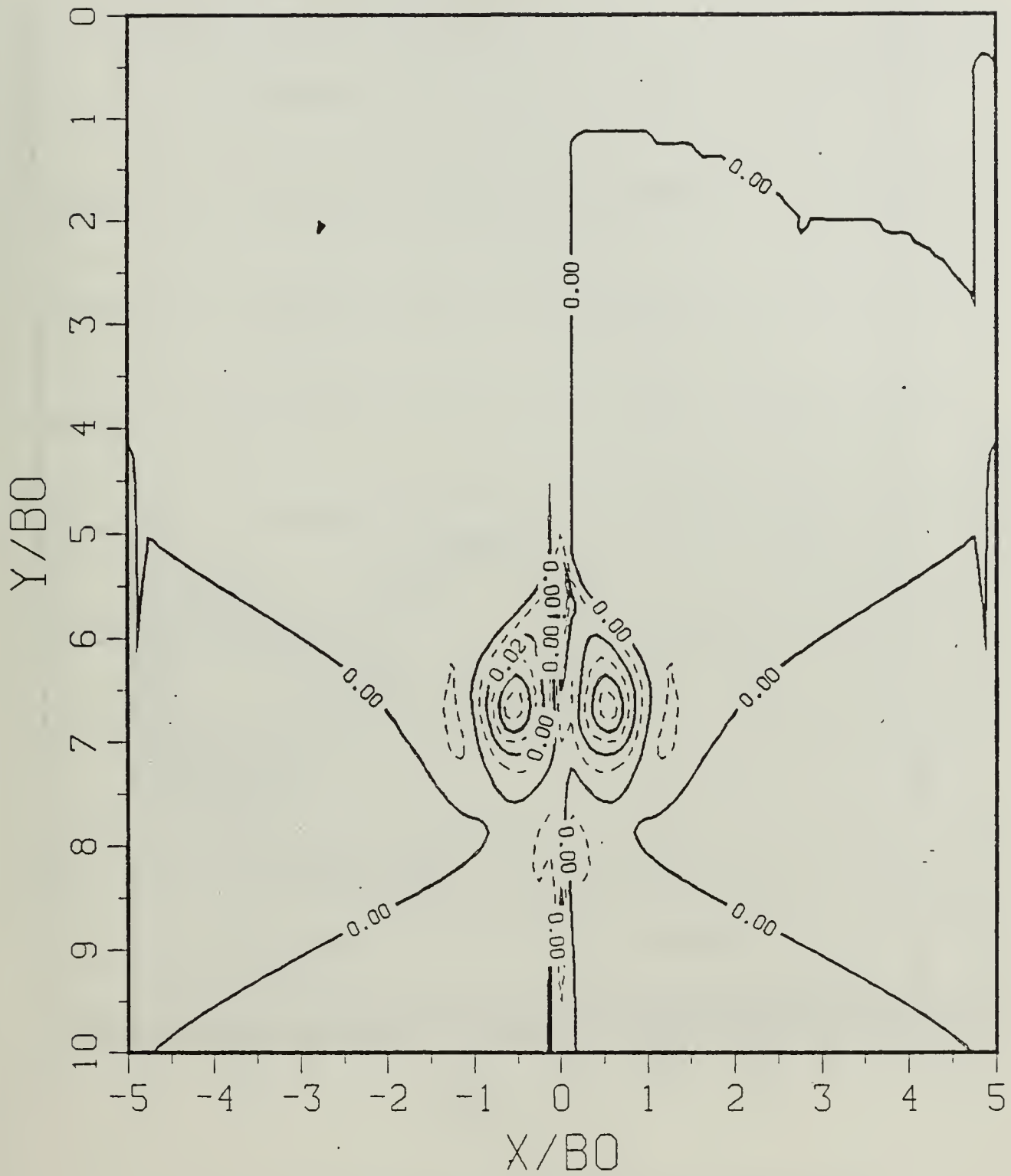


Figure B.22d Vorticity Field: SP = 1.00.

$$T^* = 2.75040$$

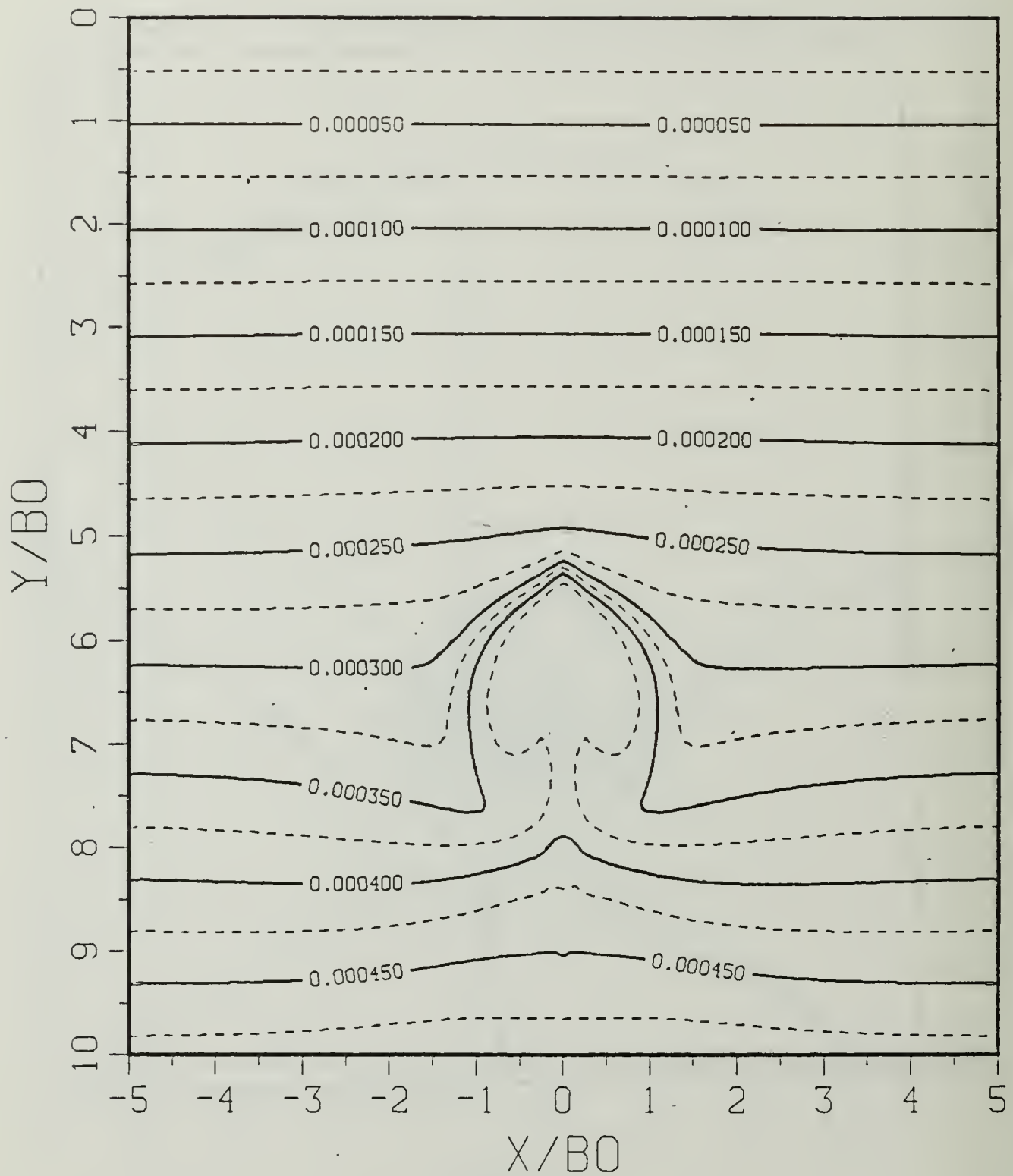


Figure B.23a Constant Density Contours:  $SP = 1.00$ .

$$T^* = 2.75040$$

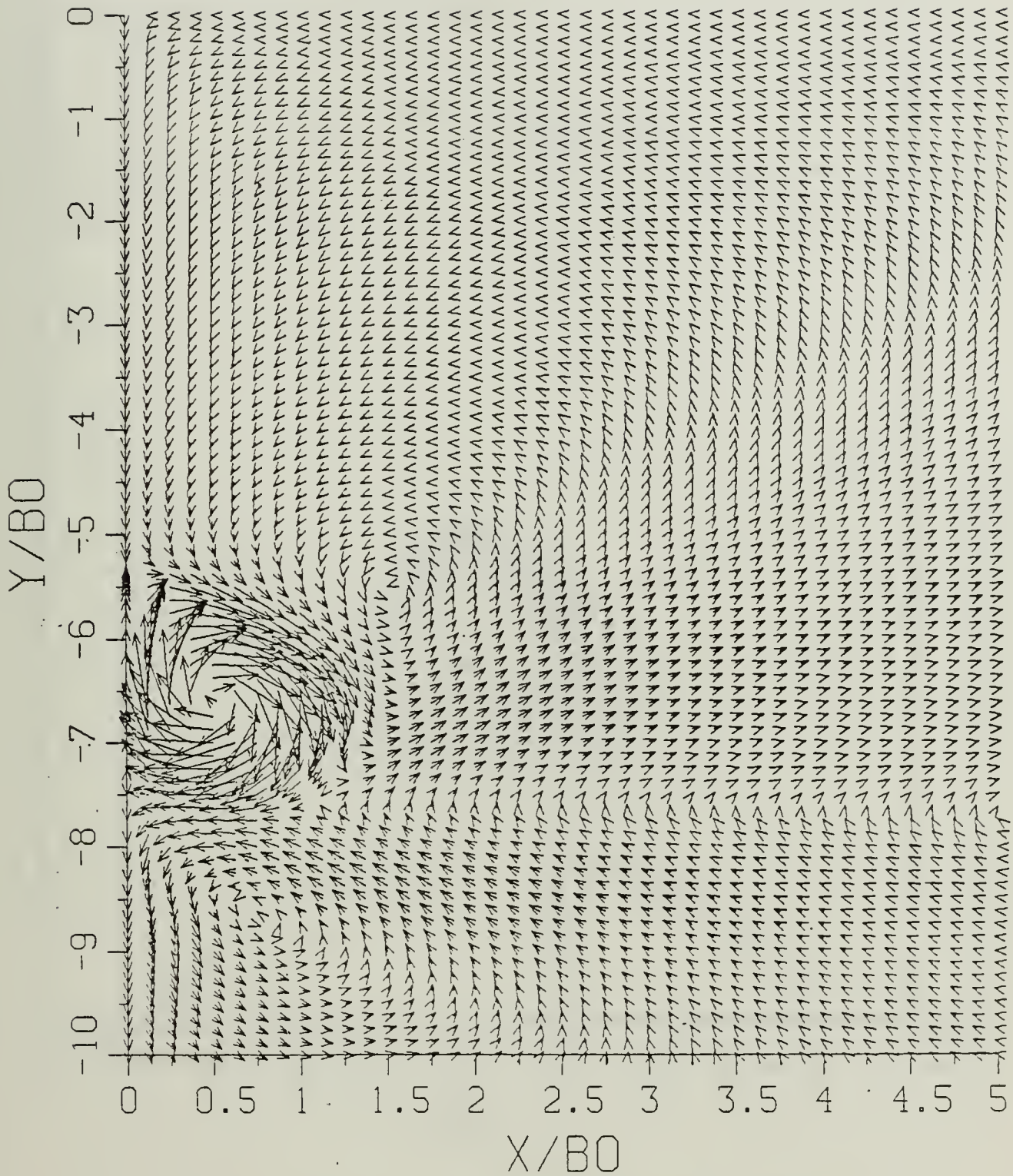


Figure B.23b Velocity Field: SP = 1.00.

$$T^* = 2.75040$$

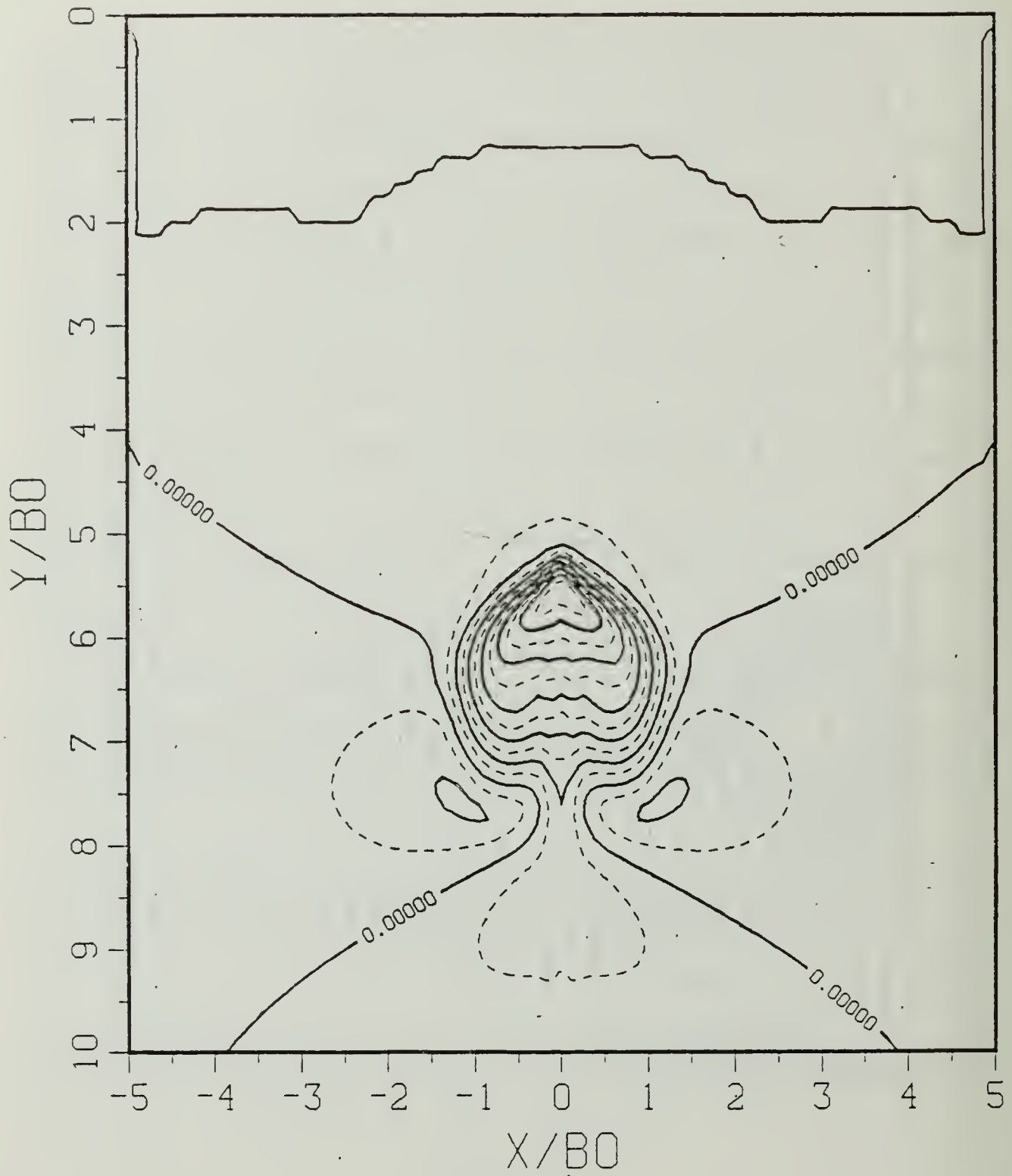


Figure B.23c Density Perturbation Contours:  $SP = 1.00$ .

$$T^* = 2.75040$$

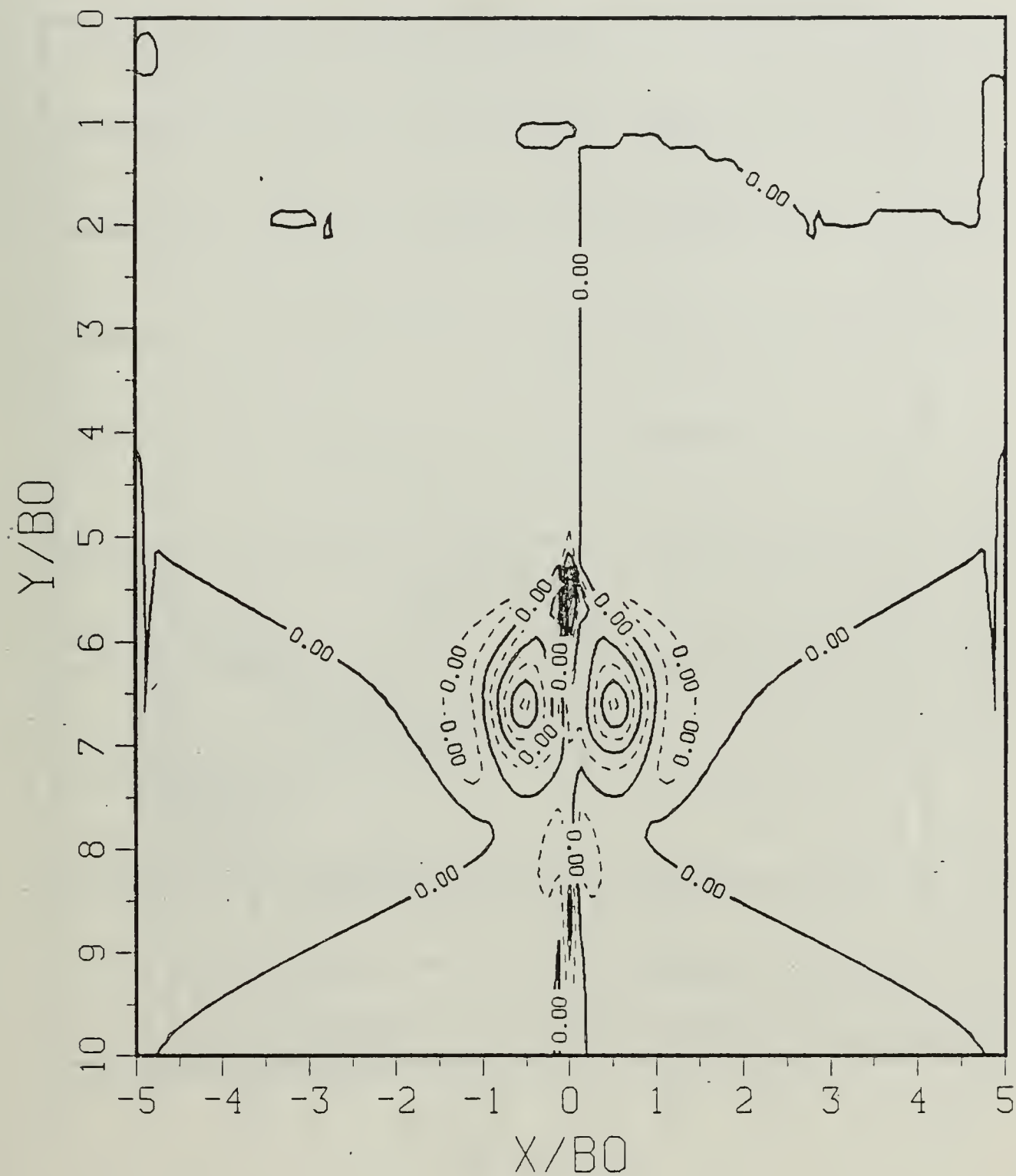


Figure B.23d Vorticity Field: SP = 1.00.

$$T^* = 3.09420$$

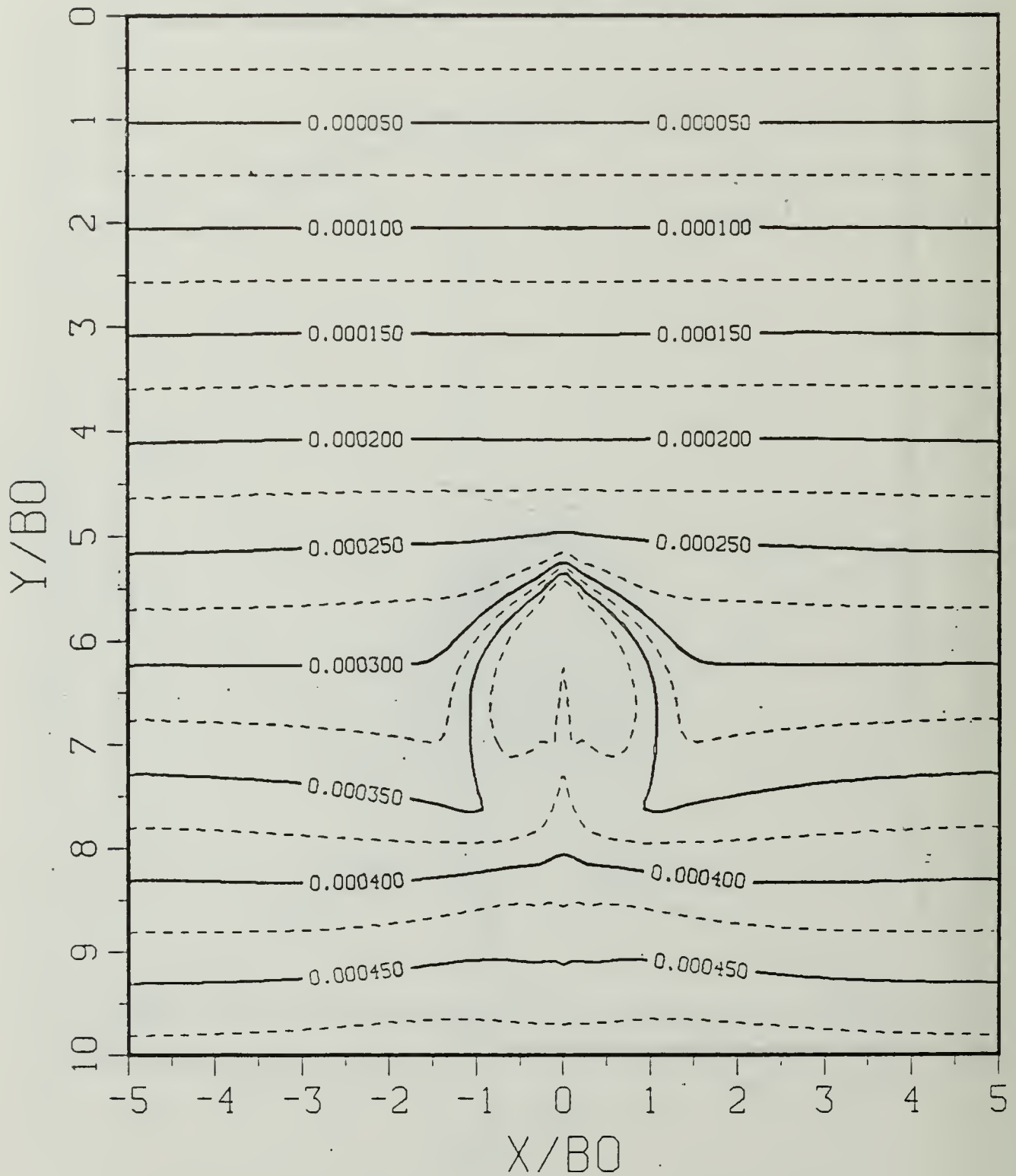


Figure B.24a Constant Density Contours:  $SP = 1.00$ .

$$T^* = 3.09420$$

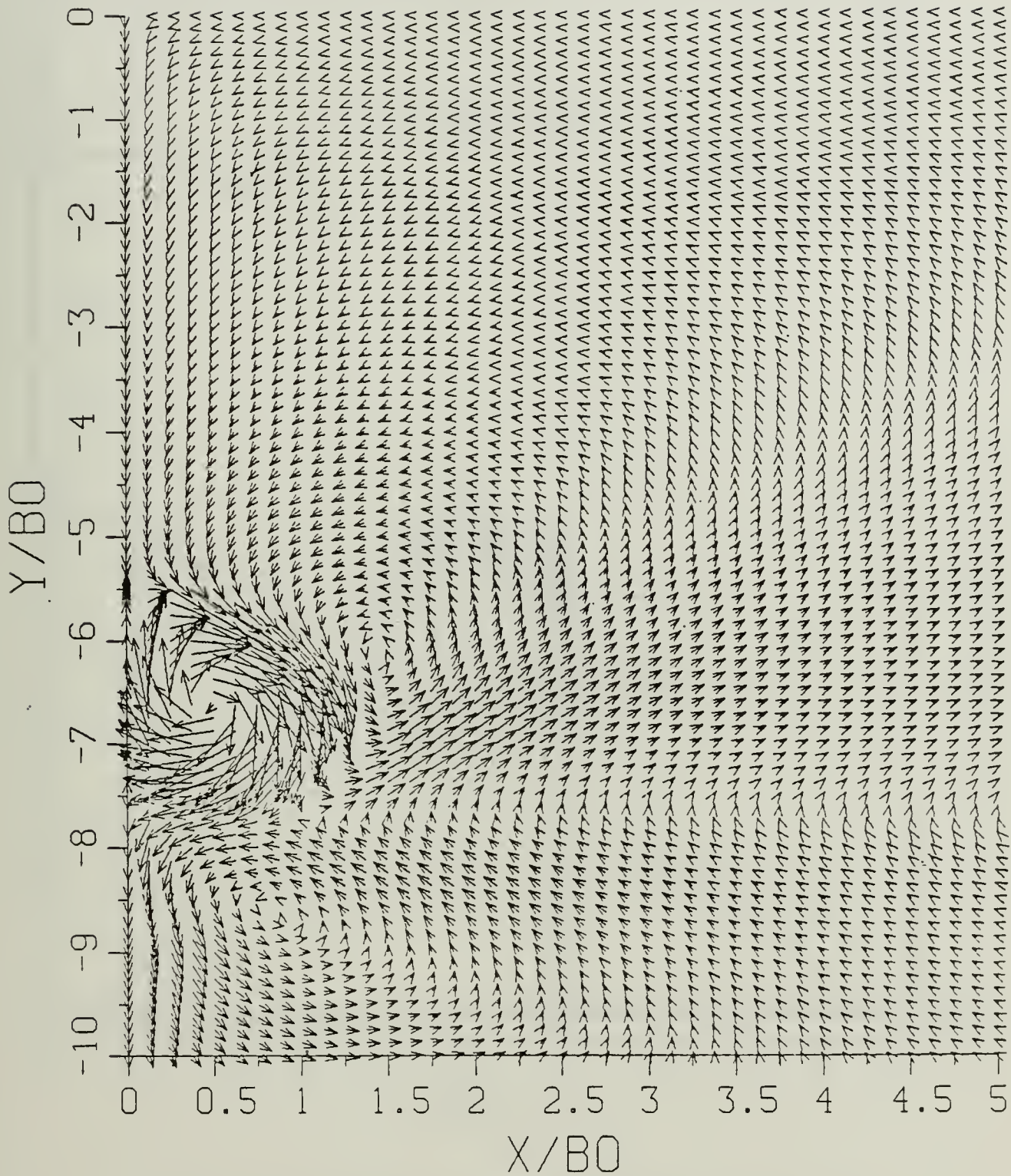


Figure B.24b Velocity Field: SP = 1.00.

$$T^* = 3.09420$$

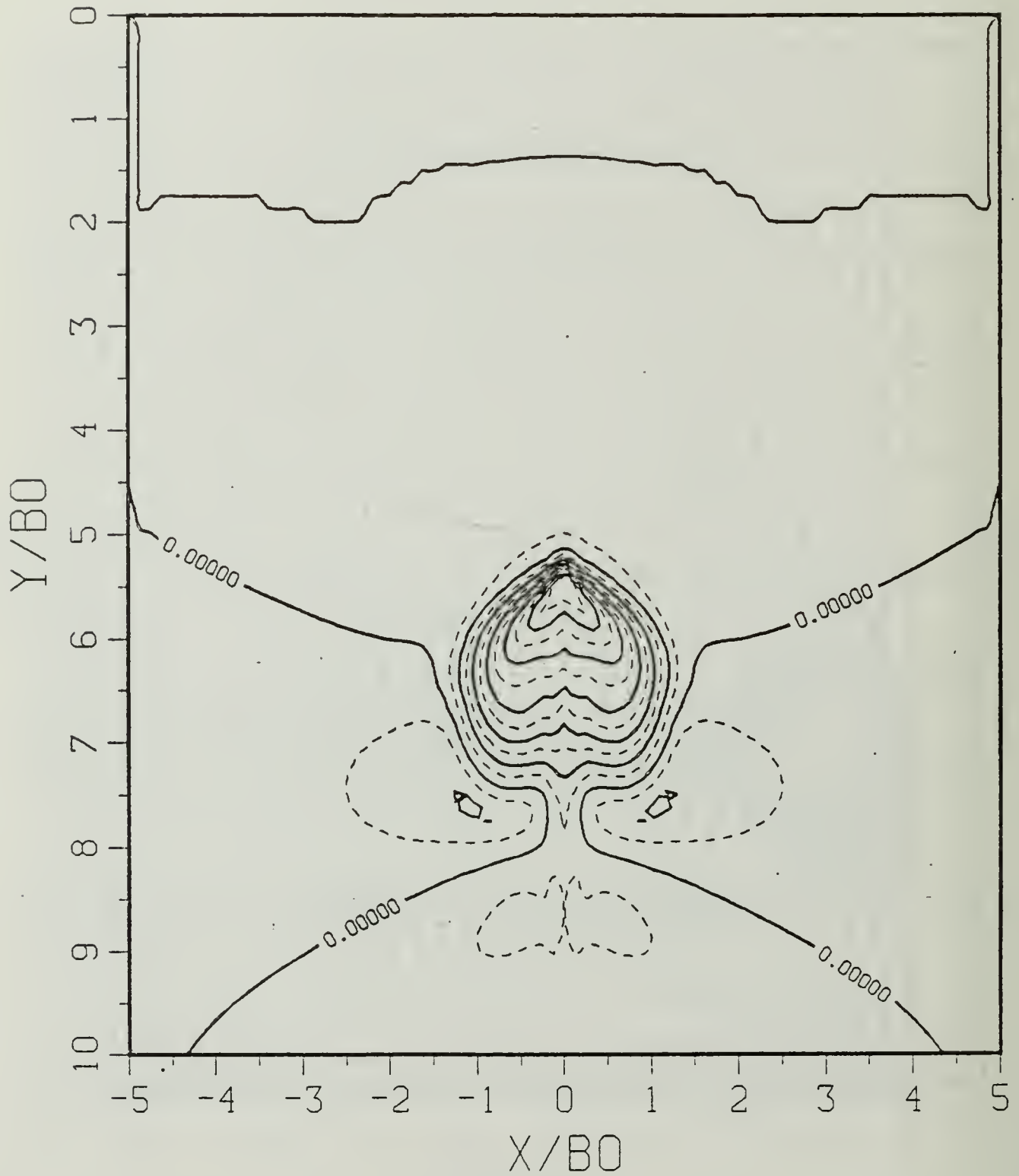


Figure B.24c Density Perturbation Contours: SP = 1.00.

$$T^* = 3.09420$$

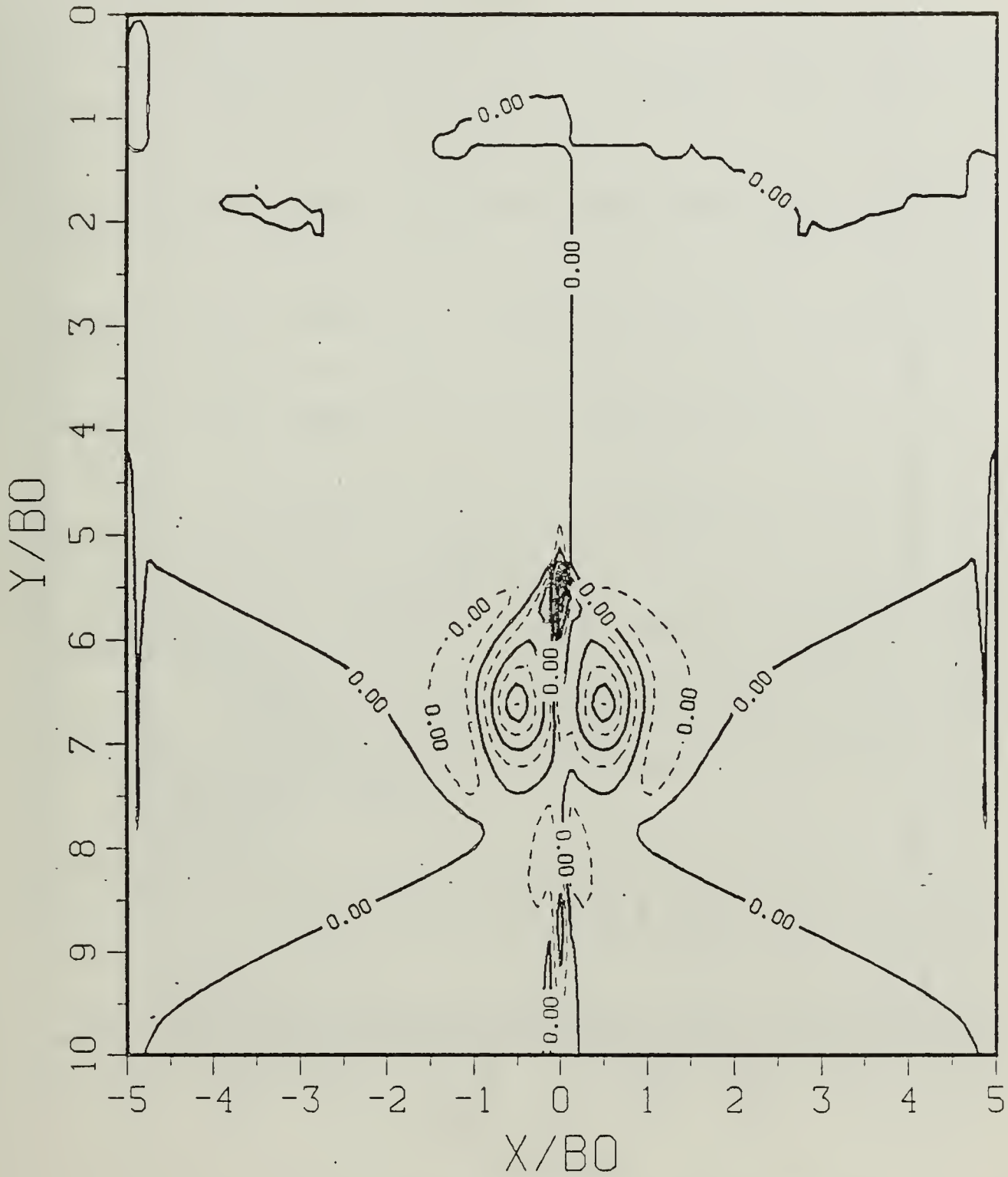


Figure B.24d Vorticity Field:  $SP = 1.00$ .

$$T^* = 3.43800$$

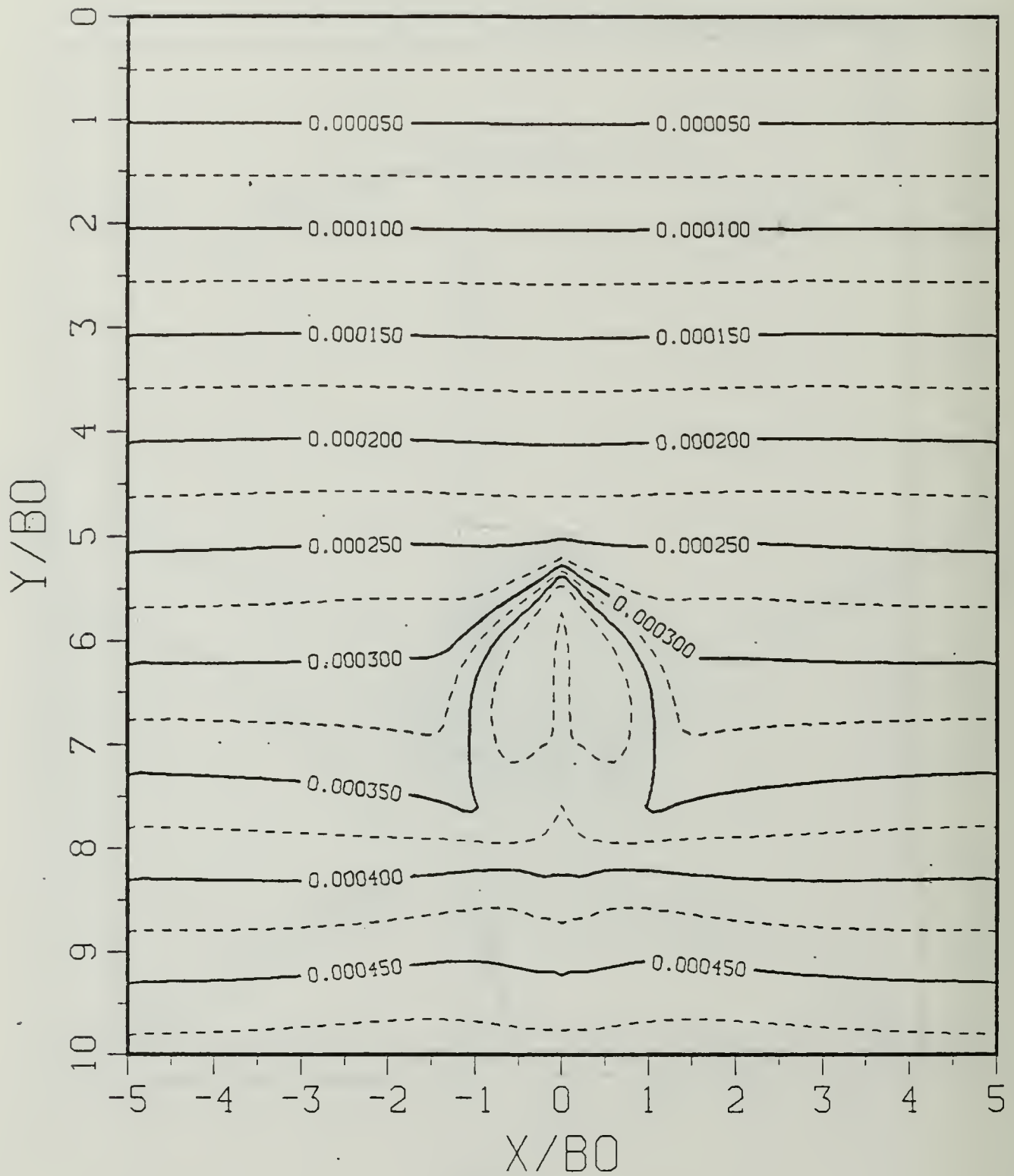


Figure B.25a Constant Density Contours:  $SP = 1.00$ .

$$T^* = 3.43800$$

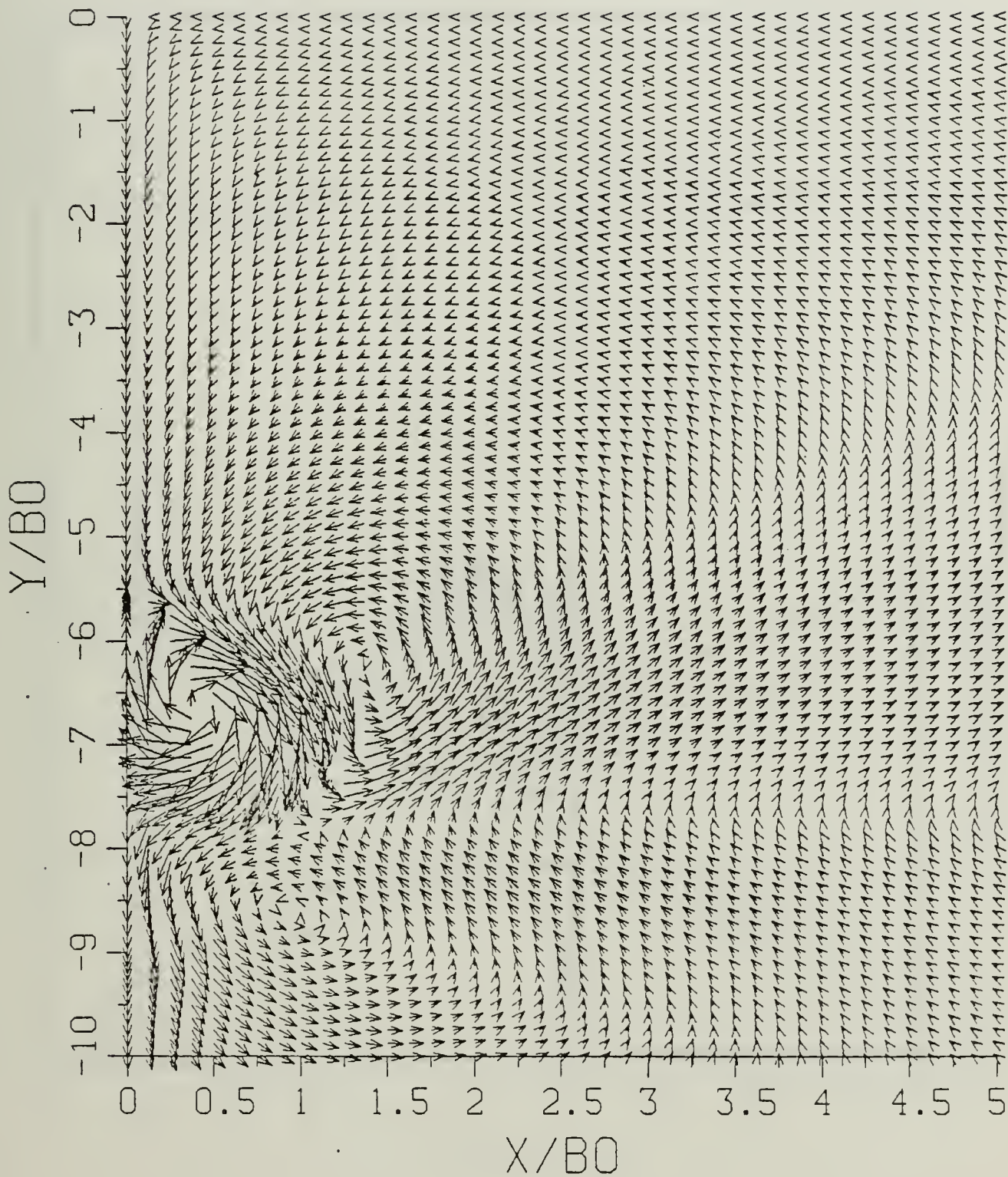


Figure B.25b .Velocity Field: SP = 1.00.

$$T^* = 3.43800$$

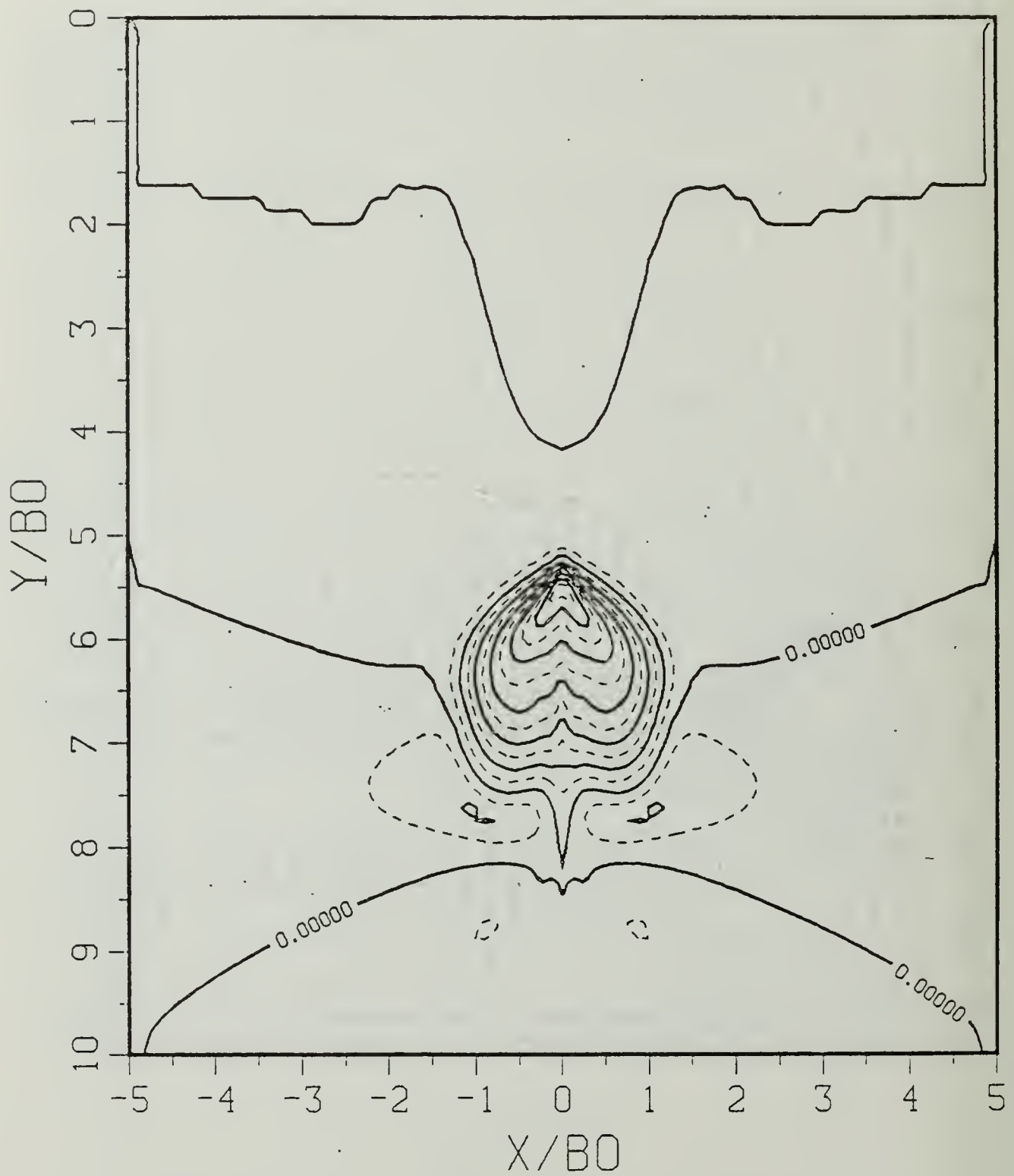


Figure B.25c Density Perturbation Contours:  $SP = 1.00$ .



$$T^* = 3.78180$$

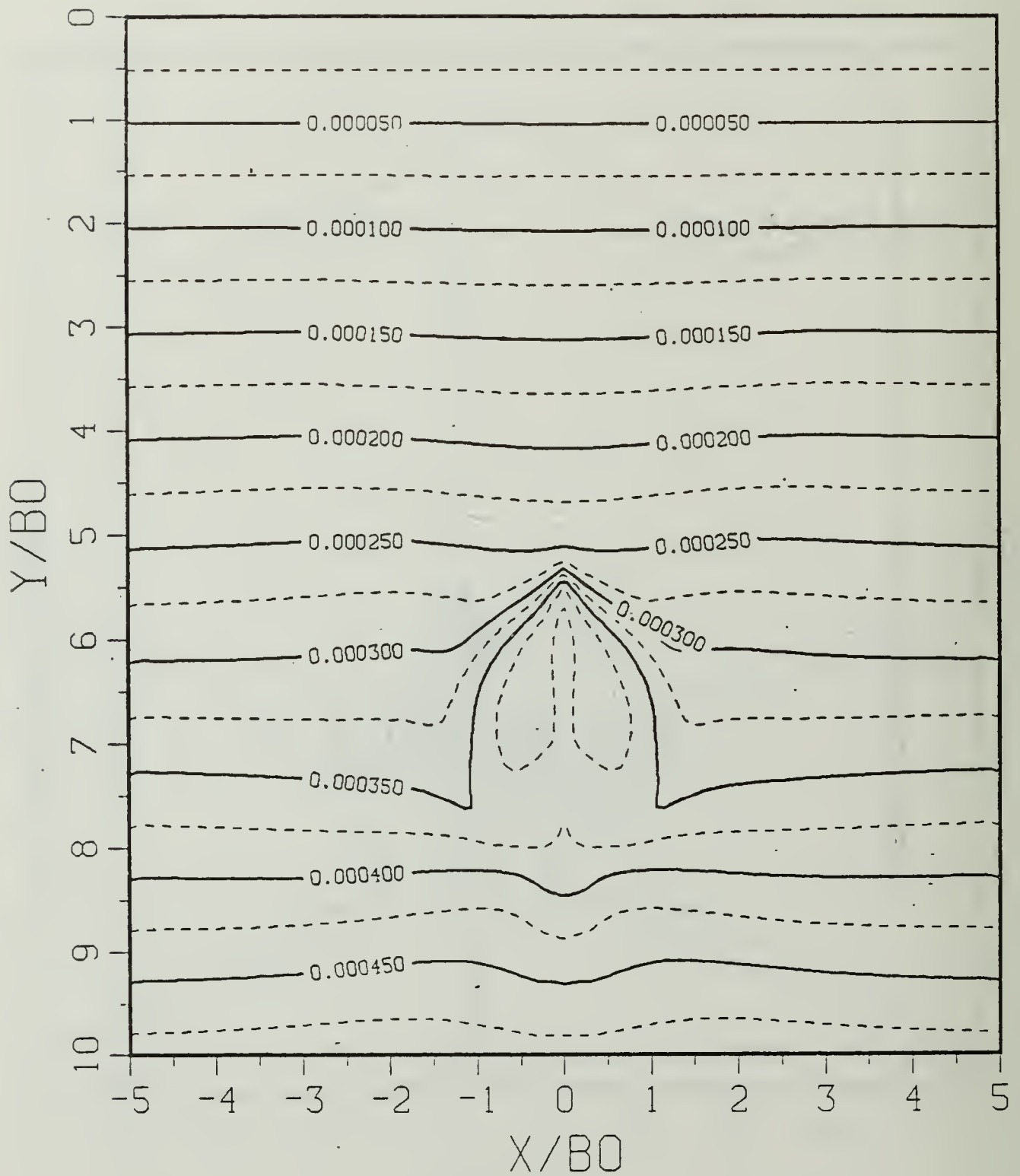


Figure B.26a Constant Density Contours:  $SP = 1.00$ .

$$T^* = 3.78180$$

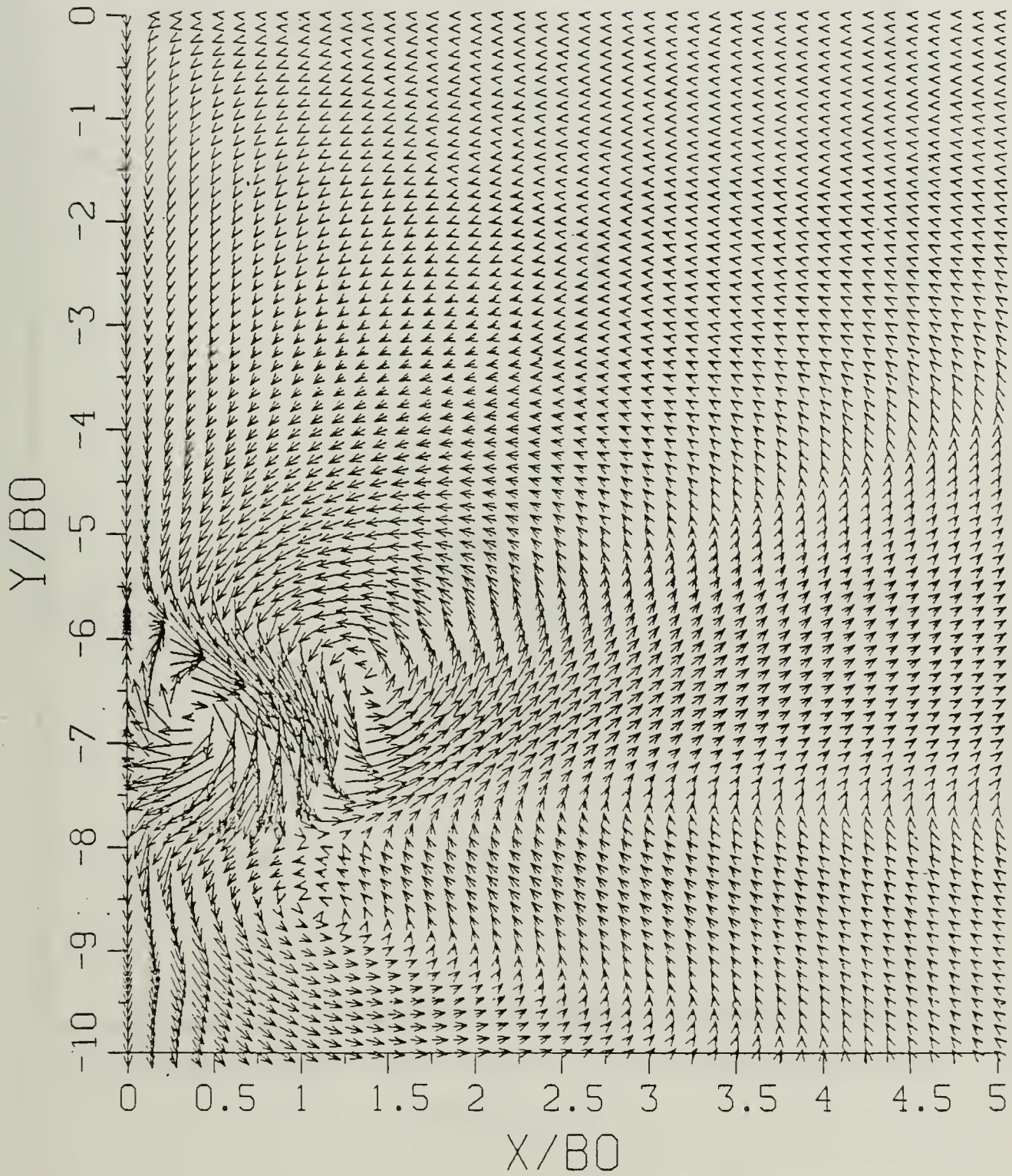


Figure B.26b Velocity Field: SP = 1.00.

$$T^* = 3.78180$$

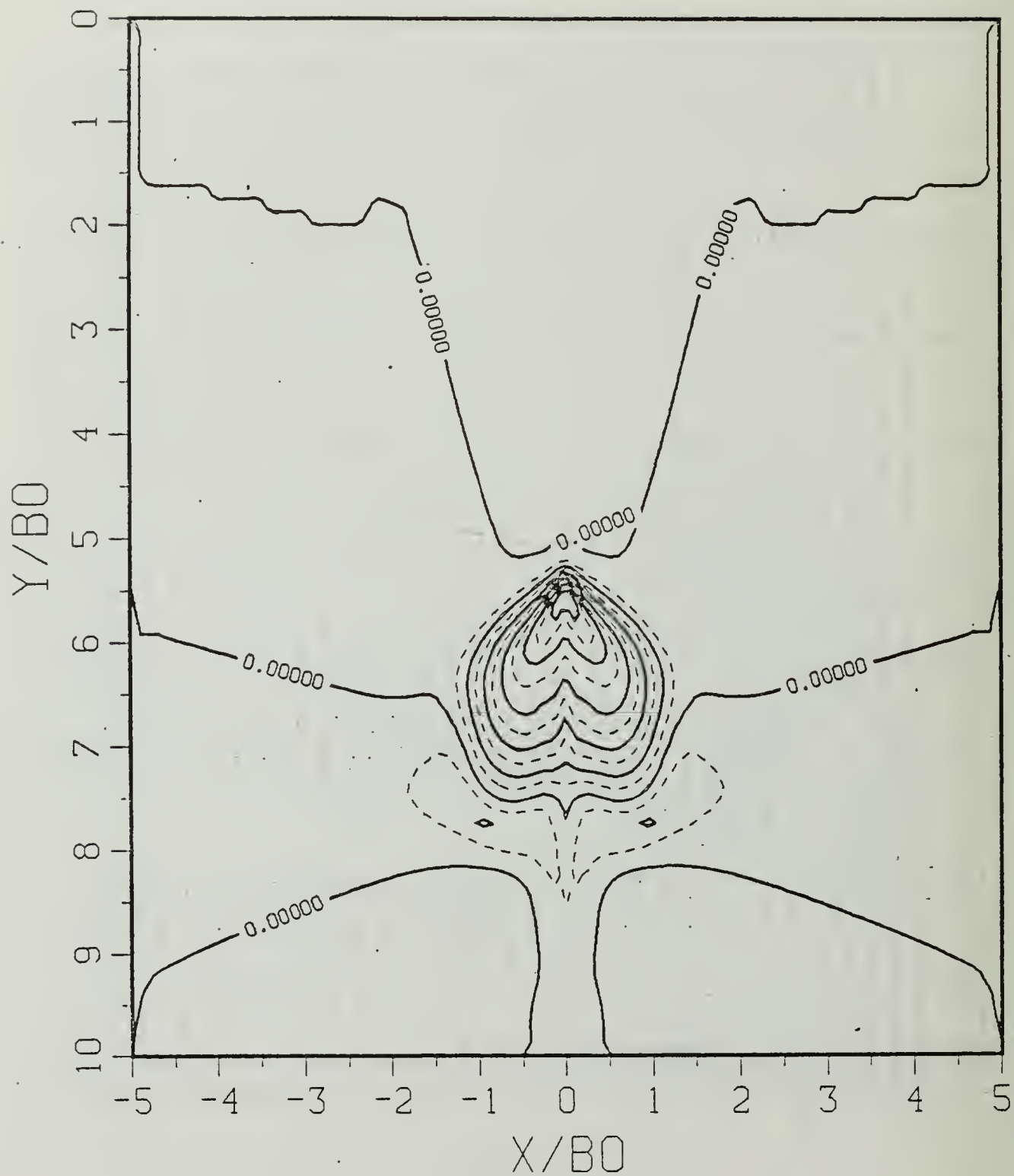


Figure B.26c Density Perturbation Contours: SP = 1.00.

$$T^* = 3.78180$$

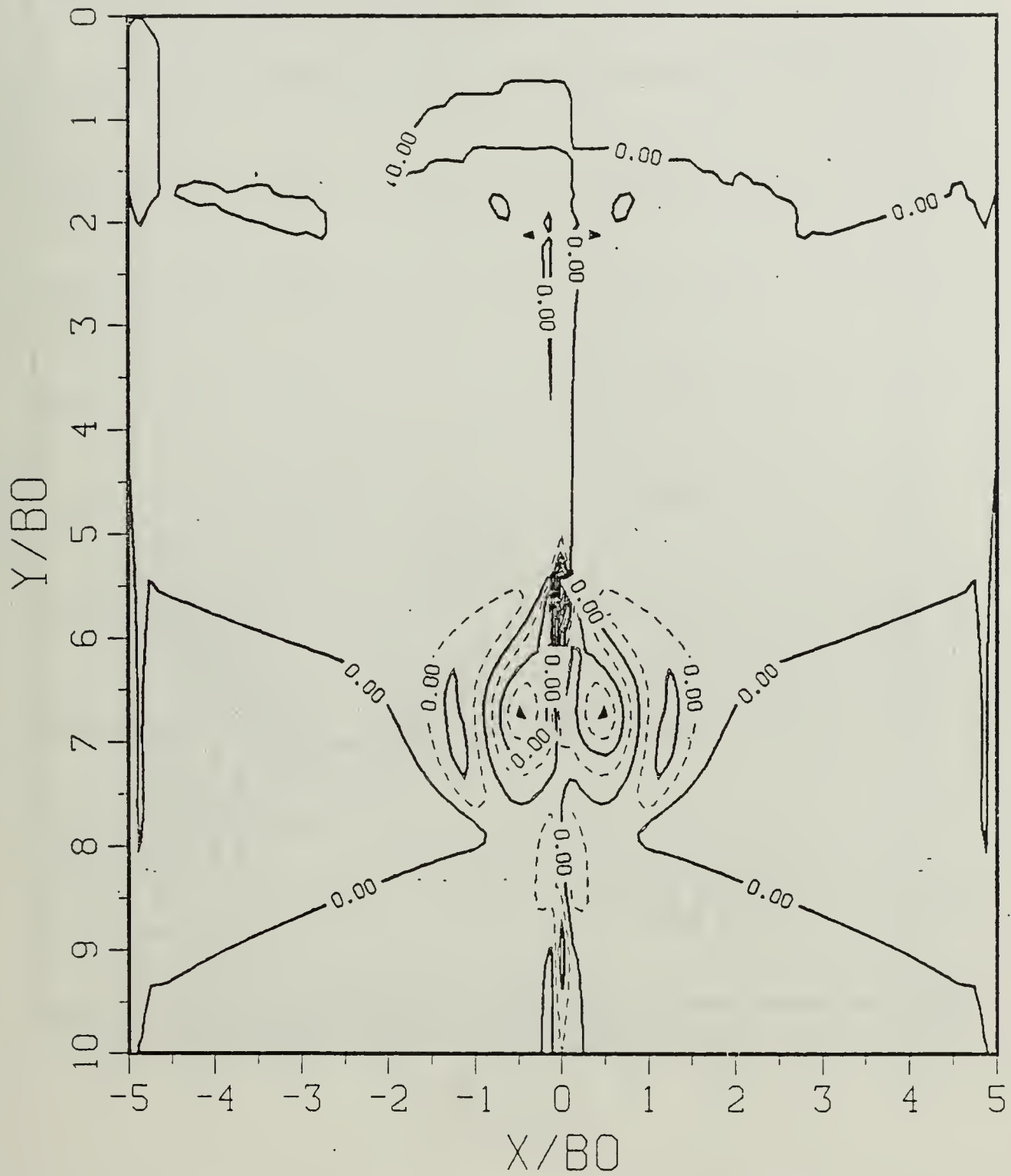


Figure B.26d Vorticity Field: SP = 1.00.

$$T^* = 4.12560$$

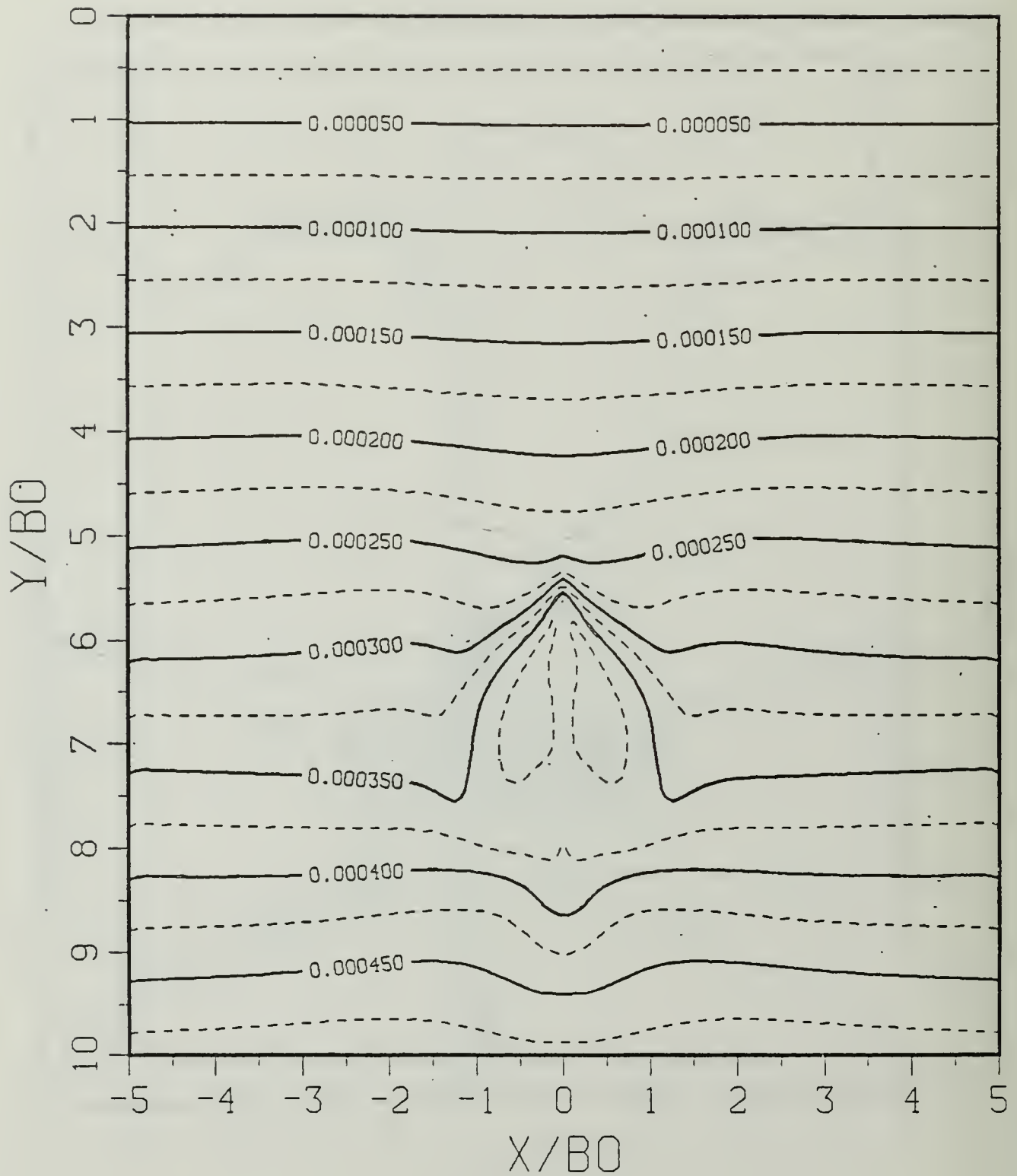


Figure B.27a Constant Density Contours:  $SP = 1.00$ .

$$T^* = 4.12560$$

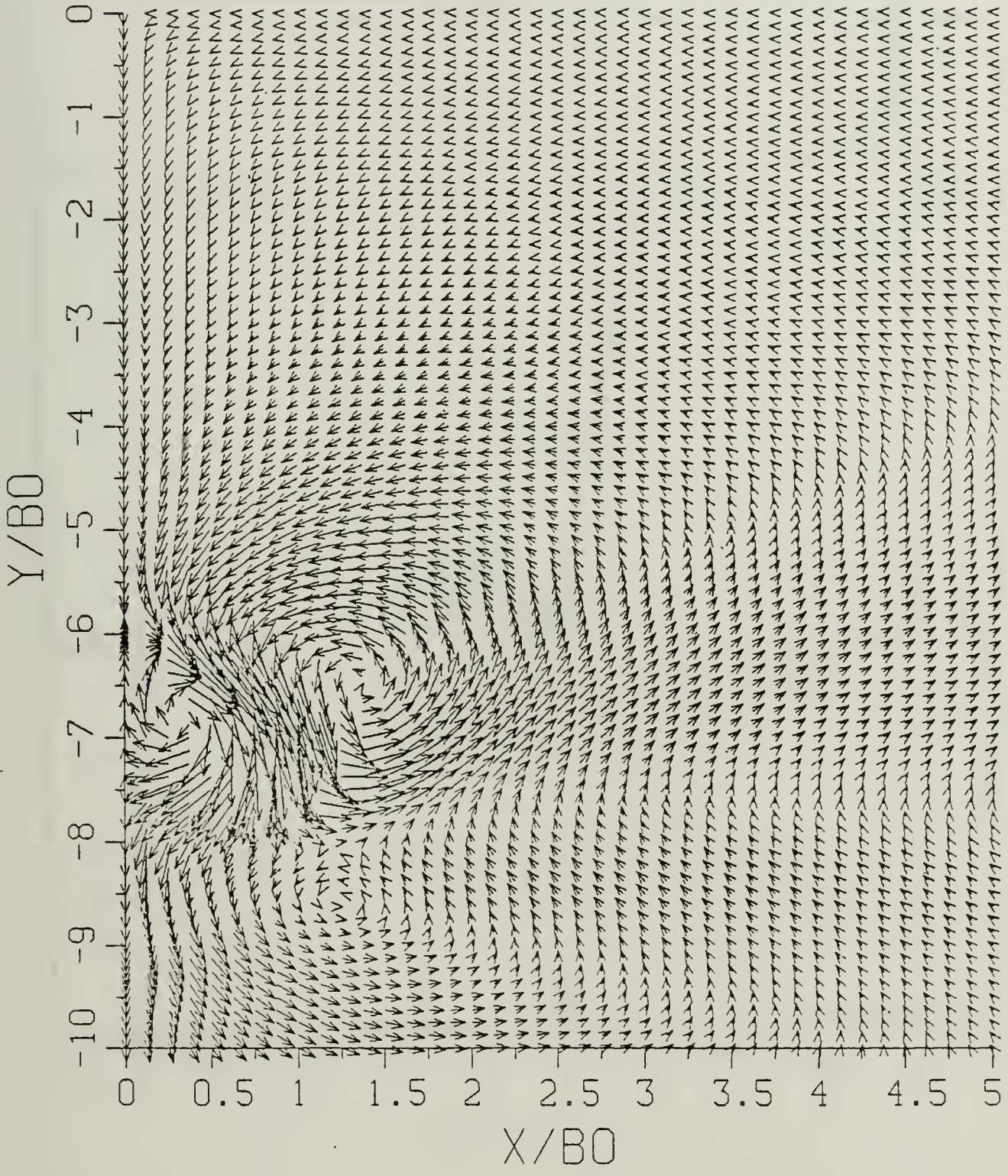


Figure B.27b Velocity Field:  $SP = 1.00$ .

$$T^* = 4.12560$$

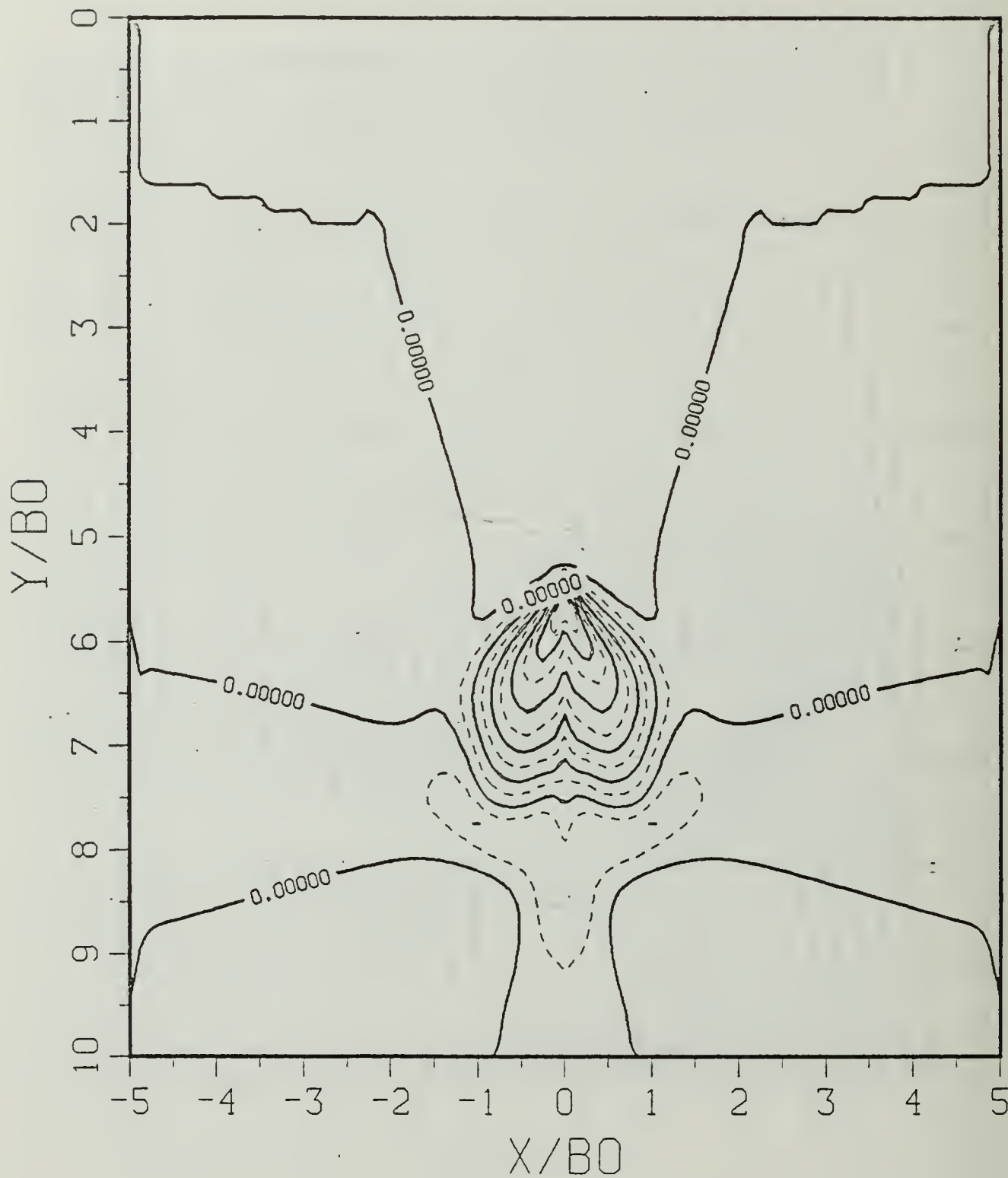


Figure B.27c Density Perturbation Contours: SP = 1.00.

$$T^* = 4.12560$$

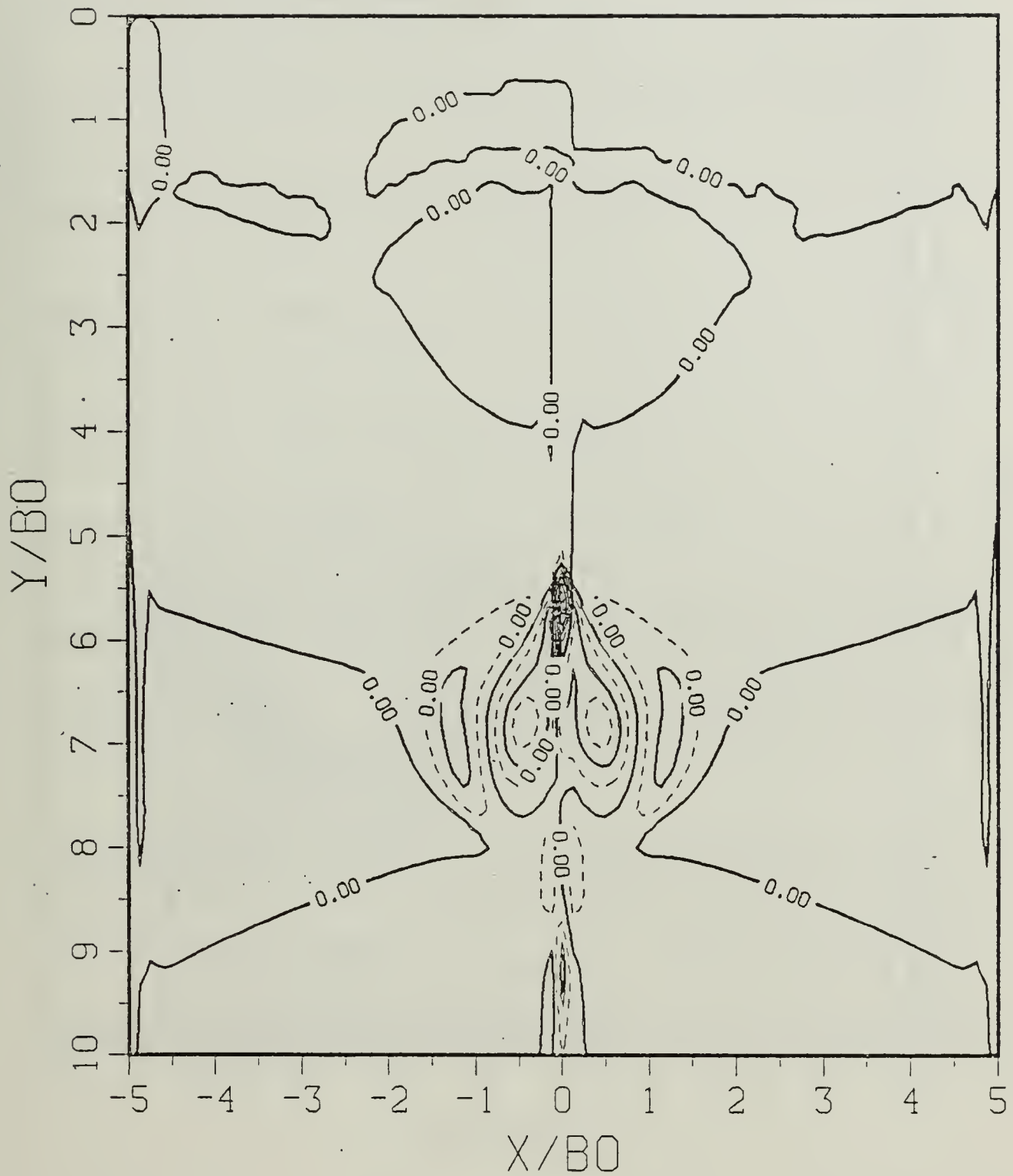


Figure B.27d Vorticity Field: SP = 1.00.

$$T^* = 4.46940$$

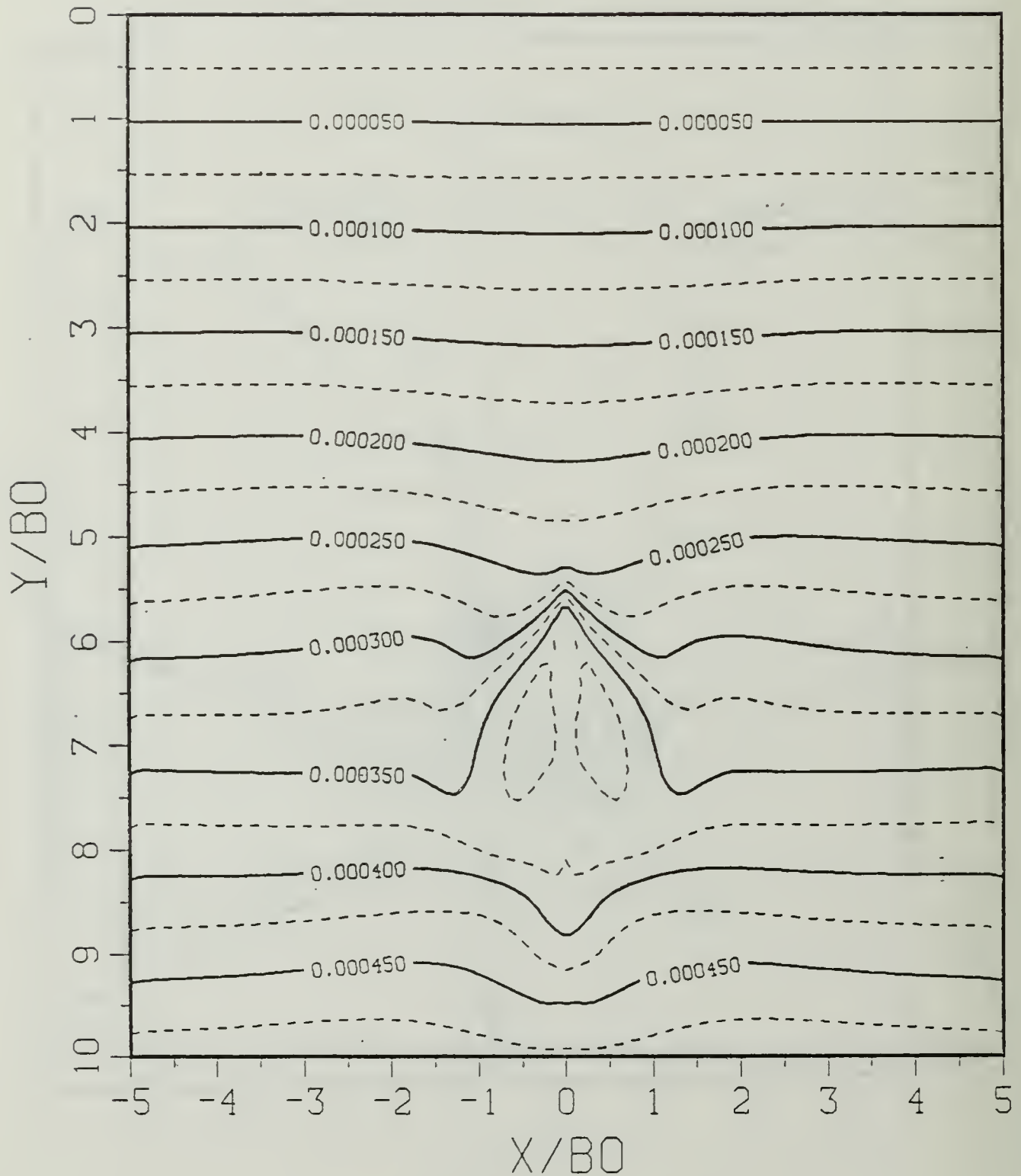


Figure B.28a Constant Density Contours:  $SP = 1.00$ .

$$T^* = 4.46940$$

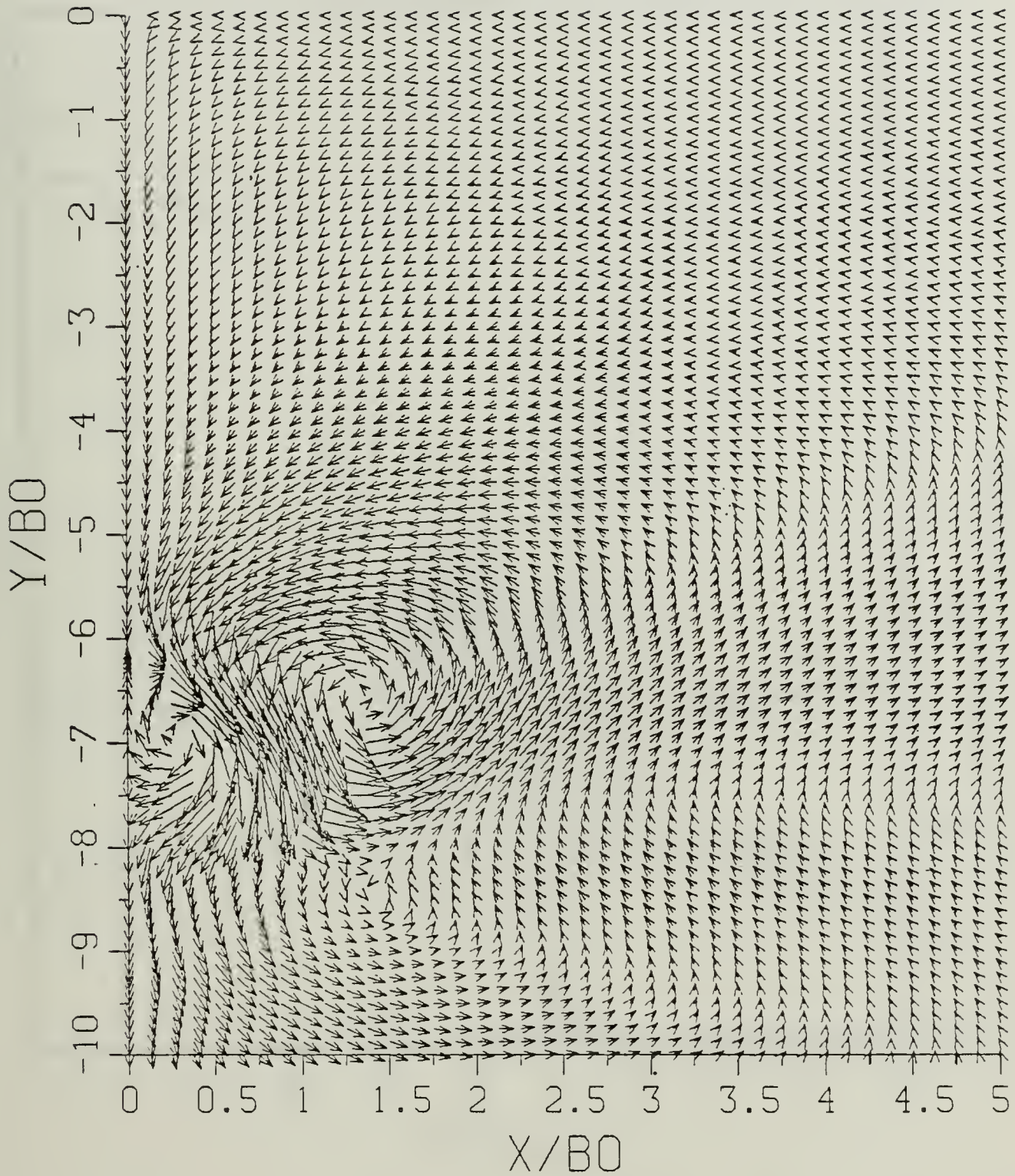


Figure B.28b Velocity Field:  $SP = 1.00$ .

$$T^* = 4.46940$$

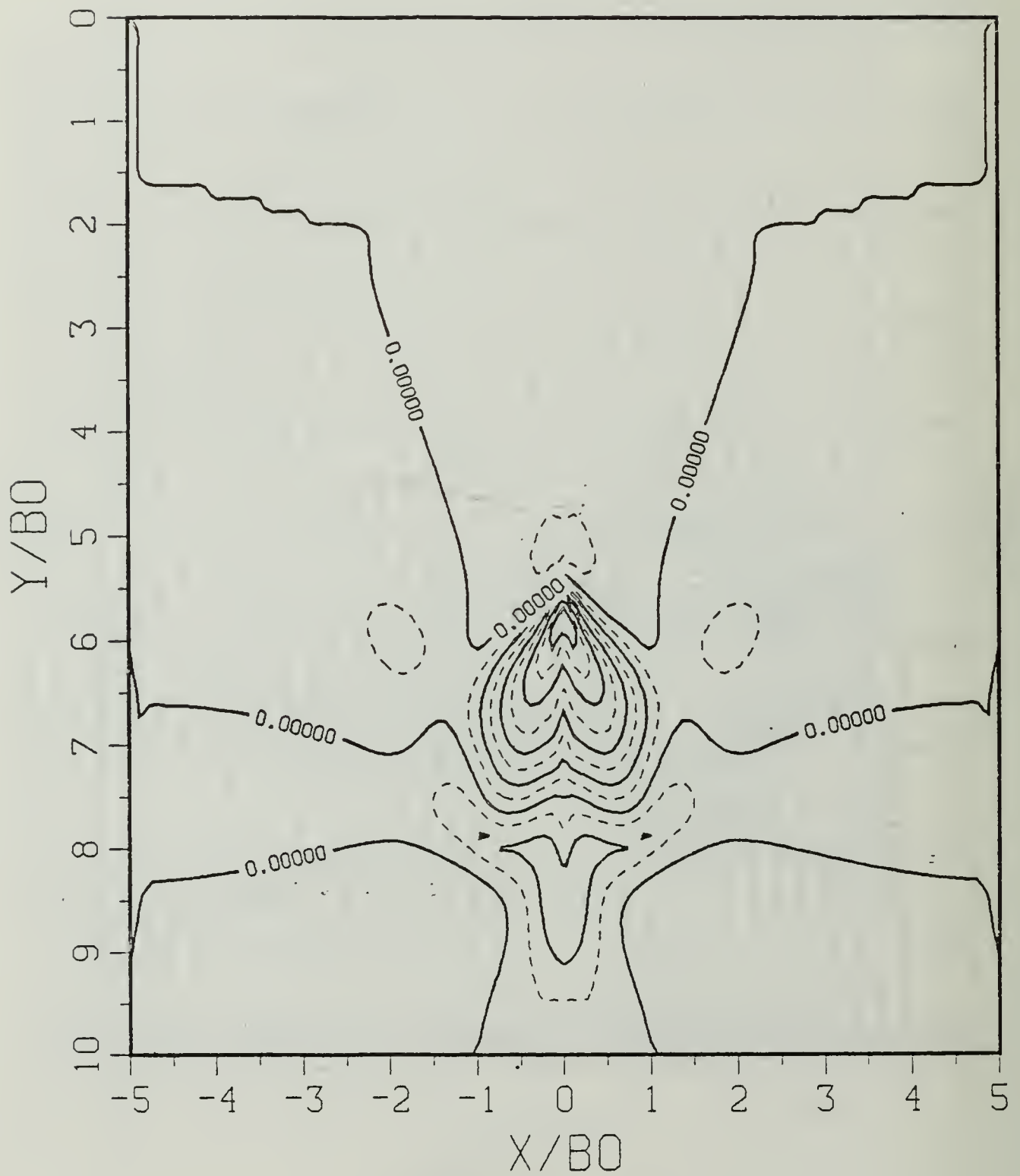


Figure B.28c Density Perturbation Contours: SP = 1.00.

$$T^* = 4.46940$$

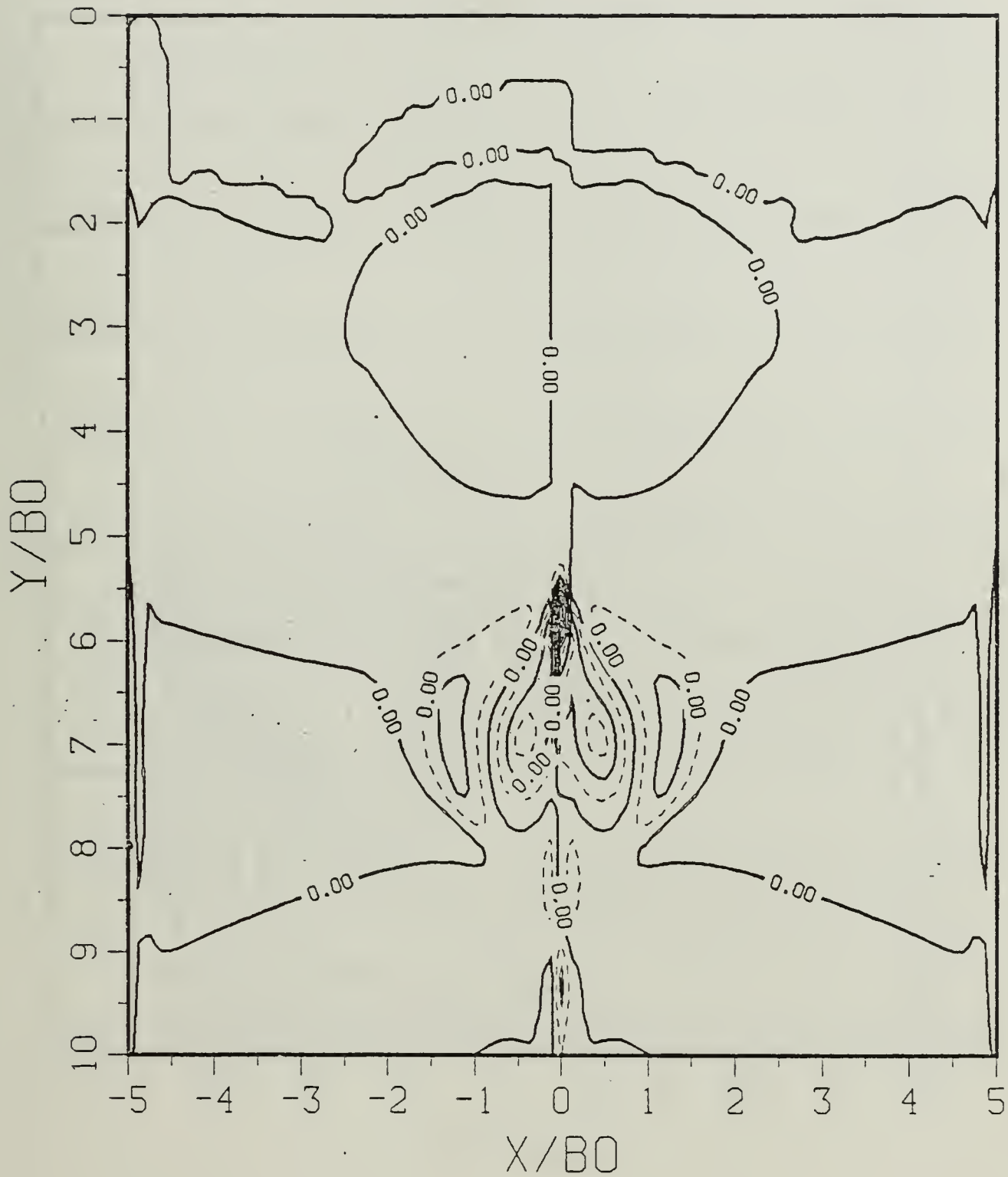


Figure B.28d Vorticity Field: SP = 1.00.

$$T^* = 4.81320$$

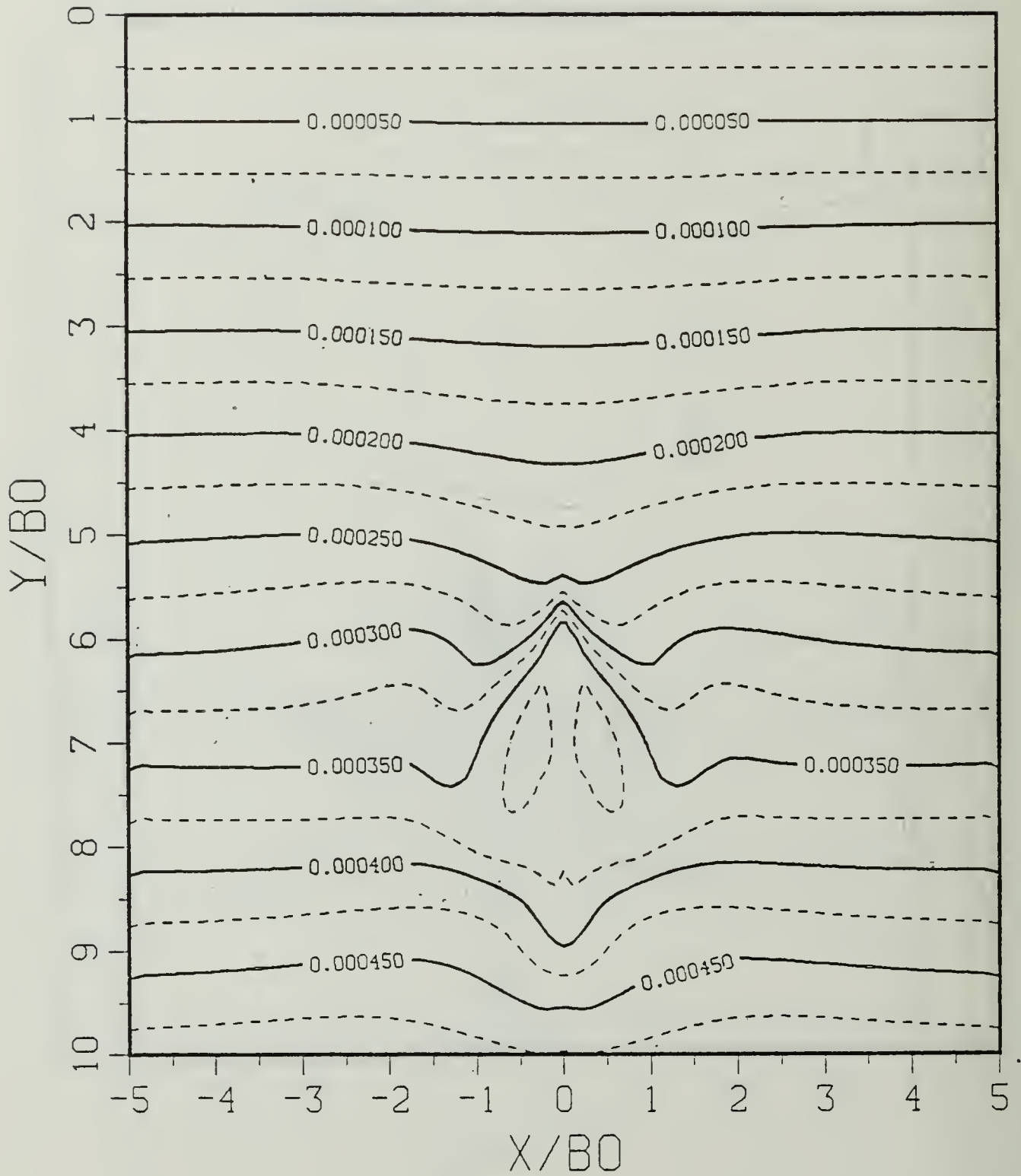


Figure B.29a Constant Density Contours:  $SP = 1.00$ .

$$T^* = 4.81320$$

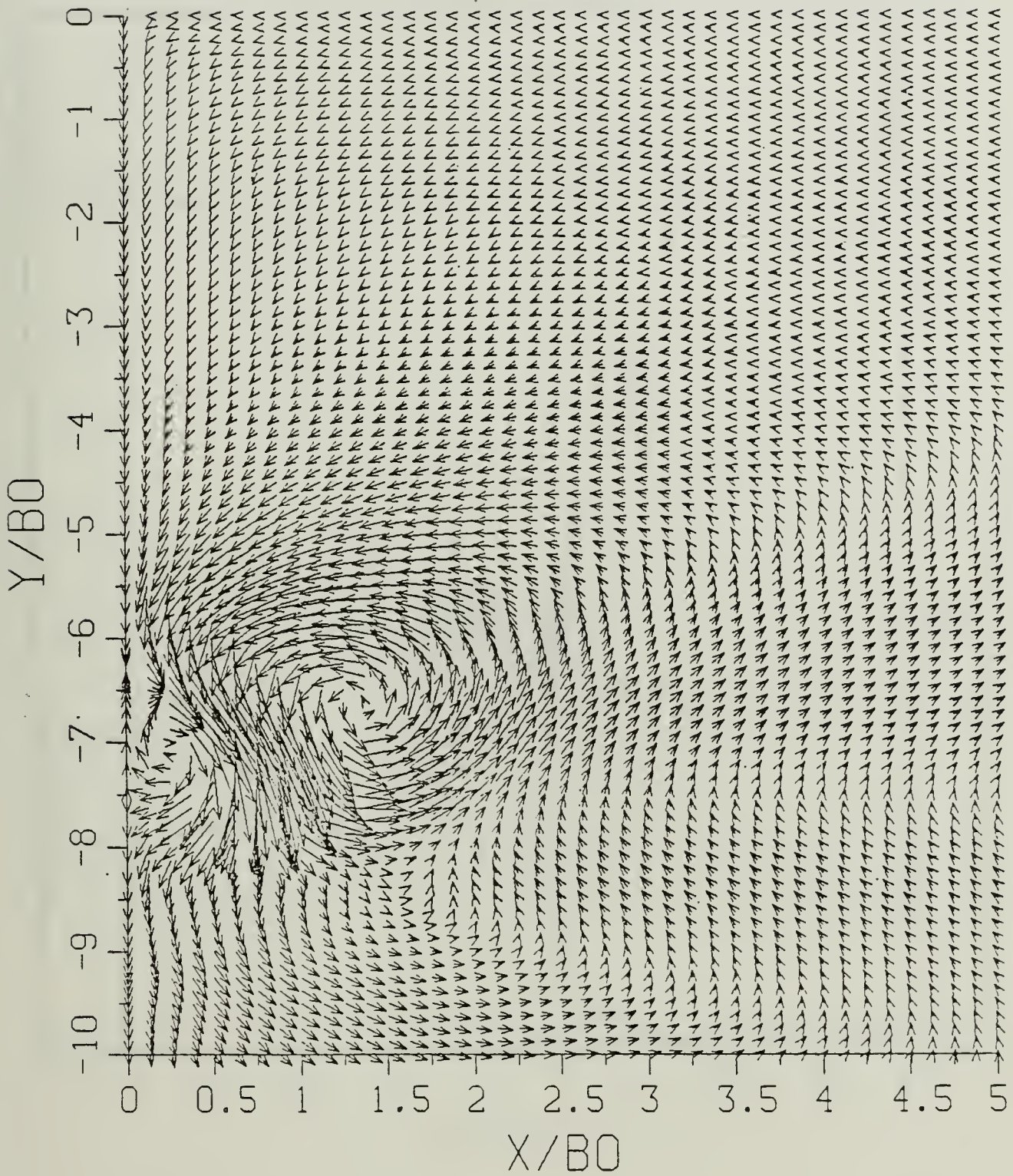


Figure B.29b Velocity Field: SP = 1.00.

$$T^* = 4.81320$$

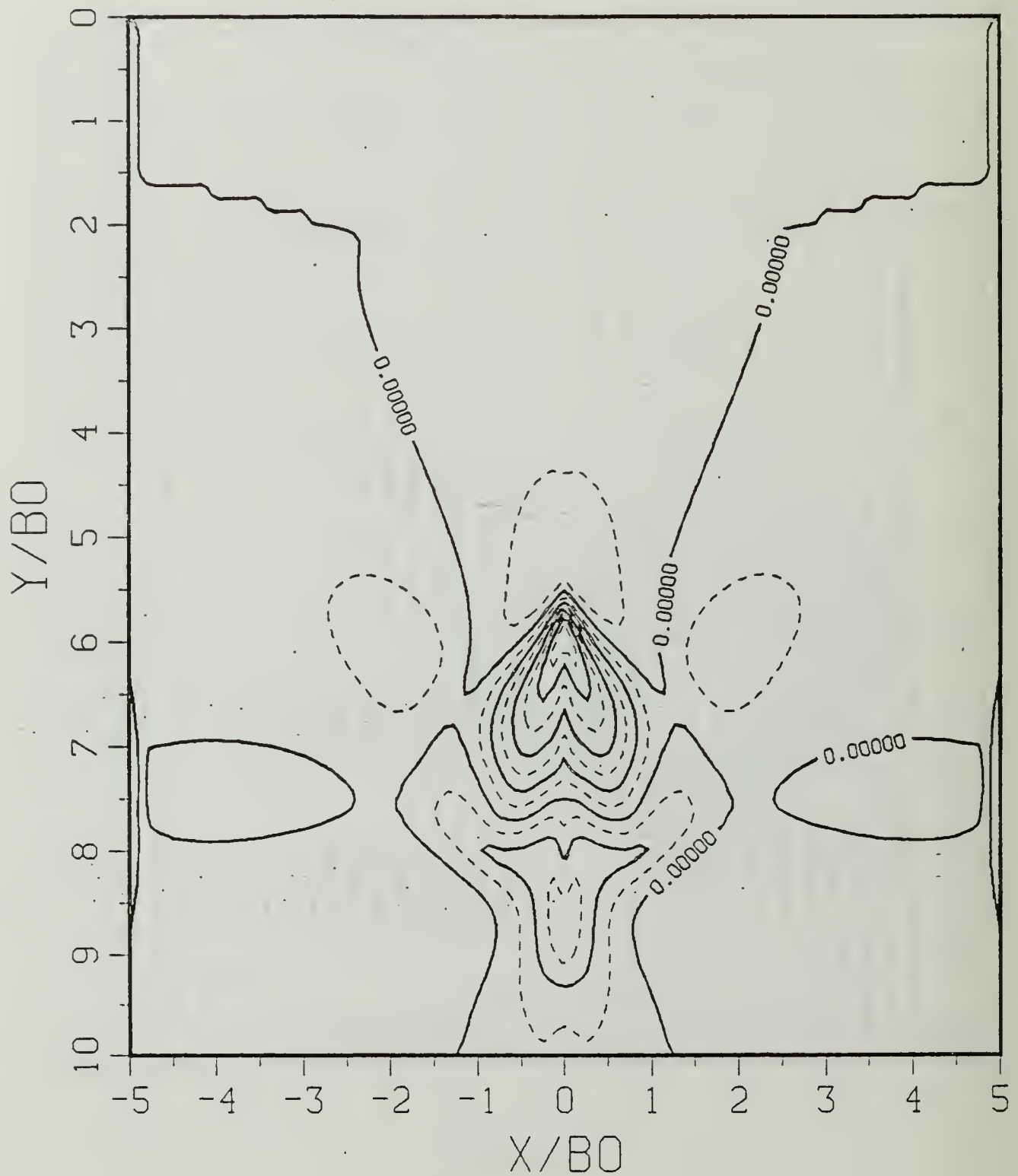


Figure B.29c Density Perturbation Contours: SP = 1.00.

$$T^* = 4.81320$$

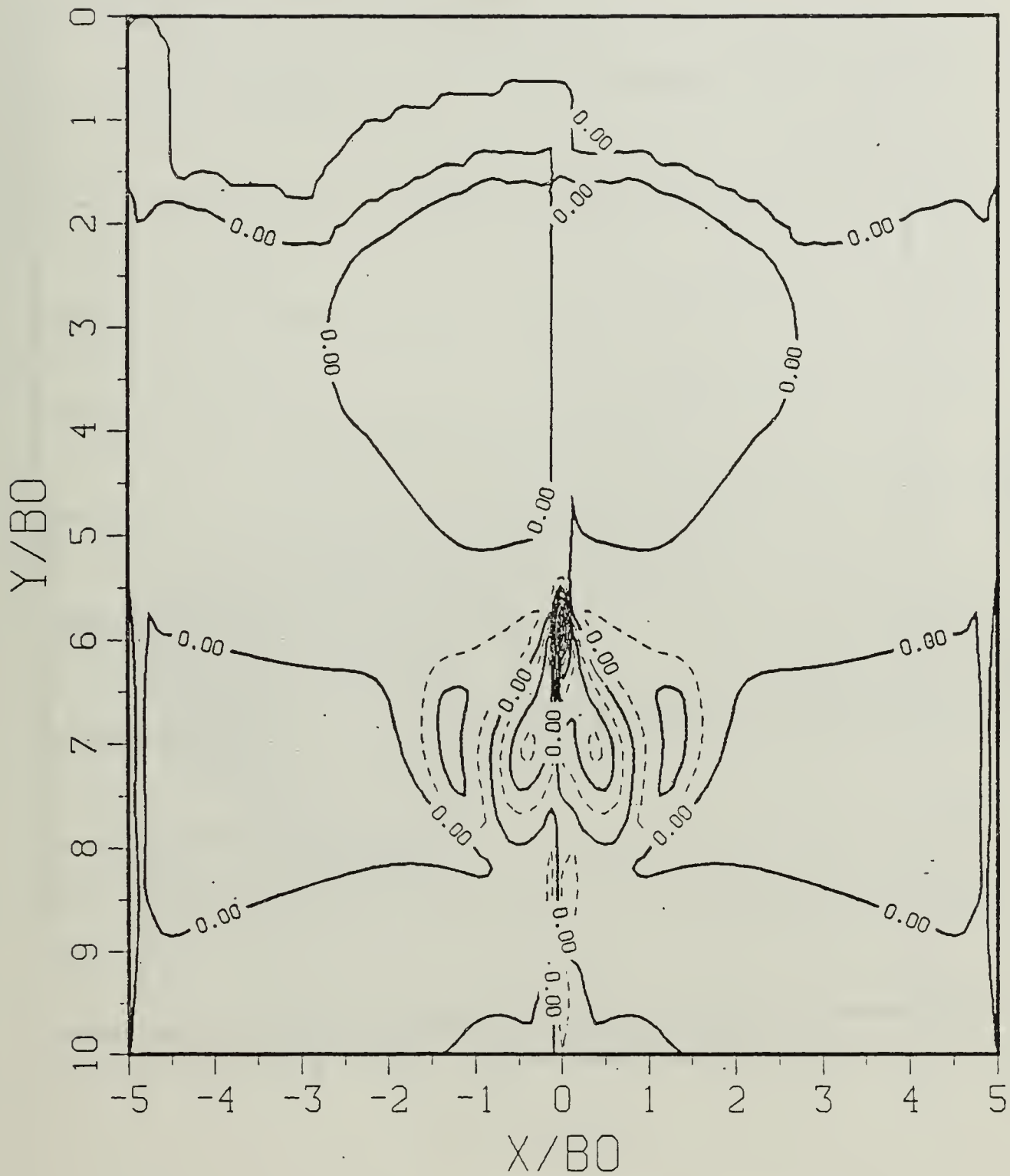


Figure B.29d Vorticity Field: SP = 1.00.

$$T^* = 5.67270$$

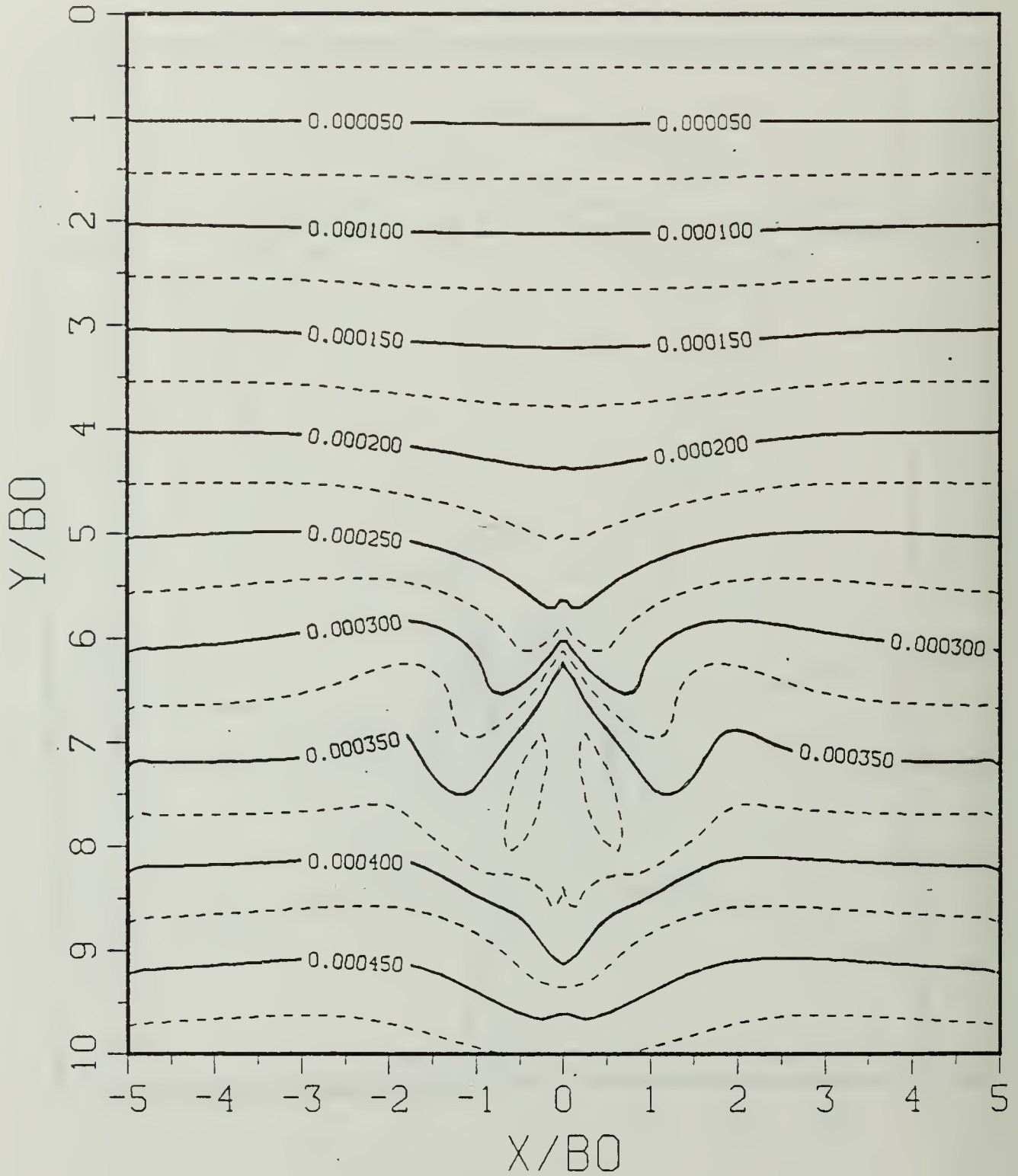


Figure B.30a Constant Density Contours:  $SP = 1.00$ .

$$T^* = 5.67270$$

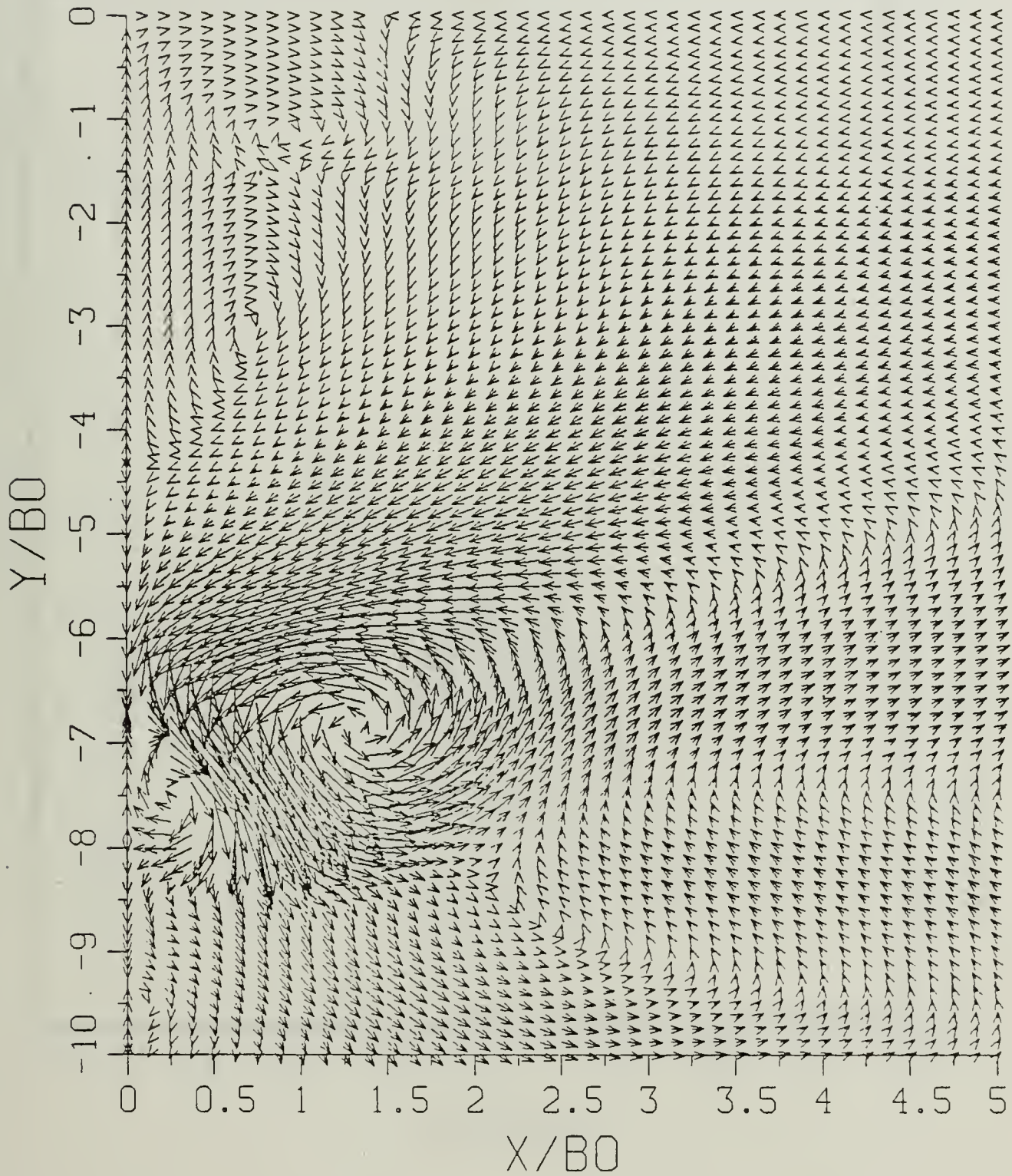


Figure B.30b Velocity Field: SP = 1.00.

$$T^* = 5.67270$$

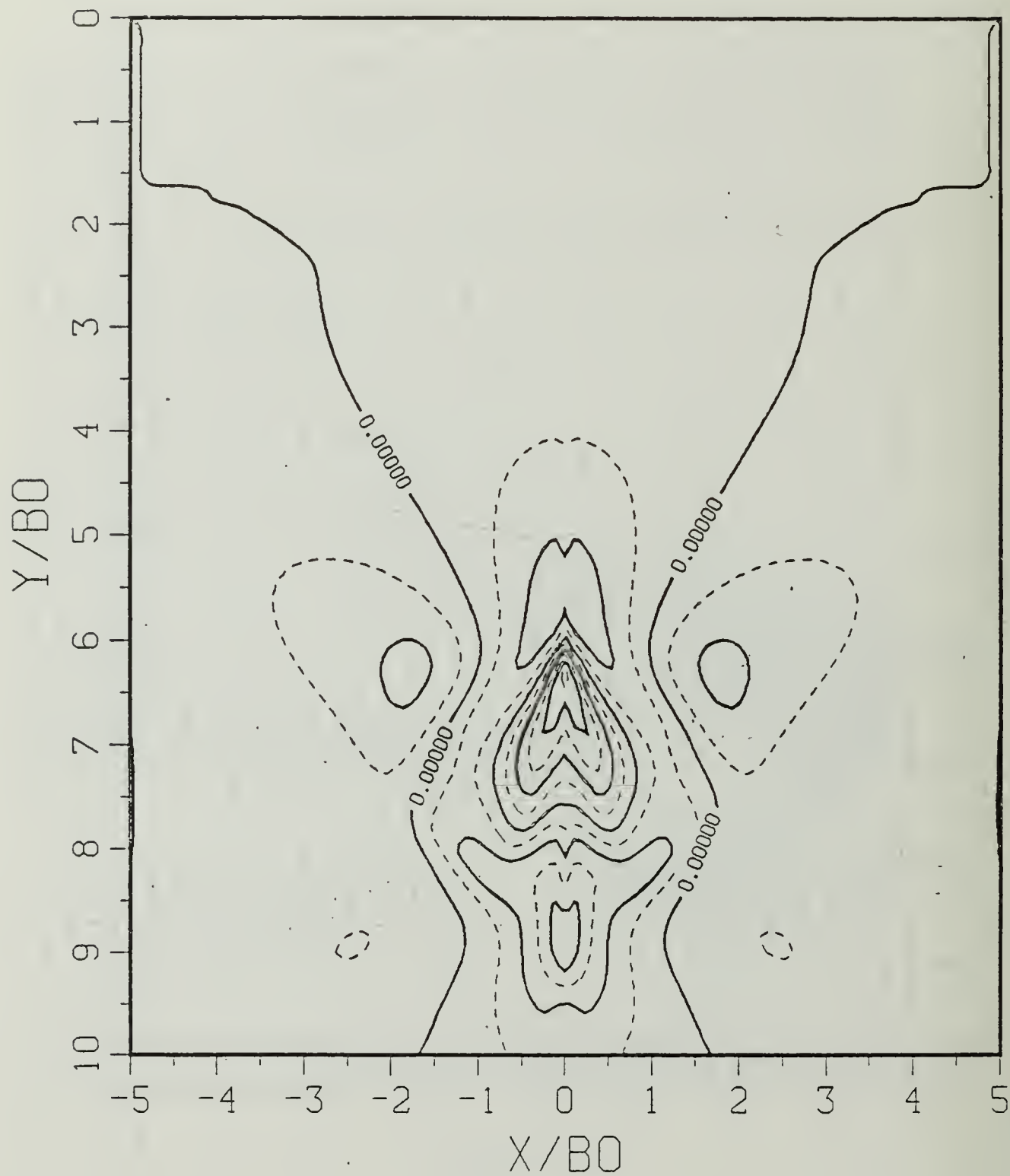


Figure B.30c Density Perturbation Contours:  $SP = 1.00$ .

$$T^* = 5.67270$$

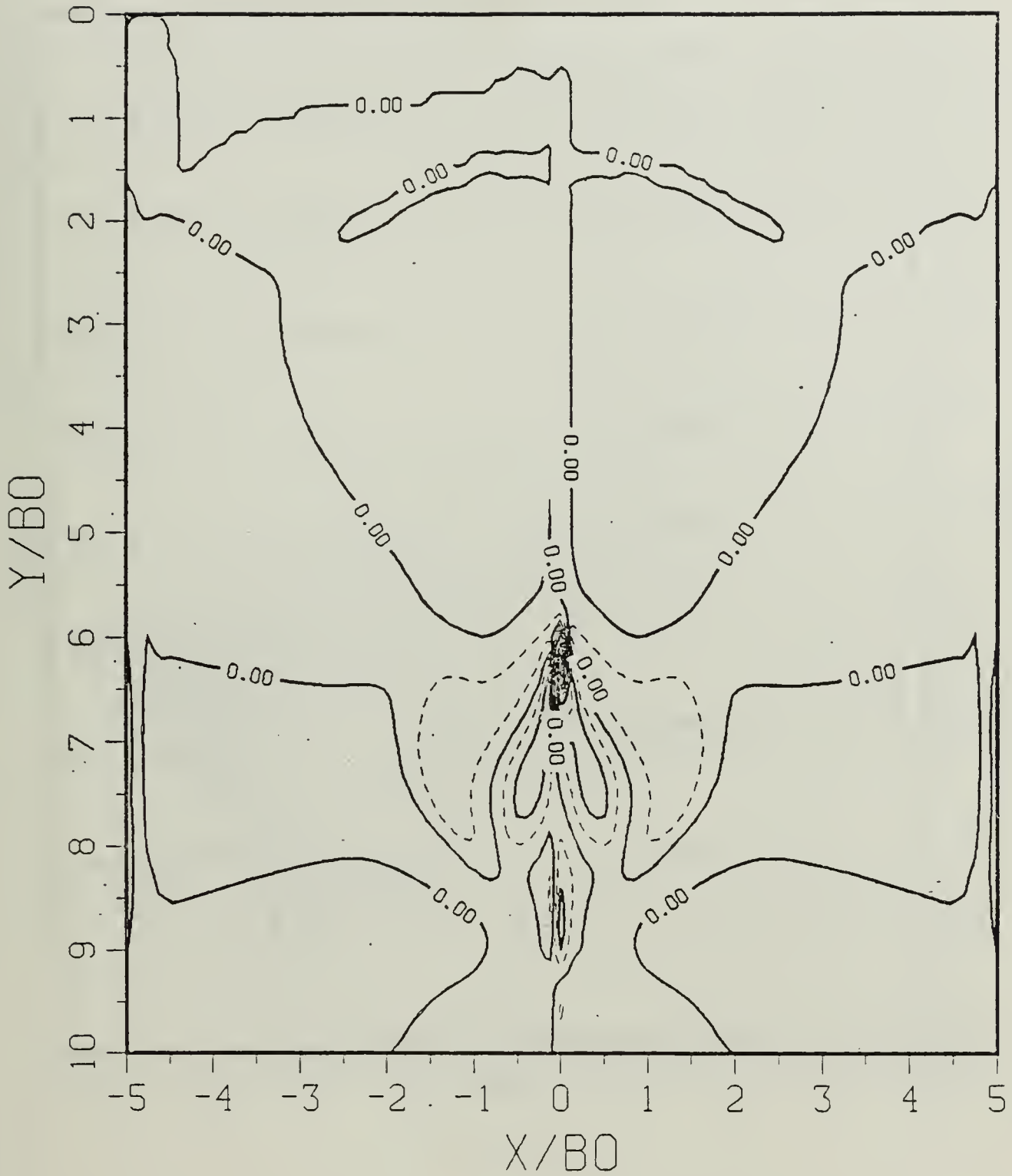


Figure B.30d Vorticity Field: SP = 1.00.

$$T^* = 5.84460$$

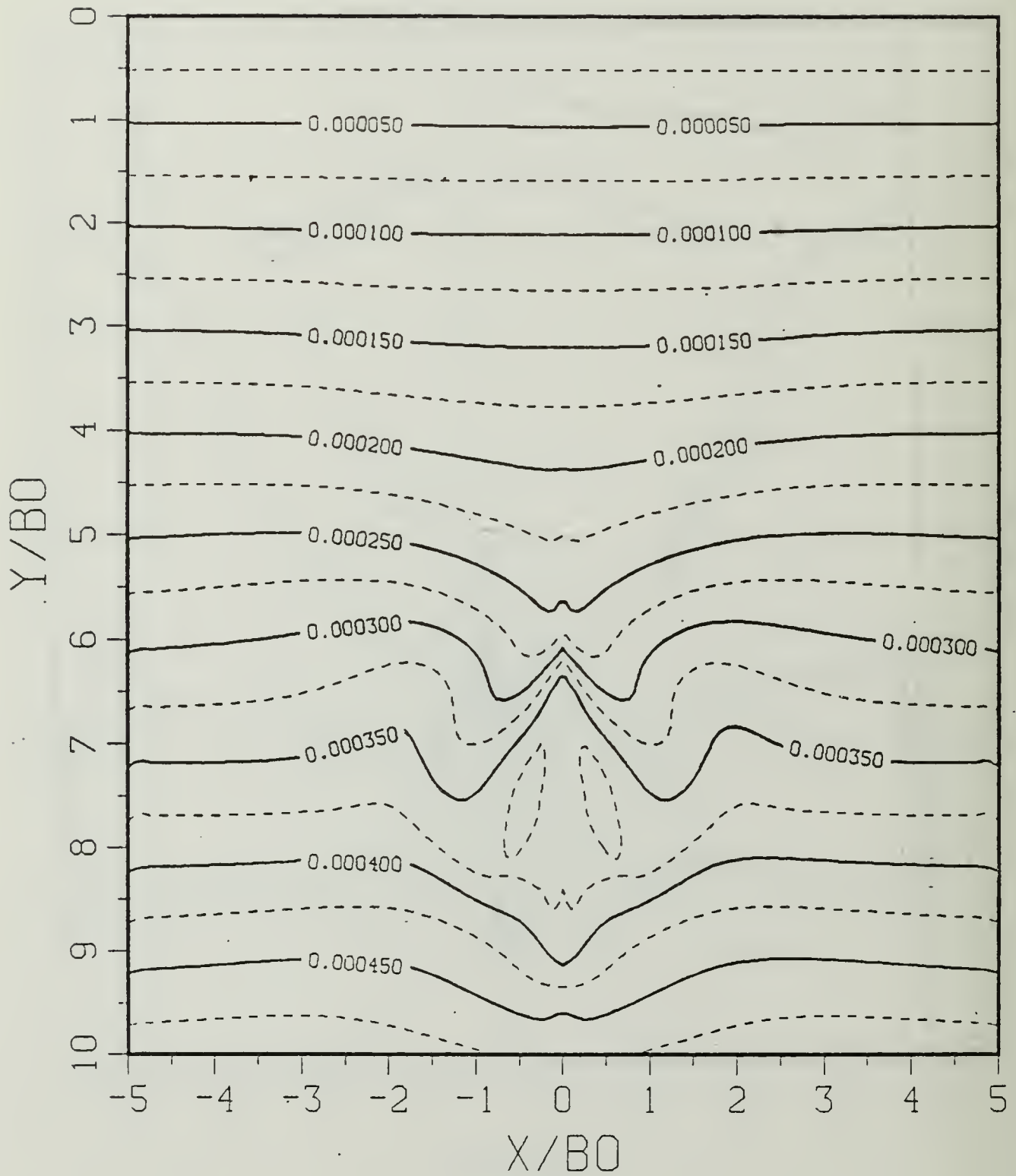


Figure B.31a Constant Density Contours:  $SP = 1.00$ .

$$T^* = 5.84460$$

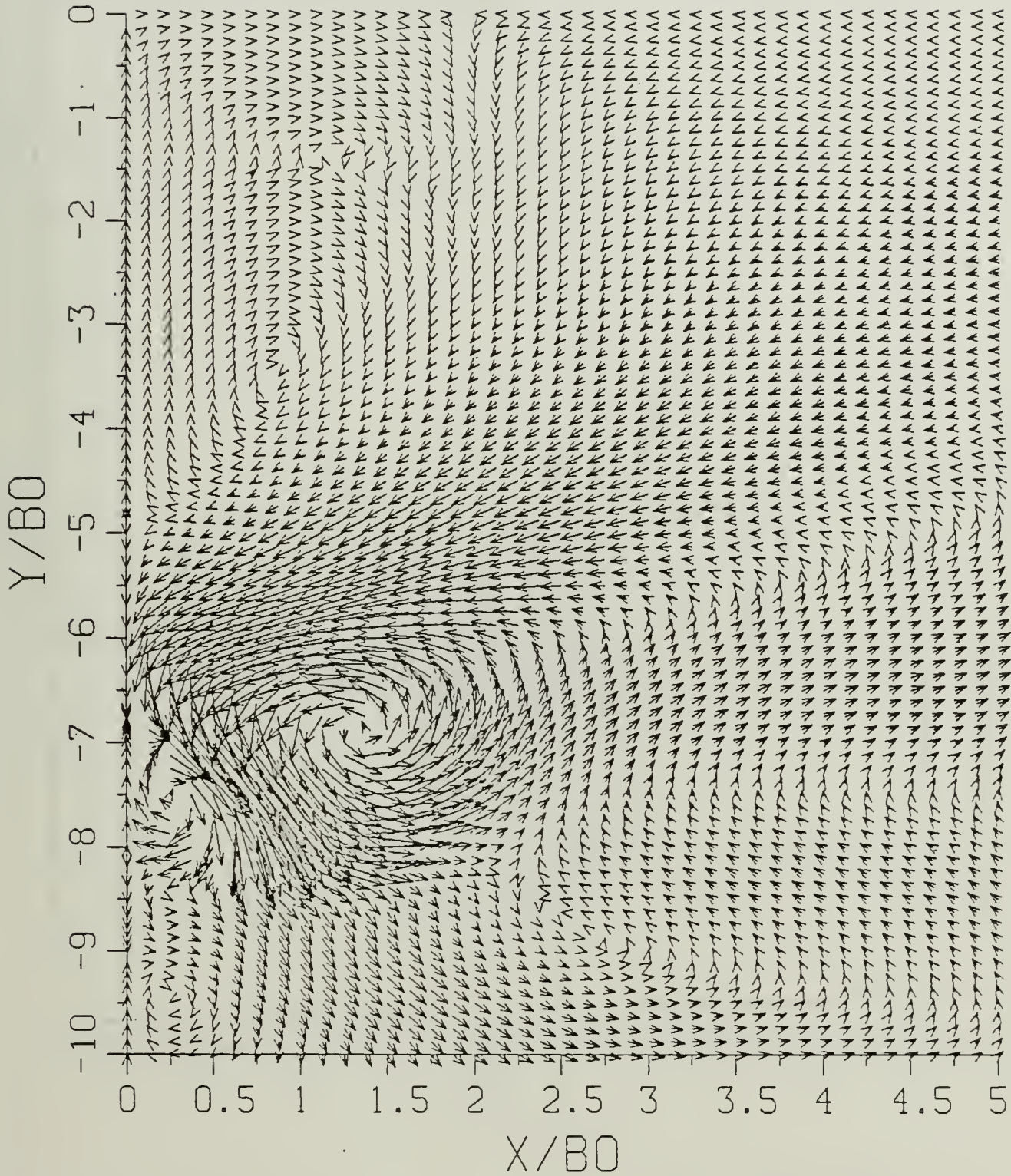


Figure B.31b Velocity Field: SP = 1.00.

$$T^* = 5.84460$$

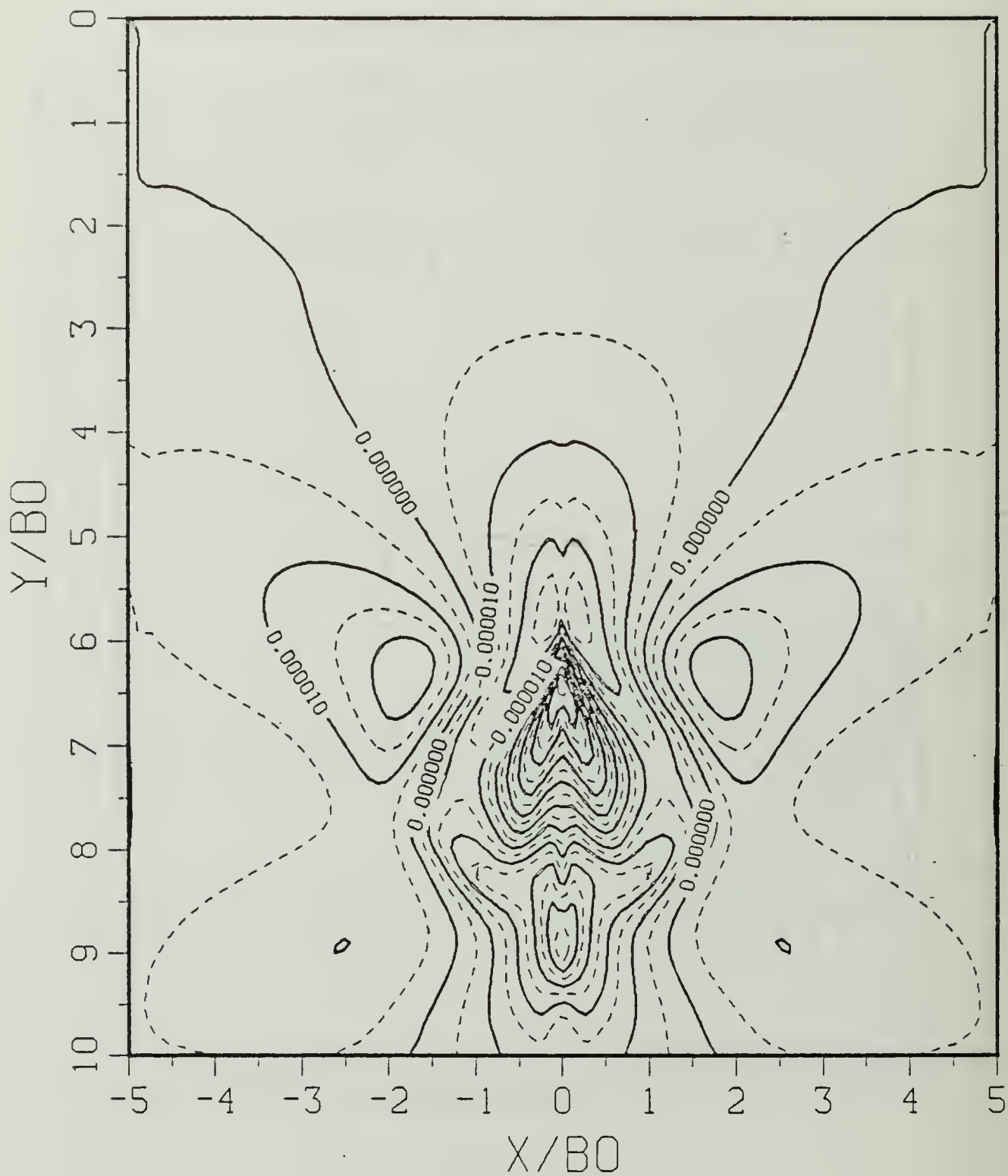


Figure B.31c Density Perturbation Contours:  $SP = 1.00$ .

$$T^* = 5.84460$$

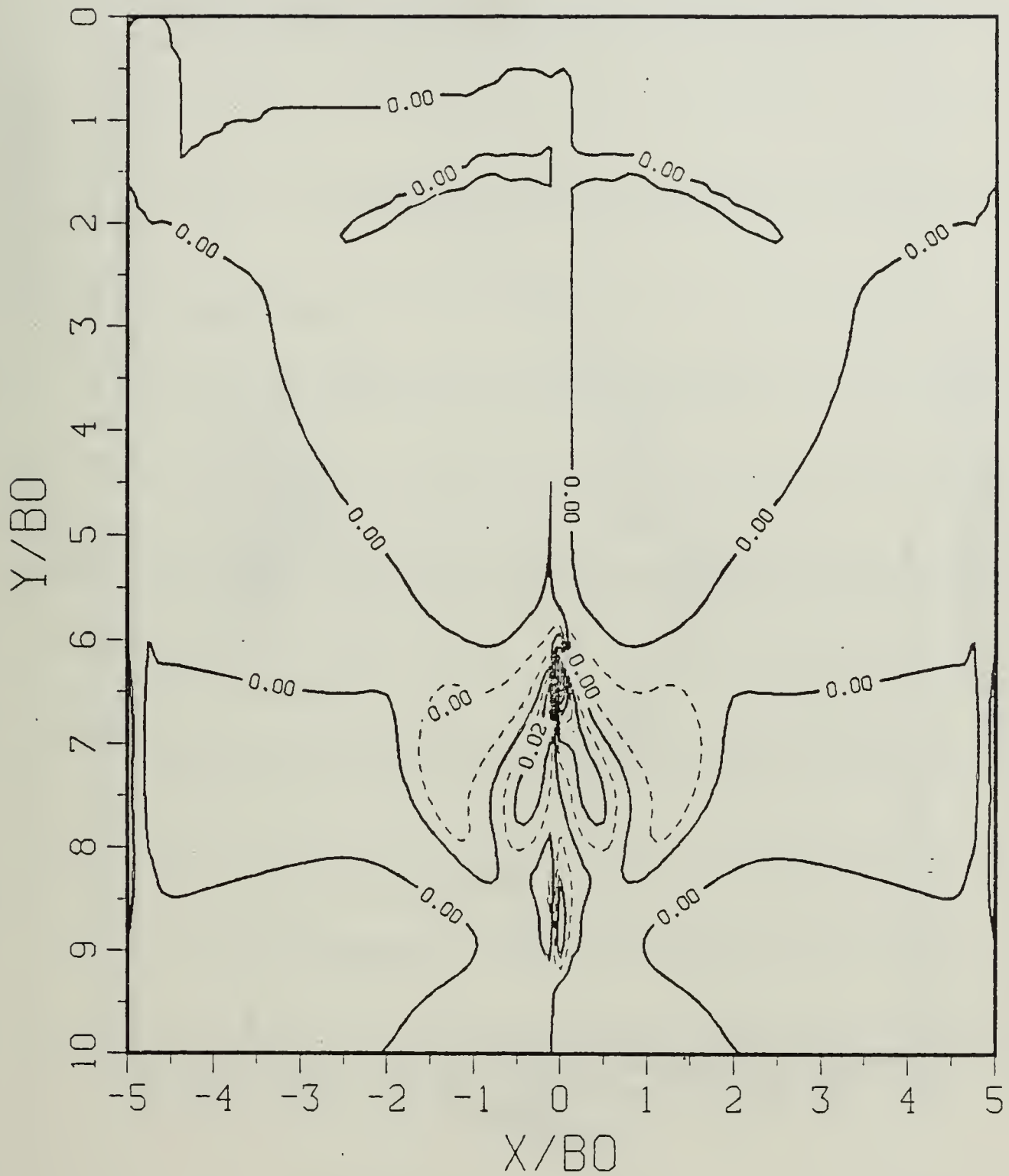


Figure B.31d Vorticity Field: SP = 1.00.

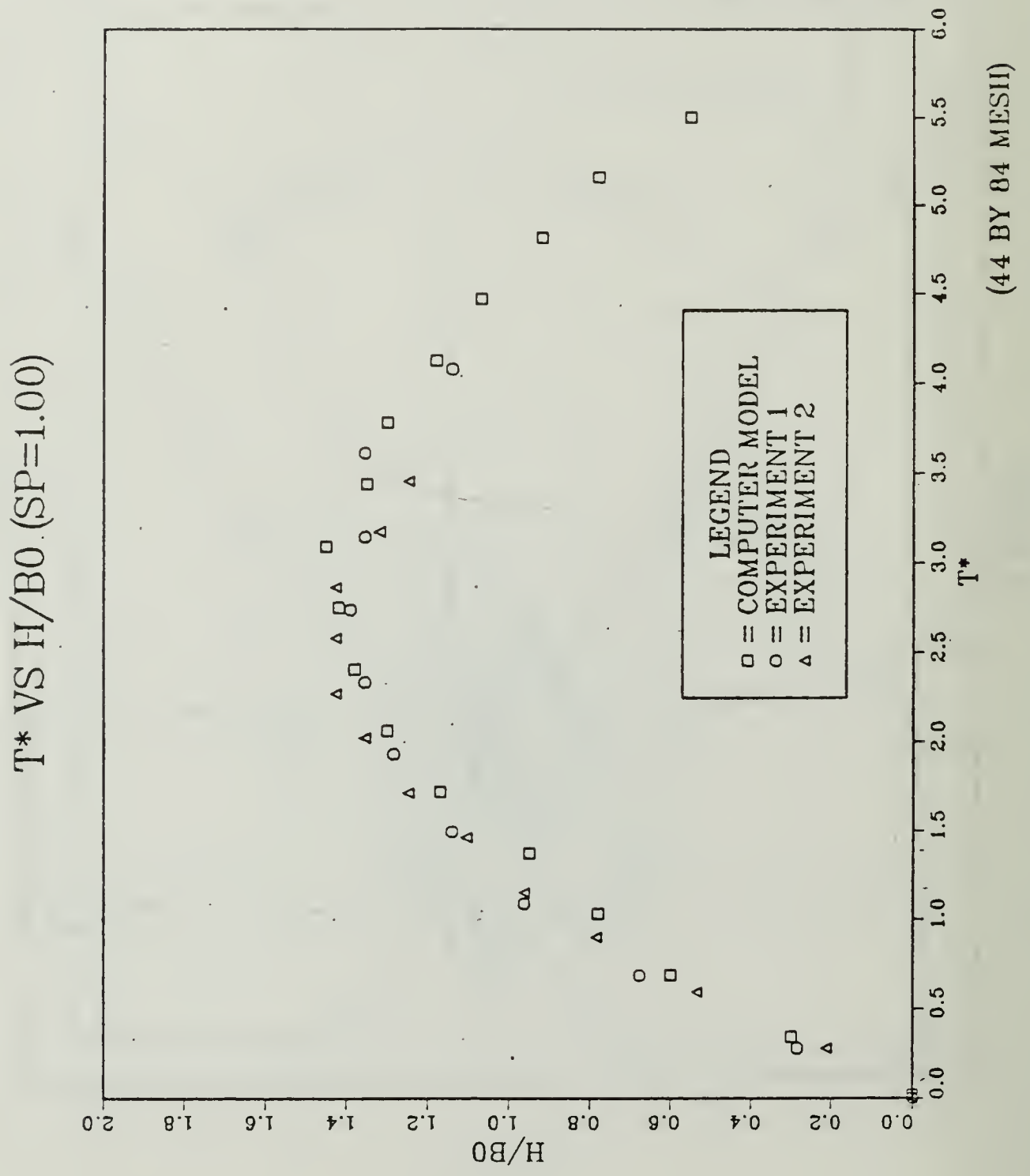


Figure B.32 . Experimental and Numerical Results for SP = 1.00.

$$T^* = 0.05952$$

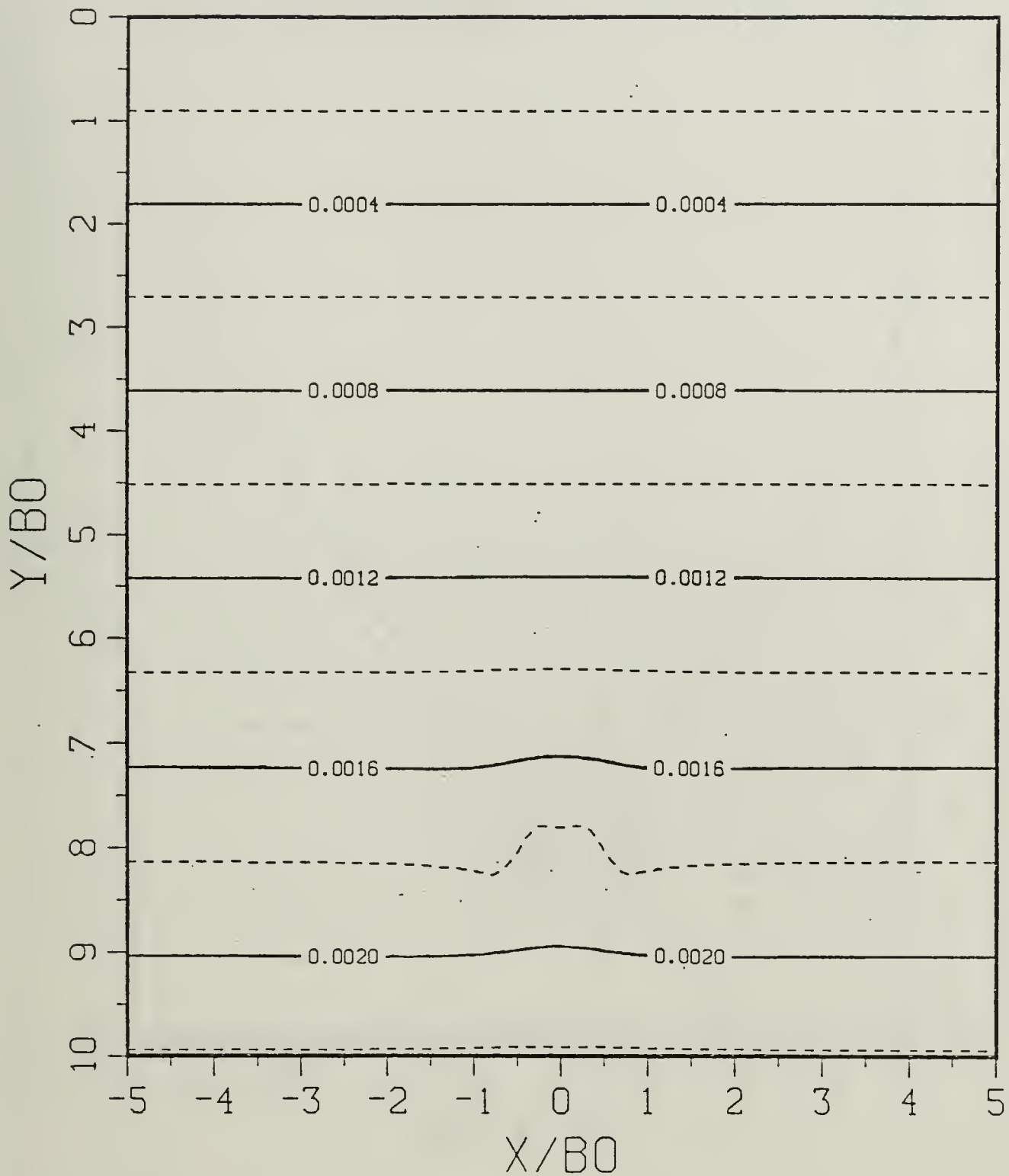


Figure B.33a Constant Density Contours:  $SP = 0.50$ .

$$T^* = 0.05952$$

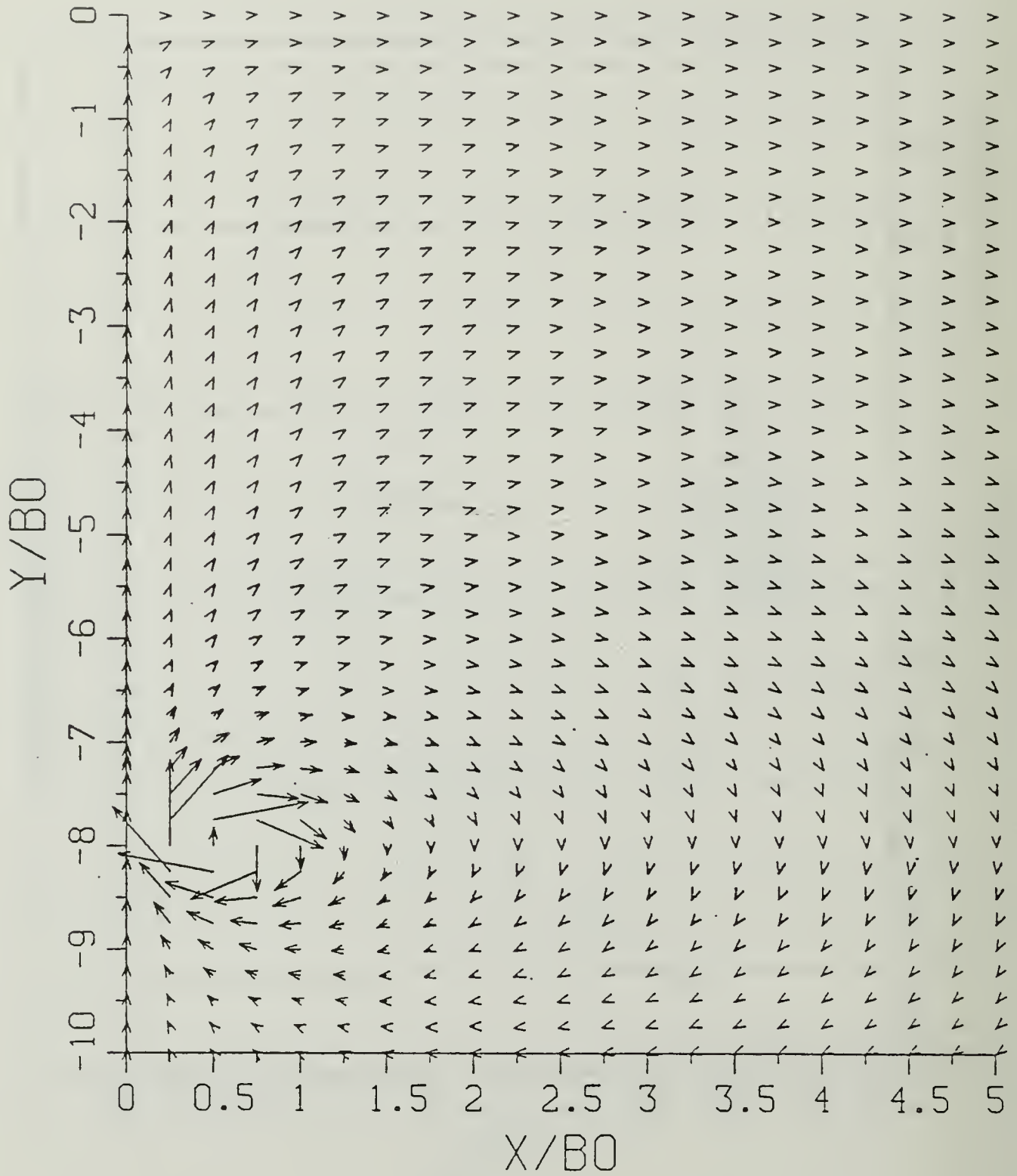


Figure B.33b Velocity Field: SP = 0.50.

$$T^* = 0.05952$$

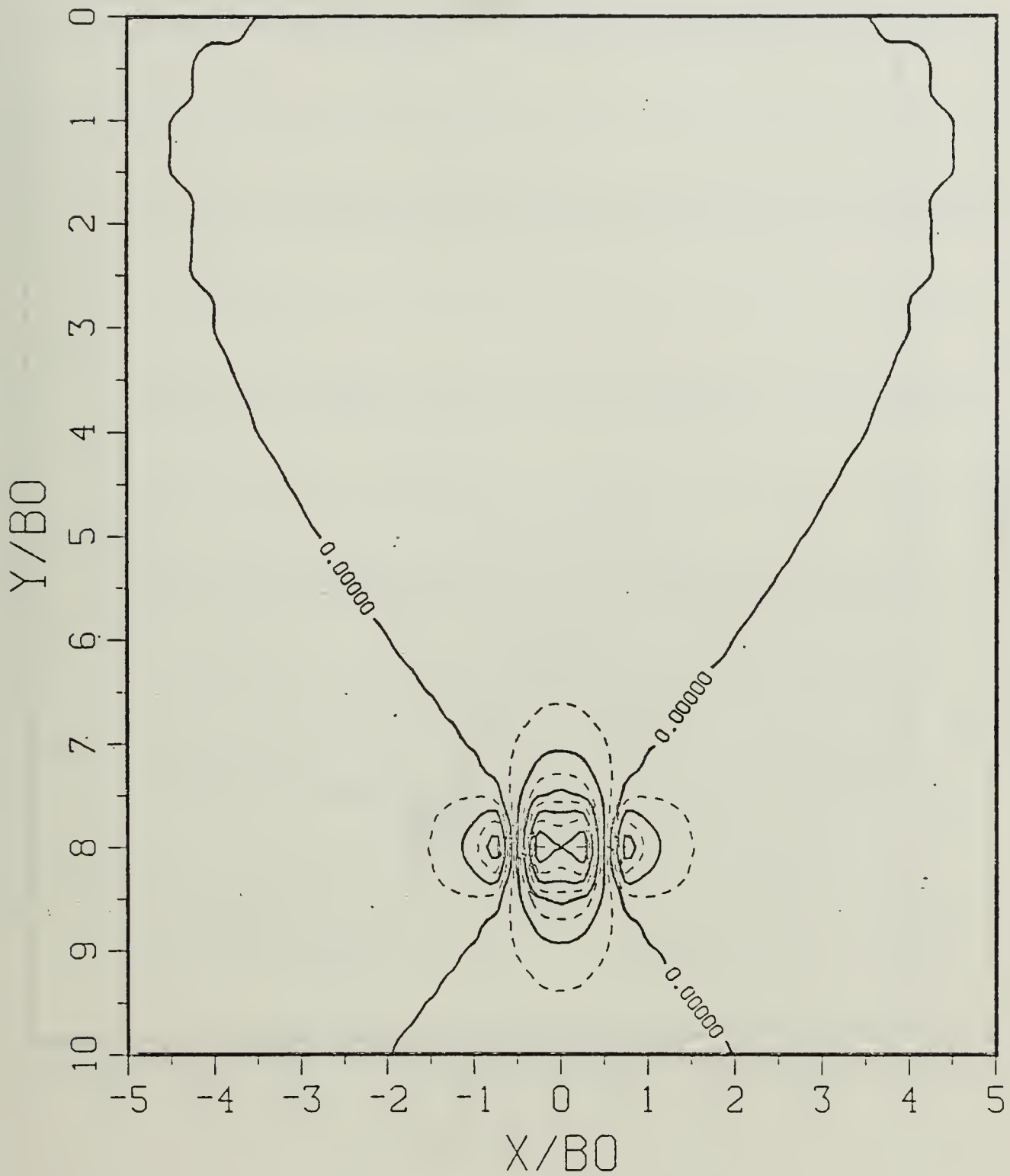


Figure B.33c Density Perturbation Contours: SP = 0.50.

$$T^* = 0.05952$$

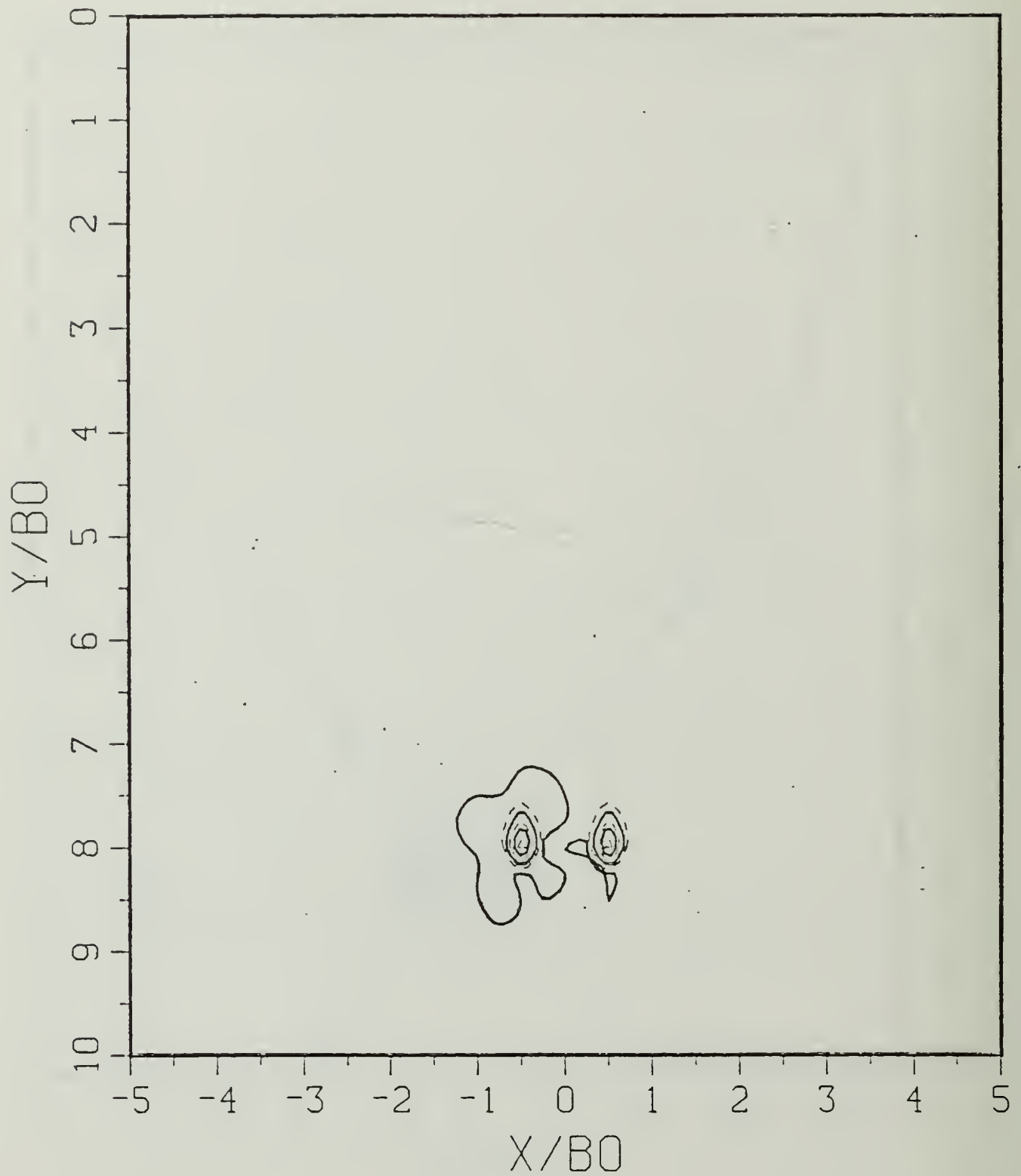


Figure B.33d Vorticity Field: SP = 0.50.

$$T^* = 0.59520$$

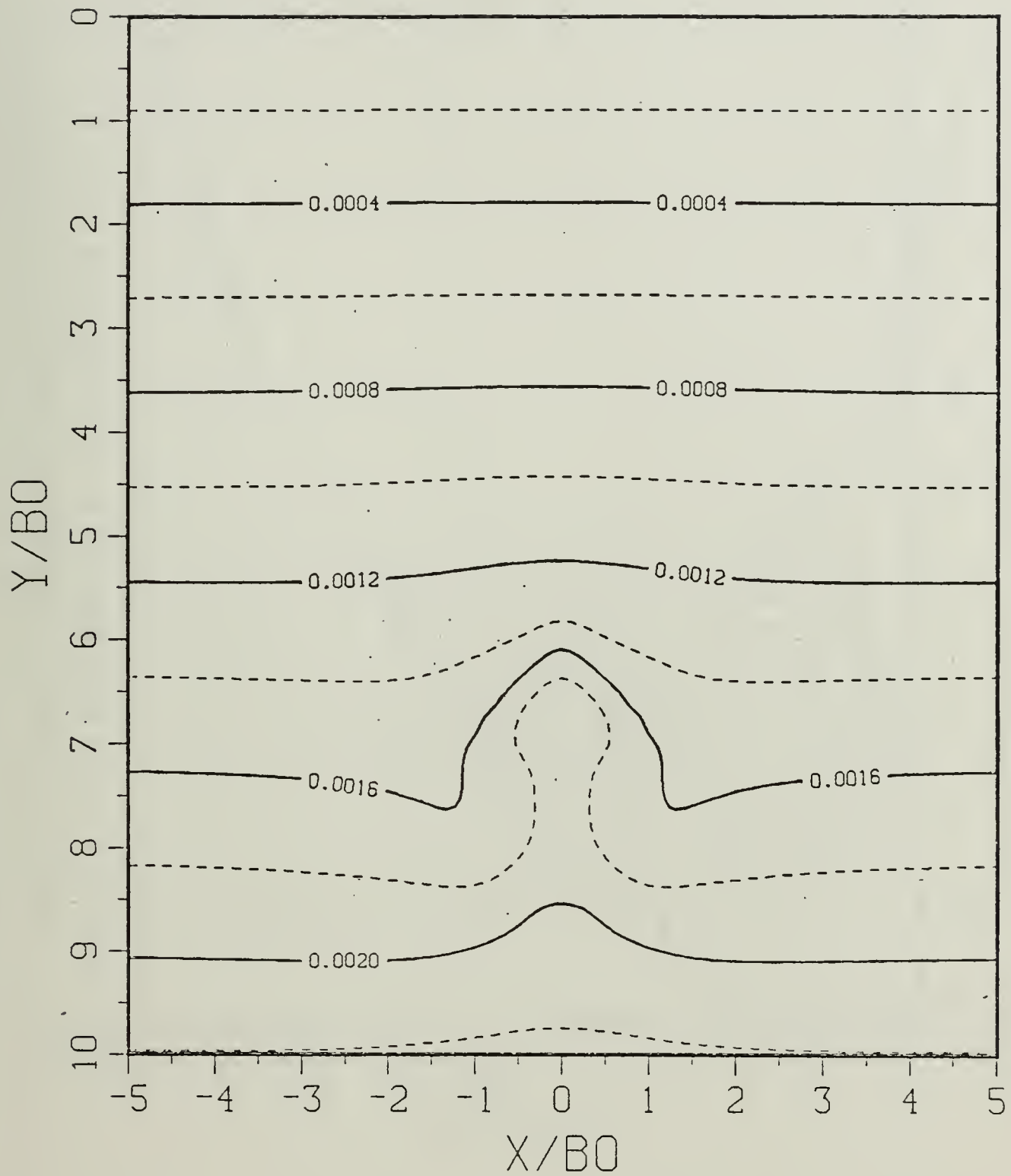


Figure B.34a Constant Density Contours:  $SP = 0.50$ .

$$T^* = 0.59520$$

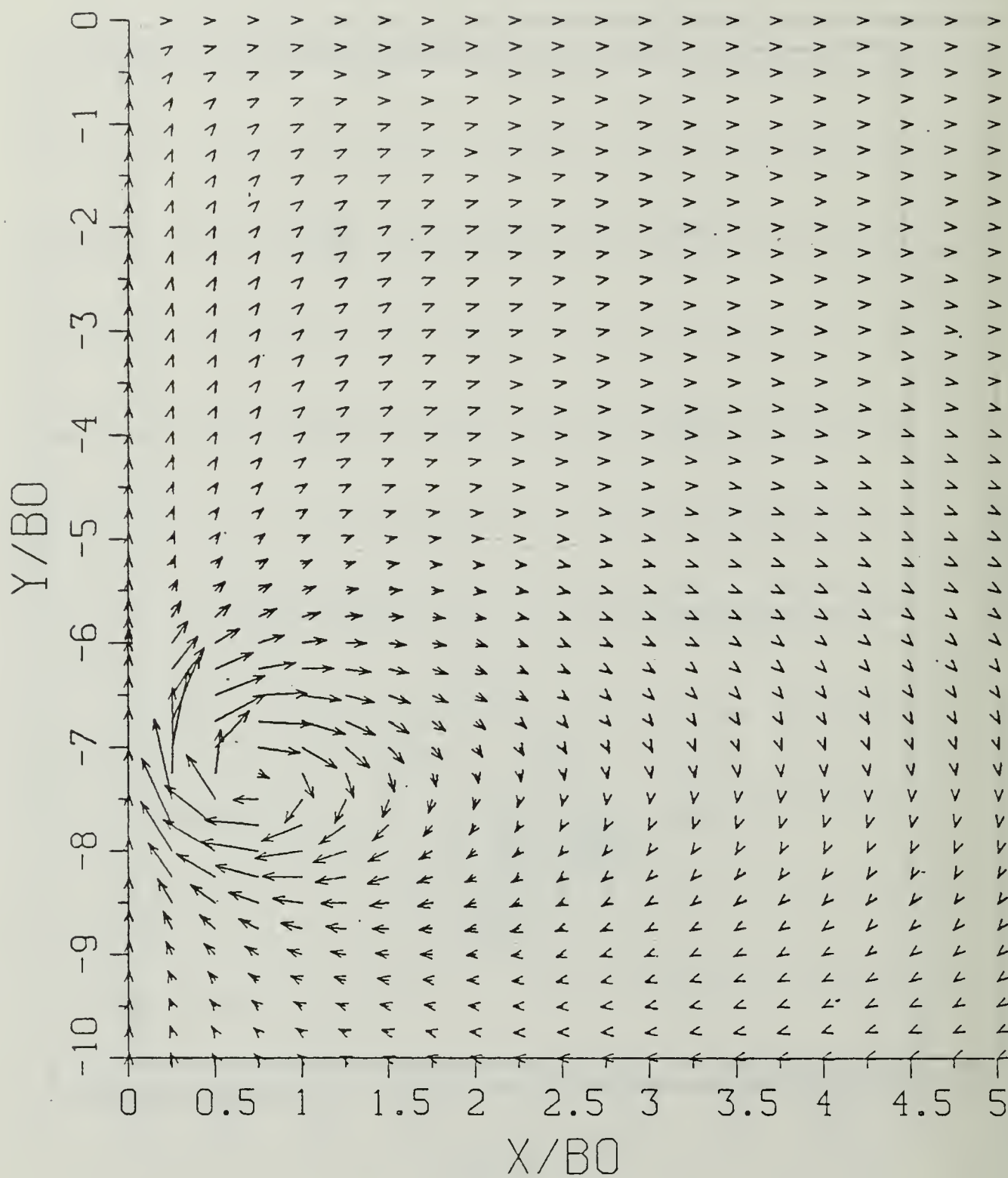


Figure B.34b Velocity Field:  $SP = 0.50$ .

$$T^* = 0.59520$$

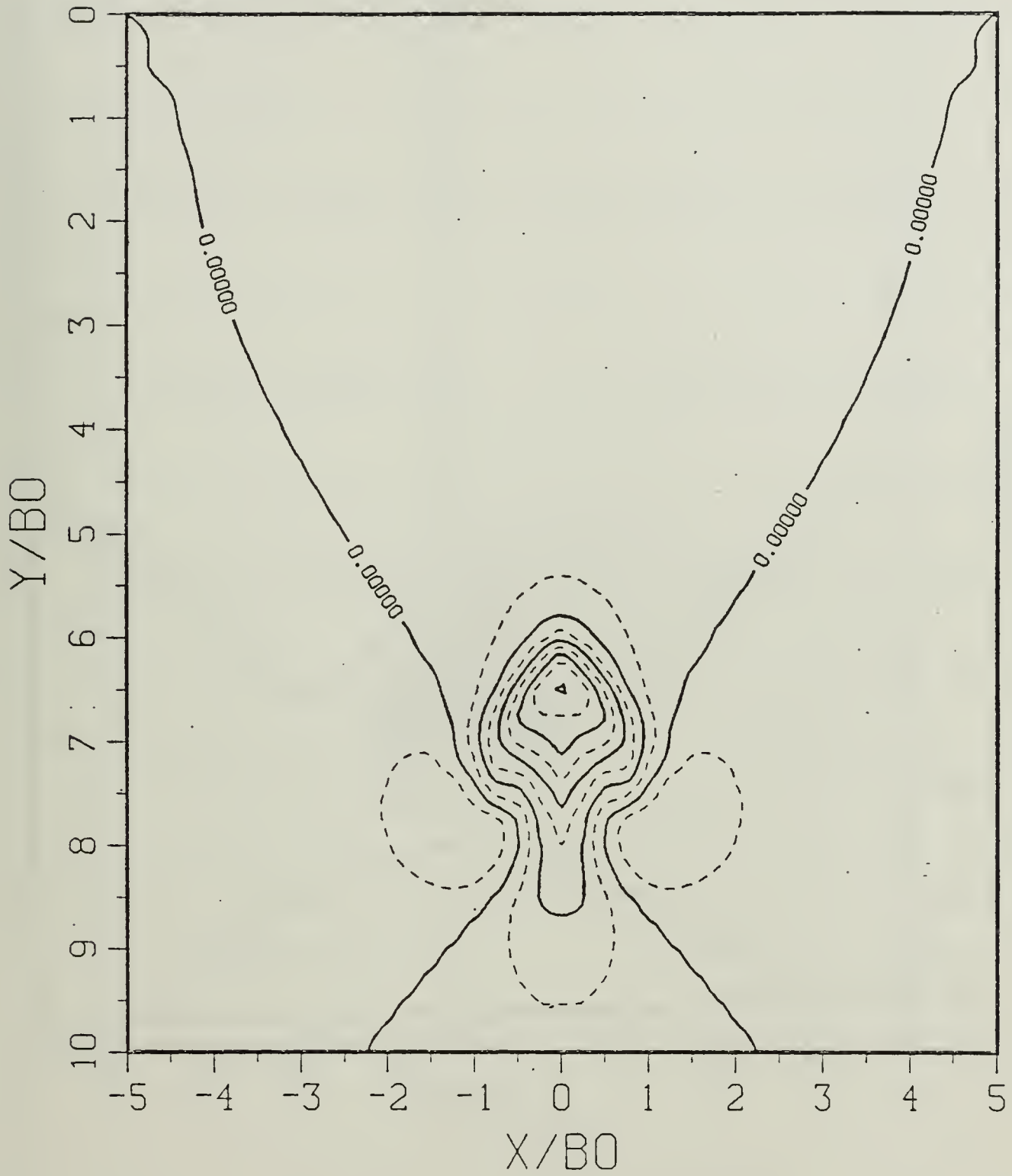


Figure B.3-4c Density Perturbation Contours: SP = 0.50.

$$T^* = 0.59520$$

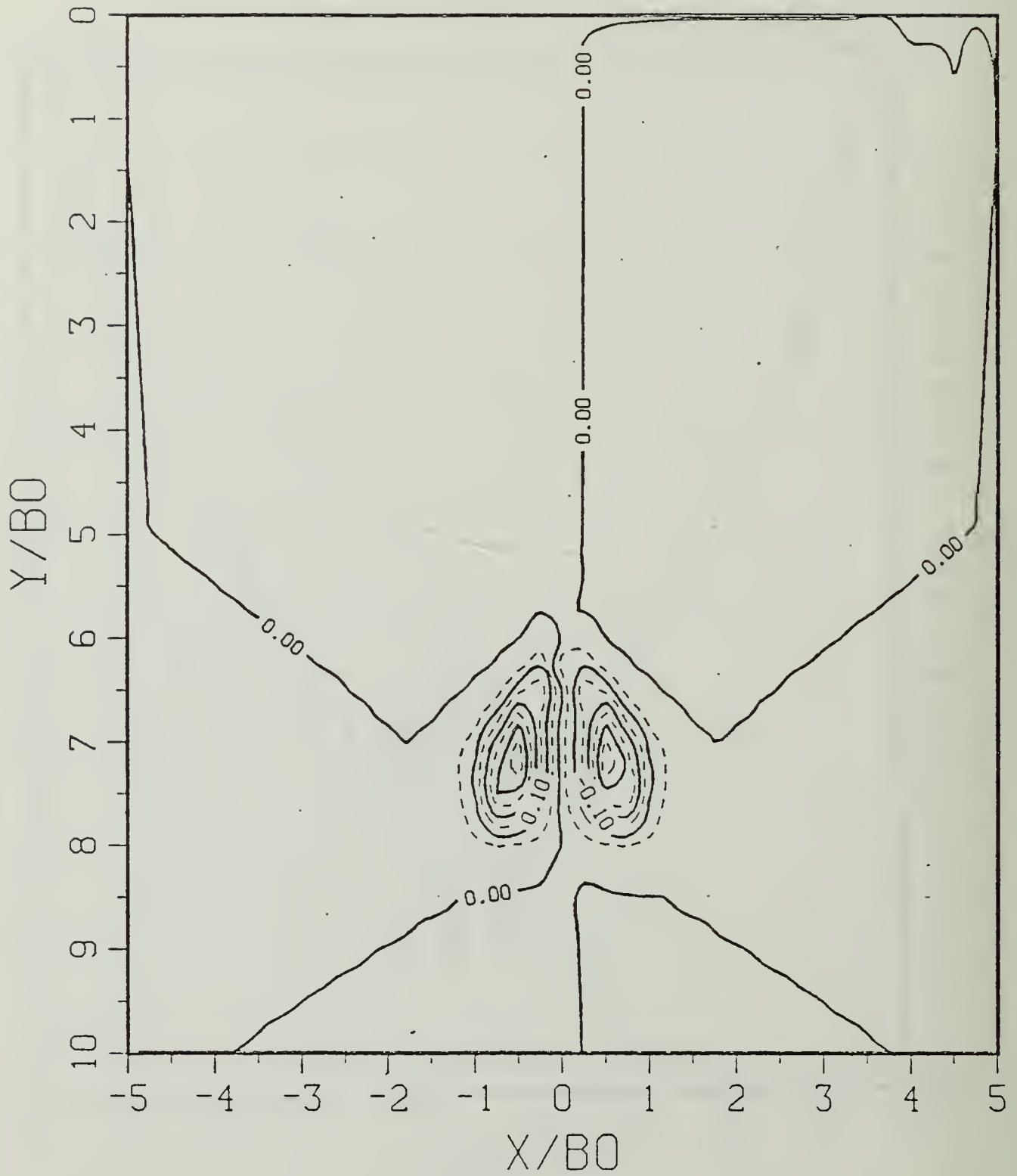


Figure B.34d Vorticity Field: SP = 0.50.

$$T^* = 1.19040$$

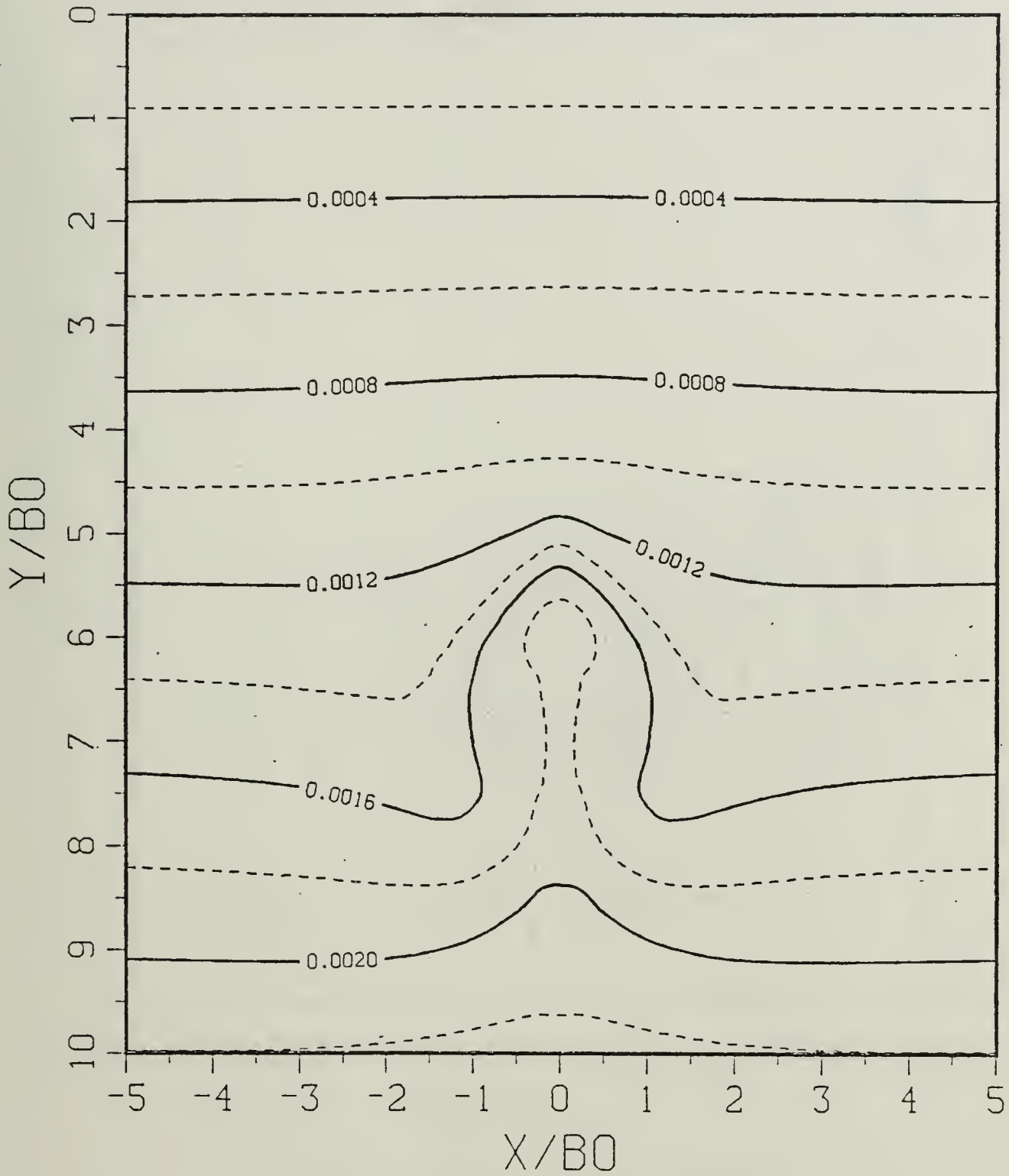


Figure B.35a Constant Density Contours:  $SP = 0.50..$

$$T^* = 1.19040$$

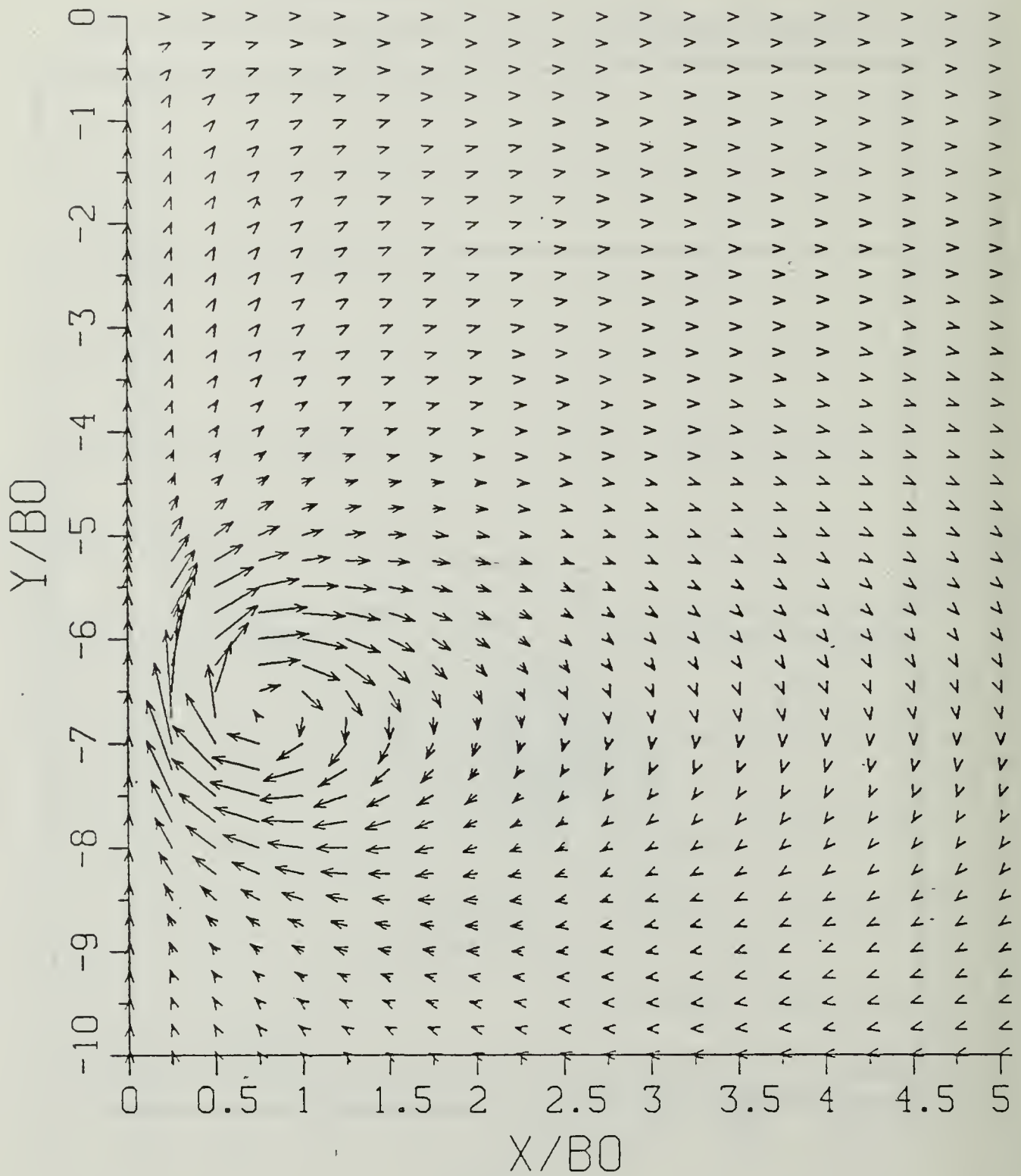


Figure B.35b Velocity Field:  $SP = 0.50$ .

$$T^* = 1.19040$$

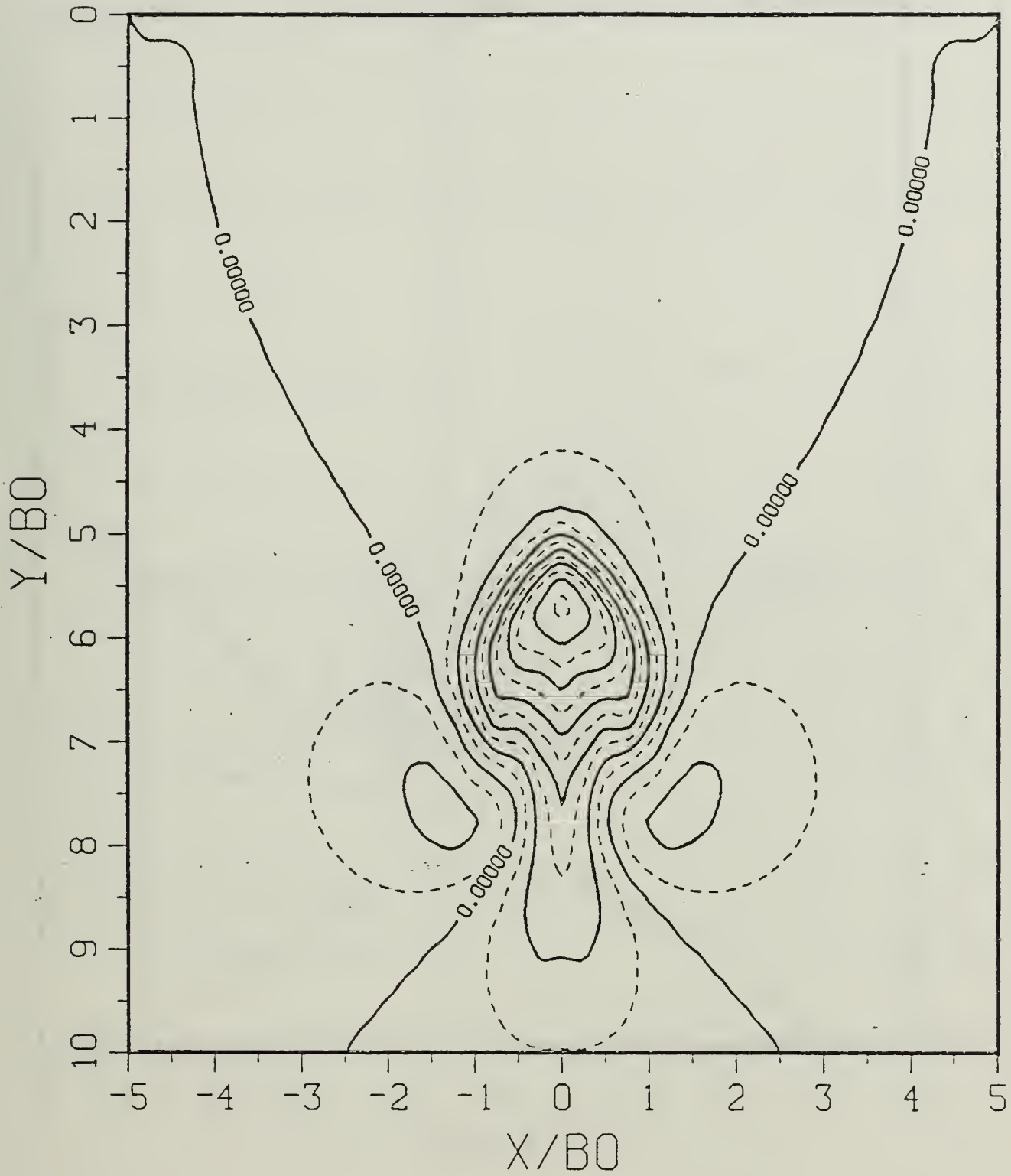


Figure B.35c Density Perturbation Contours:  $SP = 0.50$ .

$$T^* = 1.19040$$

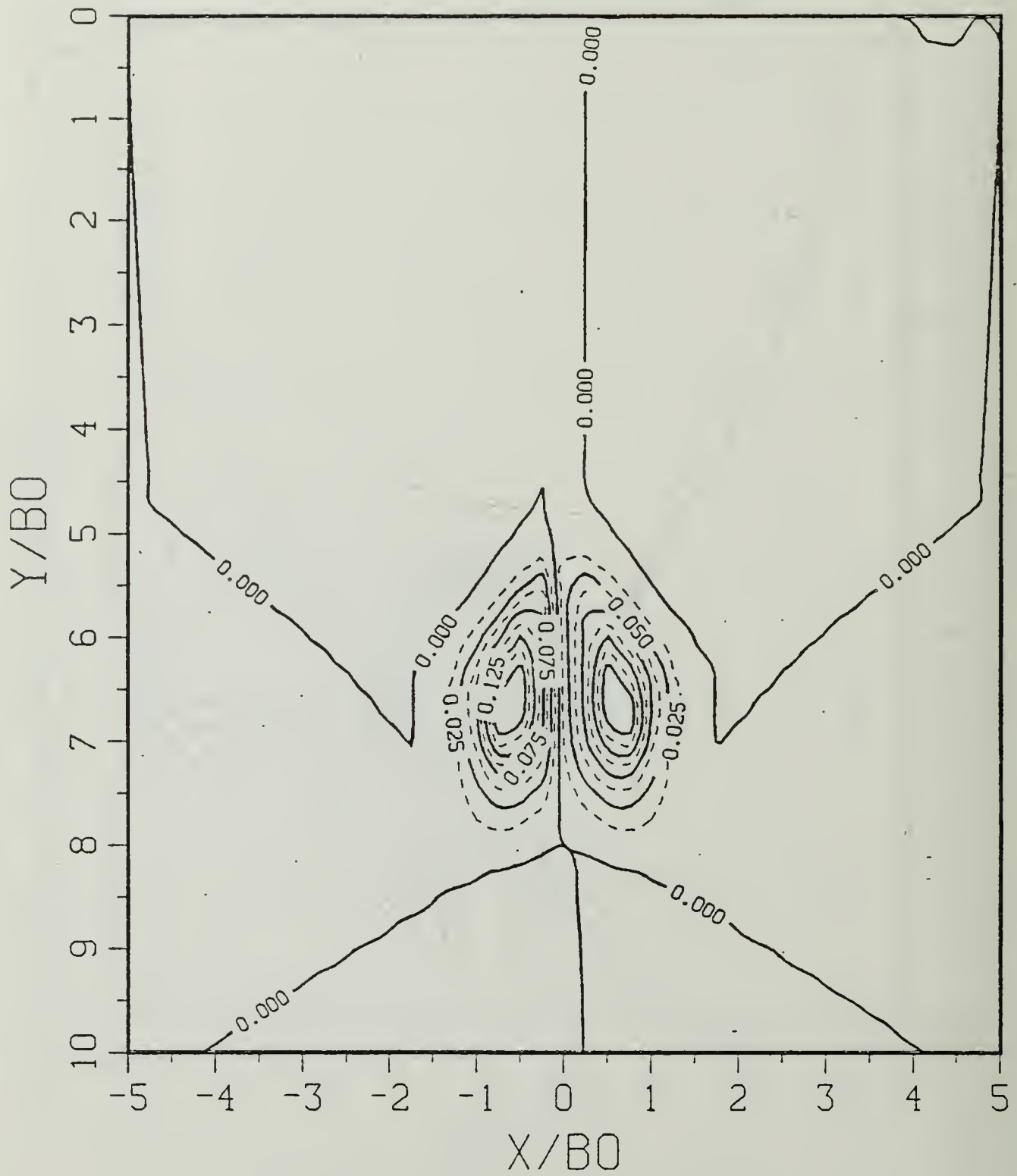


Figure B.35d Vorticity Field:  $SP = 0.50$ .

$$T^* = 1.78560$$

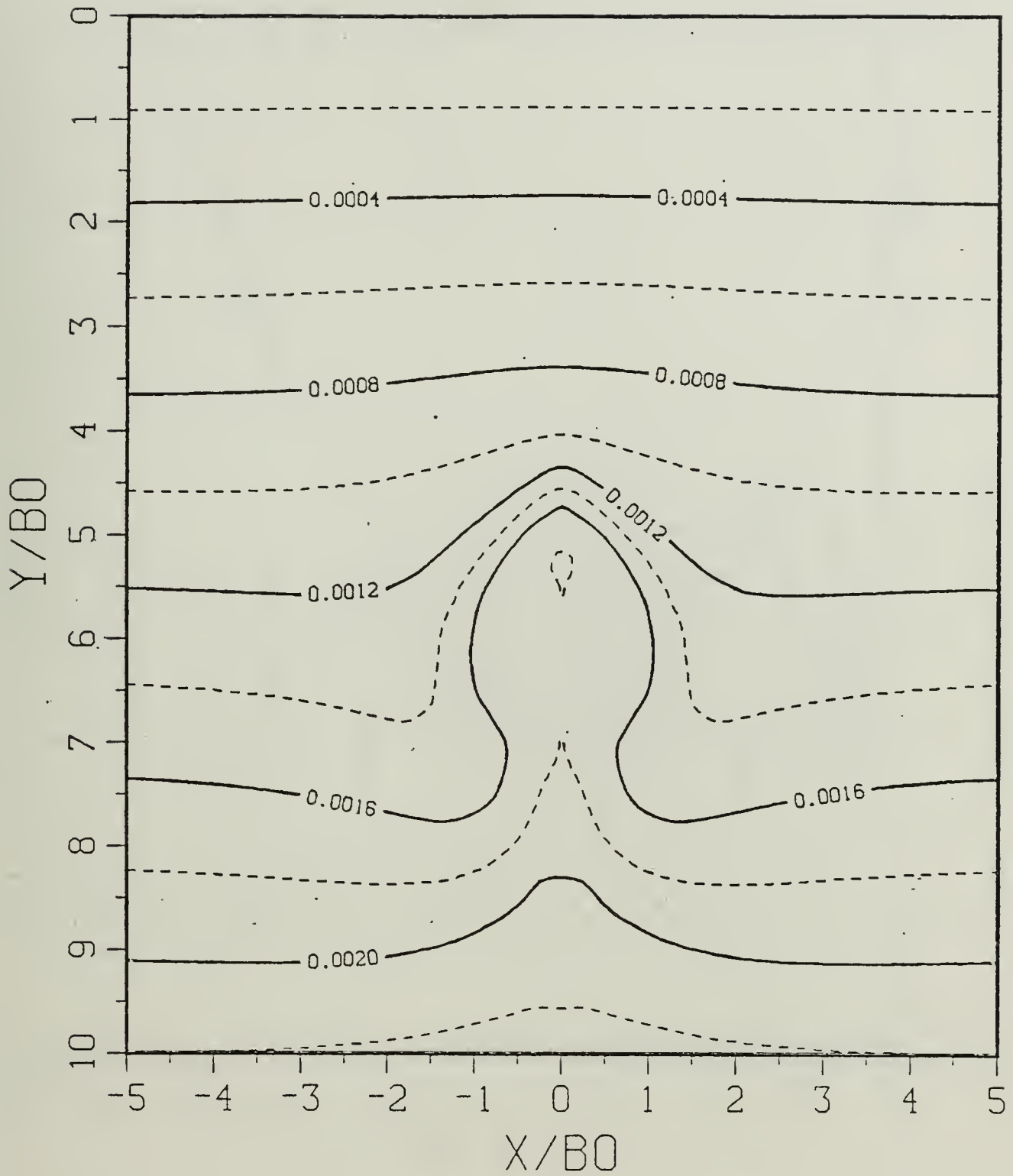


Figure B.36a Constant Density Contours: SP = 0.50.

$$T^* = 1.78560$$

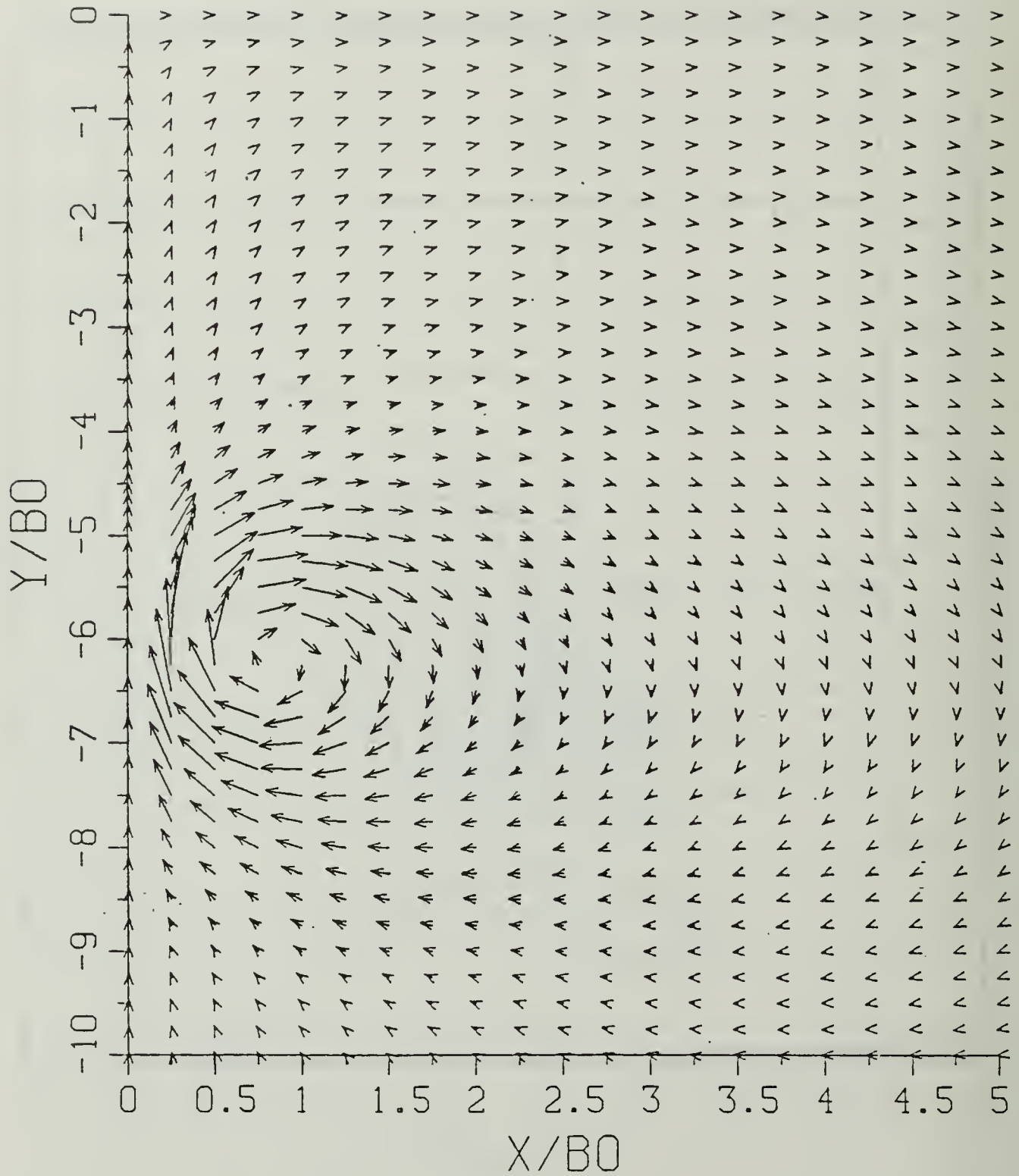


Figure B.36b Velocity Field:  $SP = 0.50$ .

$$T^* = 1.78560$$

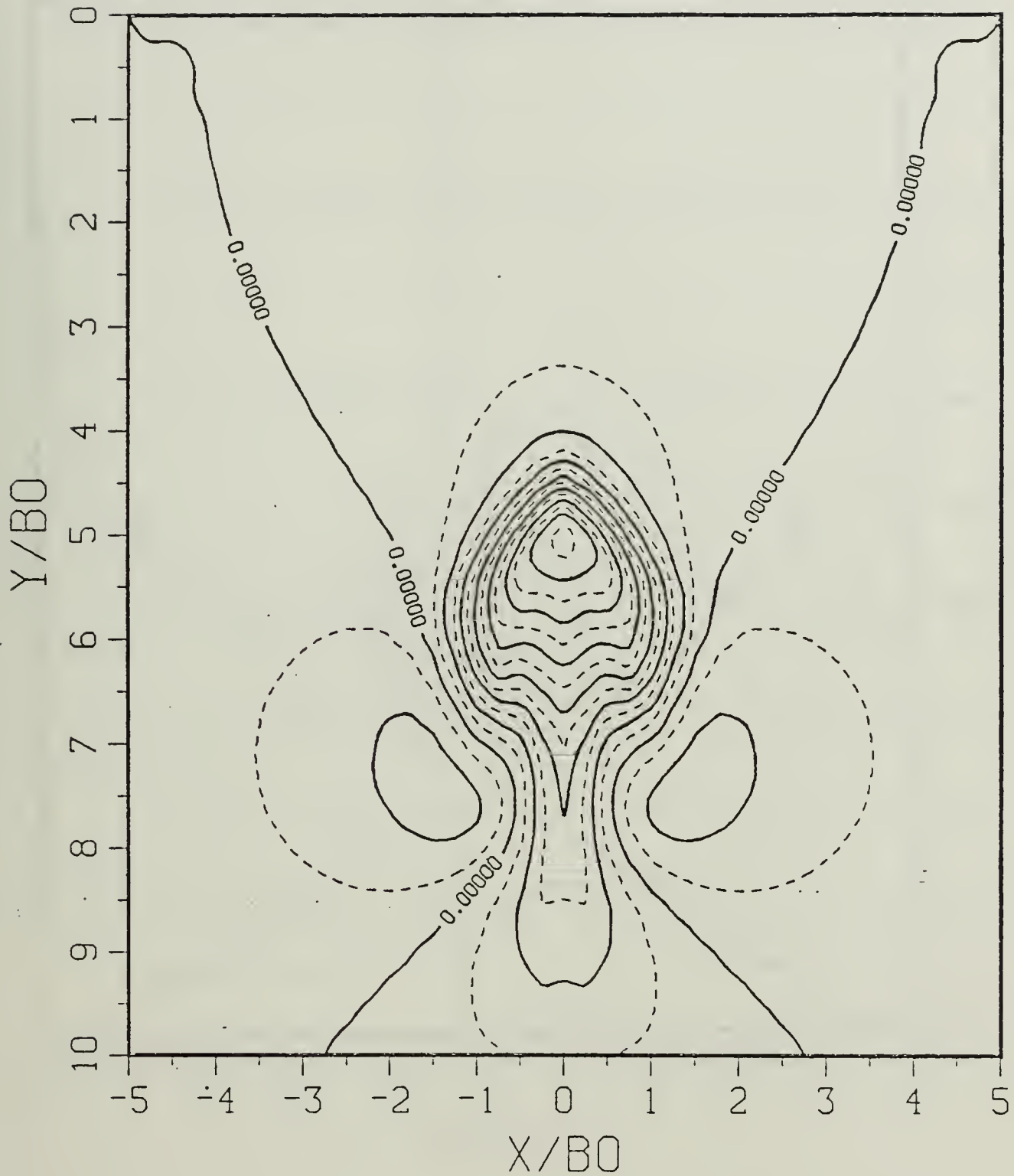


Figure B.36c Density Perturbation Contours:  $SP = 0.50$ .

$$T^* = 1.78560$$

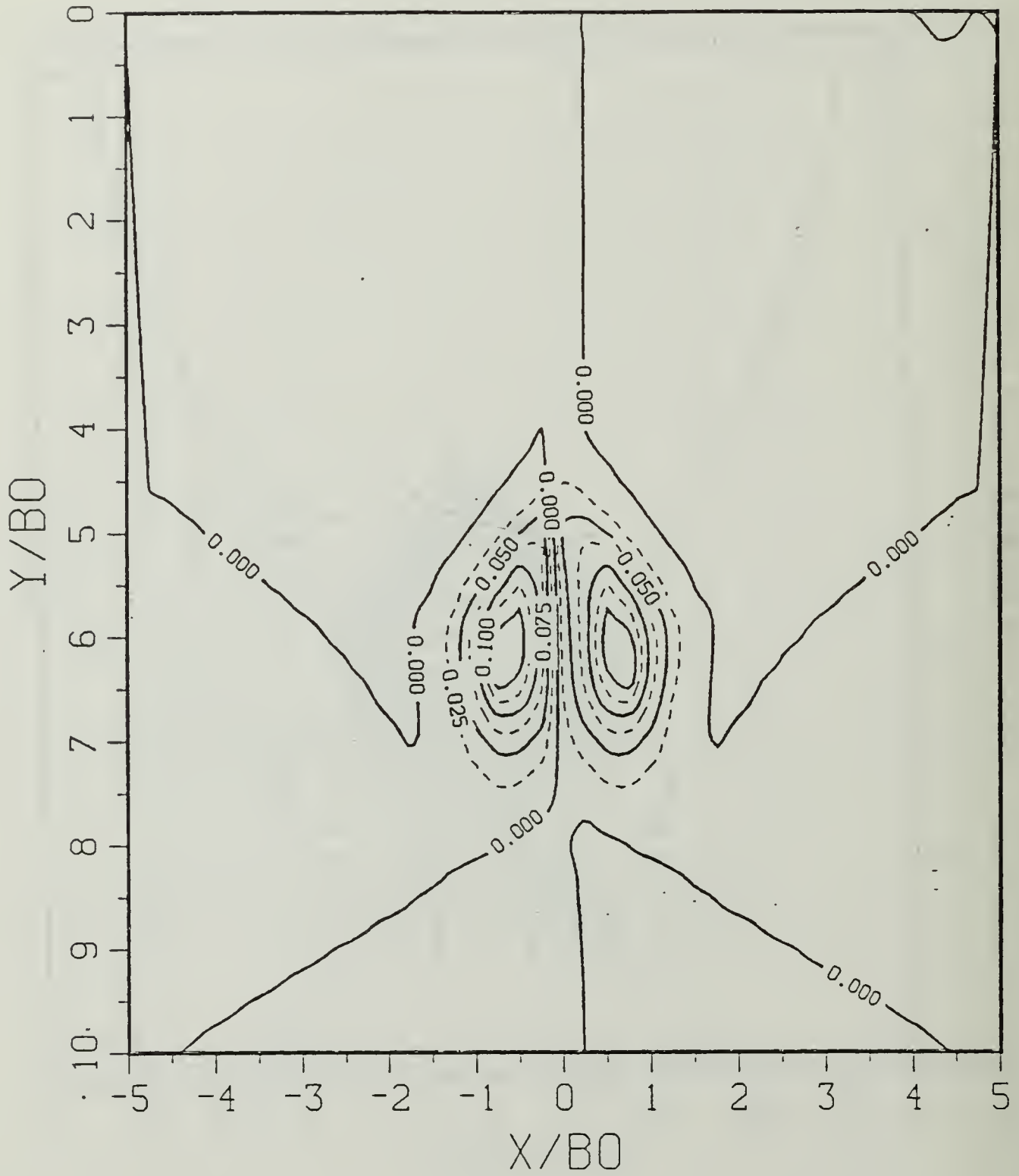


Figure B.36d Vorticity Field:  $SP = 0.50$ .

$$T^* = 2.38080$$

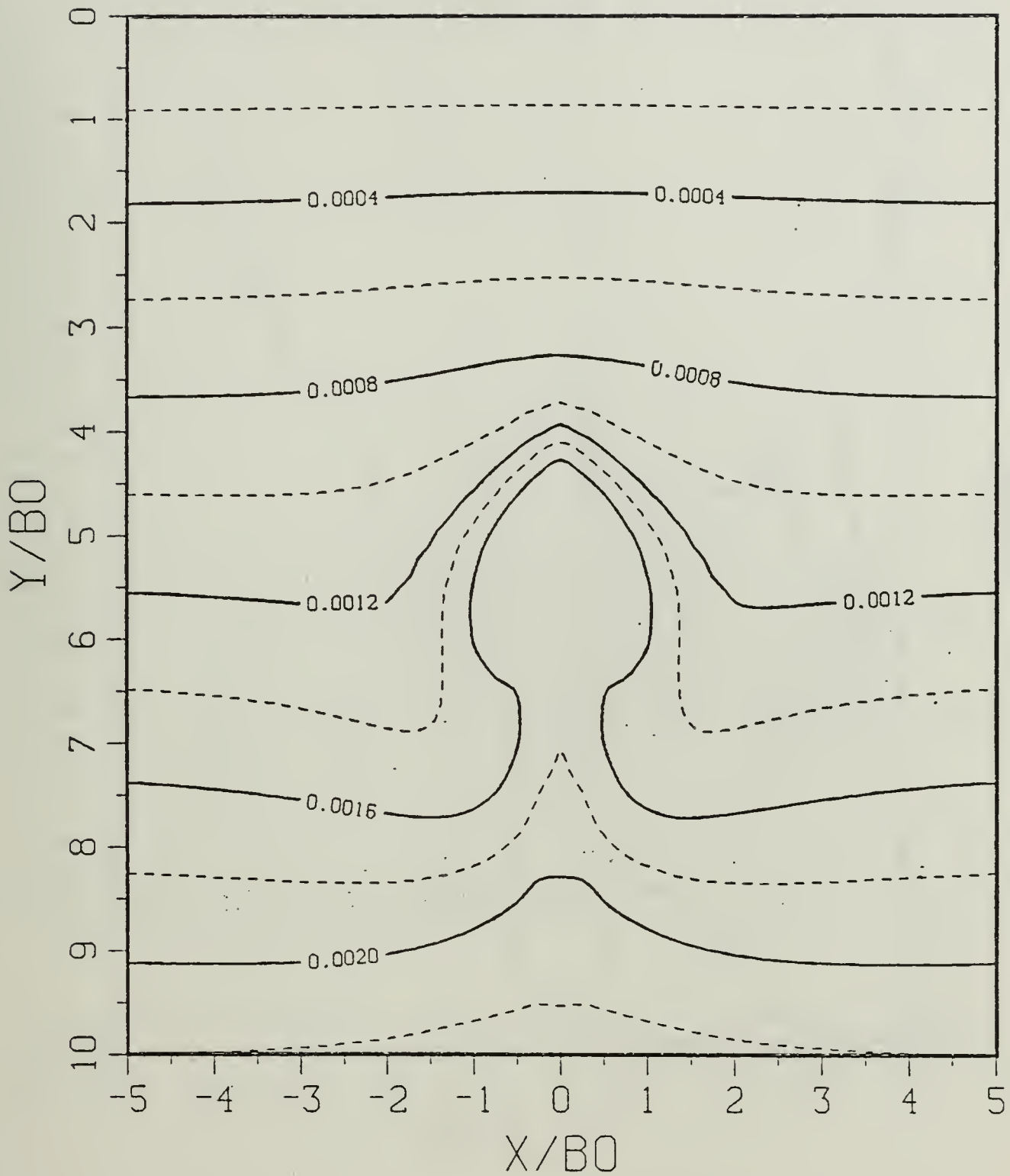


Figure B.37a Constant Density Contours:  $SP = 0.50$ .

$$T^* = 2.38080$$

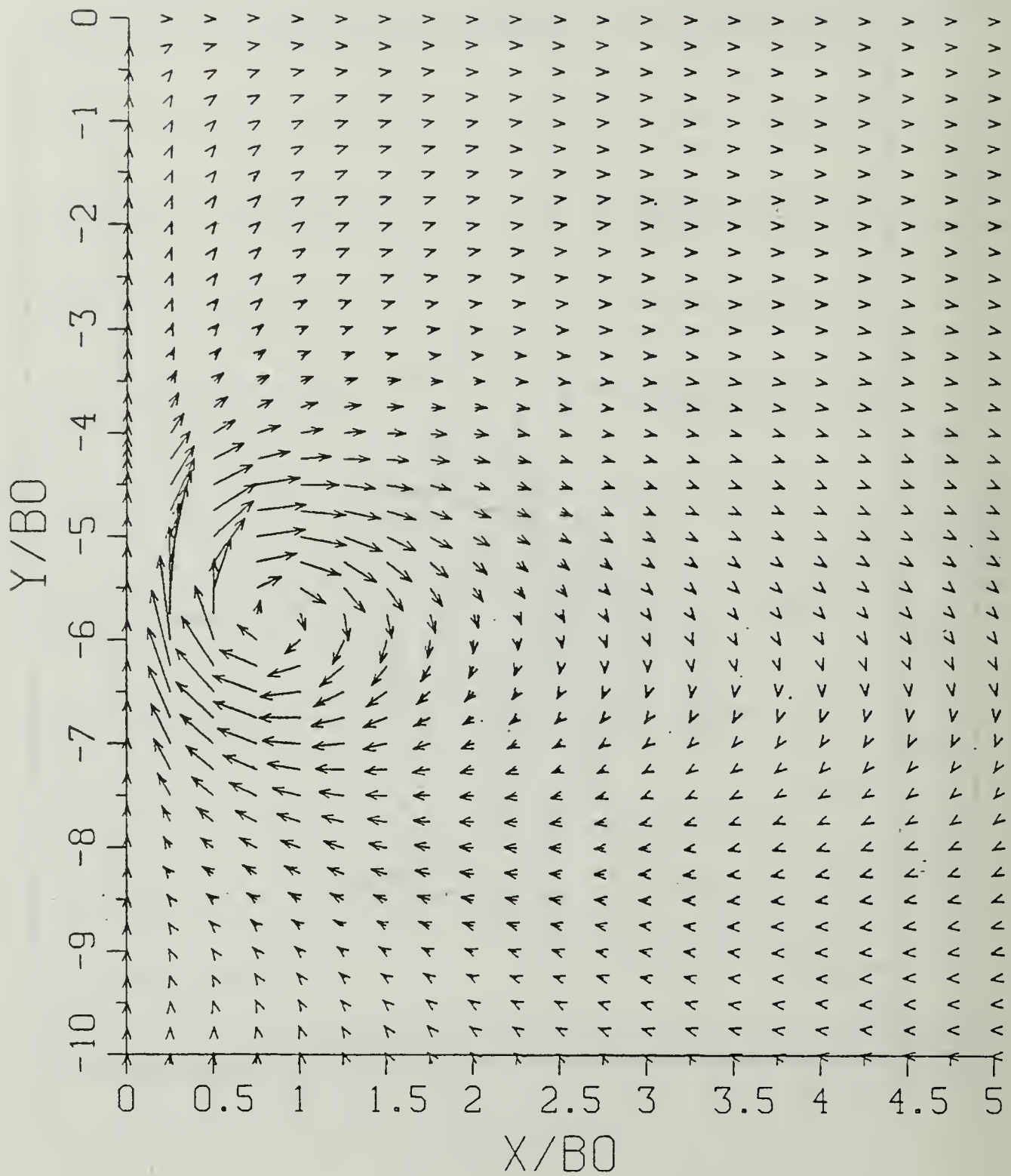


Figure B.37b Velocity Field:  $SP = 0.50$ .

$$T^* = 2.38080$$

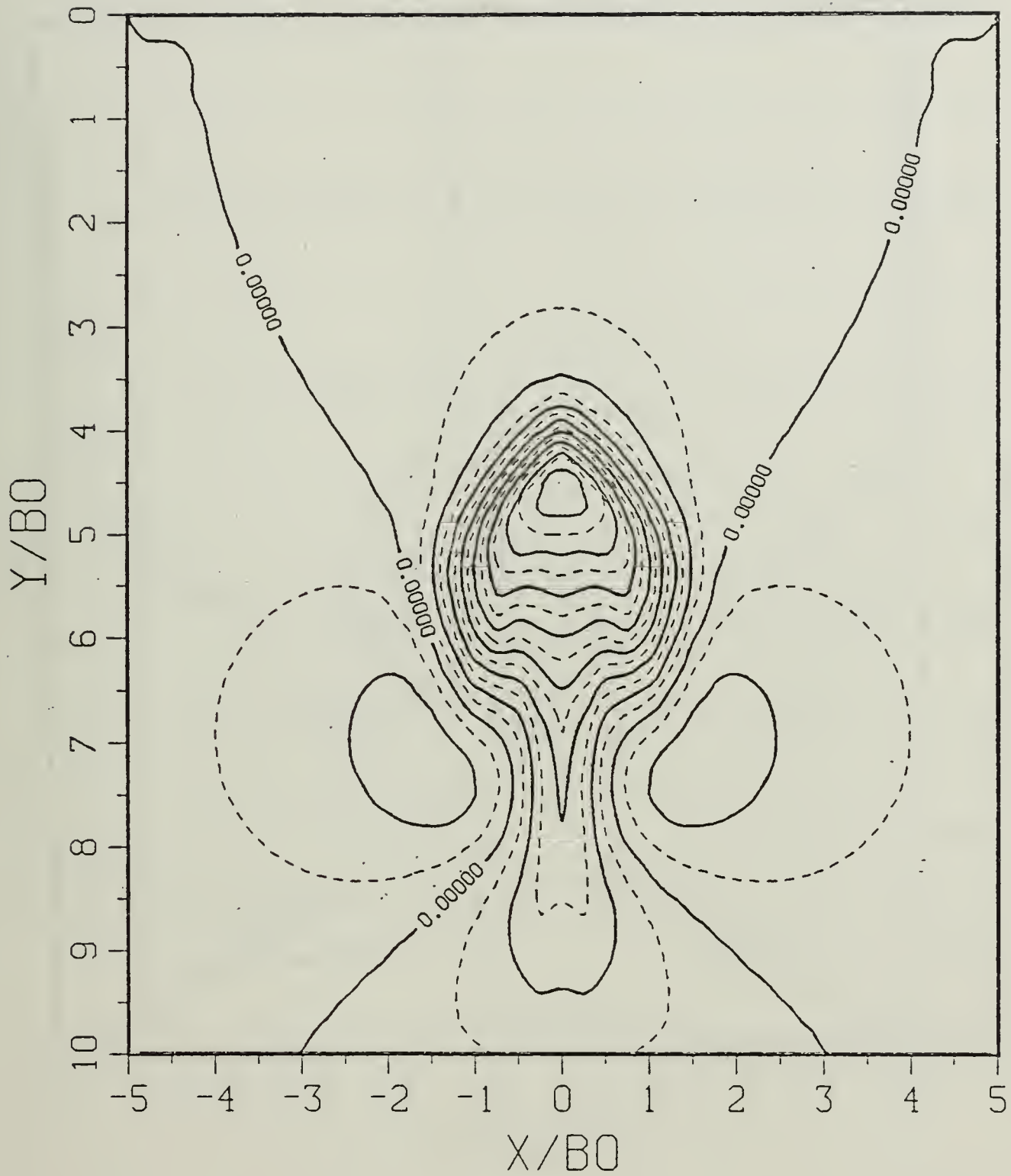


Figure B.37c Density Perturbation Contours:  $SP = 0.50$ .

$$T^* = 2.38080$$

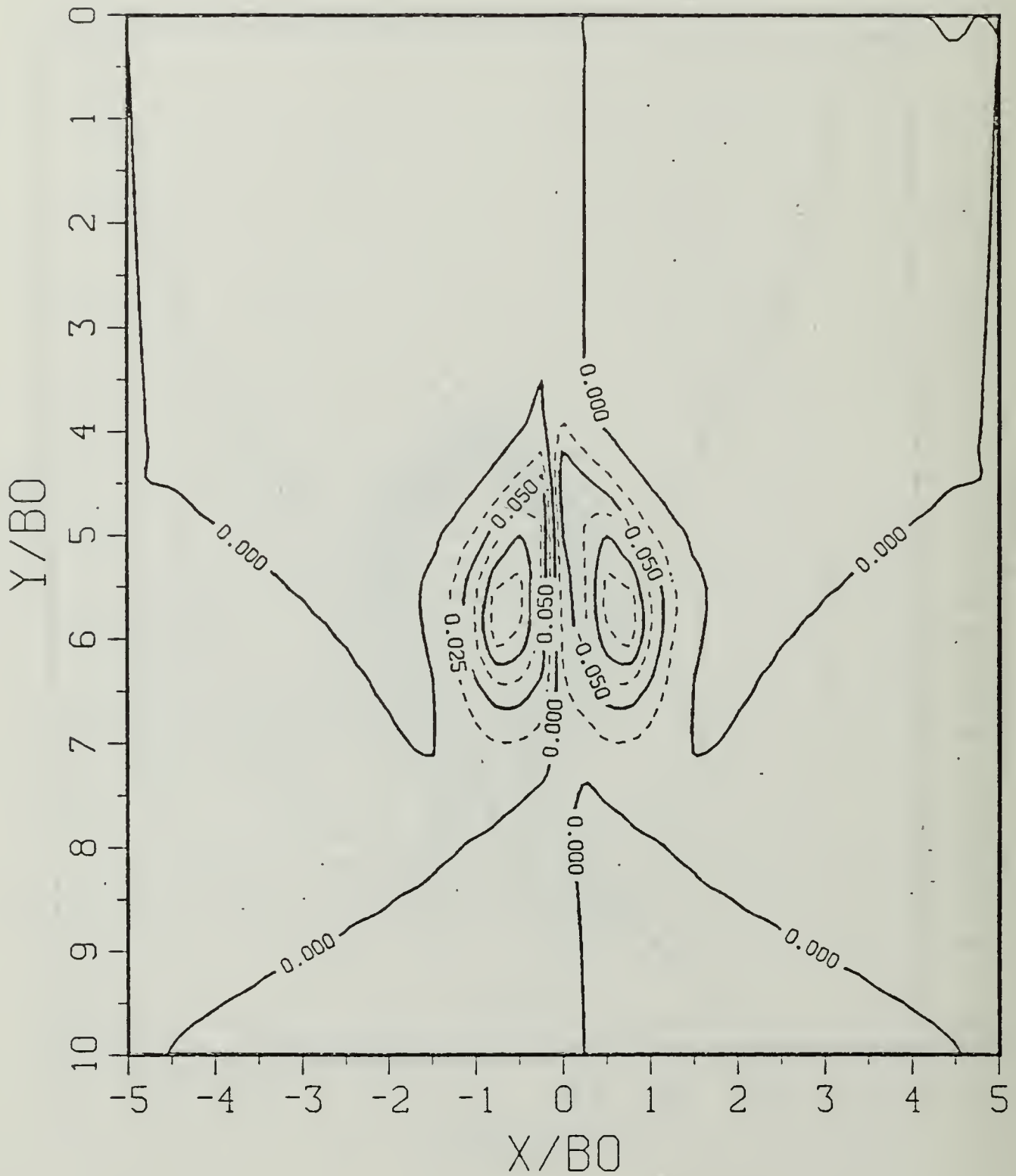


Figure B.37d Vorticity Field:  $SP = 0.50$ .

$$T^* = 2.97600$$

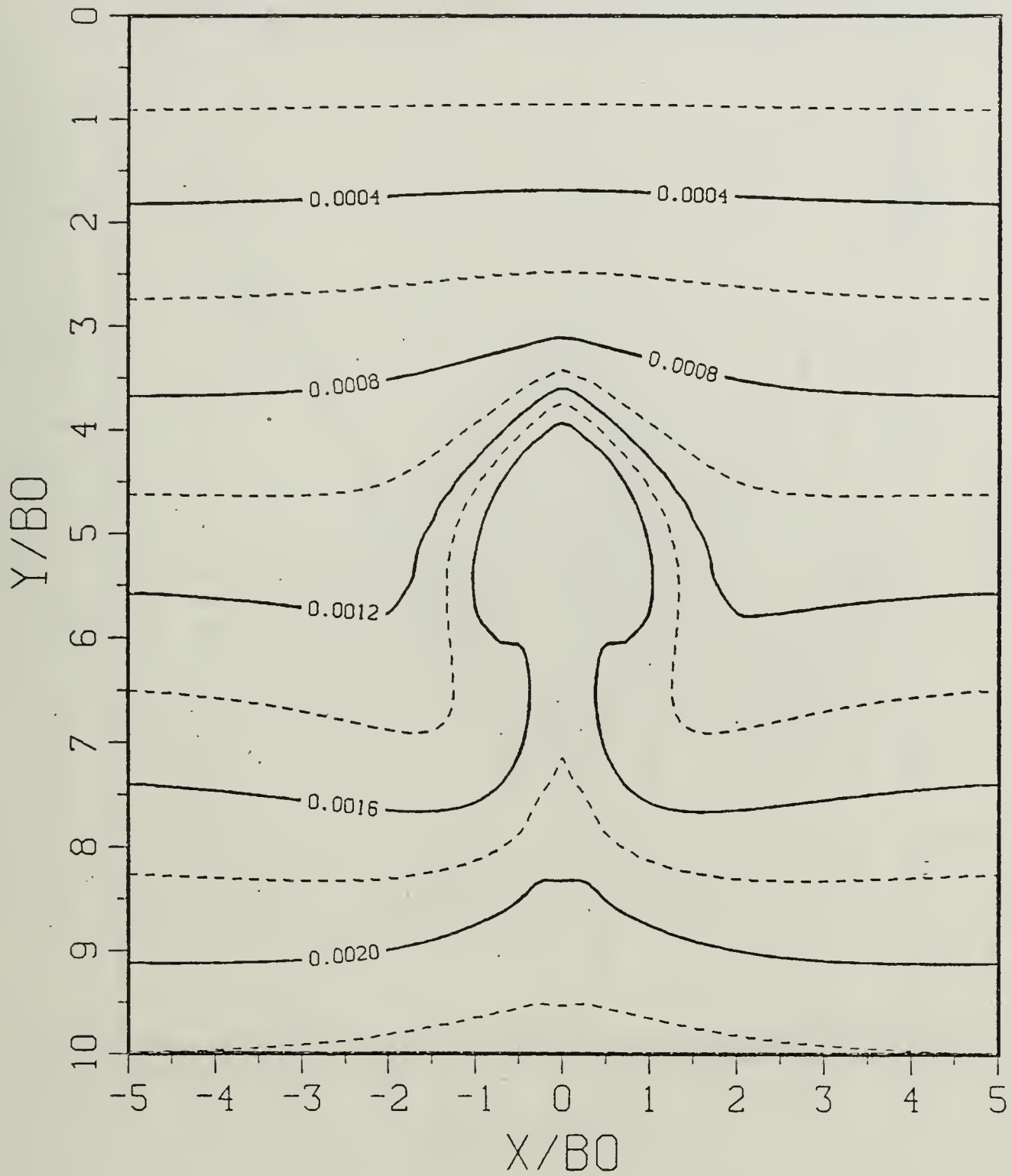


Figure B.38a Constant Density Contours:  $SP = 0.50$ .

$$T^* = 2.97600$$

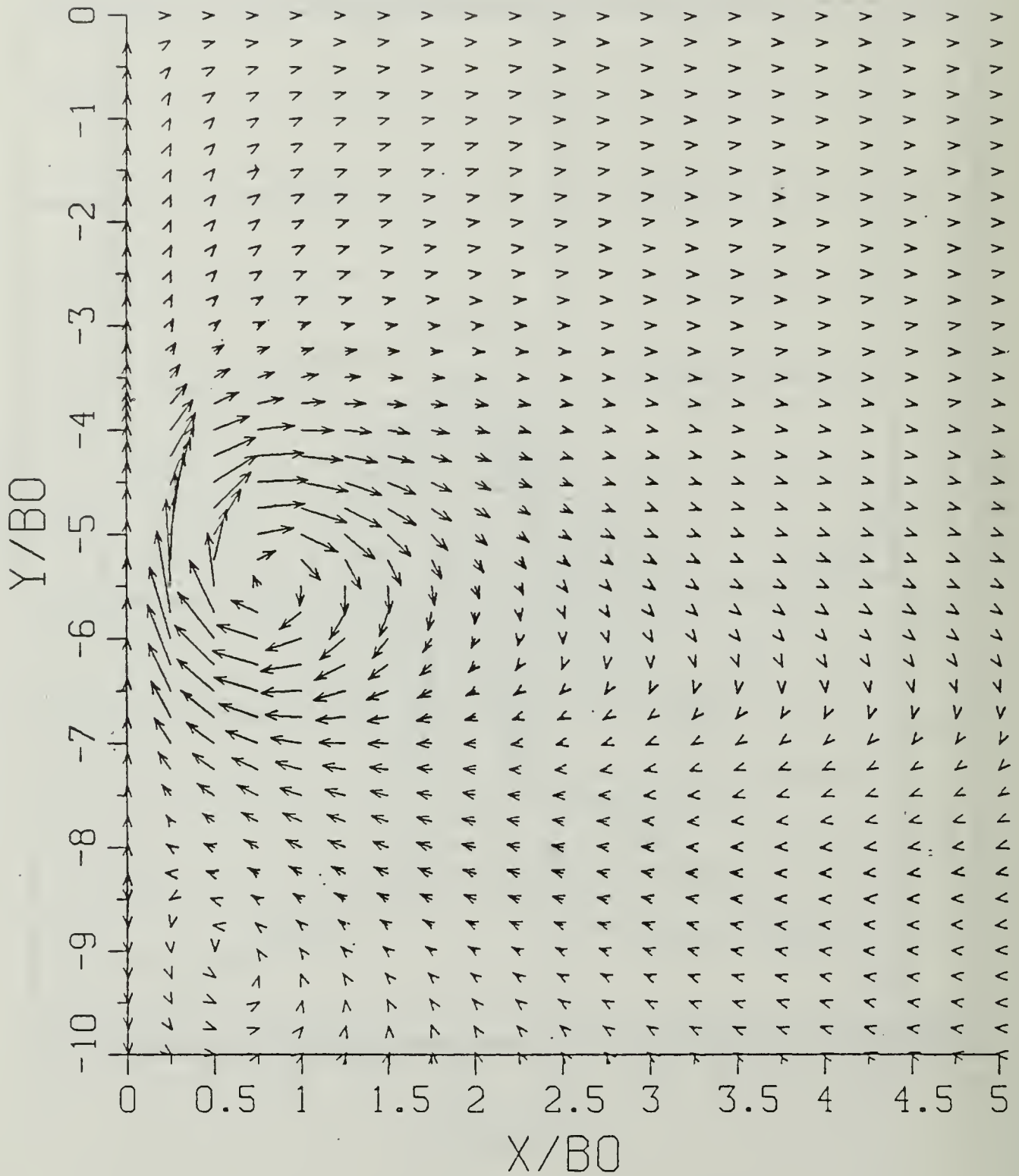


Figure B.38b Velocity Field:  $SP = 0.50$ .

$$T^* = 2.97600$$

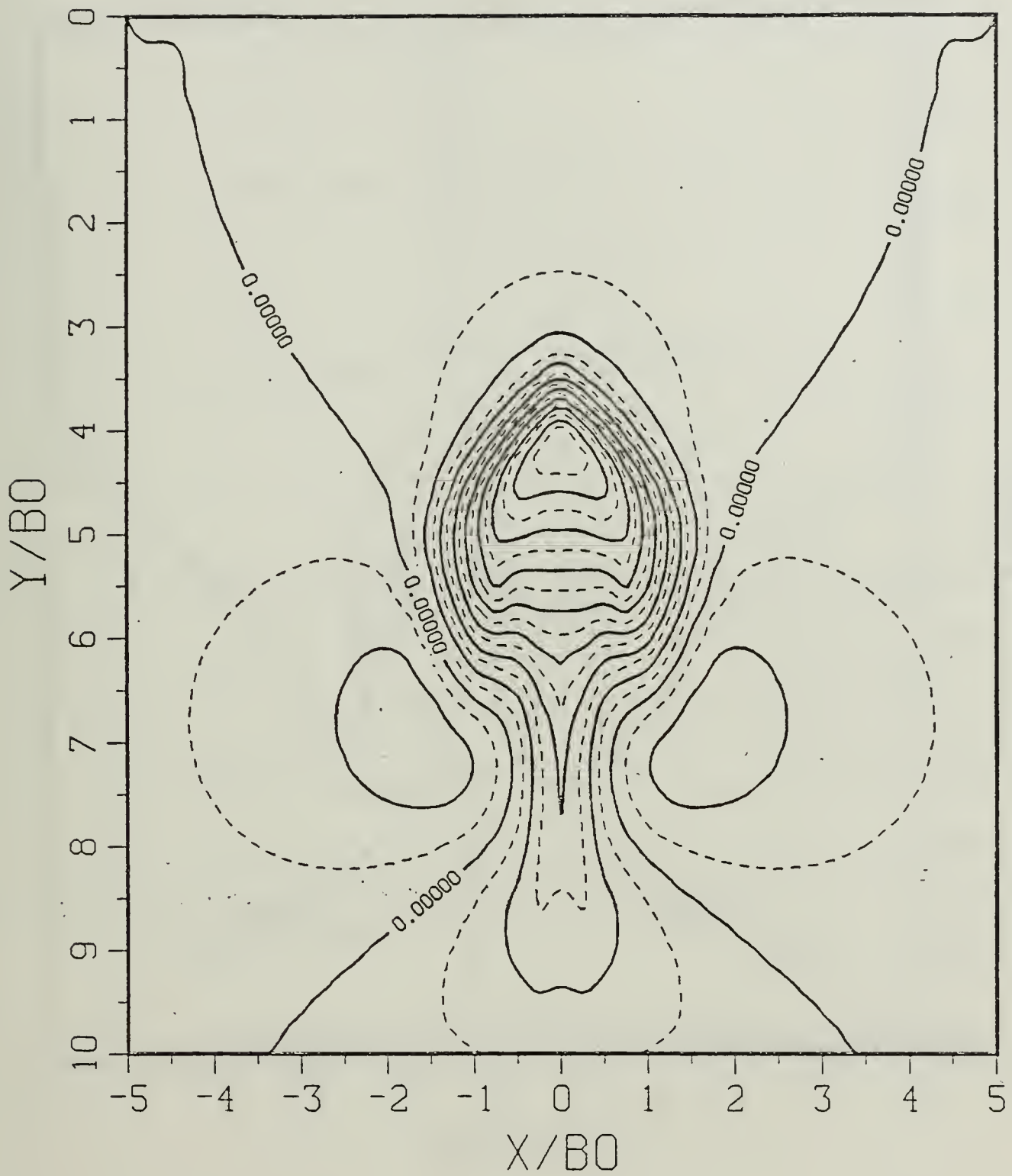


Figure B.38c Density Perturbation Contours:  $SP = 0.50$ .

$$T^* = 2.97600$$

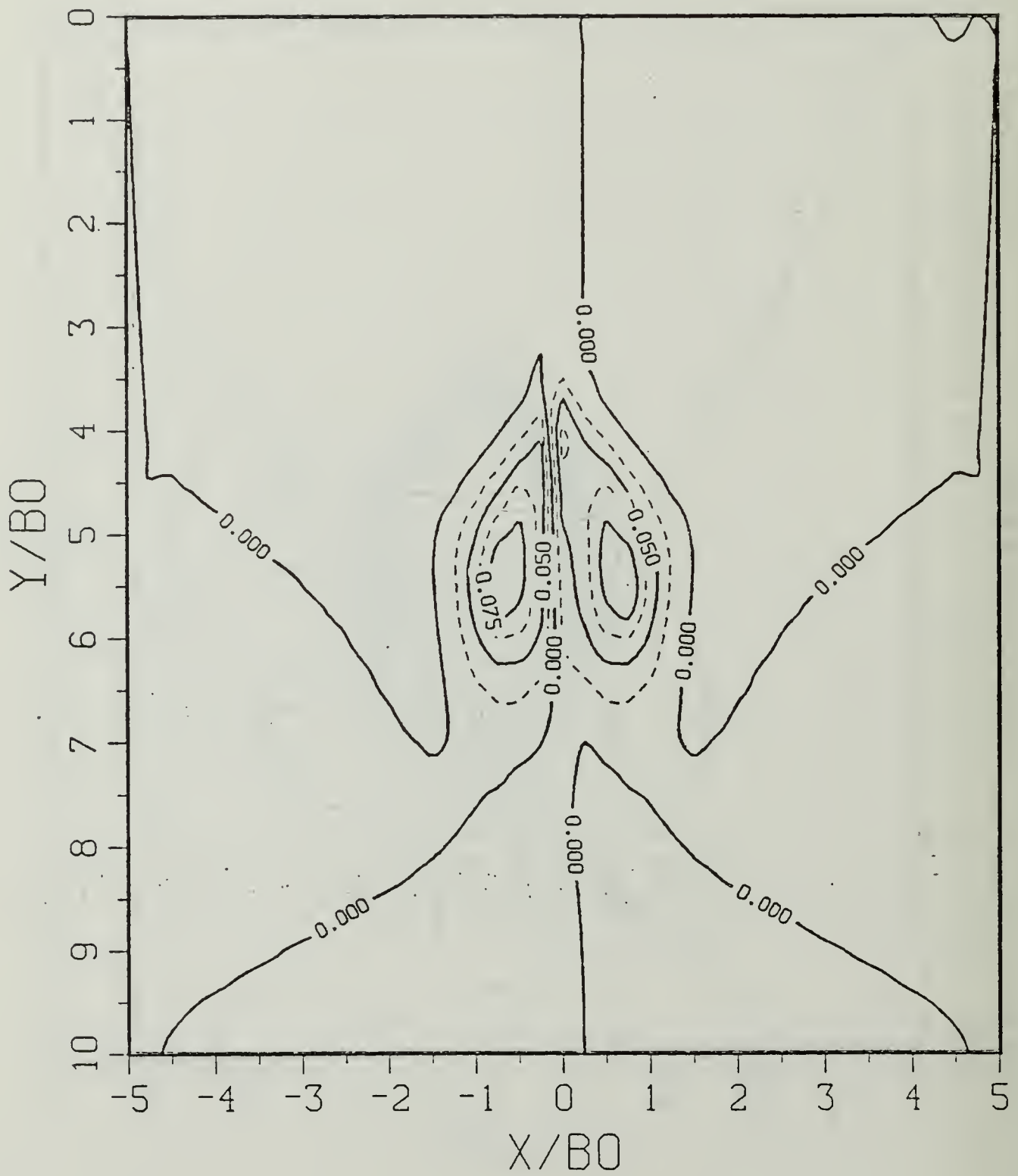


Figure B.38d Vorticity Field: SP = 0.50.

$$T^* = 3.57120$$

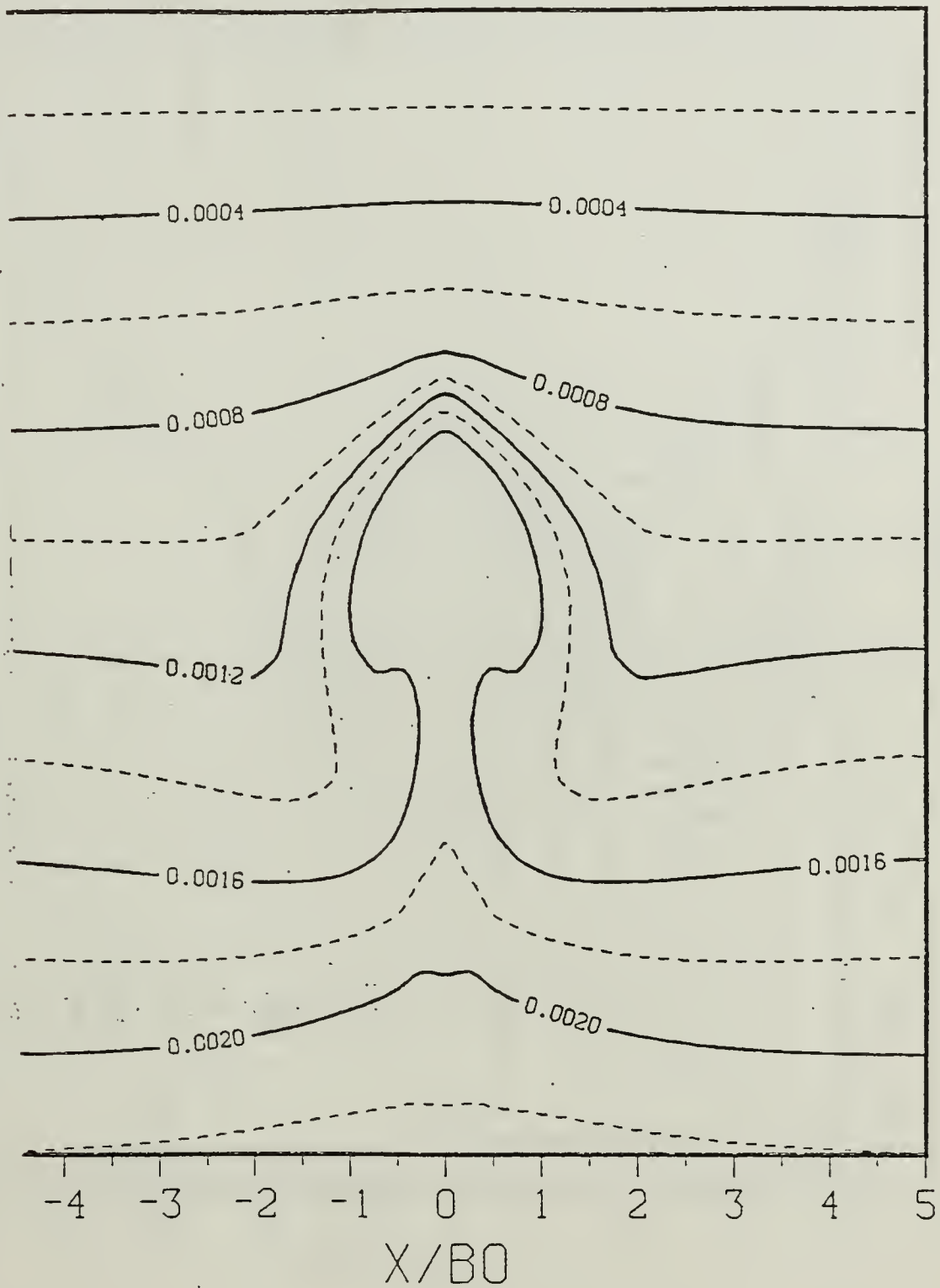


Figure B.39a Constant Density Contours:  $SP = 0.50$ .

$$T^* = 3.57120$$

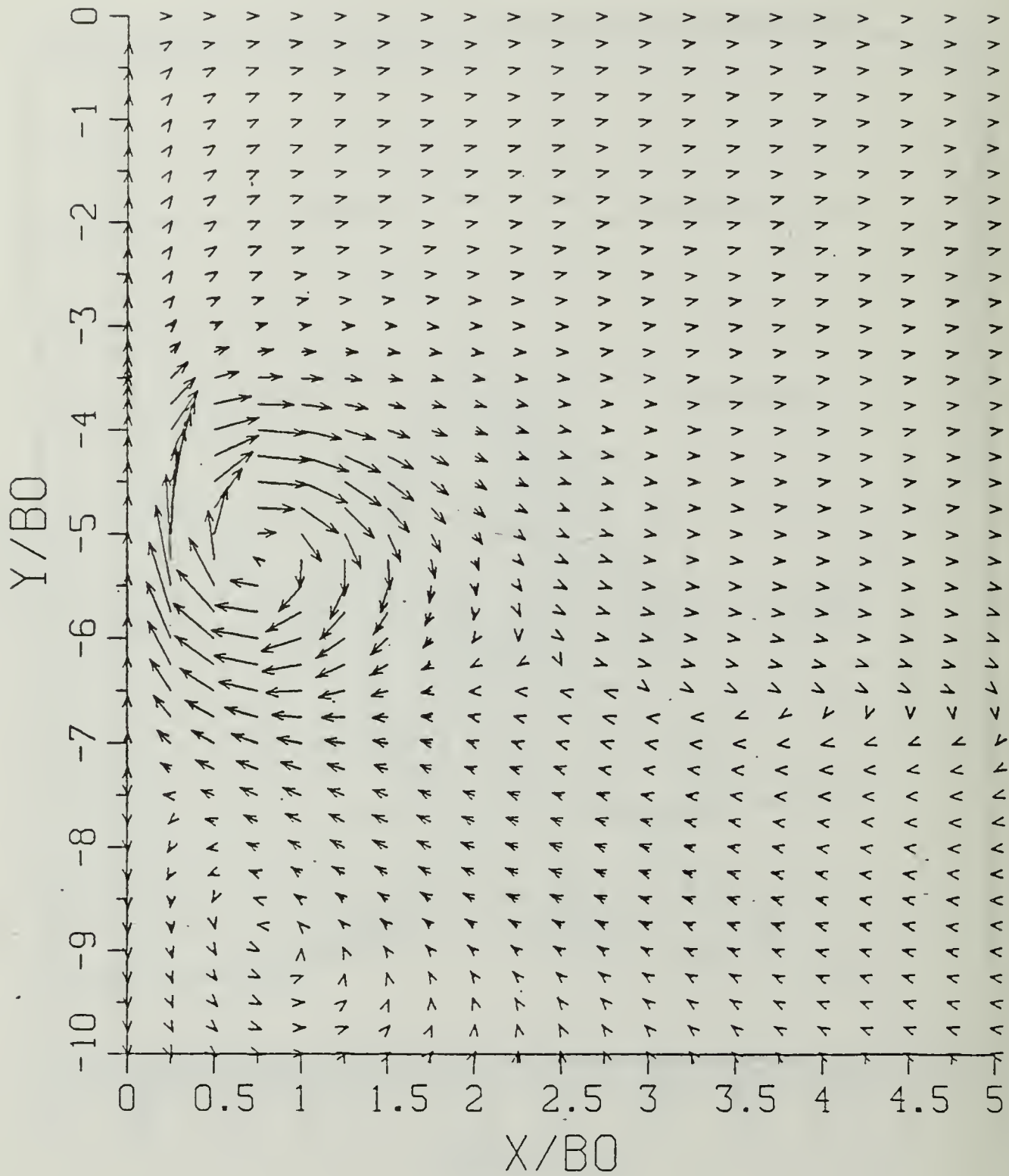


Figure B.39b Velocity Field:  $SP = 0.50$ .

$$T^* = 3.57120$$

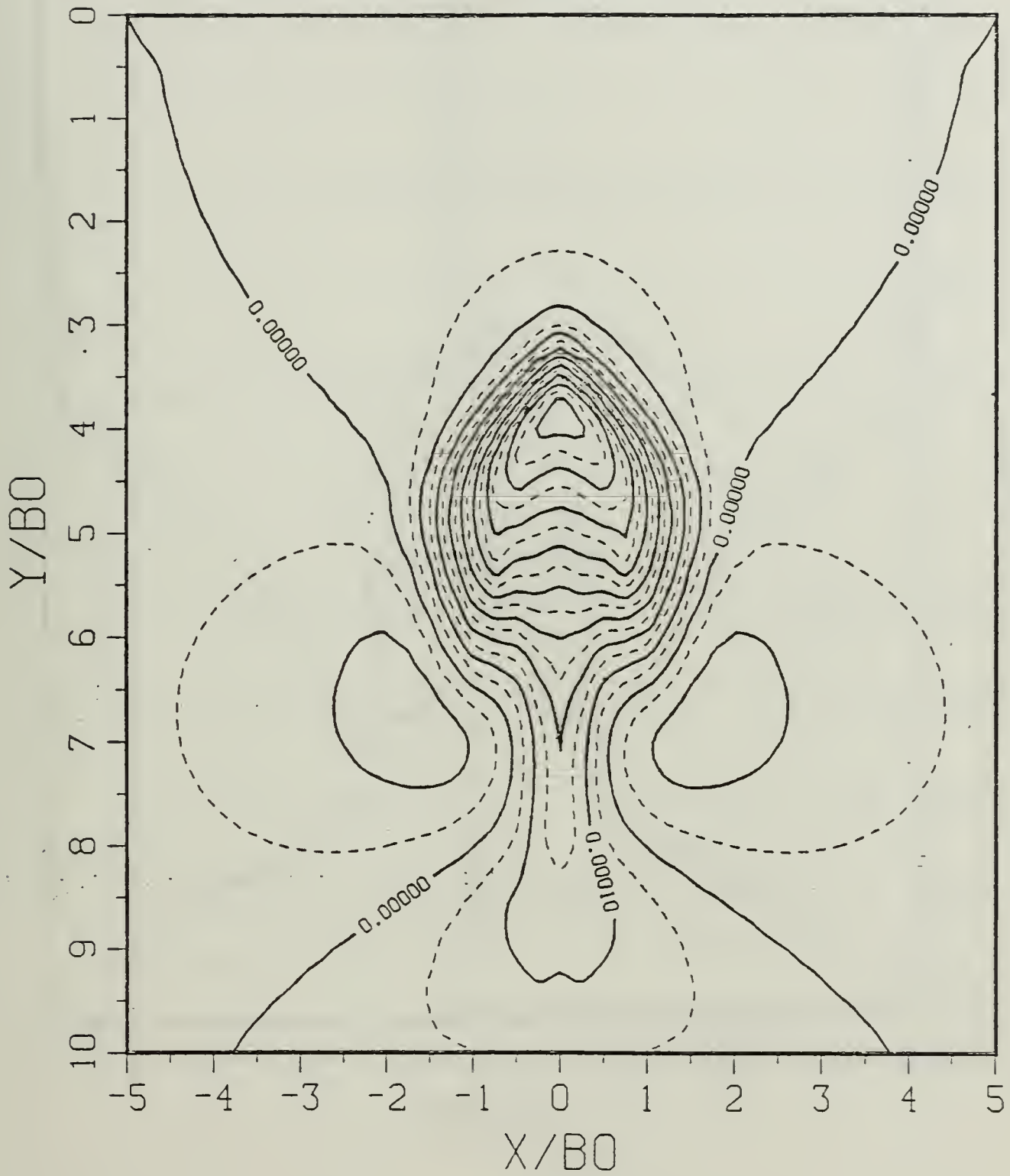


Figure B.39c Density Perturbation Contours: SP = 0.50.

$$T^* = 3.57120$$

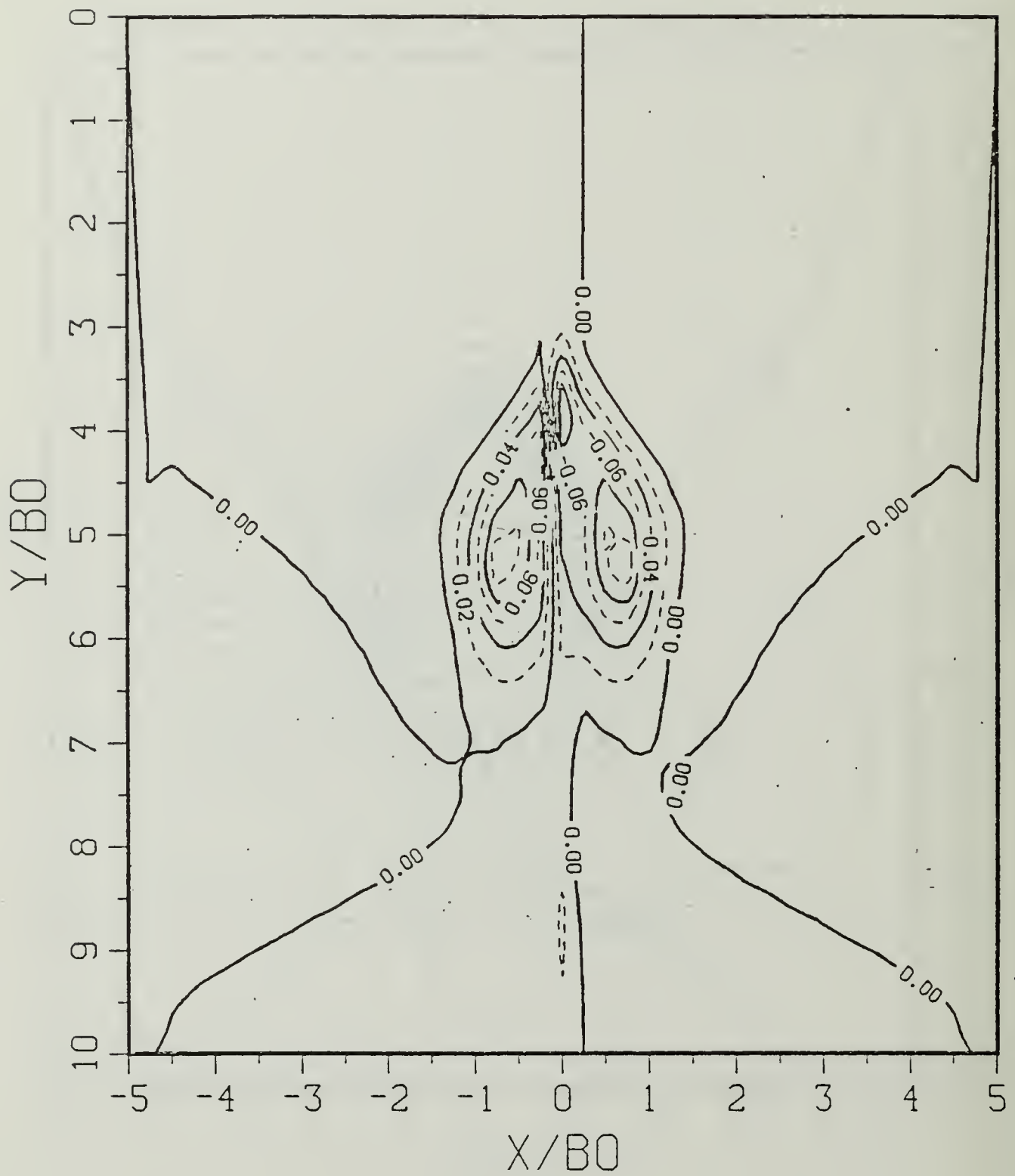


Figure B.39d Vorticity Field:  $SP = 0.50$ .

$$T^* = 4.16640$$

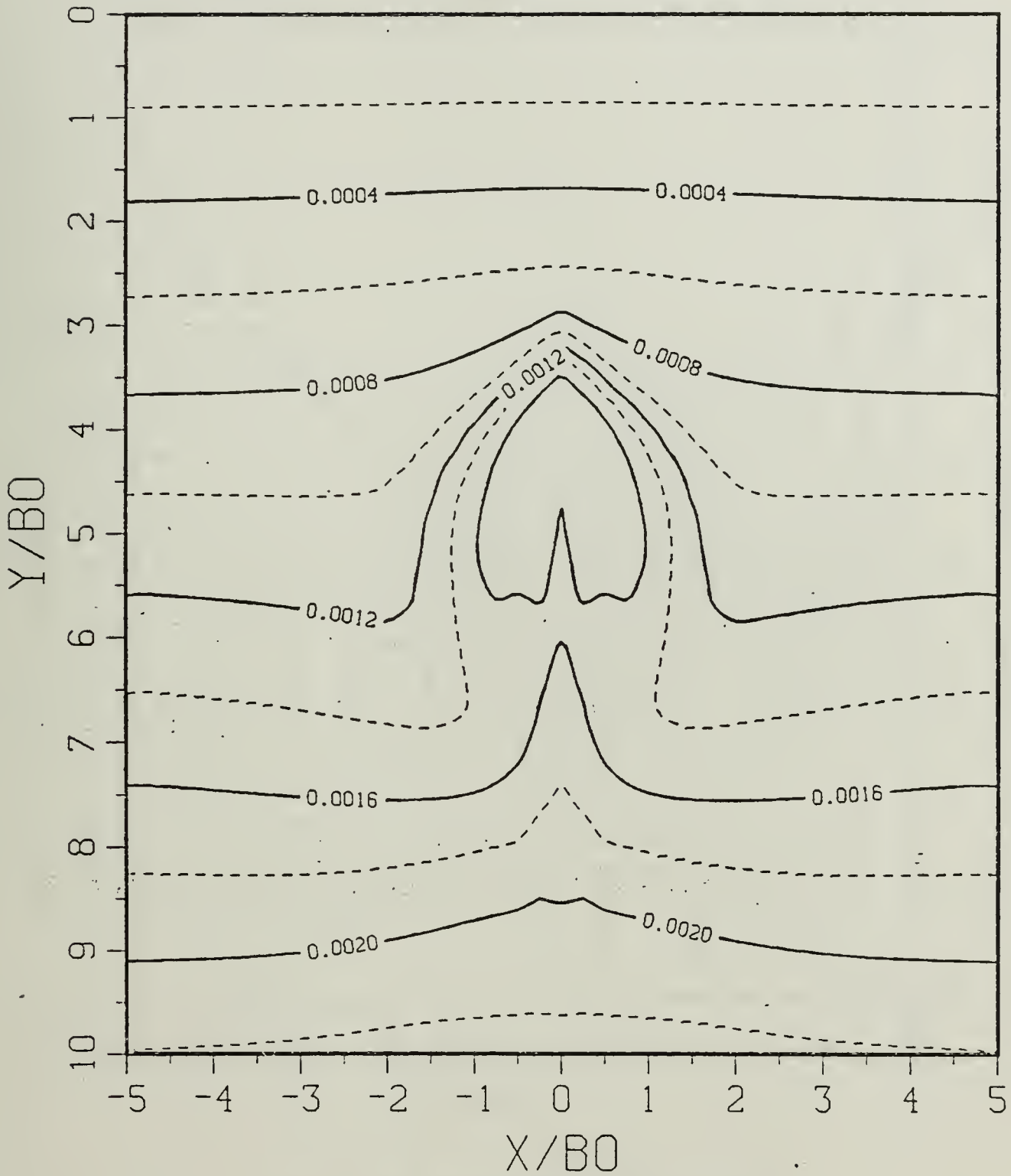


Figure B.40a Constant Density Contours:  $SP = 0.50$ .

$$T^* = 4.16640$$

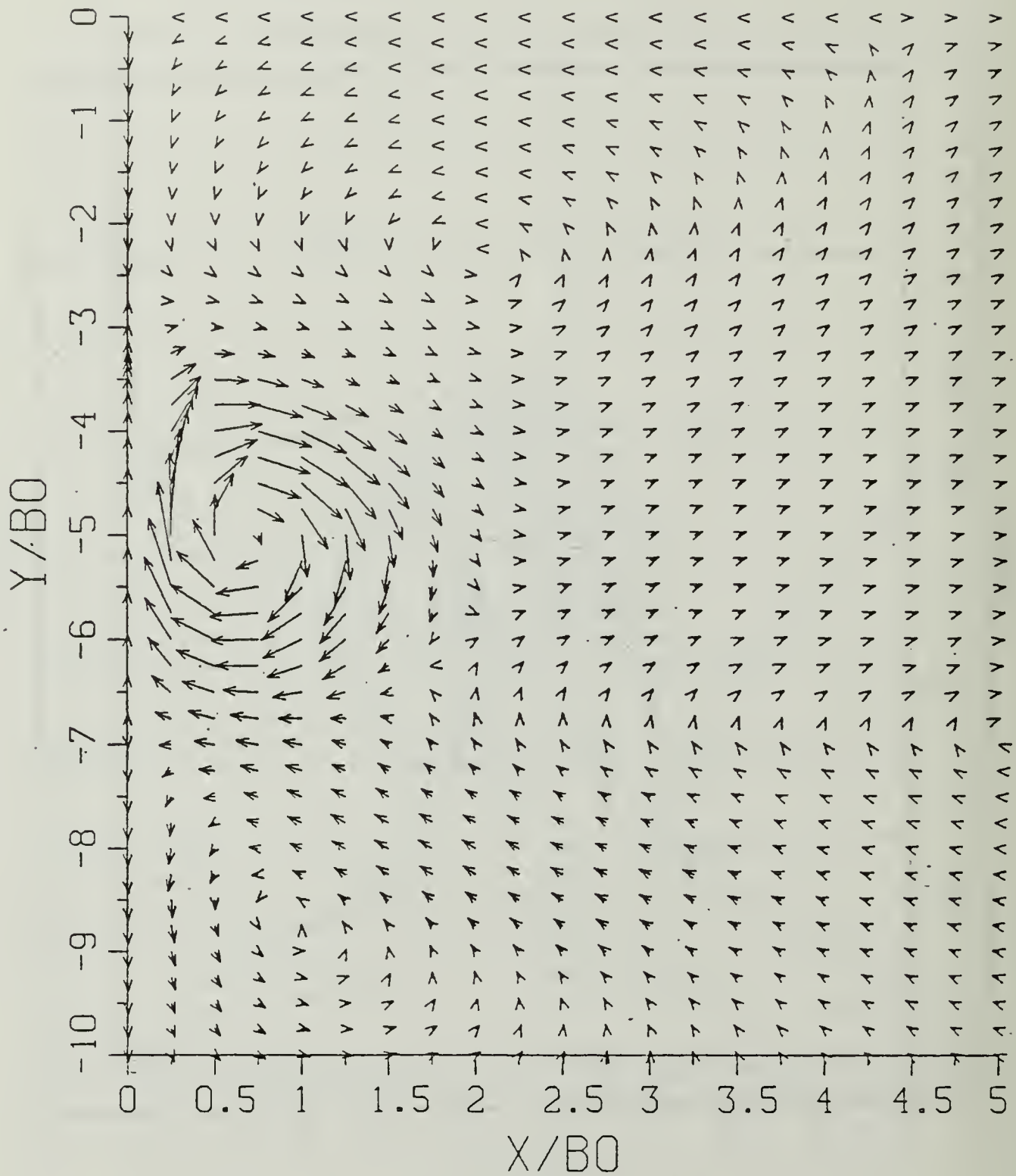


Figure B.40b Velocity Field:  $SP = 0.50$ .

$$T^* = 4.16640$$

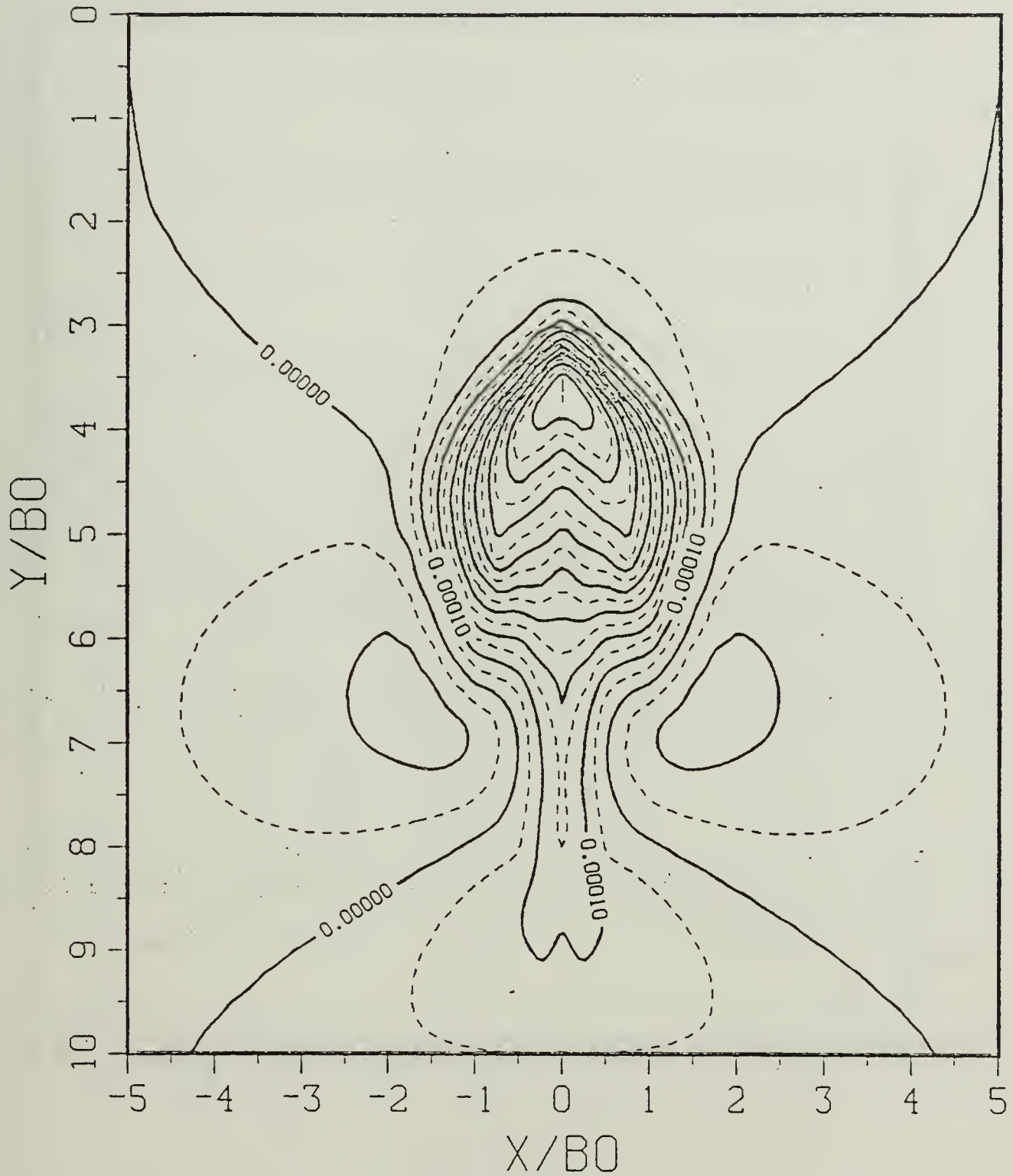


Figure B.40c Density Perturbation Contours:  $SP = 0.50$ .

$$T^* = 4.16640$$

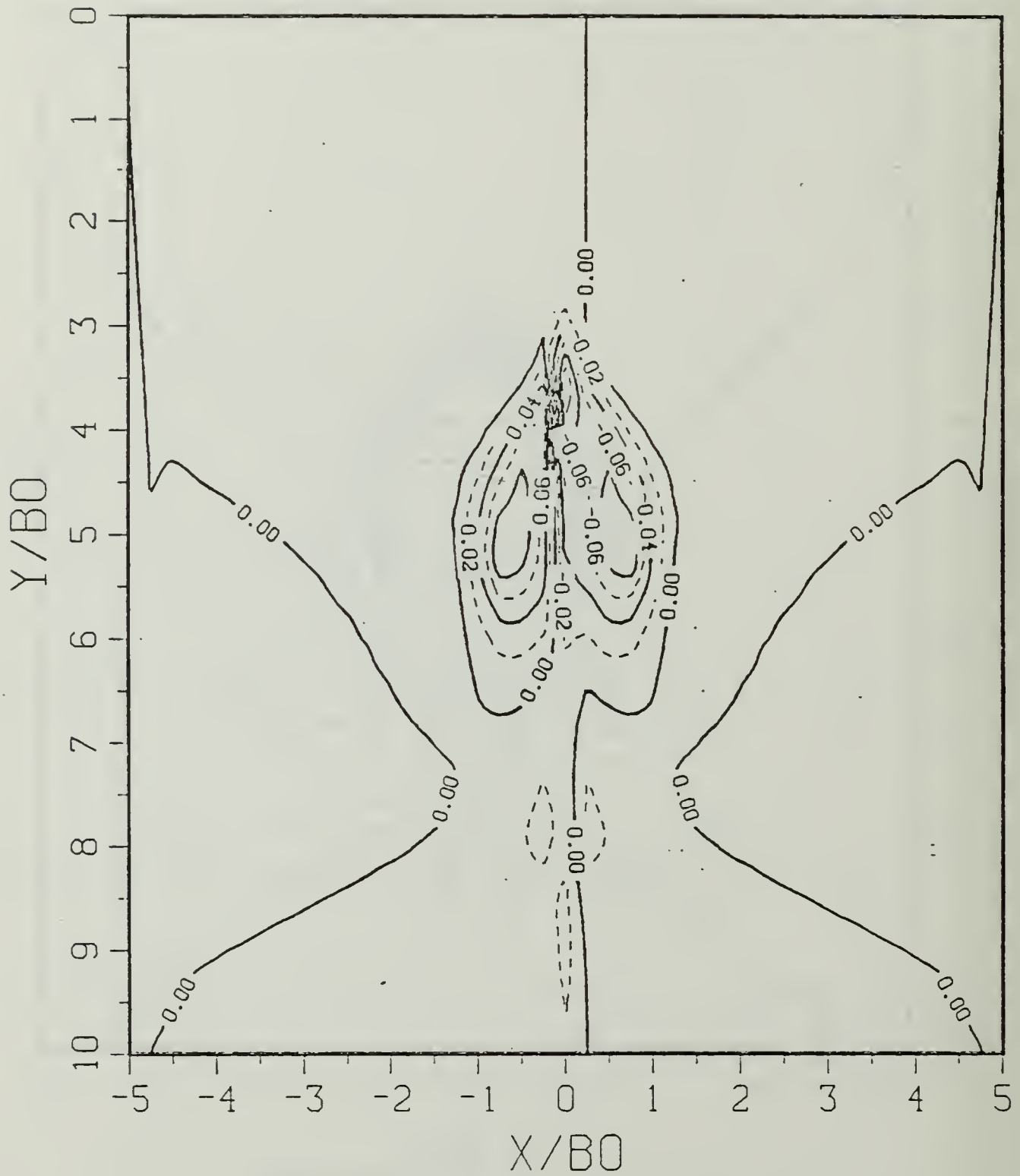


Figure B.40d Vorticity Field: SP = 0.50.

$$T^* = 4.76160$$

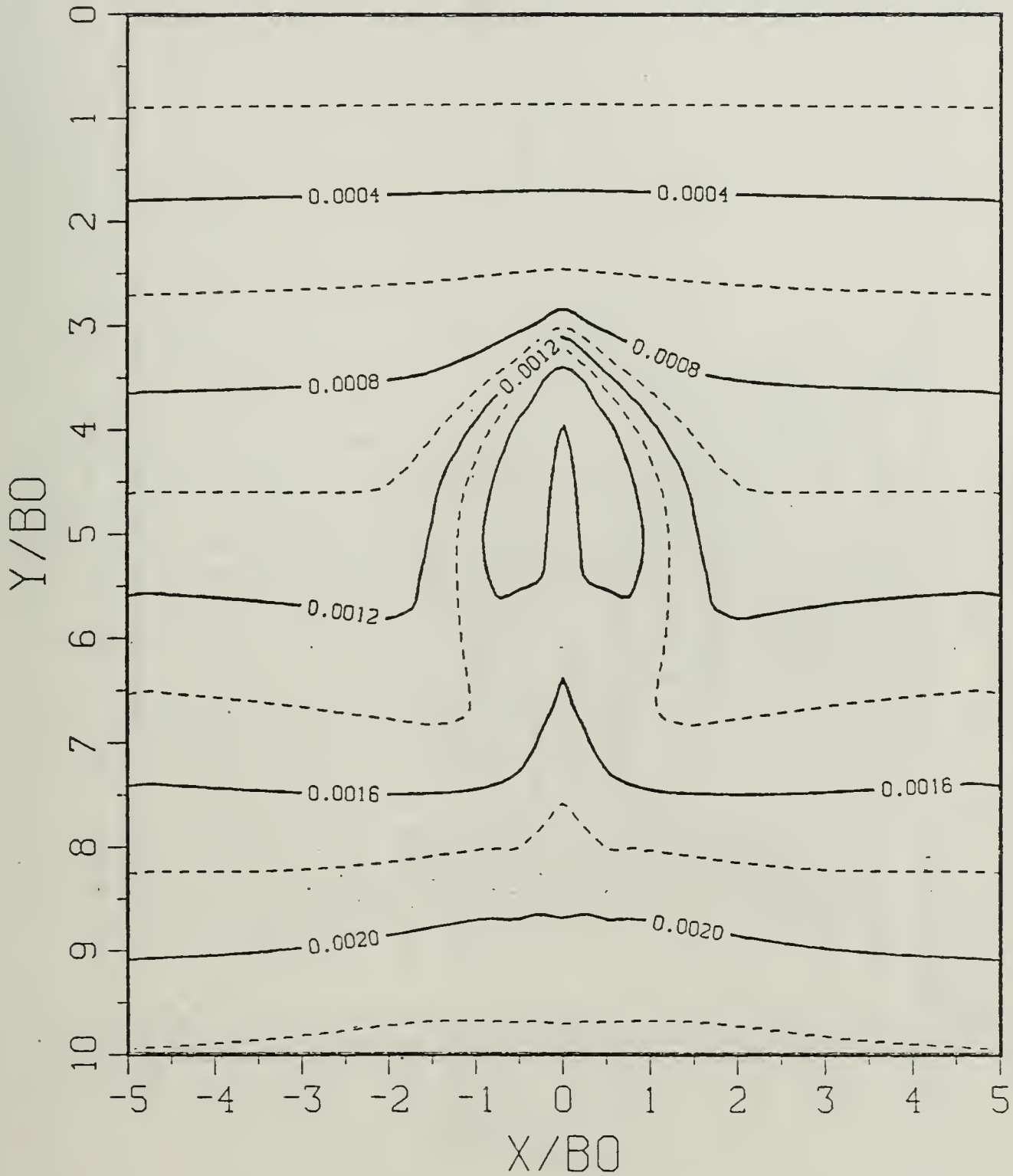


Figure B.41a Constant Density Contours:  $SP = 0.50$ .

$$T^* = 4.76160$$

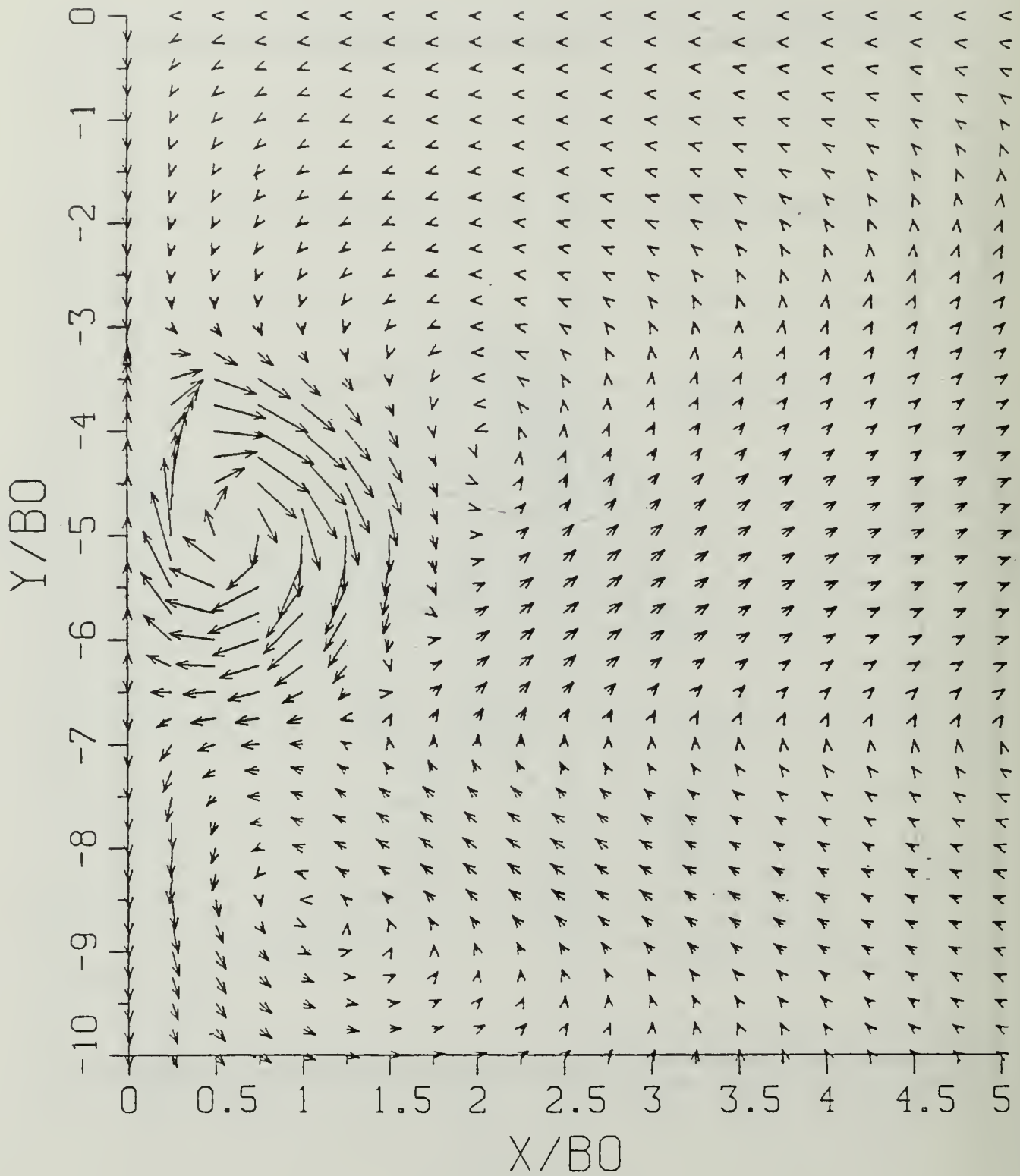


Figure B.41b Velocity Field:  $SP = 0.50$ .

$$T^* = 4.76160$$

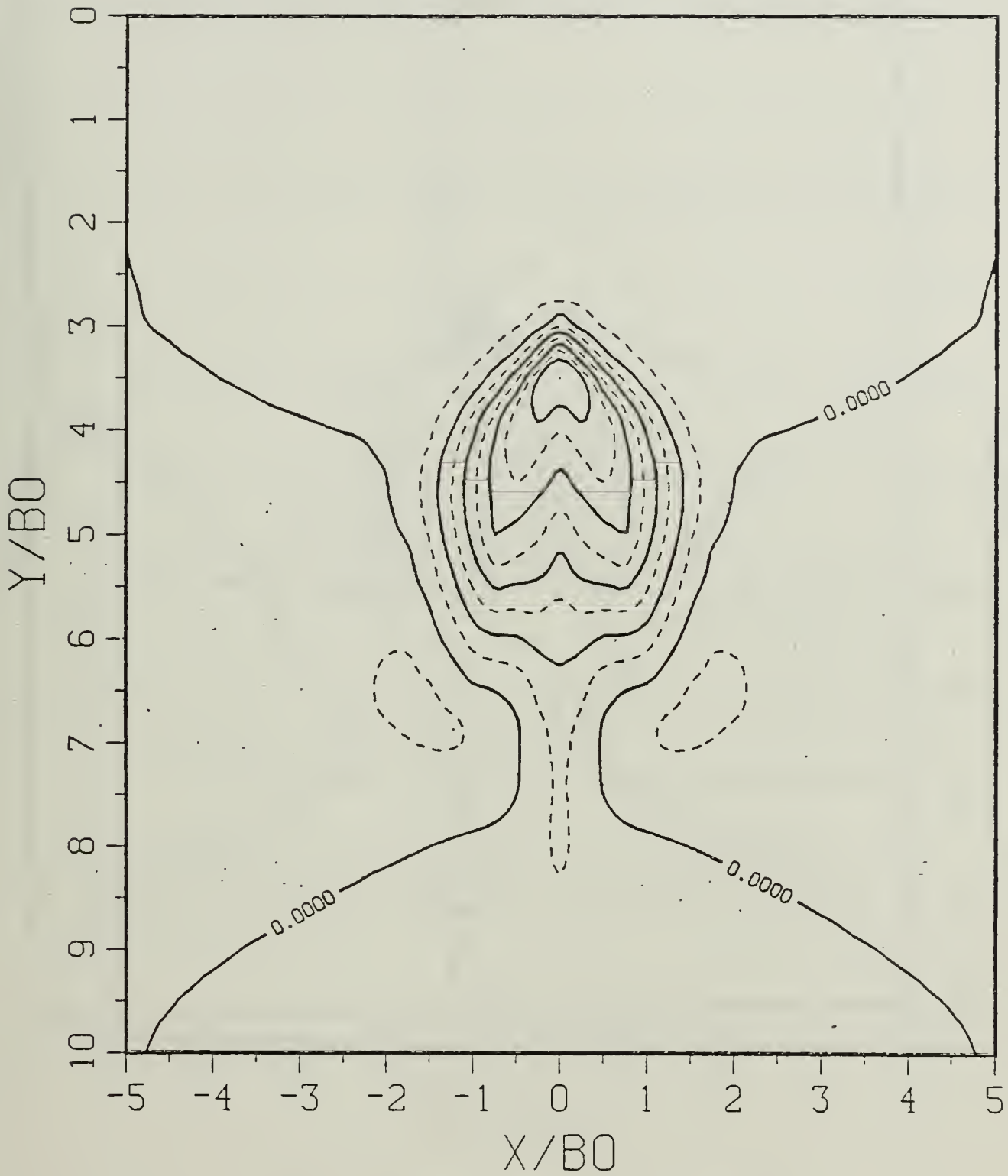


Figure B.41c Density Perturbation Contours:  $SP = 0.50$ .

$$\Gamma^* = 4.76160$$

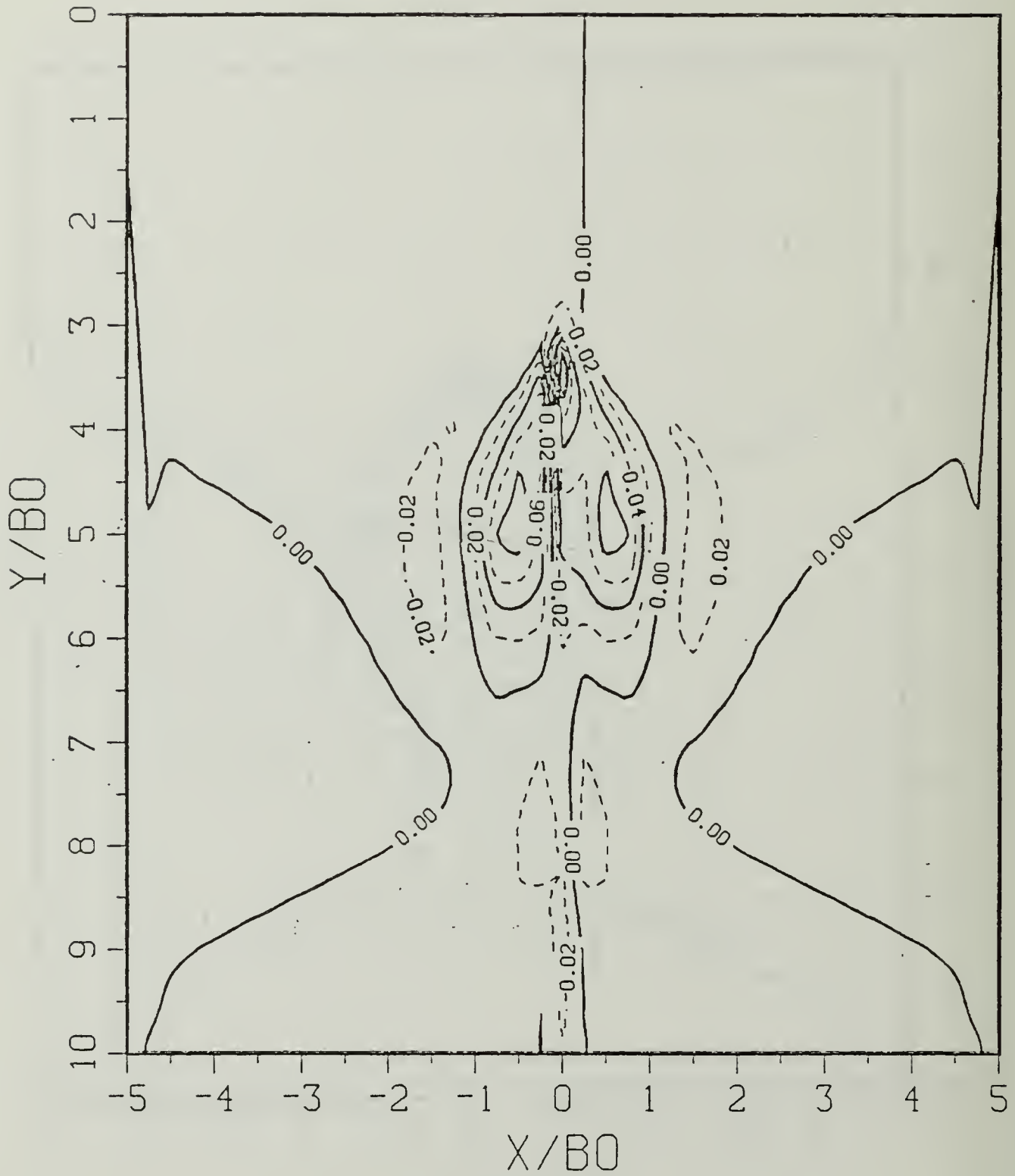


Figure B.41d Vorticity Field:  $SP = 0.50$ .

$$T^* = 5.35680$$

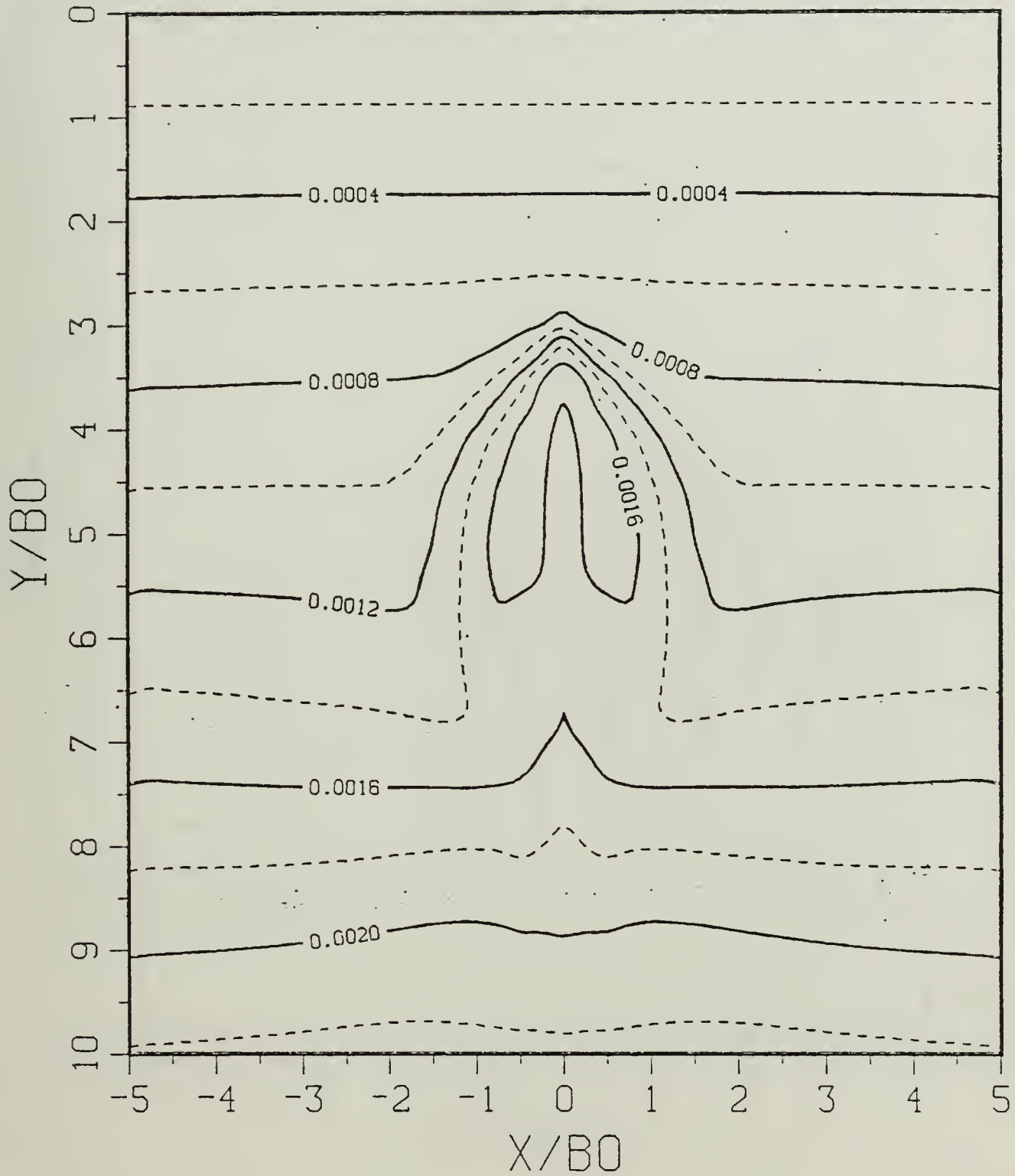


Figure B.42a Constant Density Contours:  $SP = 0.50$ .

$$T^* = 5.35680$$

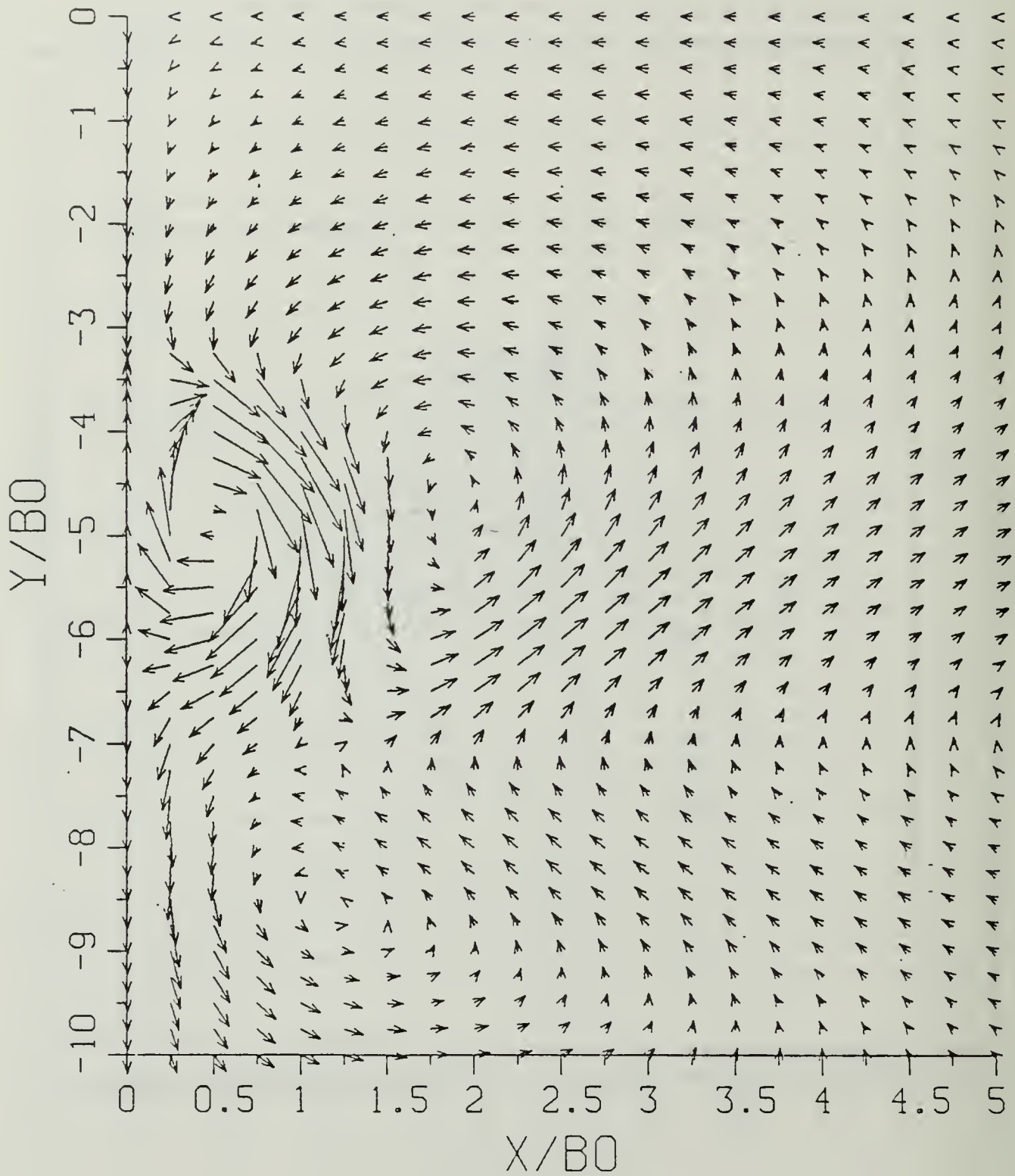


Figure B.42b Velocity Field:  $SP = 0.50$ .

$$T^* = 5.35680$$

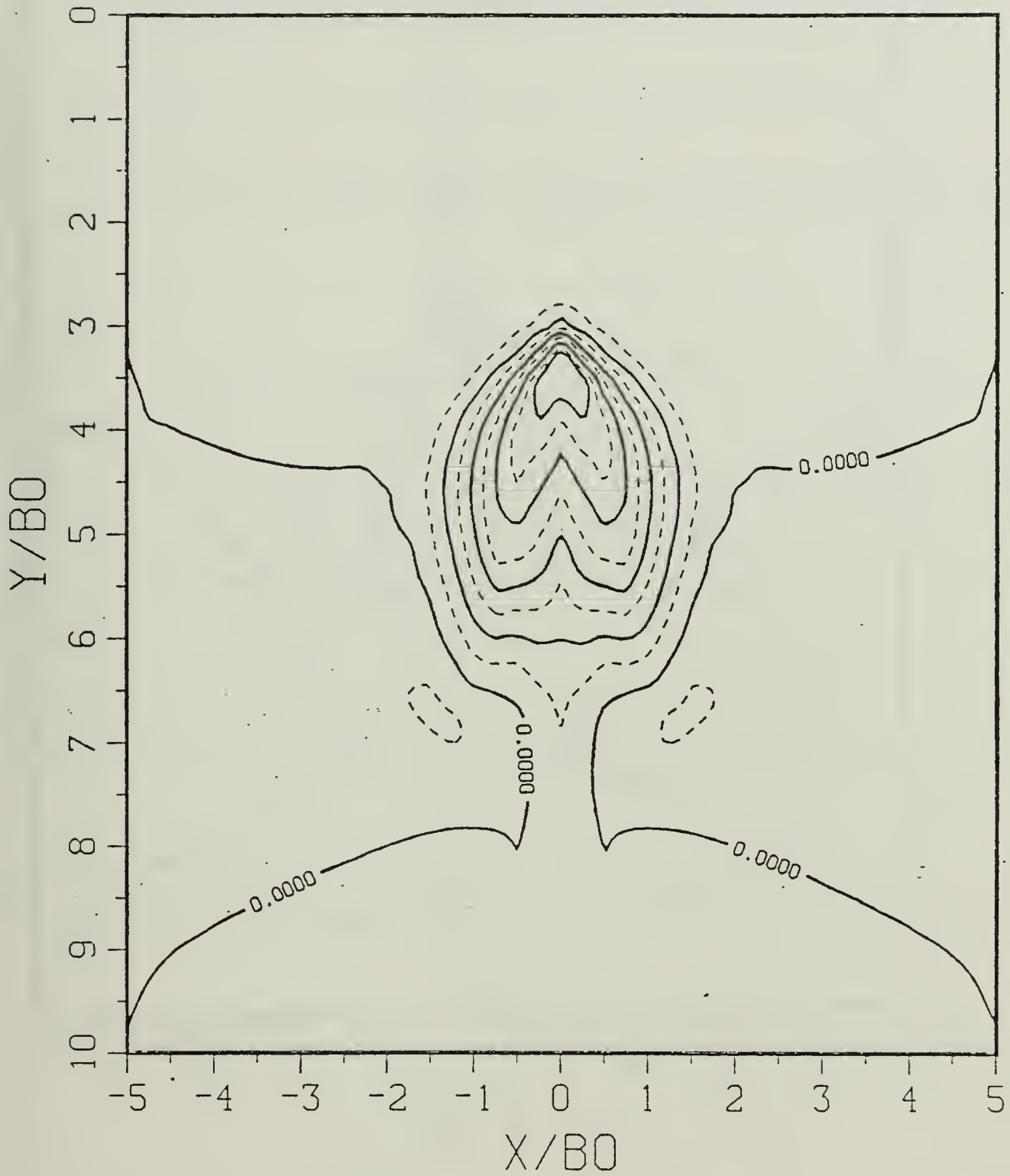


Figure B.42c Density Perturbation Contours:  $SP = 0.50$ .

$$\Gamma^* = 5.35680$$

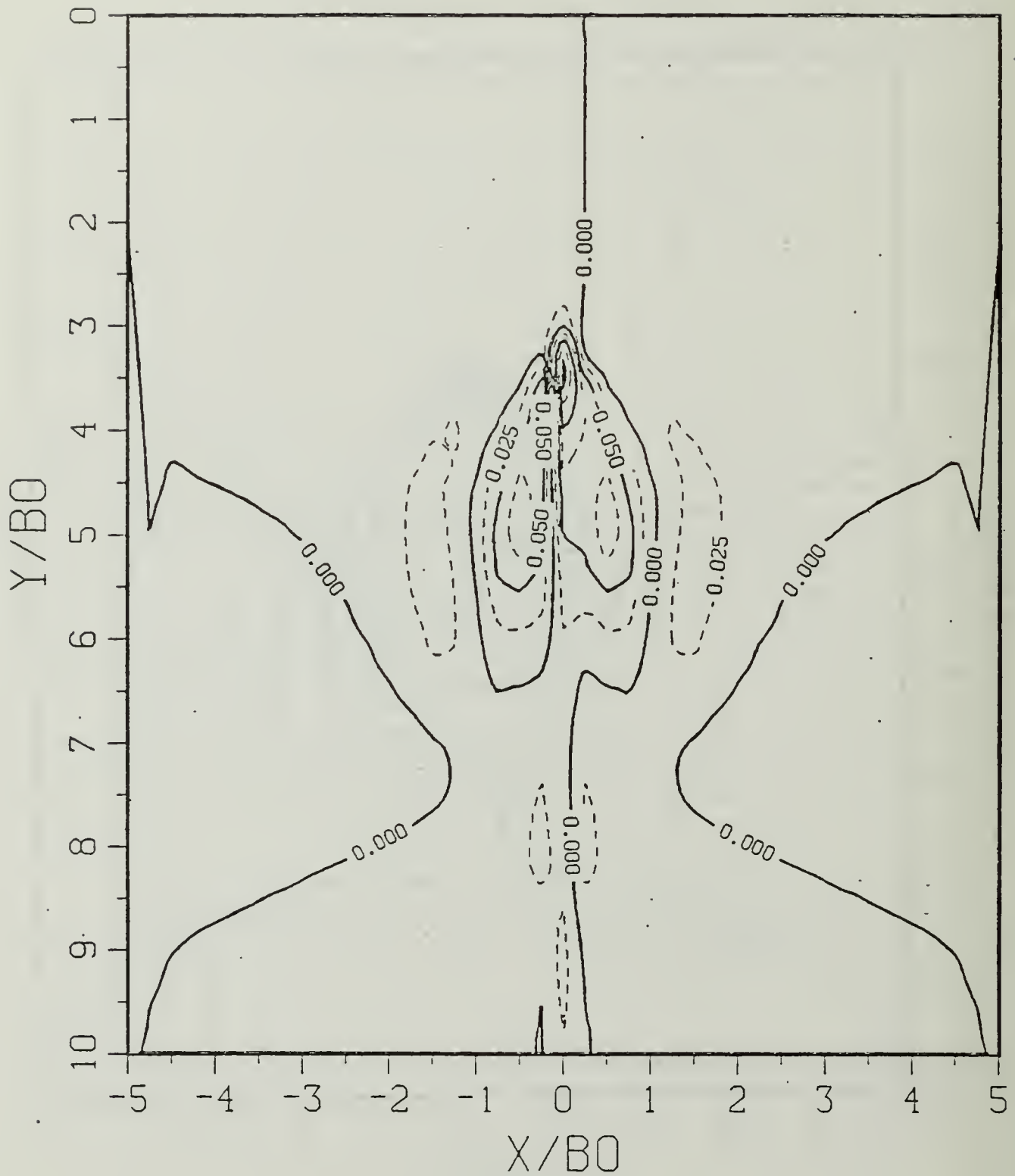


Figure B.42d Vorticity Field:  $SP = 0.50$ .

$$T^* = 5.95200$$

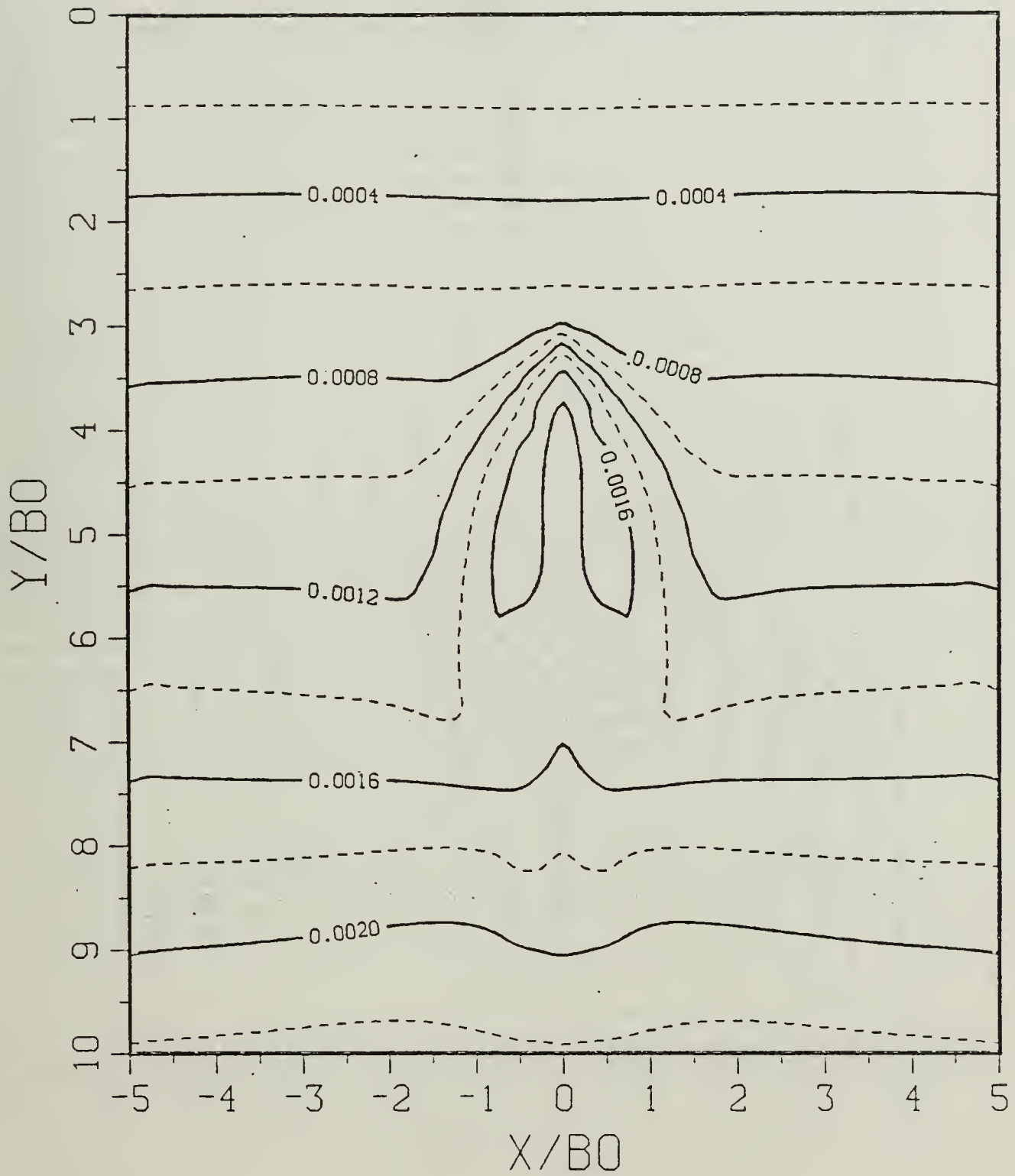


Figure B.43a Constant Density Contours:  $SP = 0.50$ .

$$T^* = 5.95200$$

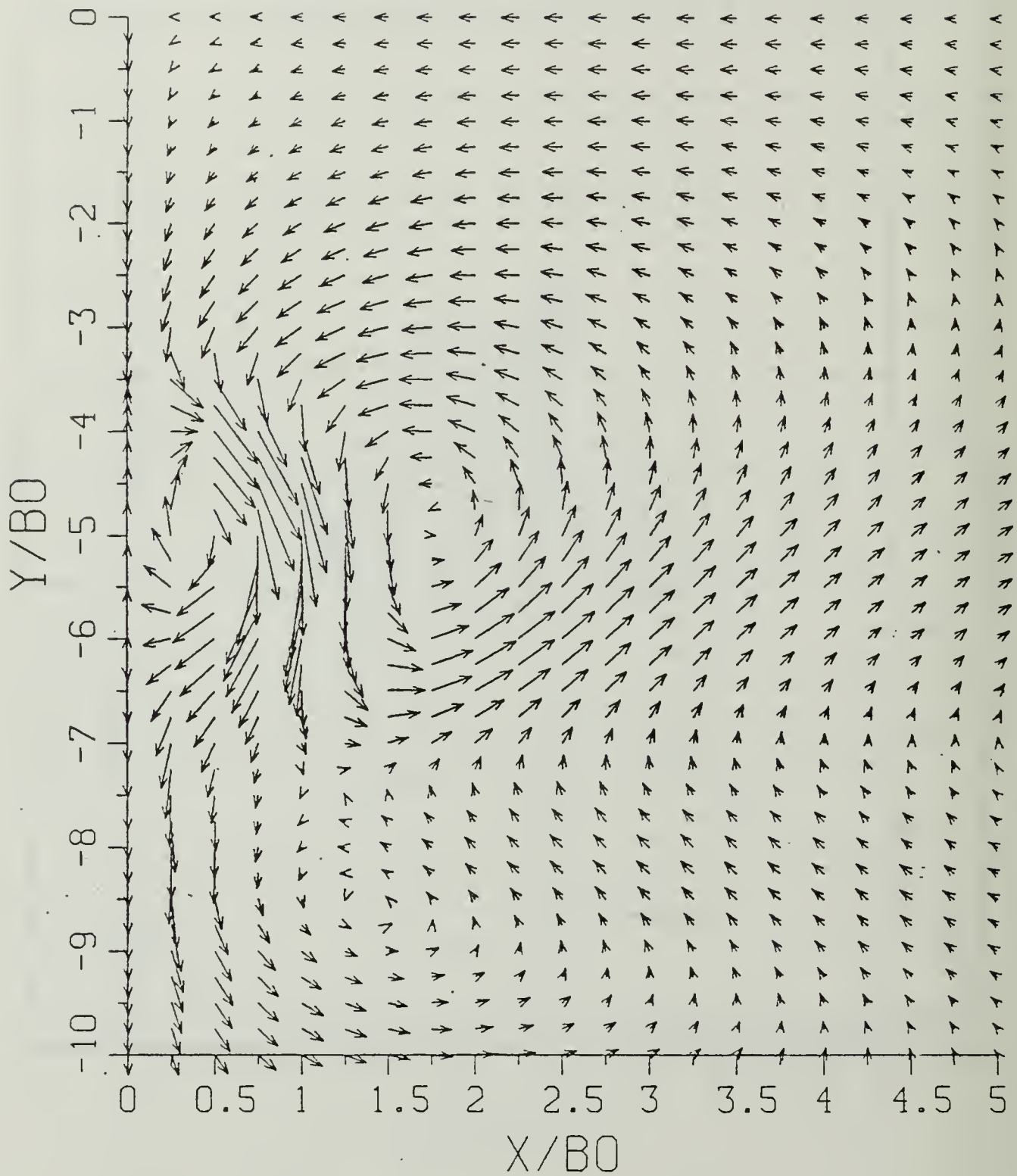


Figure B.43b Velocity Field:  $SP = 0.50$ .

$$T^* = 5.95200$$

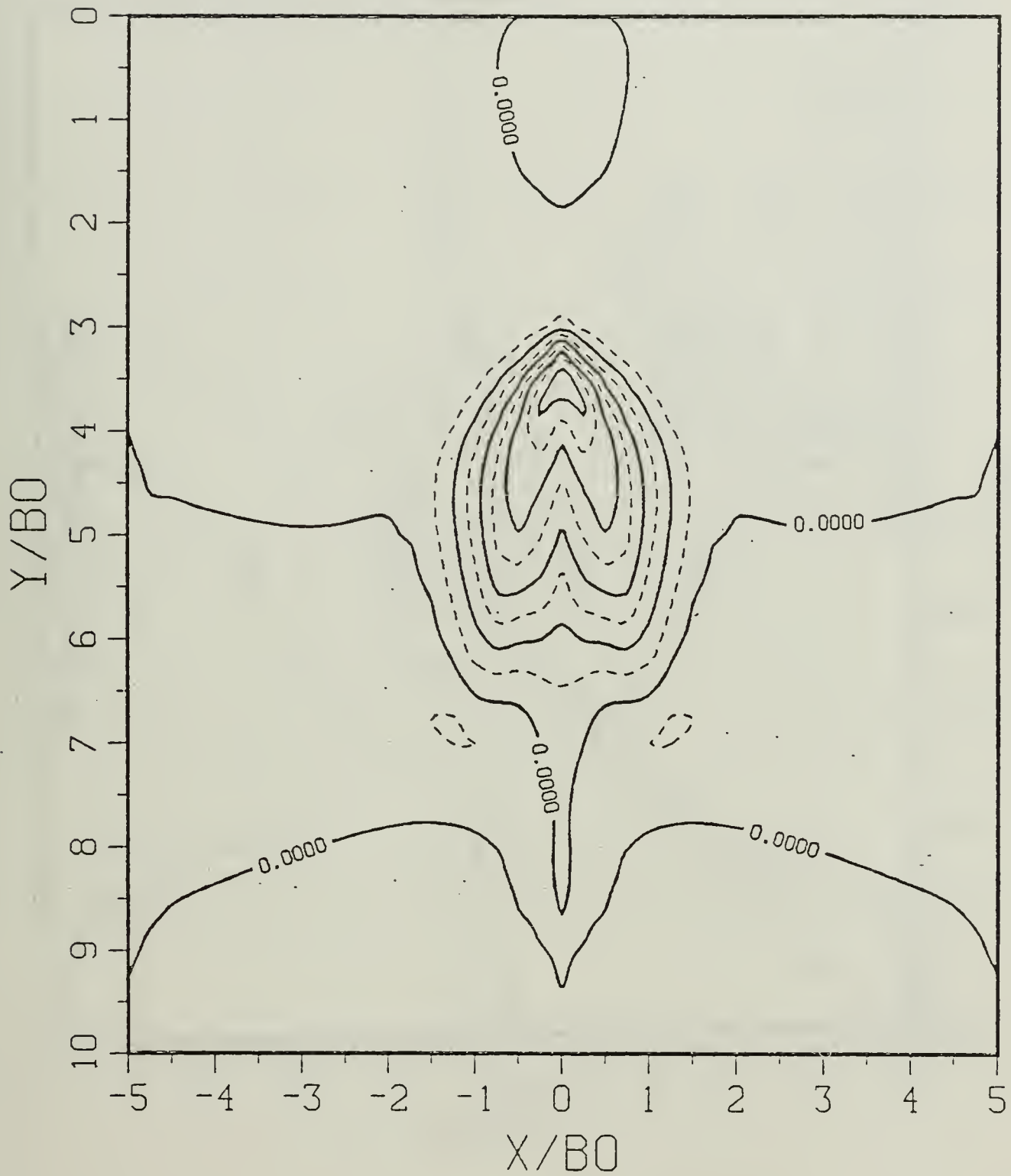


Figure B.43c Density Perturbation Contours:  $SP = 0.50$ .

$$T^* = 5.95200$$

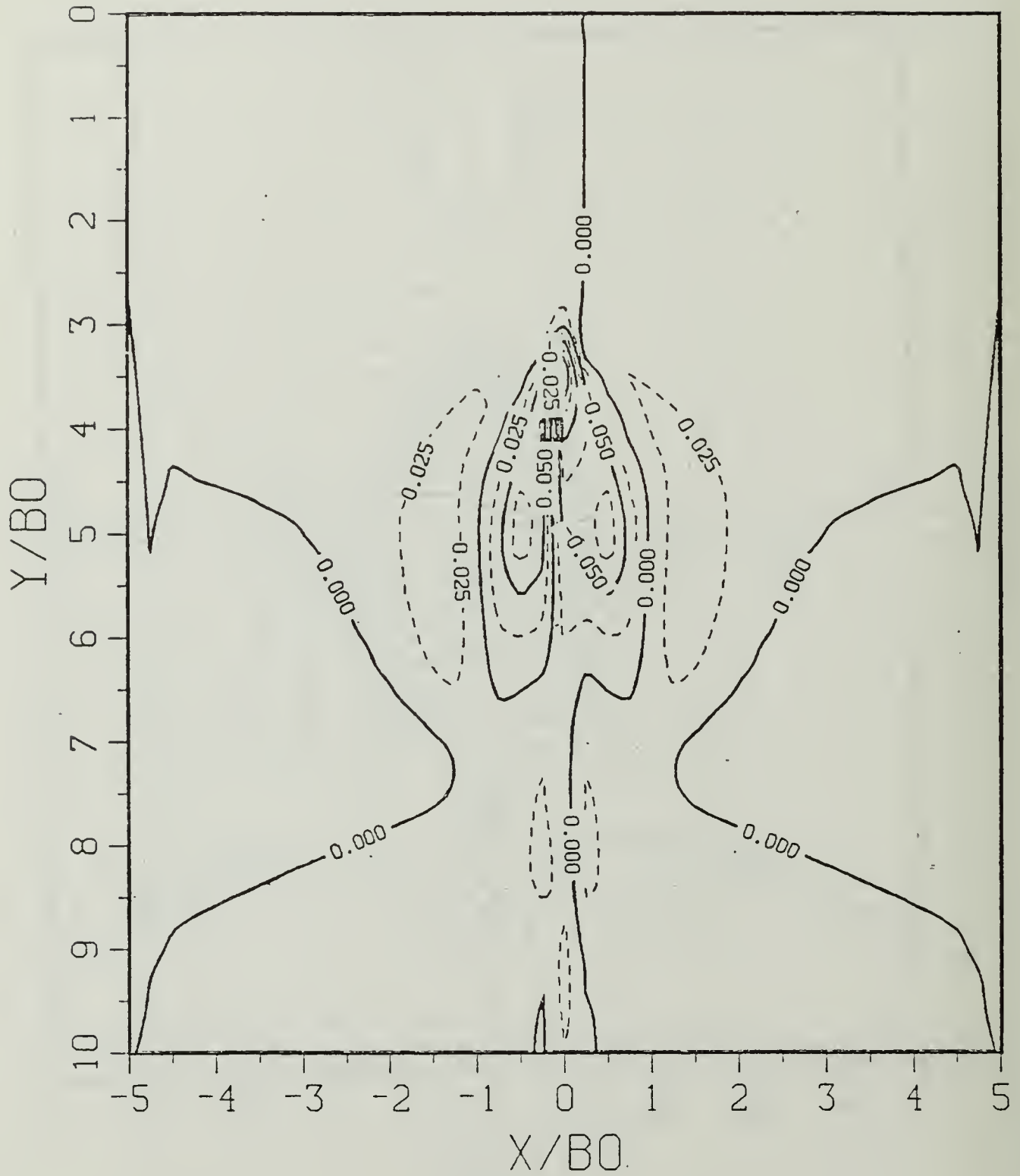


Figure B.43d Vorticity Field:  $SP = 0.50$ .

$T^* \text{ VS } H/B_0 \text{ (SP=0.50)}$

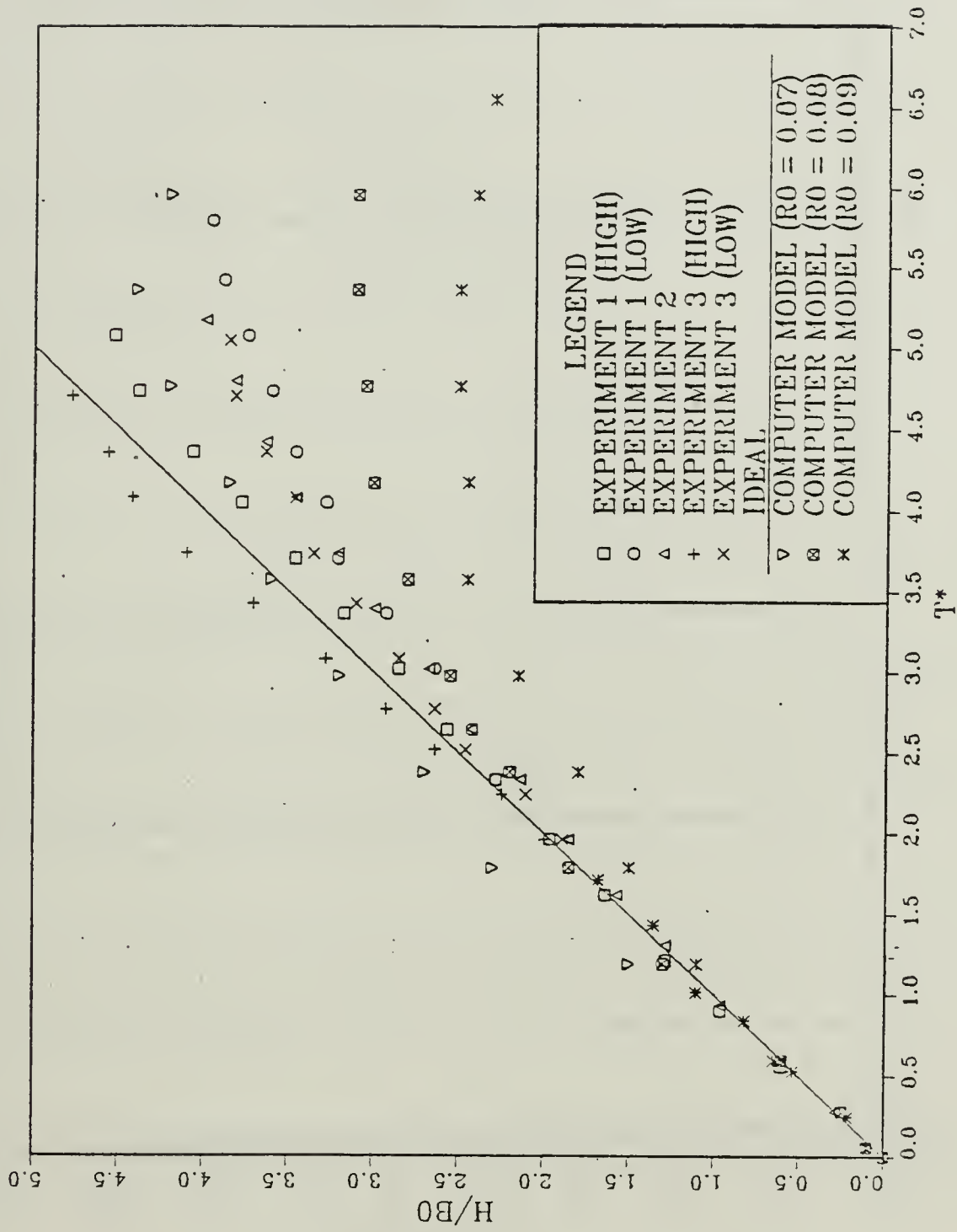


Figure B.44 Experimental and Numerical Results for Various Initial Core Radii.

$$T^* = 0.05952$$

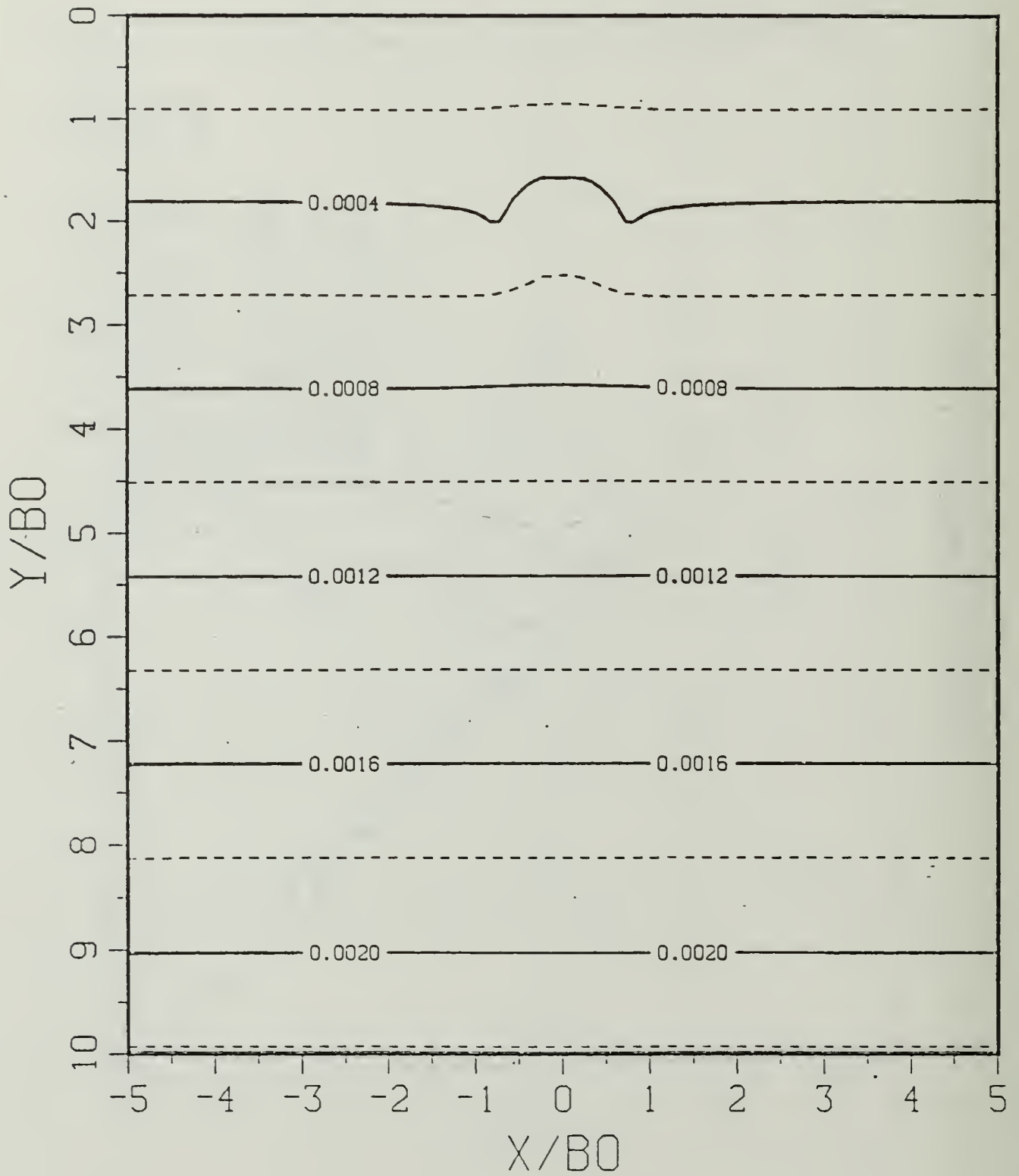


Figure B.45a Constant Density Contours:  $SP = 0.50$ .

$$T^* = 0.05952$$

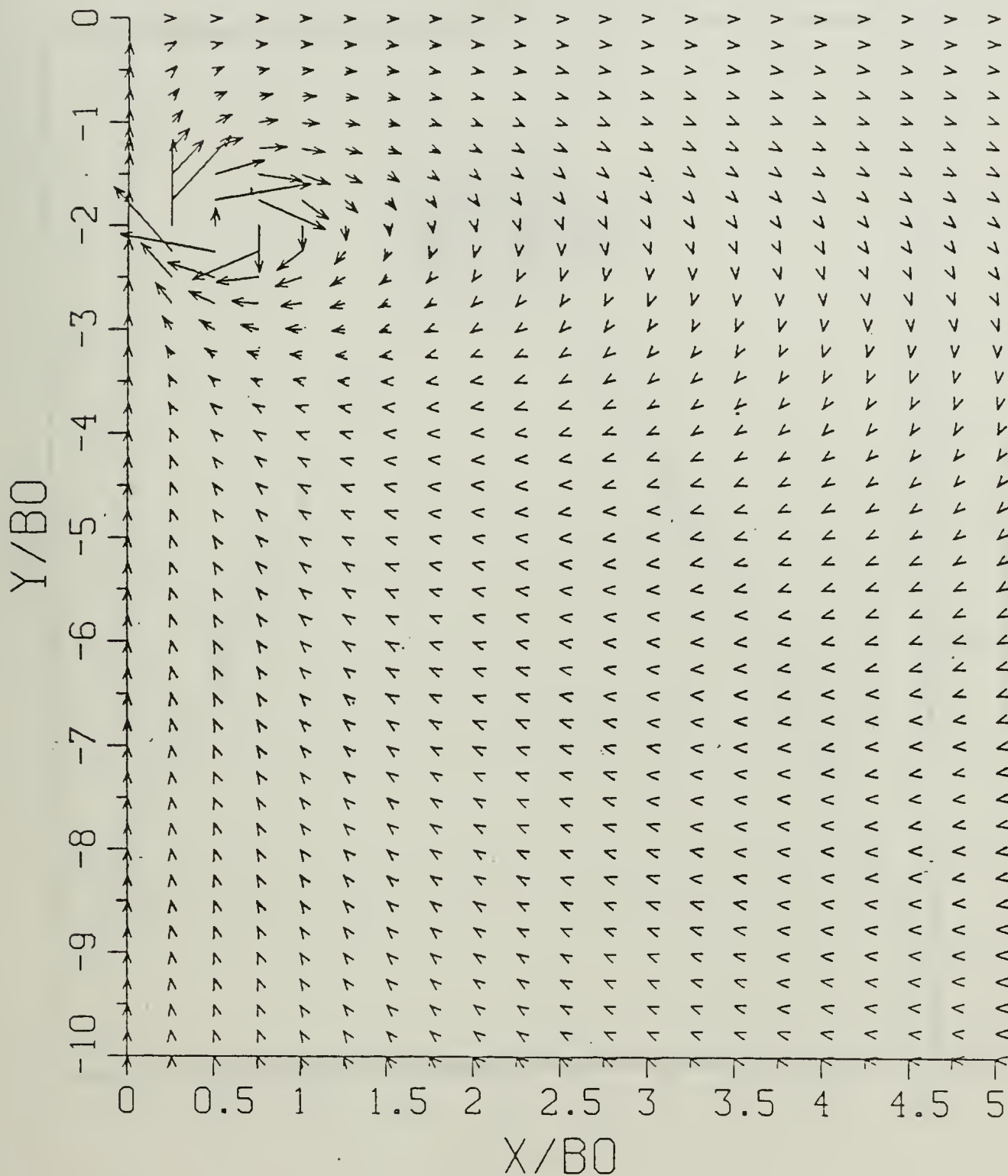


Figure B.45b Velocity Field: SP = 0.50.

$$T^* = 0.05952$$

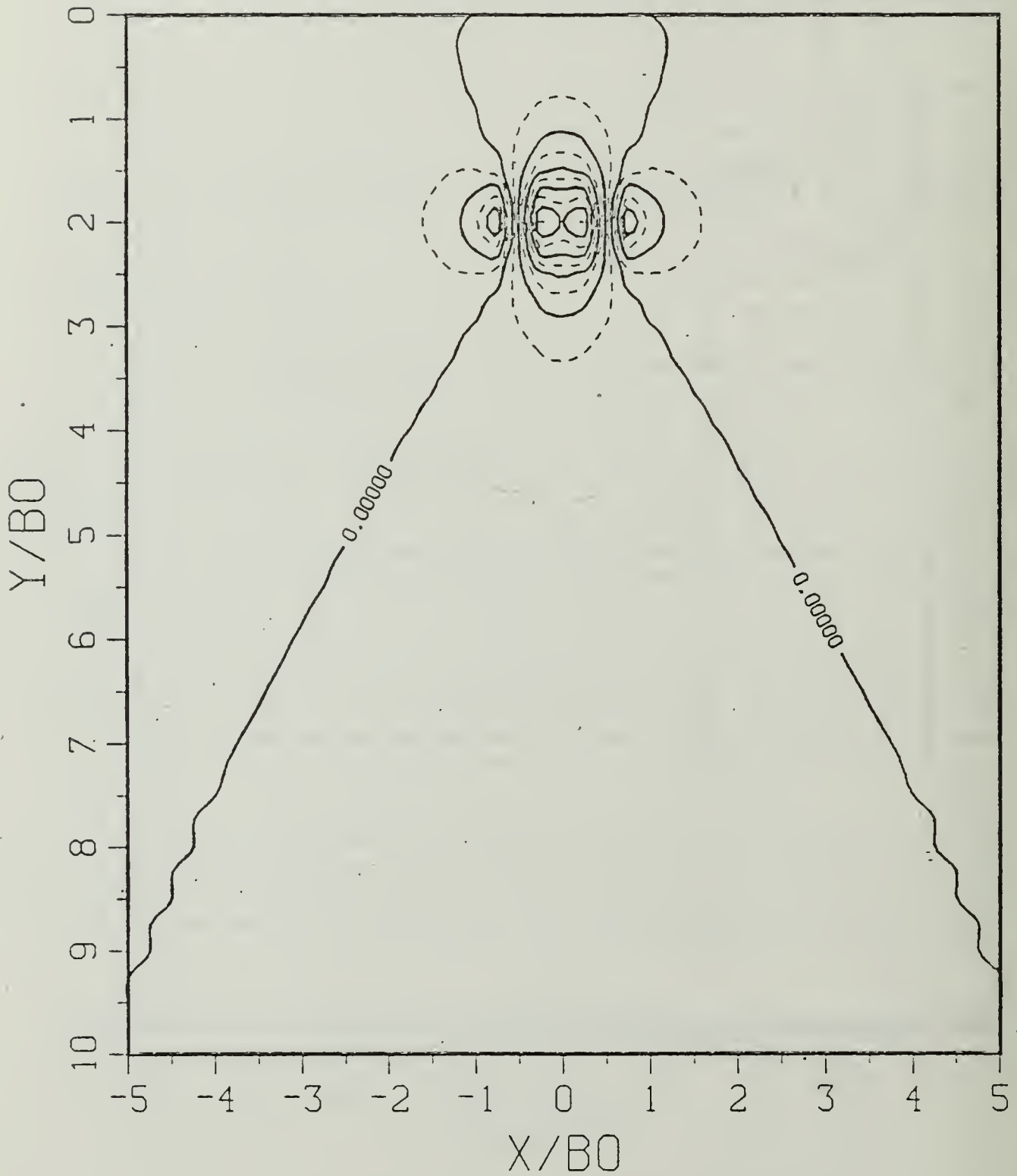


Figure B.45c Density Perturbation Contours:  $SP = 0.50$ .

$$T^* = 0.05952$$

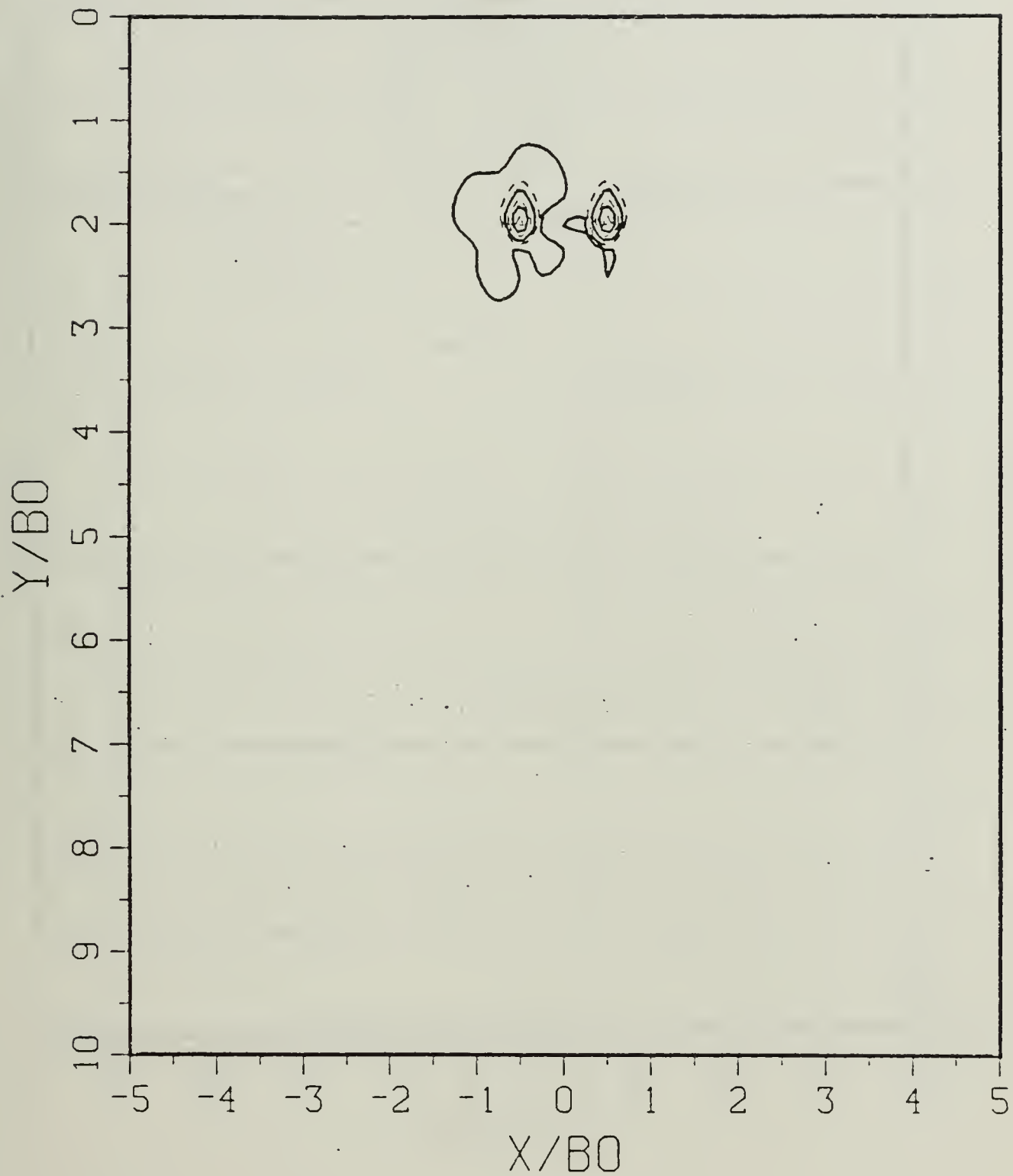


Figure B.45d Vorticity Field: SP = 0.50.

$$T^* = 0.59520$$

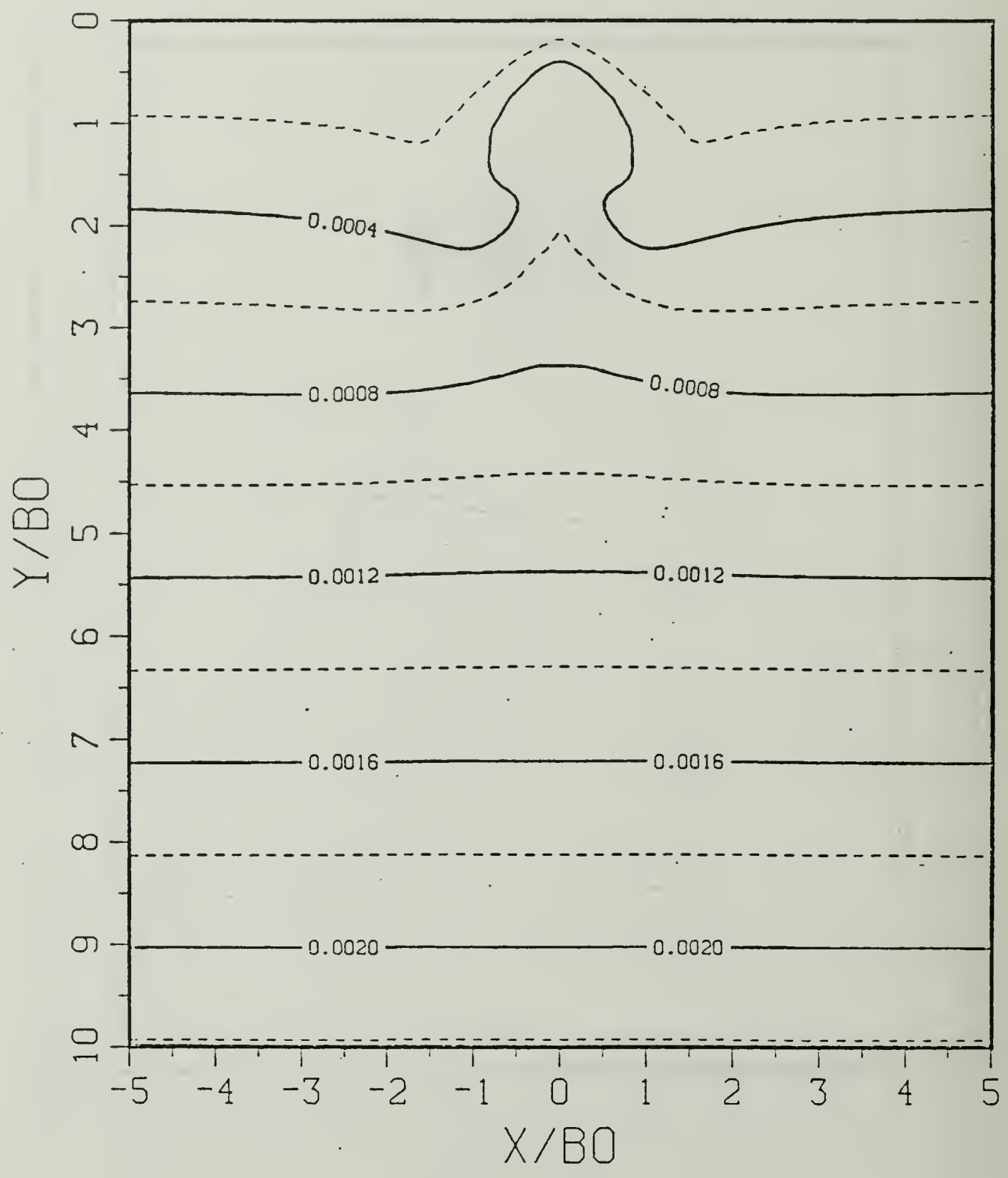


Figure B.46a Constant Density Contours:  $SP = 0.50$ .

$$T^* = 0.59520$$

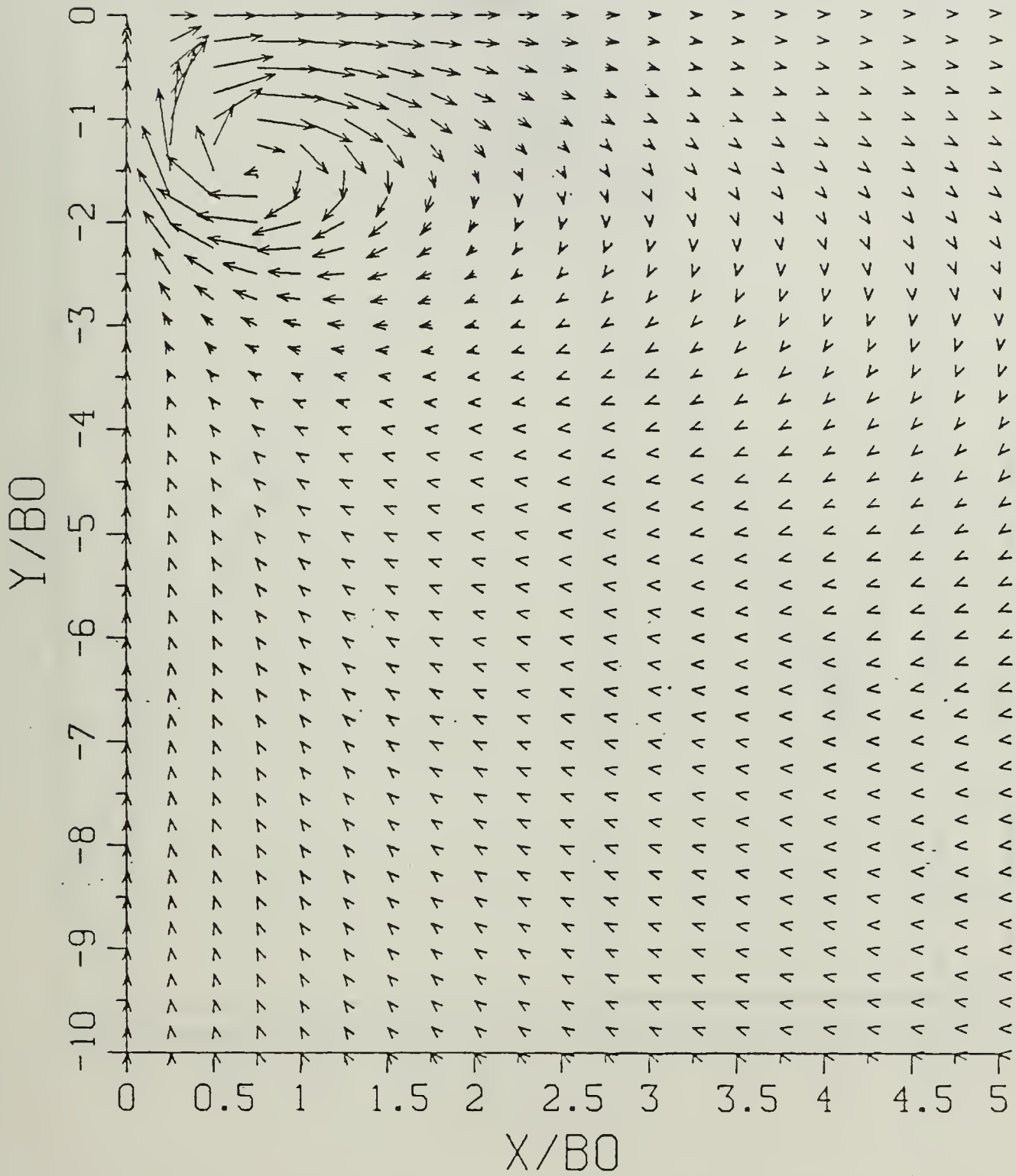


Figure B.46b Velocity Field: SP = 0.50.

$$T^* = 0.59520$$

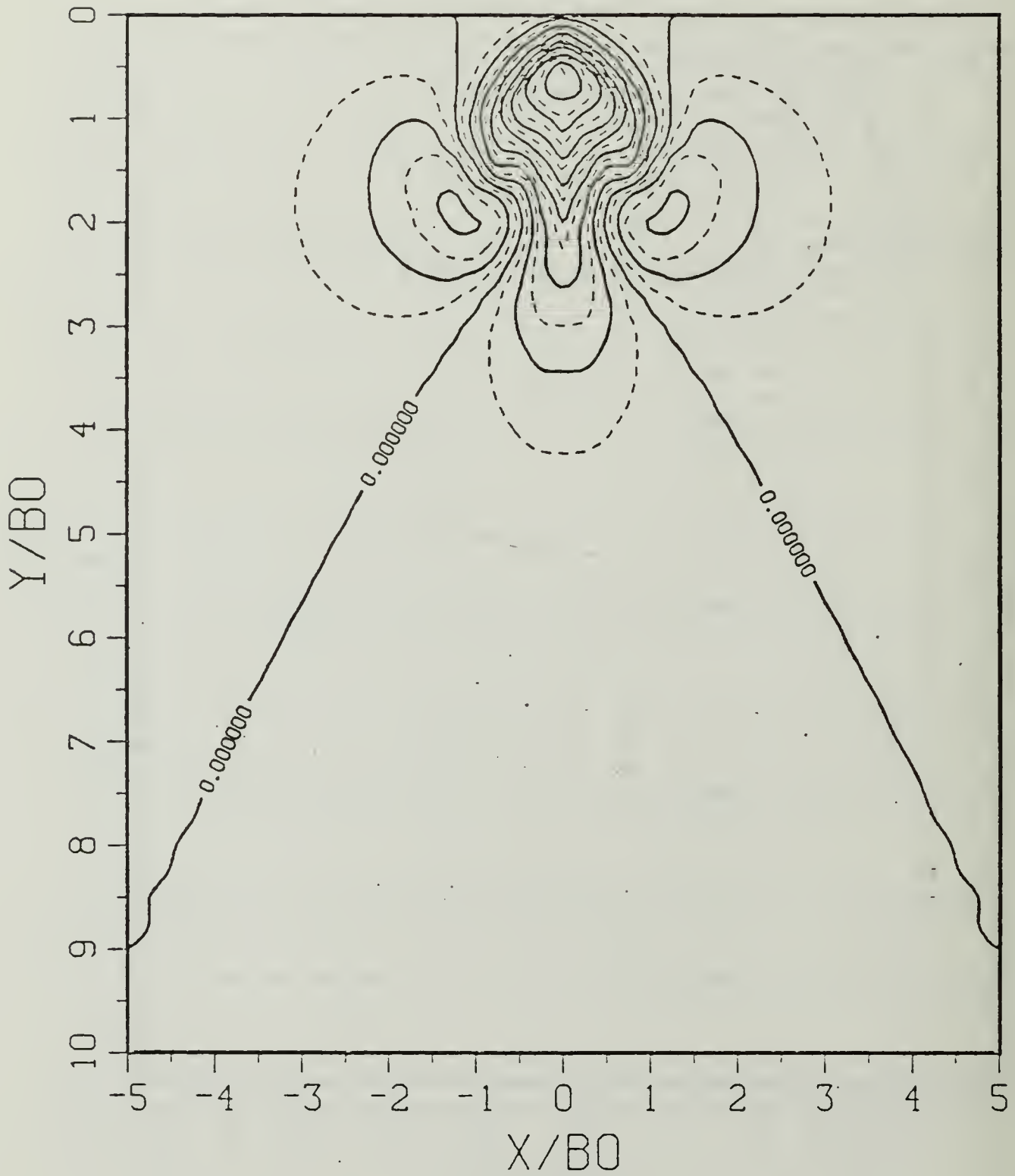


Figure B.46c Density Perturbation Contours:  $SP = 0.50$ .

$$T^* = 0.59520$$

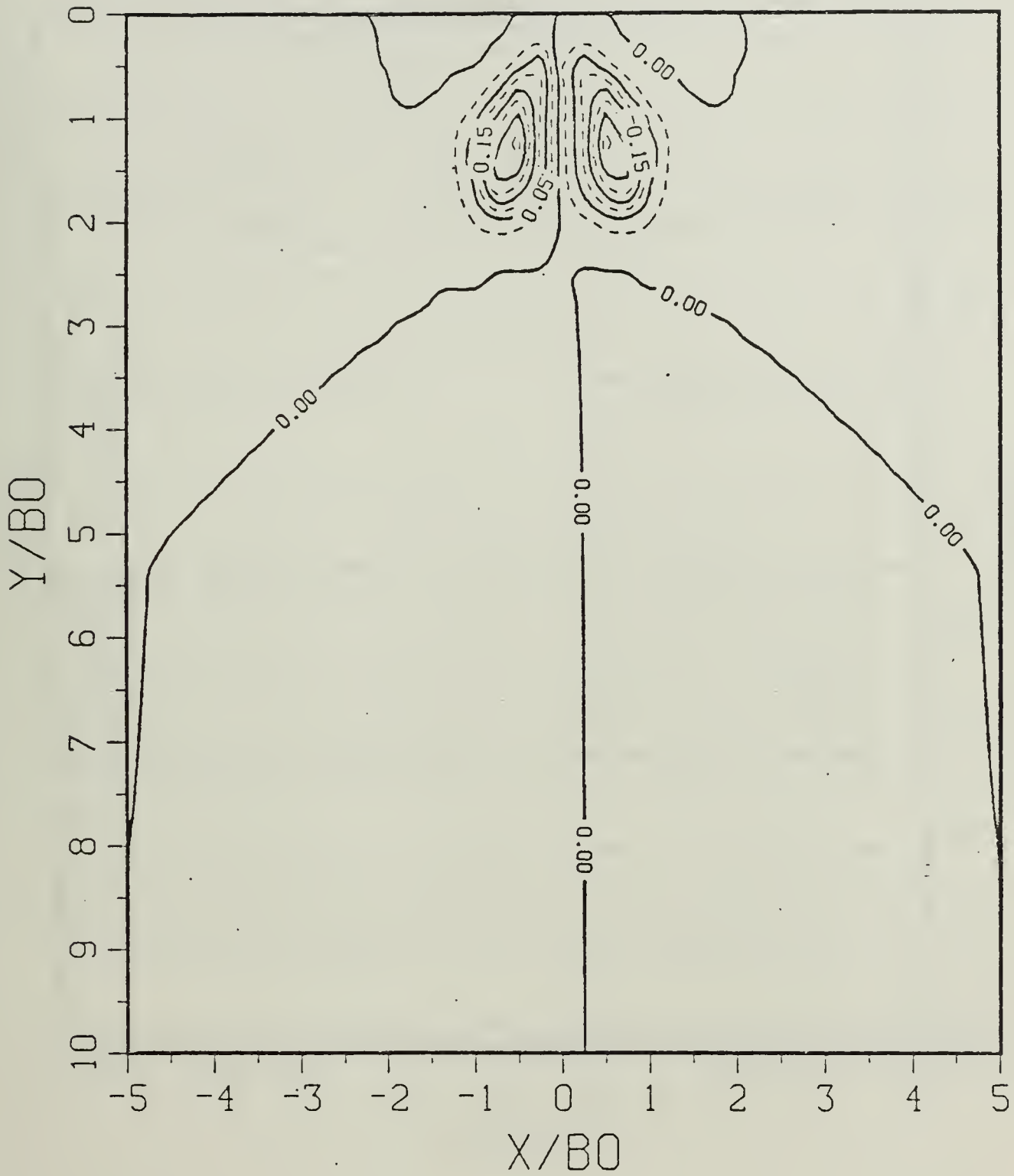


Figure B.46d Vorticity Field: SP = 0.50.

$$T^* = 1.19040$$

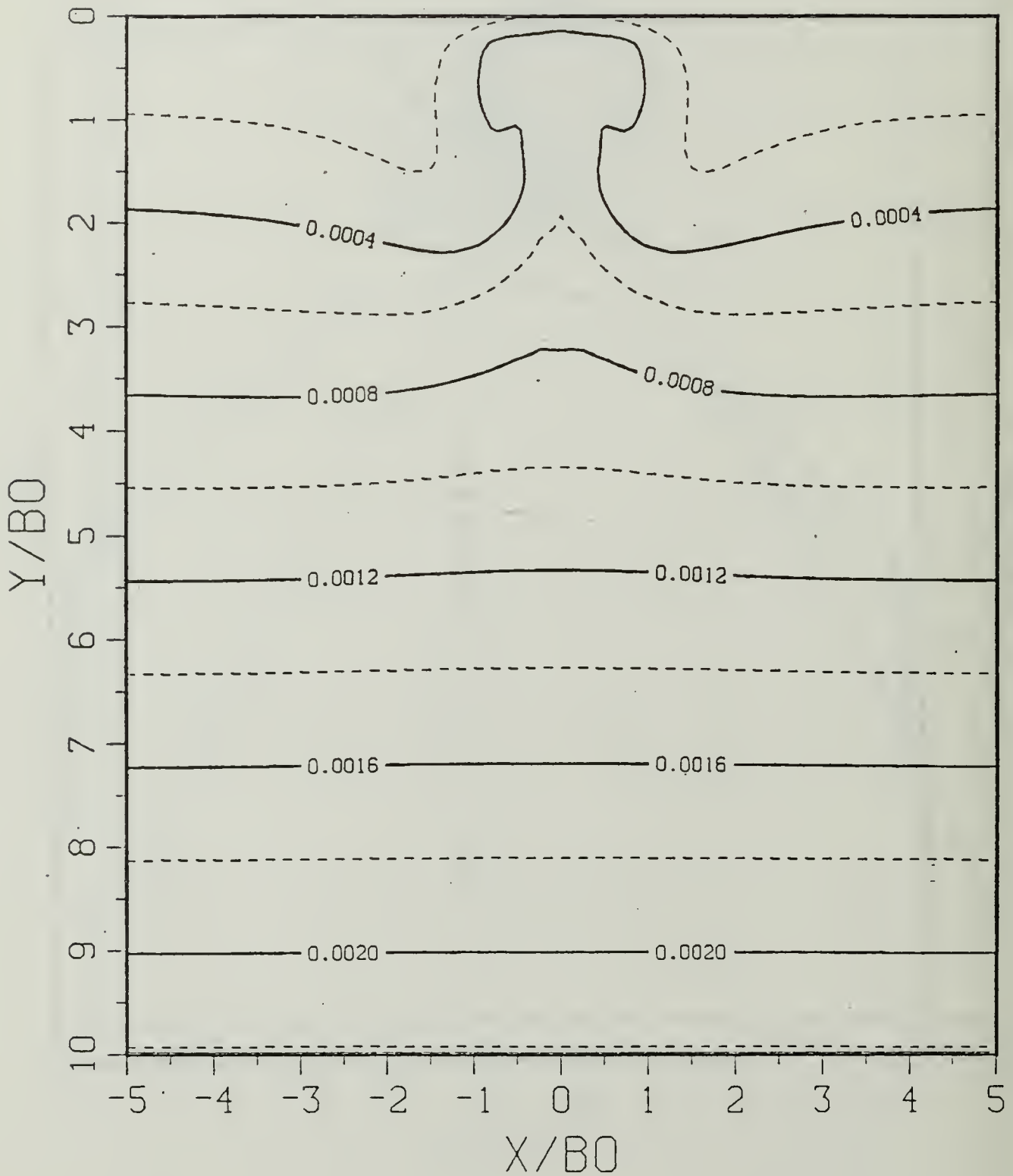


Figure B.47a Constant Density Contours:  $SP = 0.50$ .

$$T^* = 1.19040$$

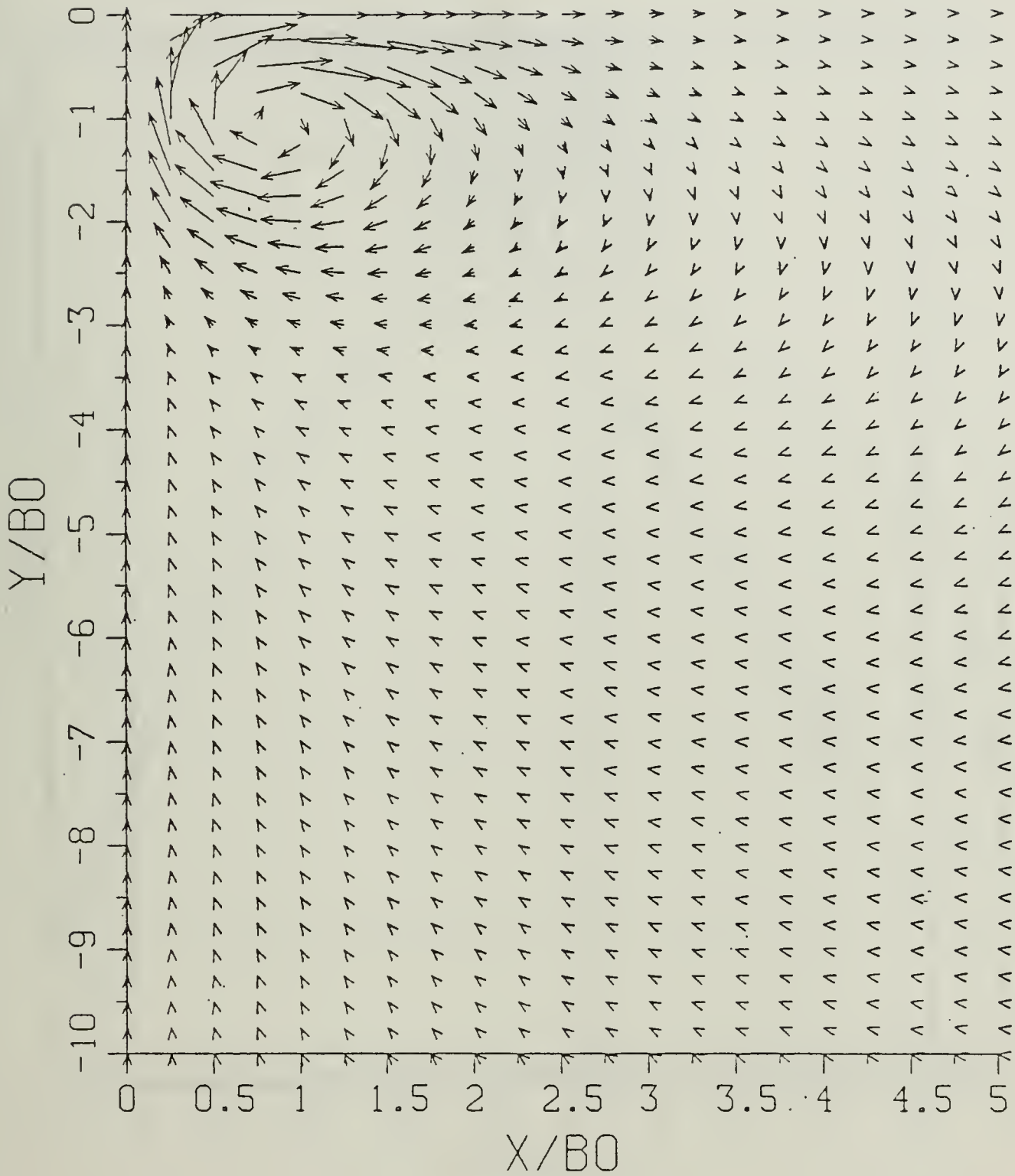


Figure B.47b Velocity Field:  $SP = 0.50$ .

$$T^* = 1.19040$$

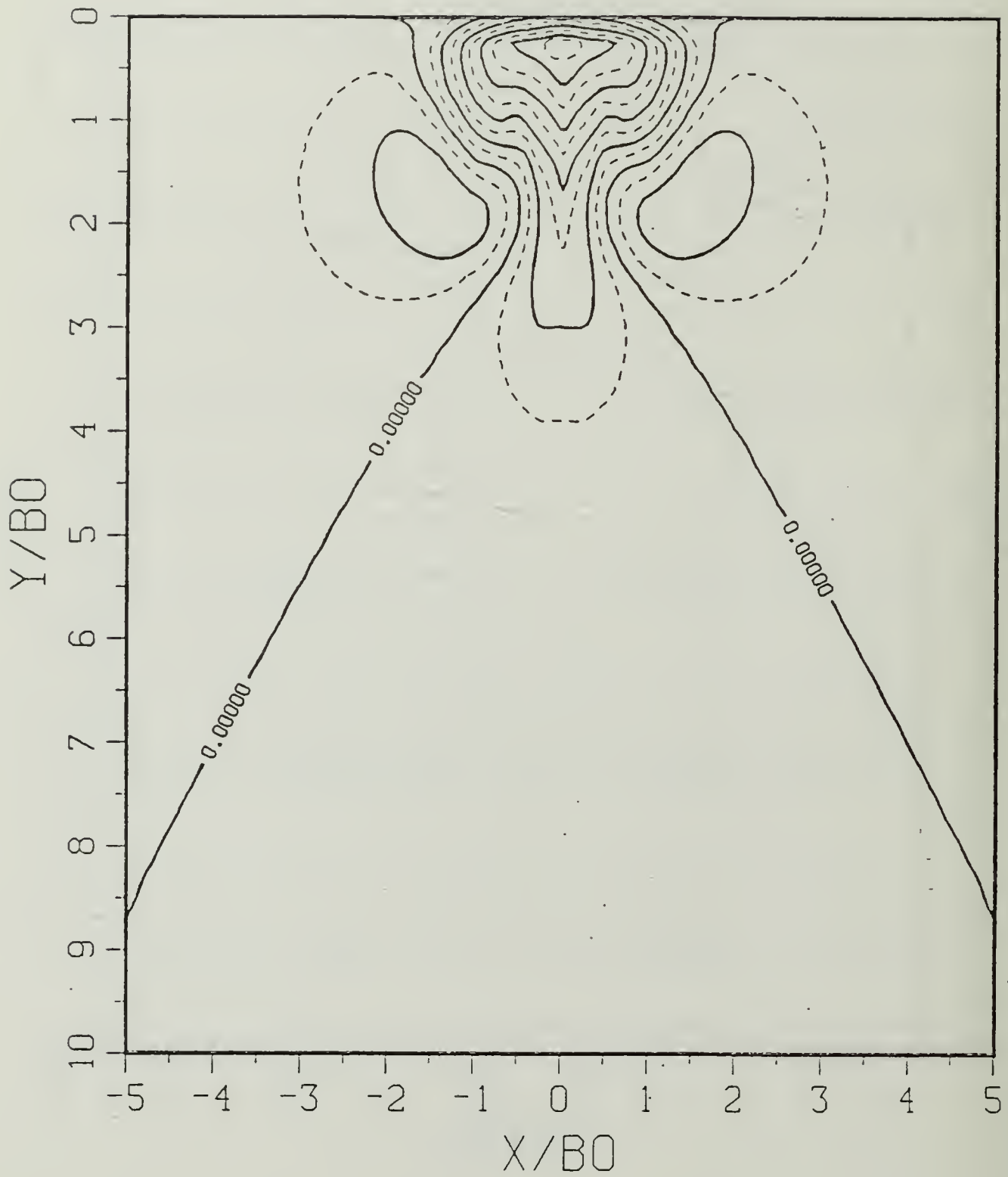


Figure B.47c Density Perturbation Contours: SP = 0.50.

$$T^* = 1.19040$$

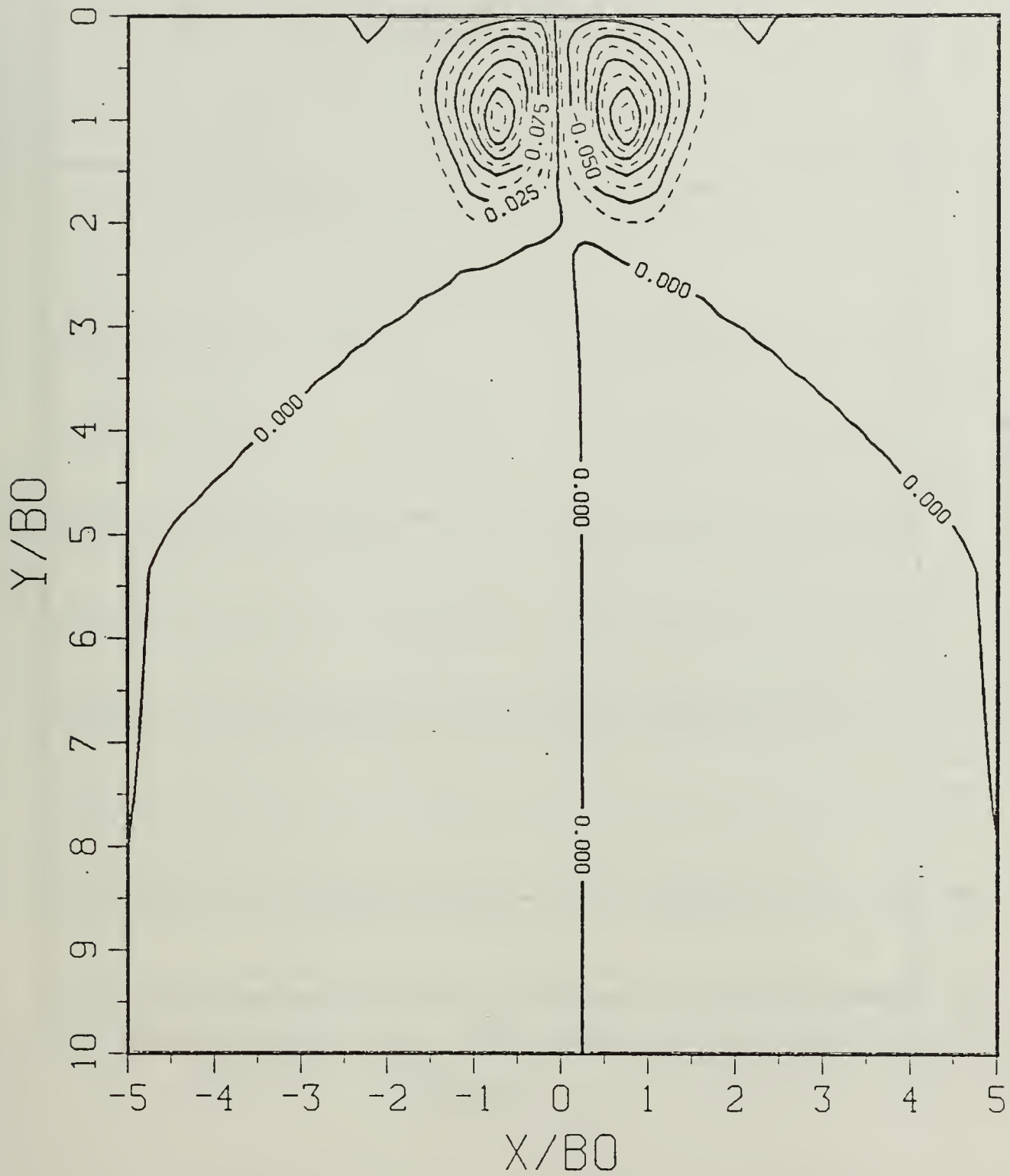


Figure B.47d Vorticity Field: SP = 0.50.

$$T^* = 1.78560$$

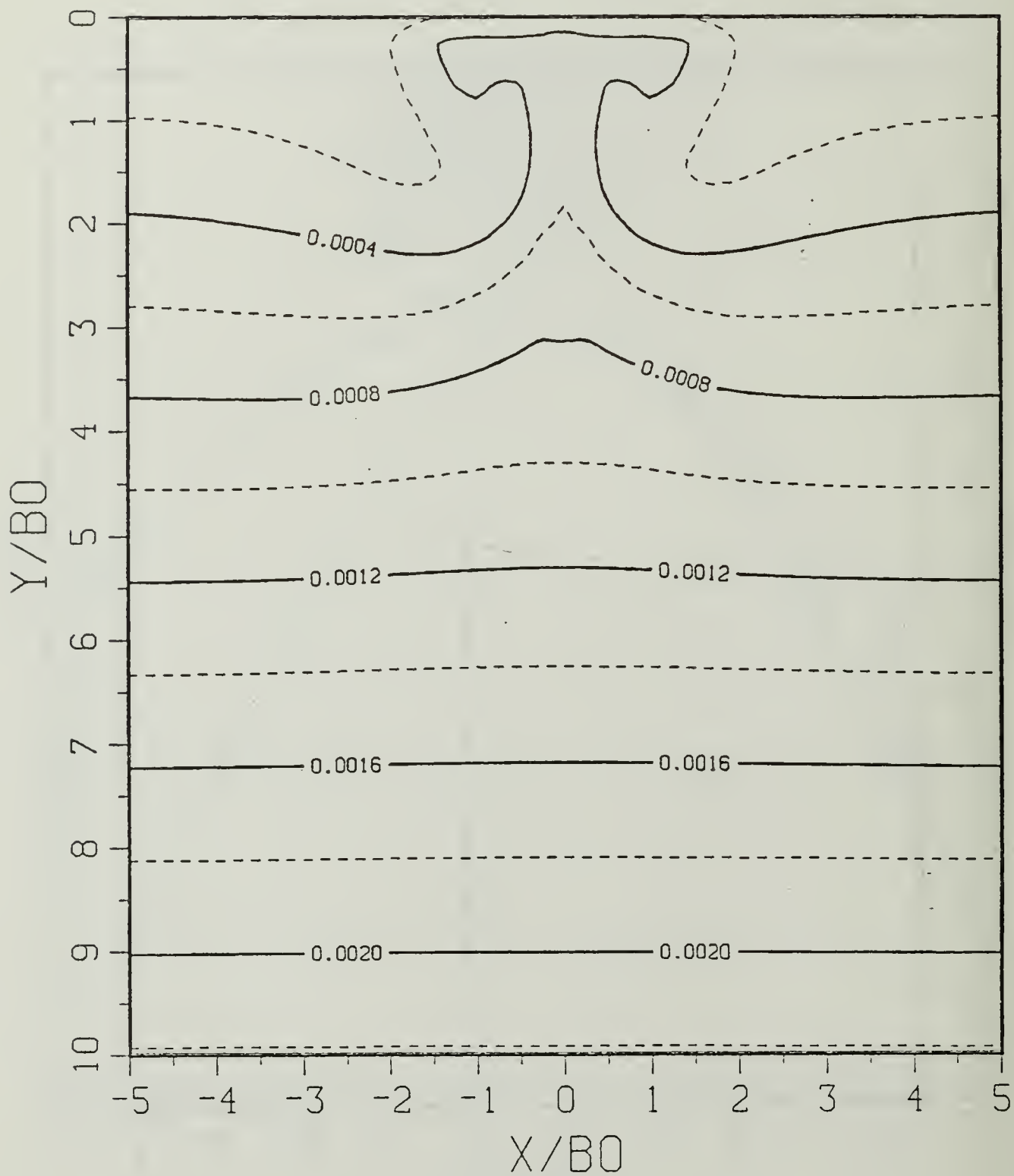


Figure B.48a Constant Density Contours:  $SP = 0.50$ .

$$T^* = 1.78560$$

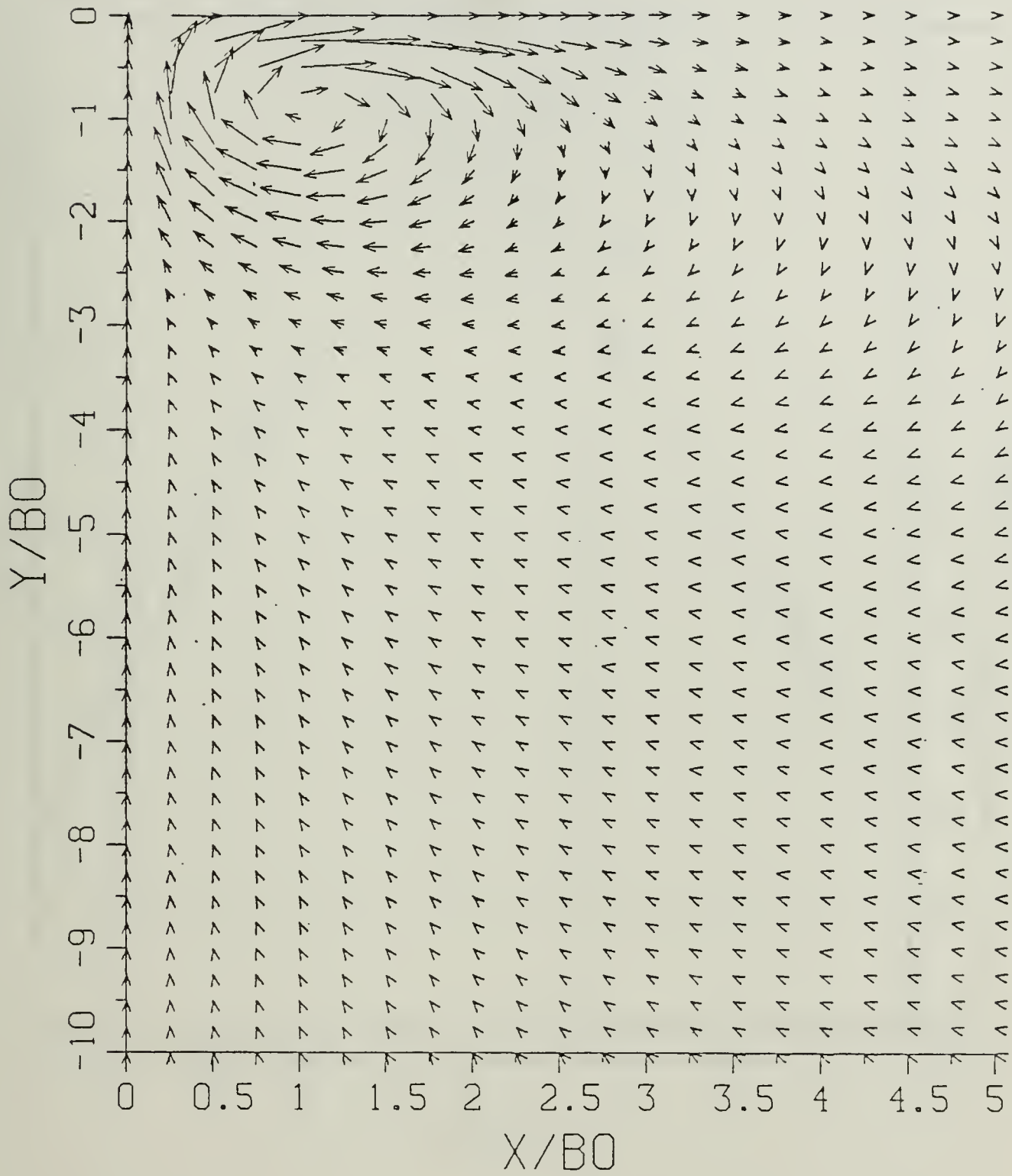


Figure B.48b Velocity Field:  $SP = 0.50$ .

$$T^* = 1.78560$$

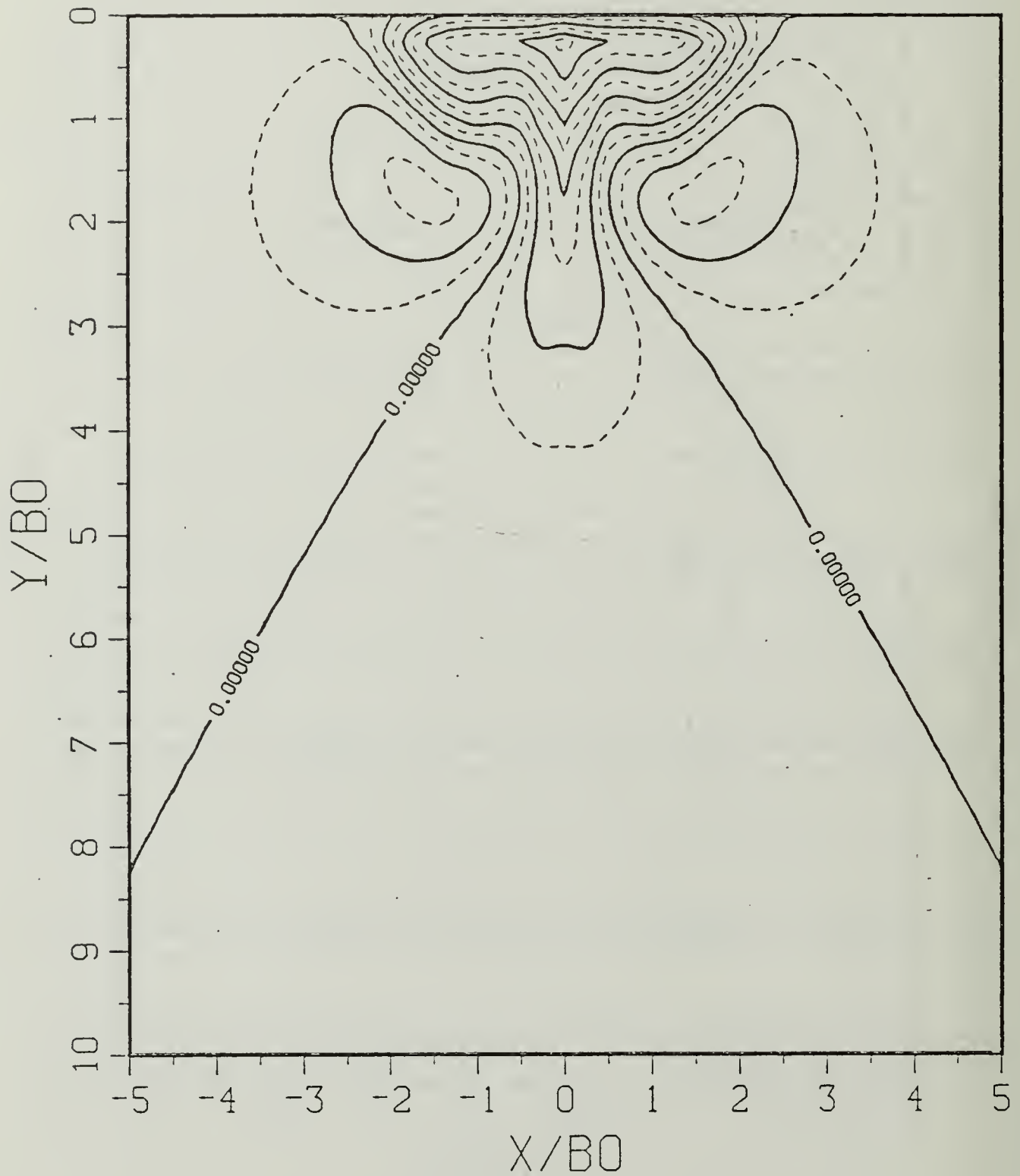


Figure B.48c Density Perturbation Contours:  $SP = 0.50$ .

$$T^* = 1.78560$$

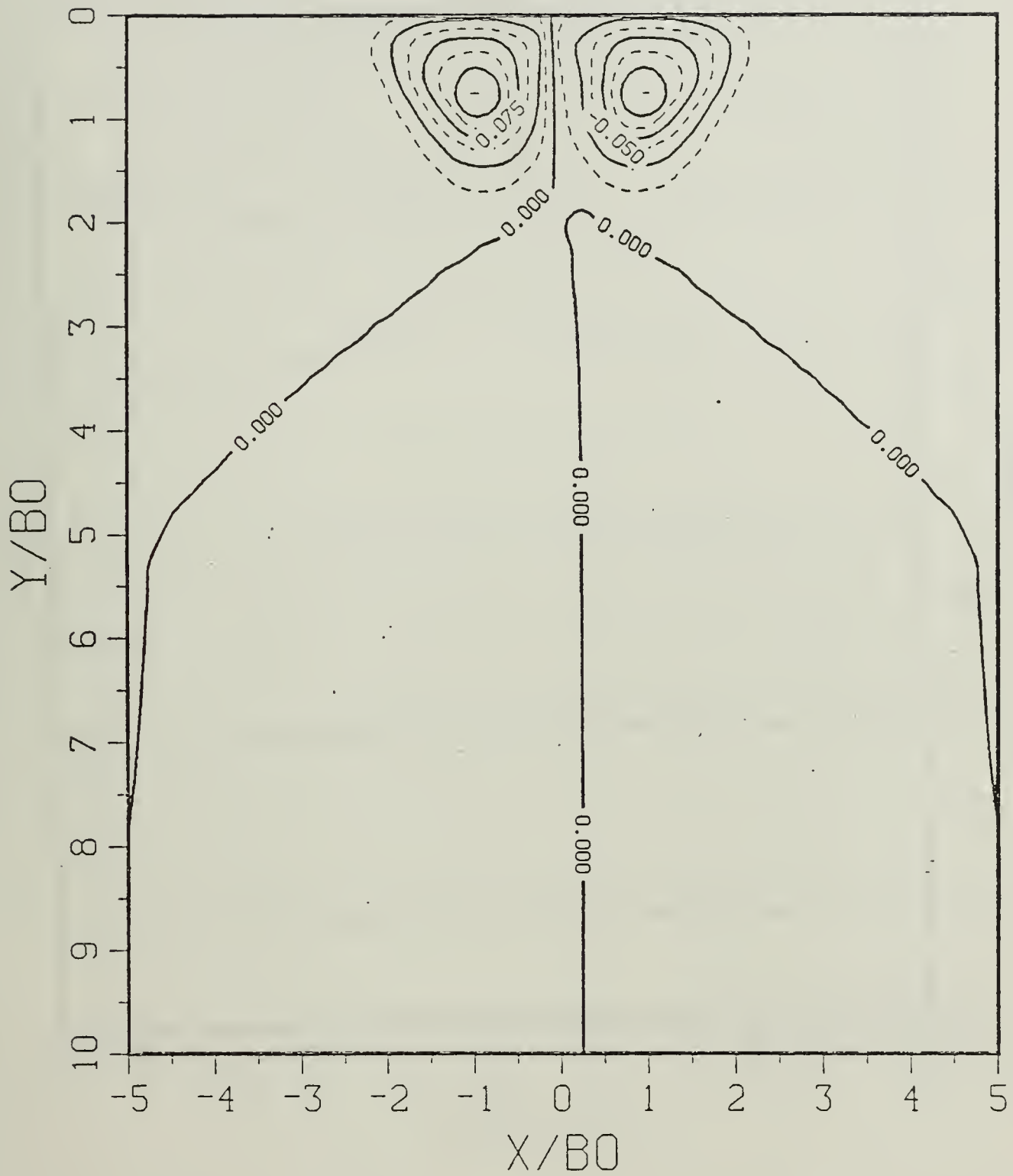


Figure B.48d Vorticity Field: SP = 0.50.

$$T^* = 2.38080$$

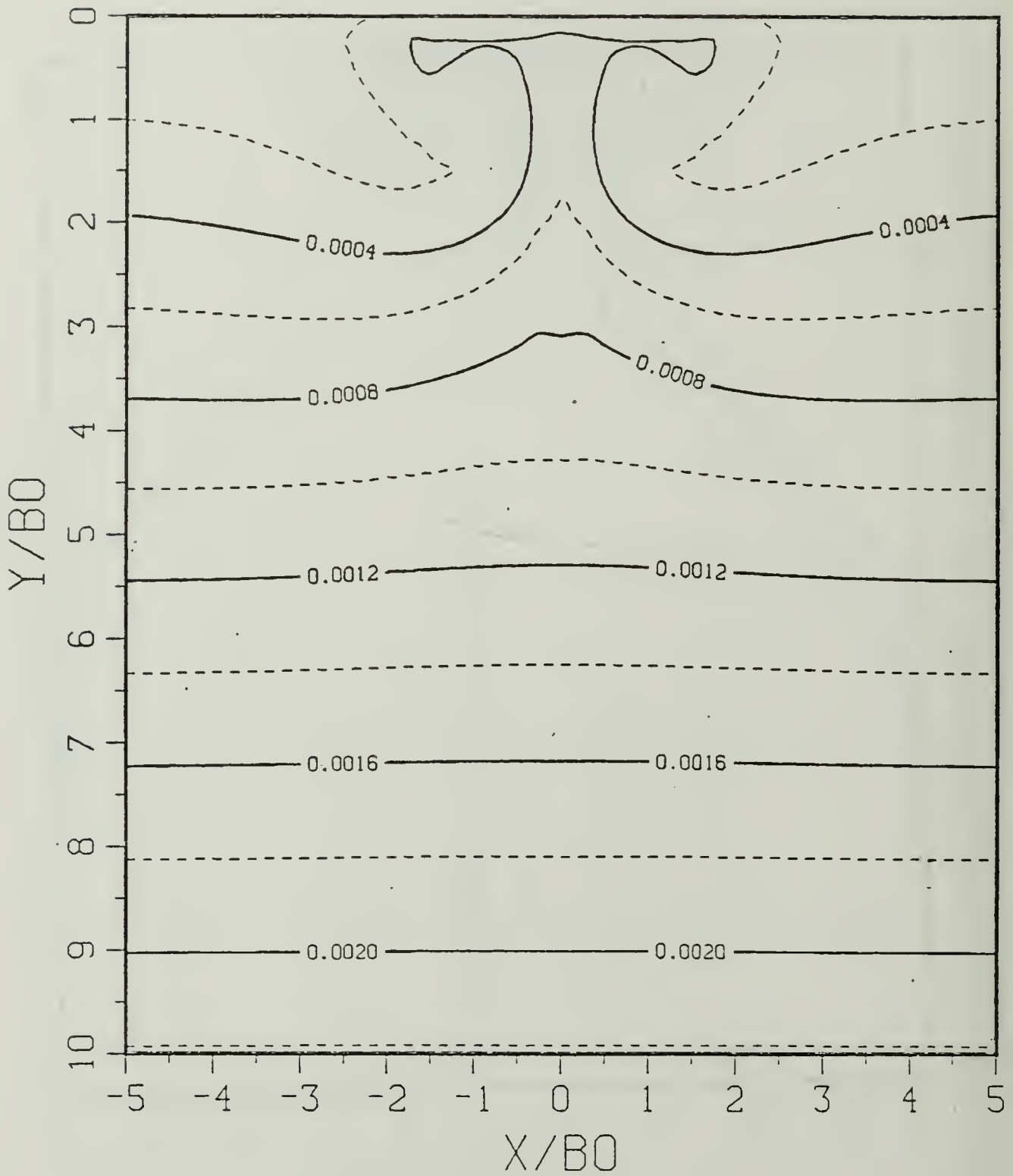


Figure B.49a Constant Density Contours:  $SP = 0.50$ .

$$T^* = 2.38080$$

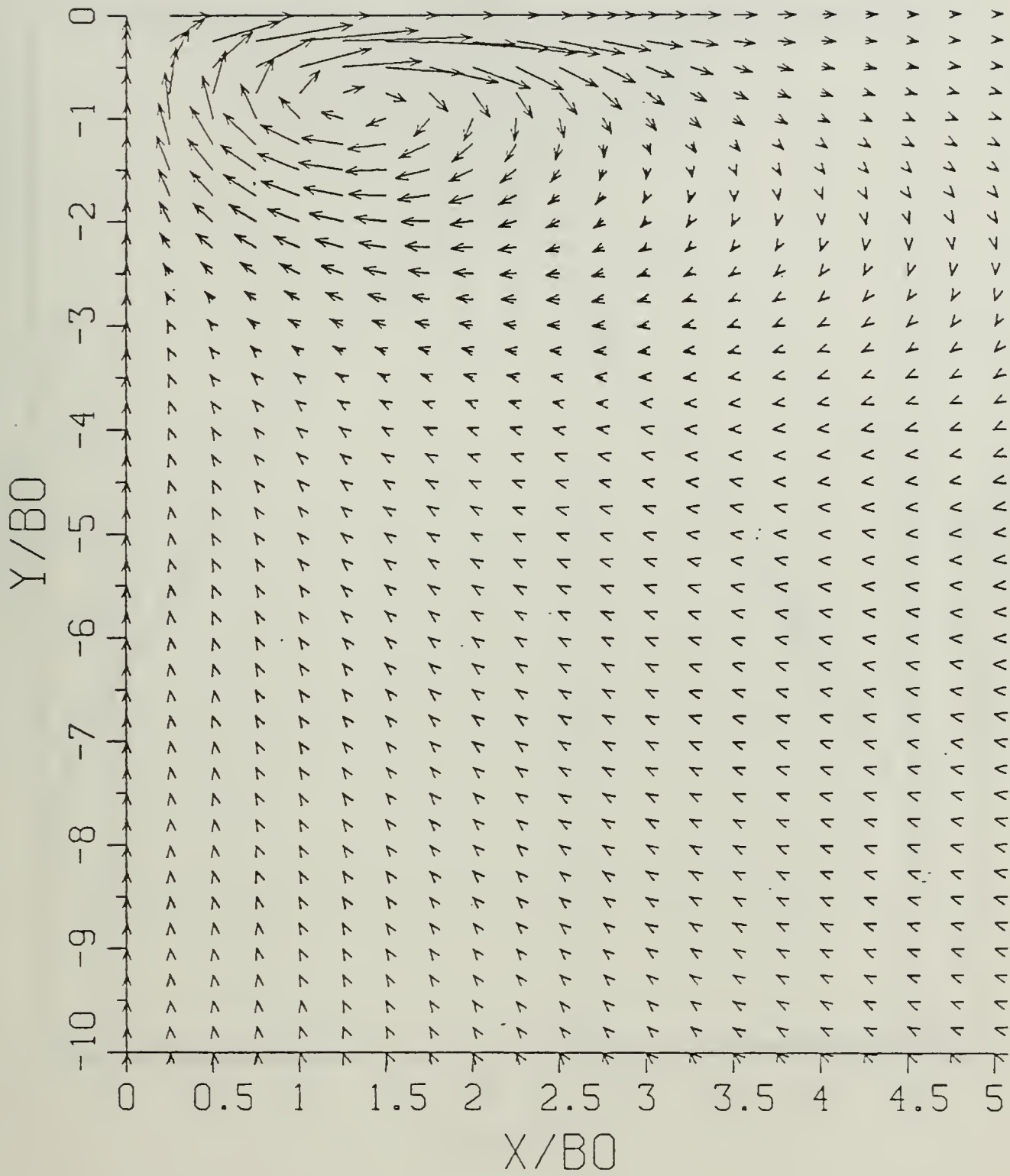


Figure B.49b Velocity Field: SP = 0.50.

$$T^* = 2.38080$$

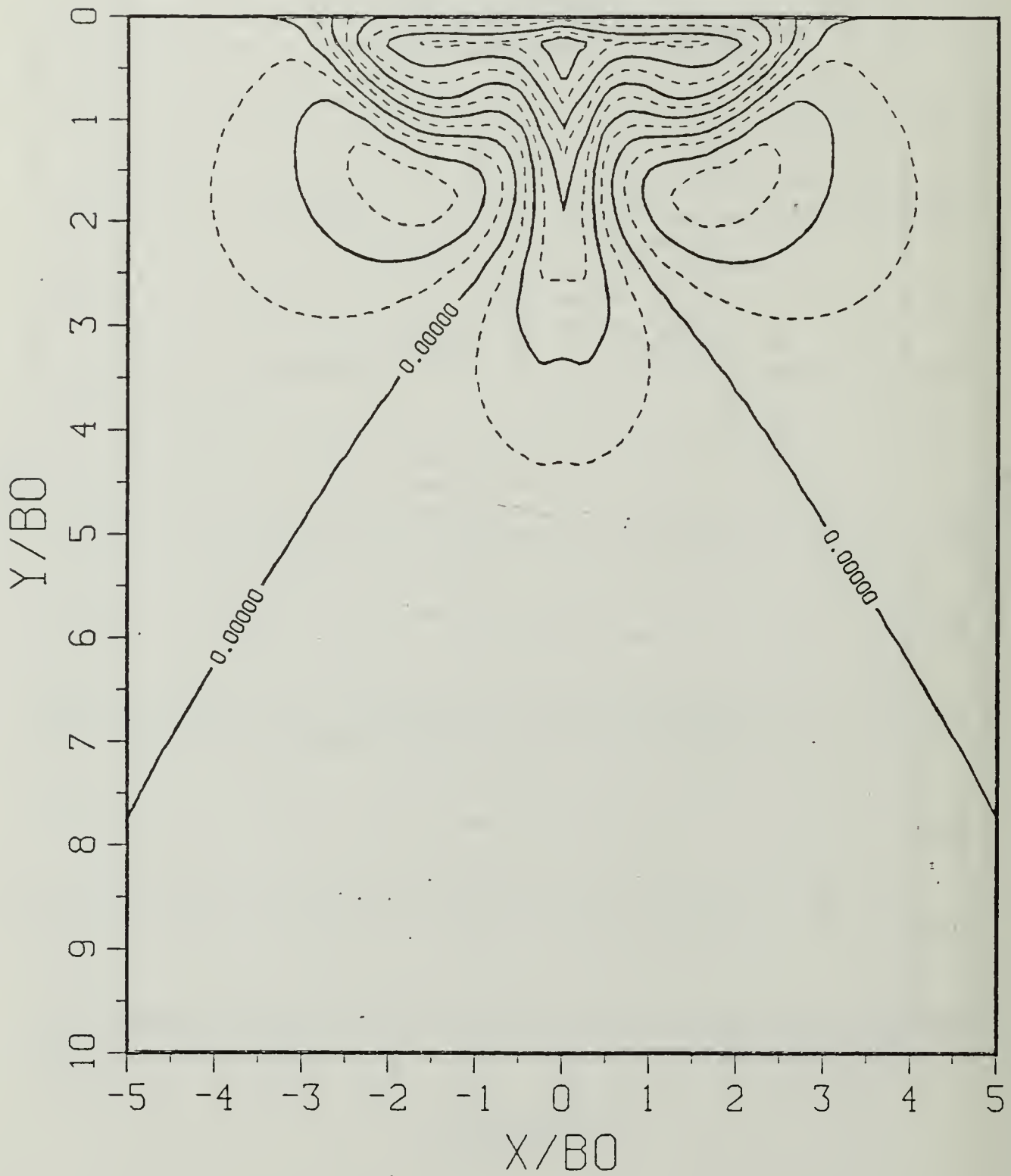


Figure B.49c Density Perturbation Contours:  $SP = 0.50$ .

$$T^* = 2.38080$$

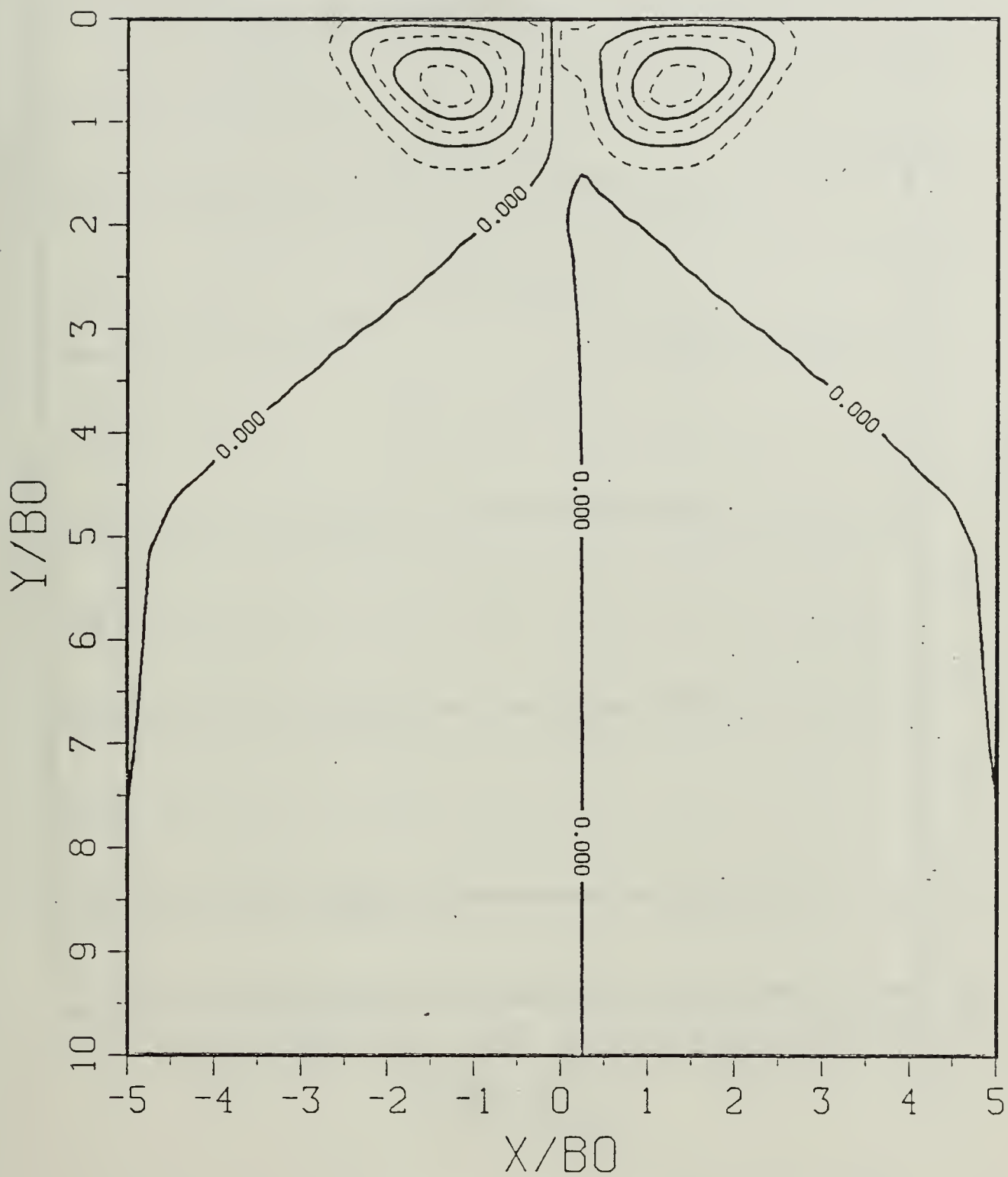


Figure B.49d Vorticity Field: SP = 0.50.

$$T^* = 2.97600$$

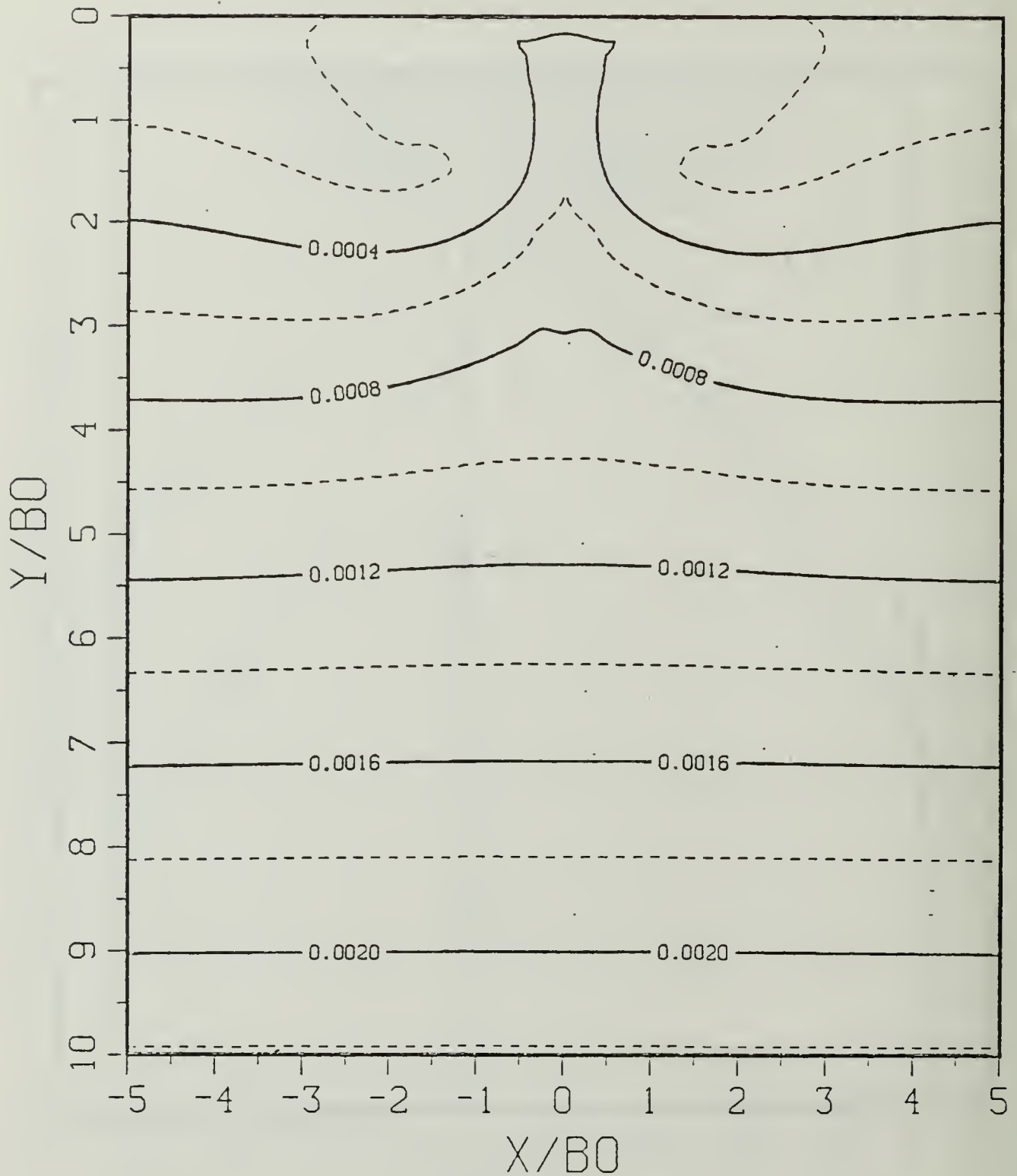


Figure B.50a Constant Density Contours:  $SP = 0.50$ .

$$T^* = 2.97600$$

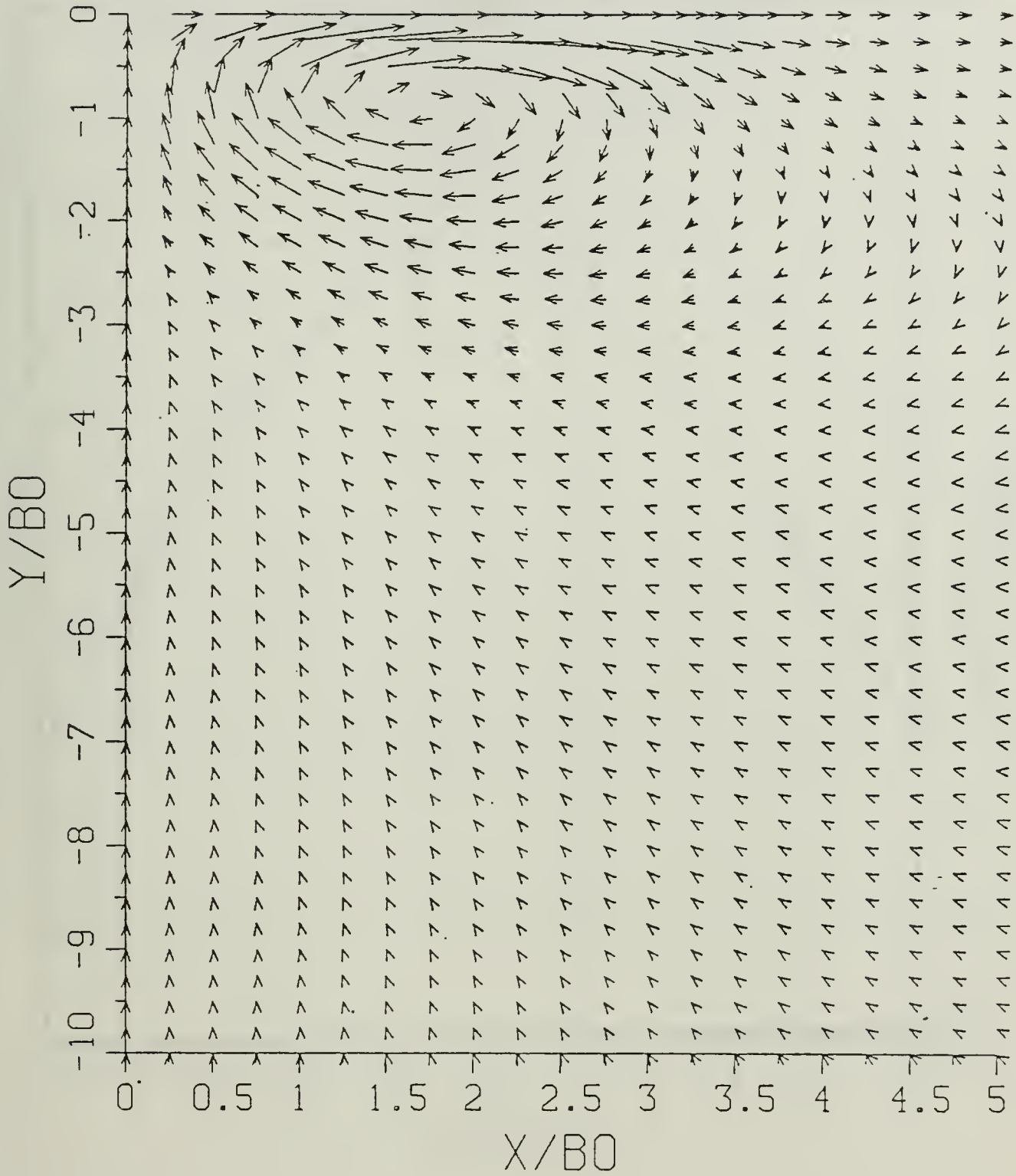


Figure B.50b Velocity Field: SP = 0.50.

$$T^* = 2.97600$$

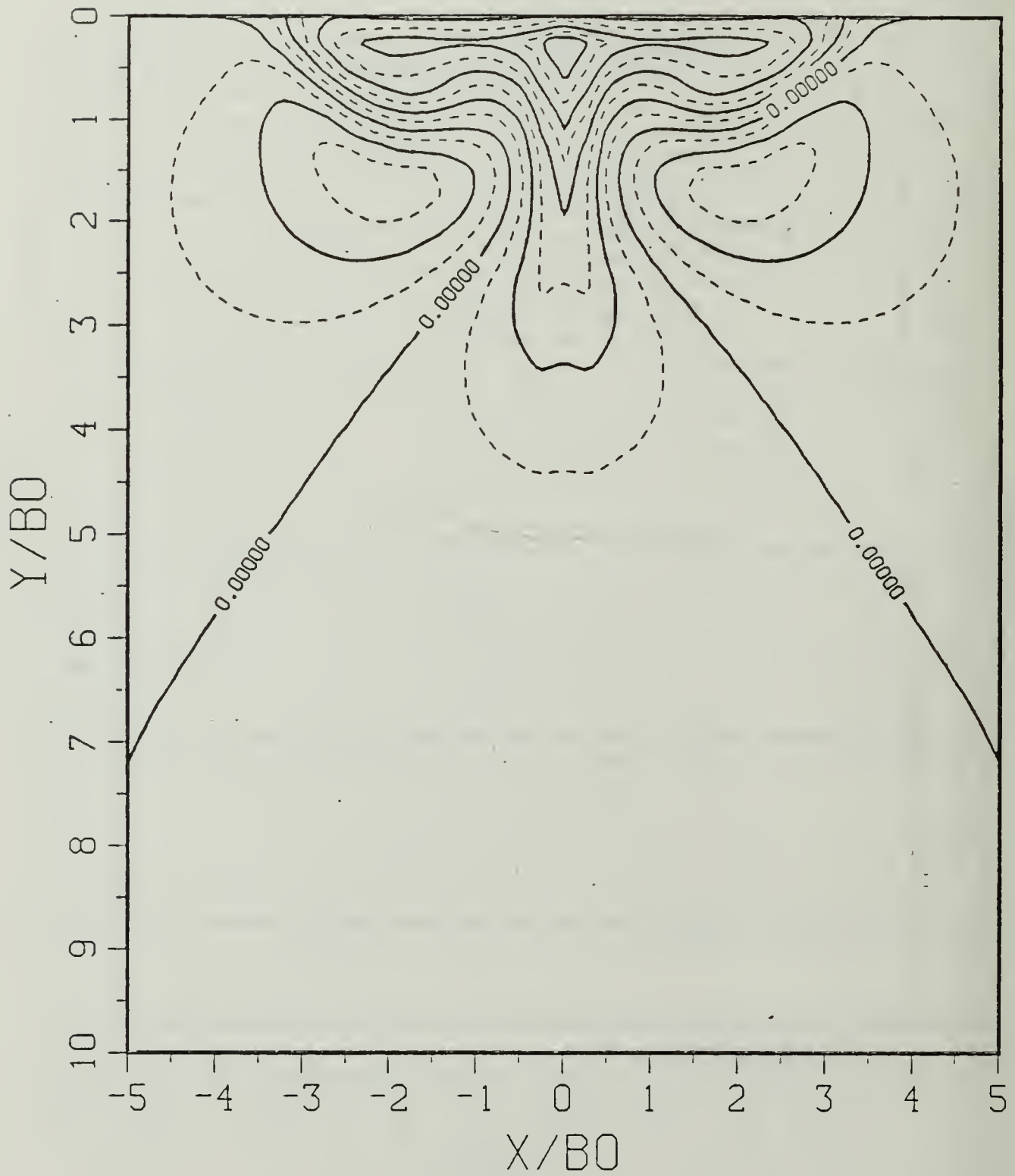


Figure B.50c Density Perturbation Contours:  $SP = 0.50$ .

$$T^* = 2.97600$$

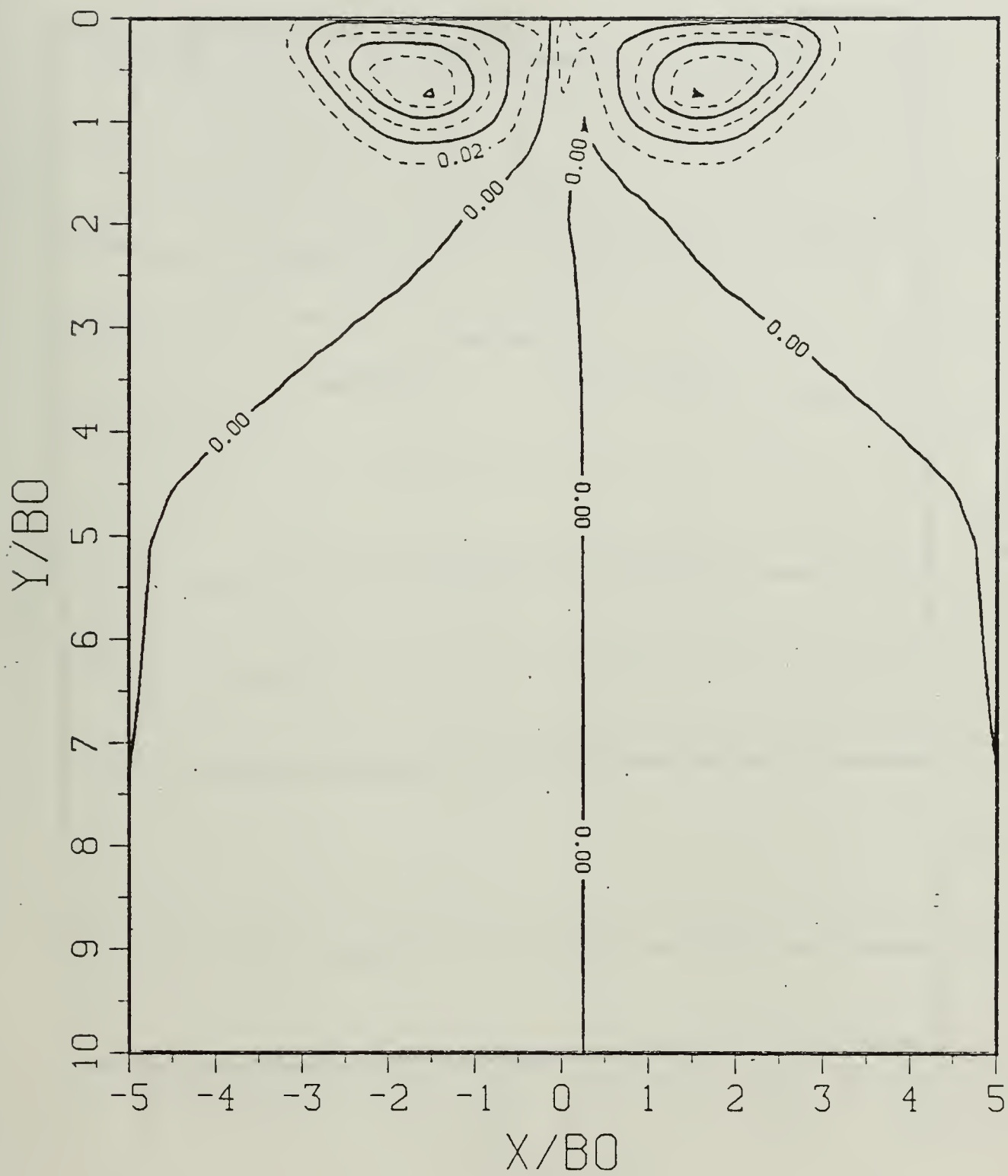


Figure B.50d Vorticity Field: SP = 0.50.

$$T^* = 3.57120$$

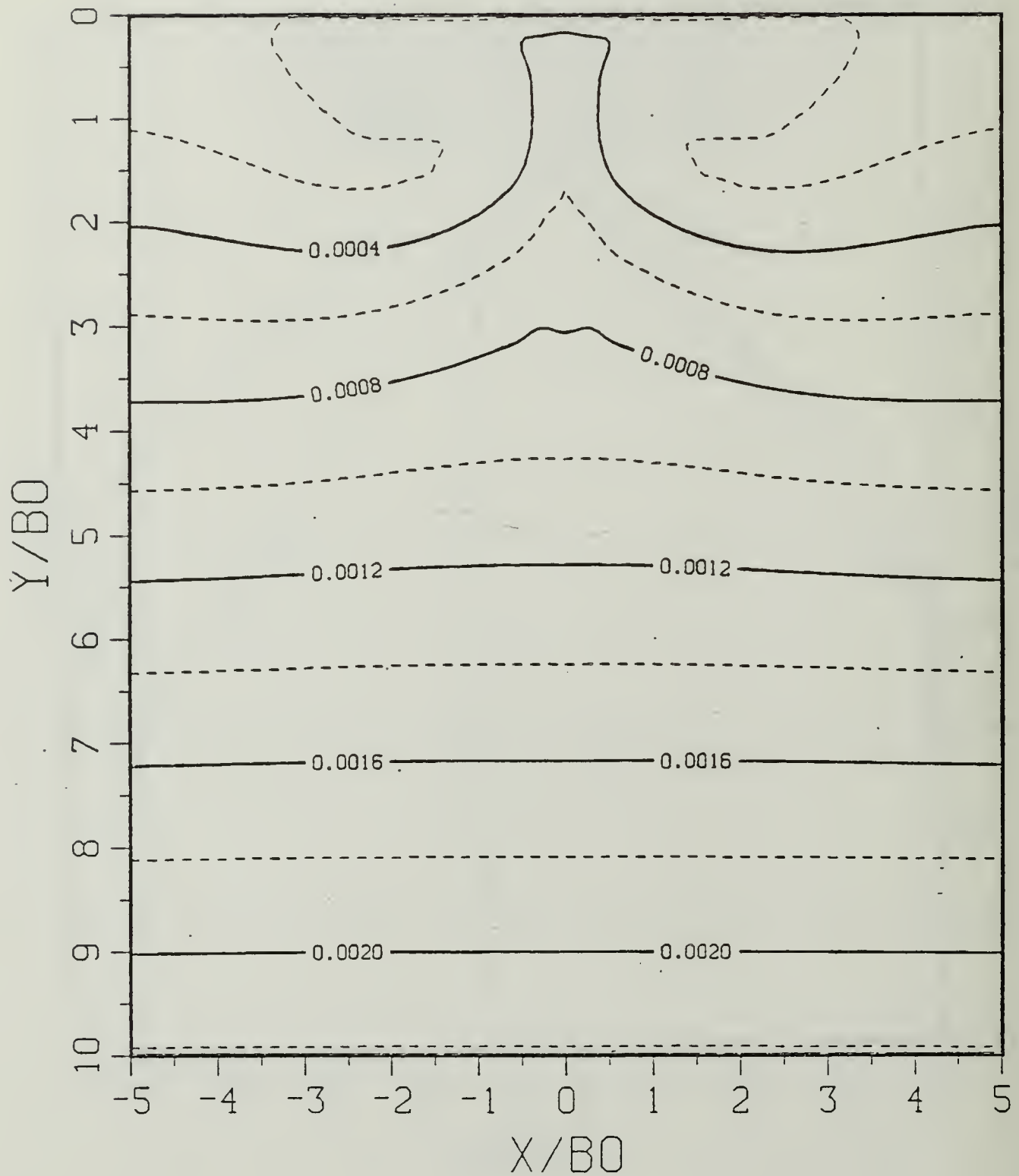


Figure B.51a Constant Density Contours:  $SP = 0.50$ .

$$T^* = 3.57120$$

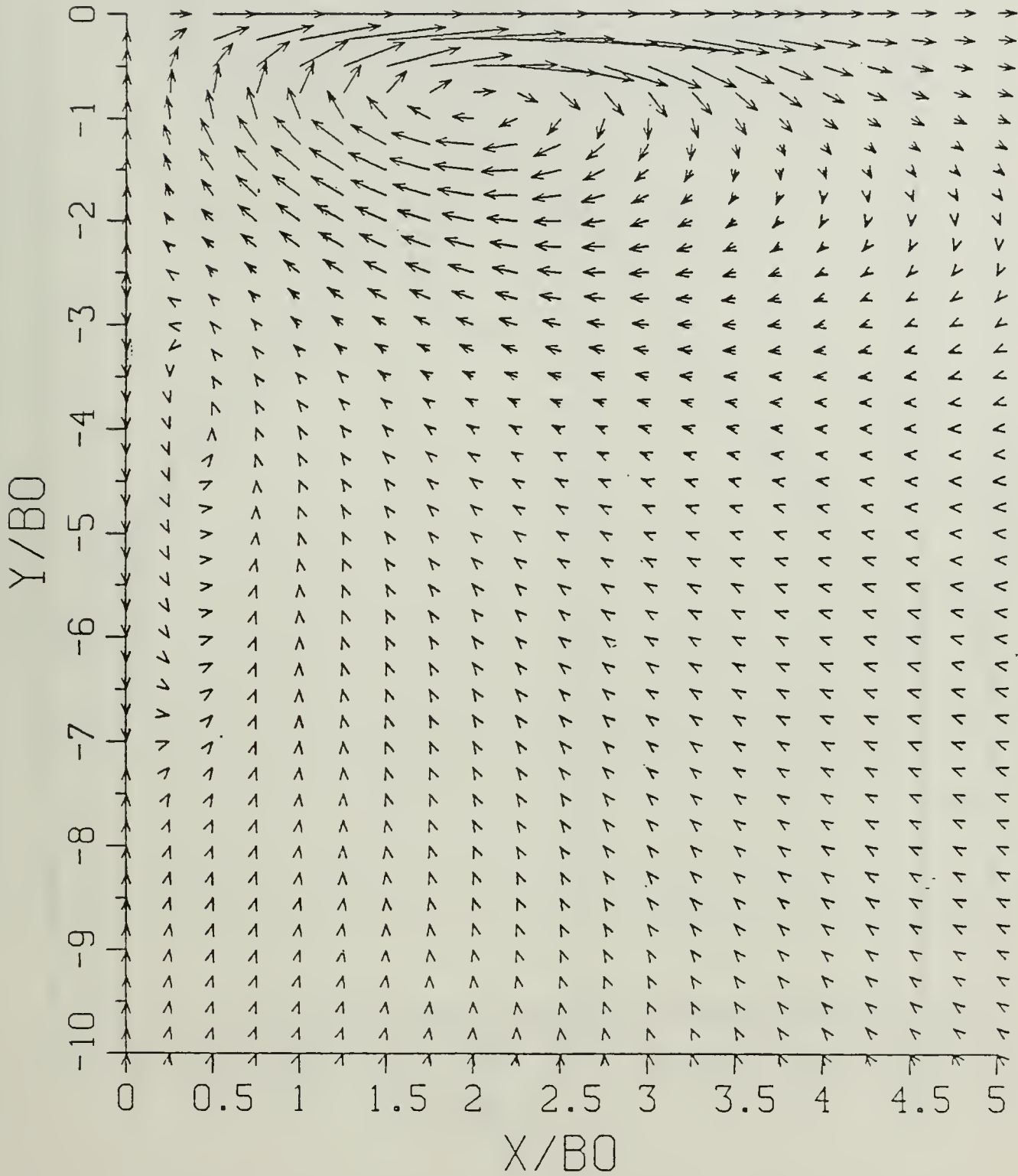


Figure B.51b Velocity Field: SP = 0.50.

$$T^* = 3.57120$$

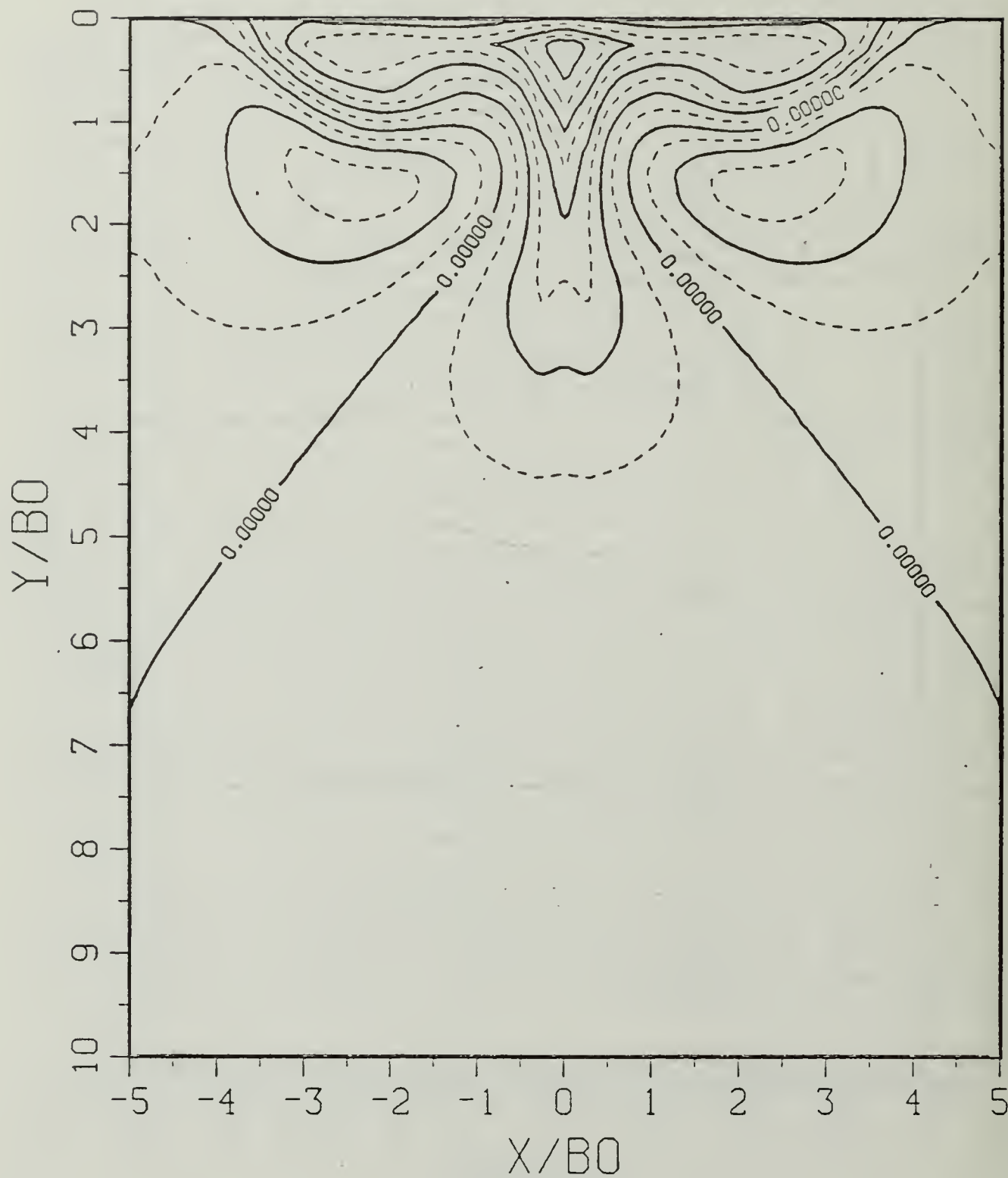


Figure B.51c Density Perturbation Contours: SP = 0.50.

$$T^* = 3.57120$$

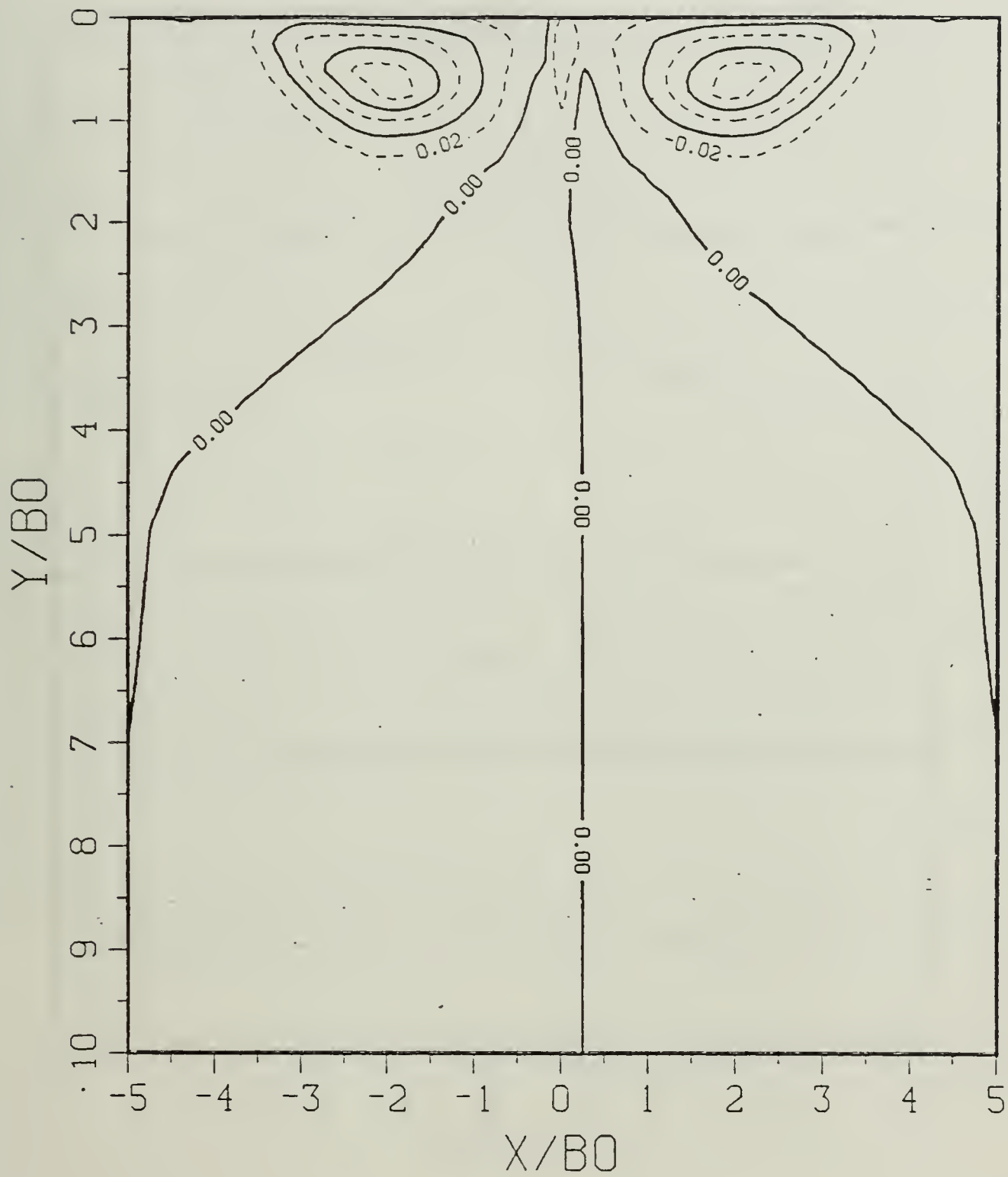


Figure B.51d Vorticity Field: SP = 0.50.

$$T^* = 4.16640$$

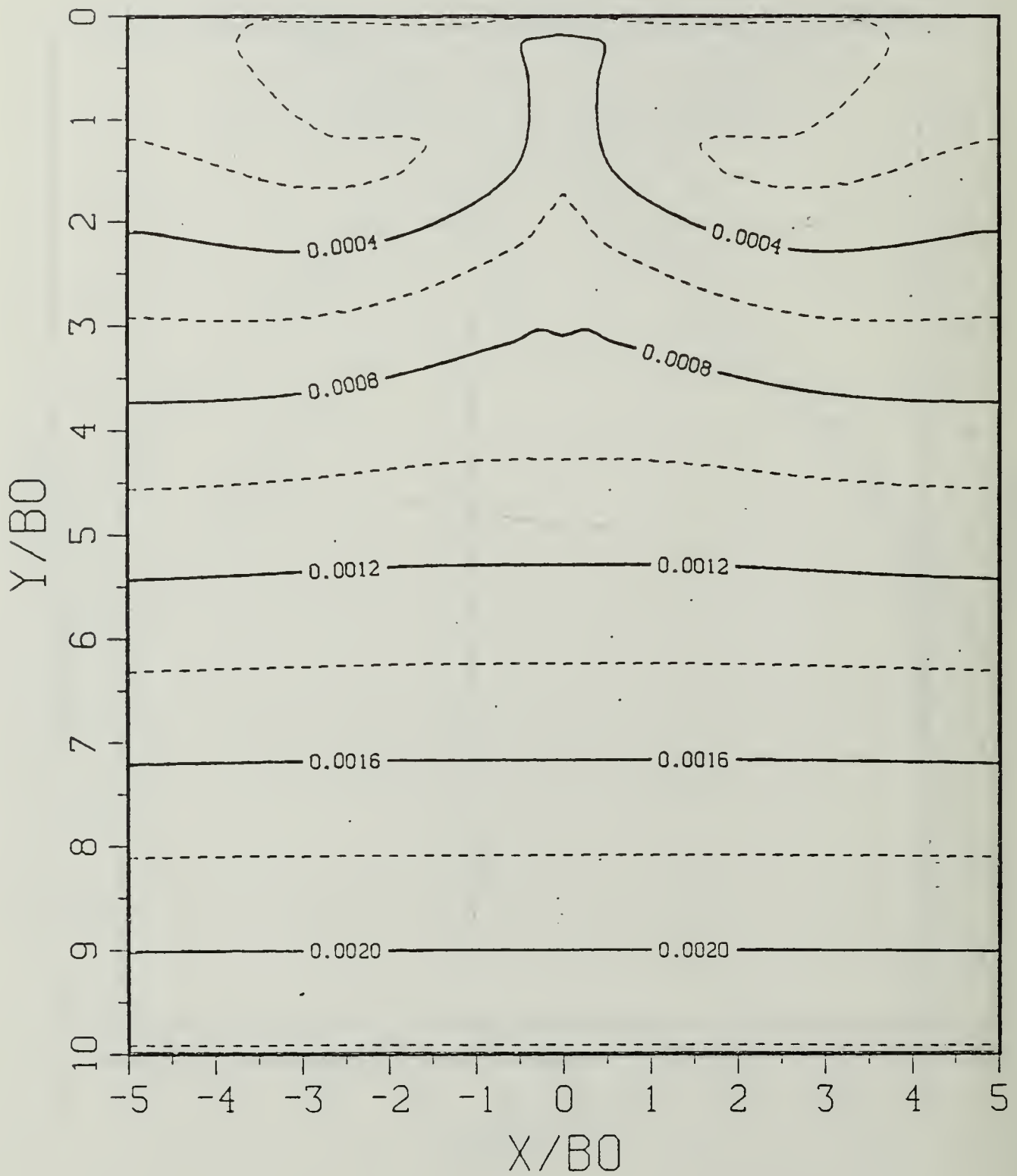


Figure B.52a Constant Density Contours:  $SP = 0.50$ .

$$T^* = 4.16640$$

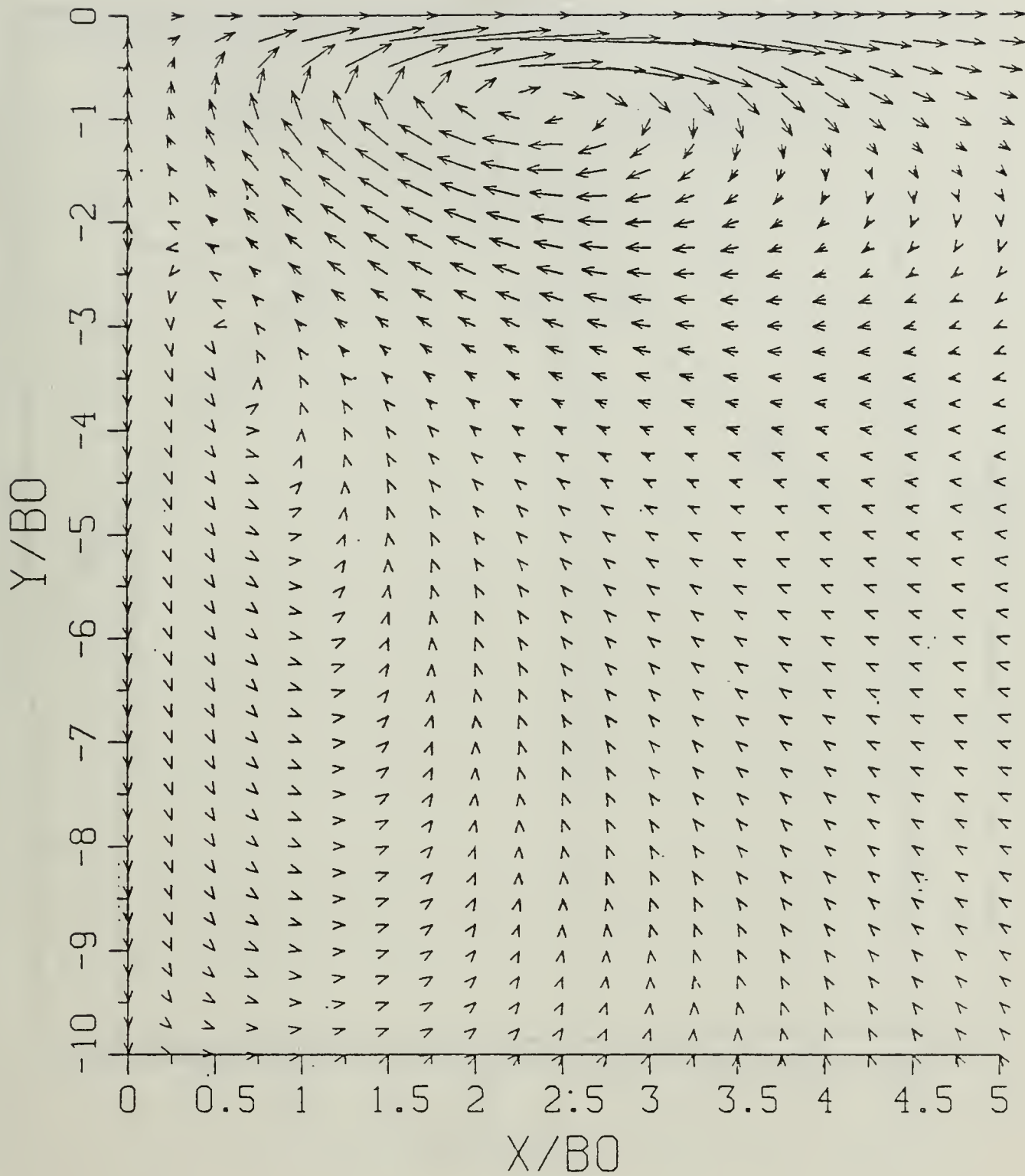


Figure B.52b Velocity Field: SP = 0.50.

$$T^* = 4.16640$$

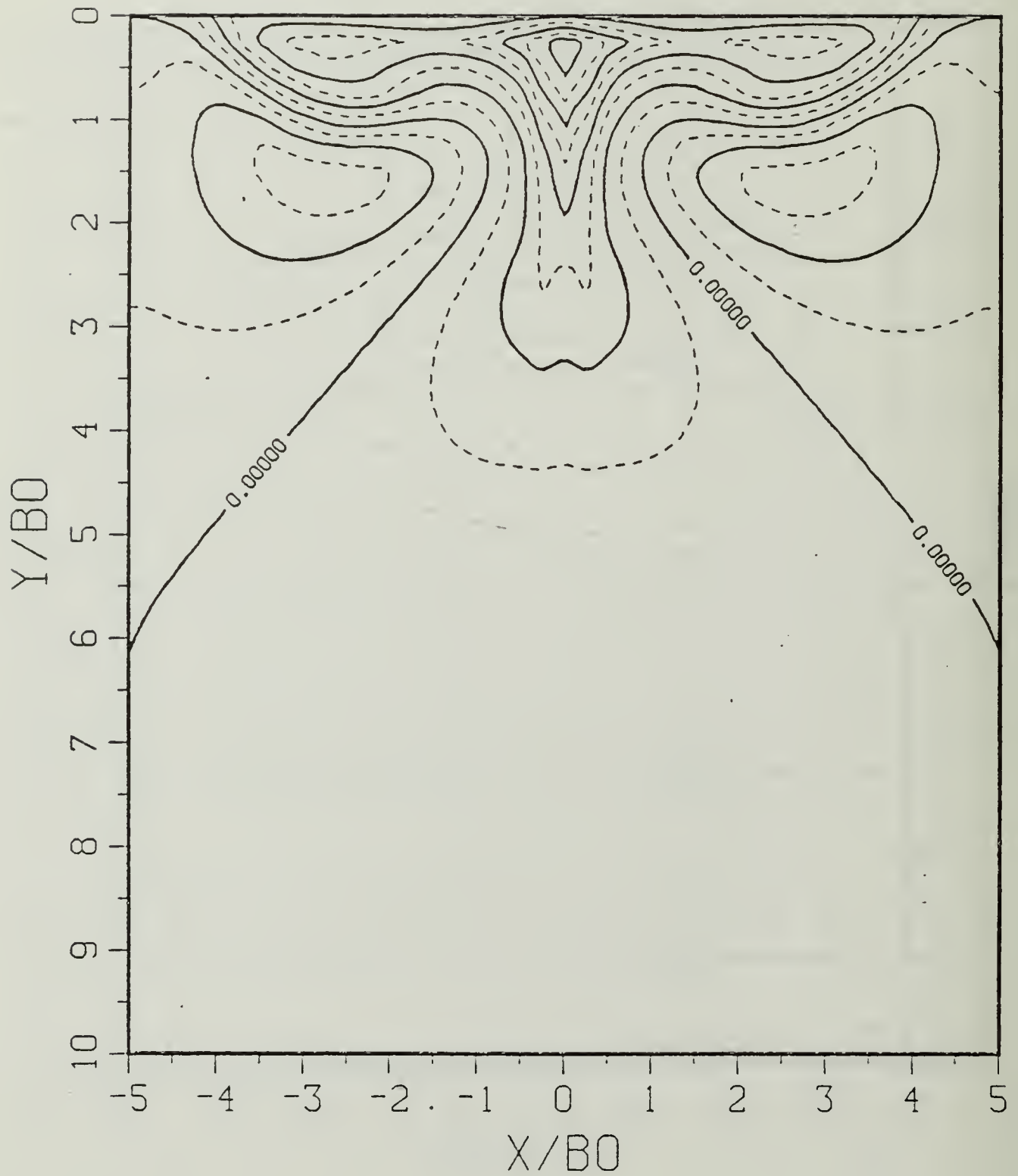


Figure B.52c Density Perturbation Contours:  $SP = 0.50$ .

$$\Gamma^* = 4.16640$$

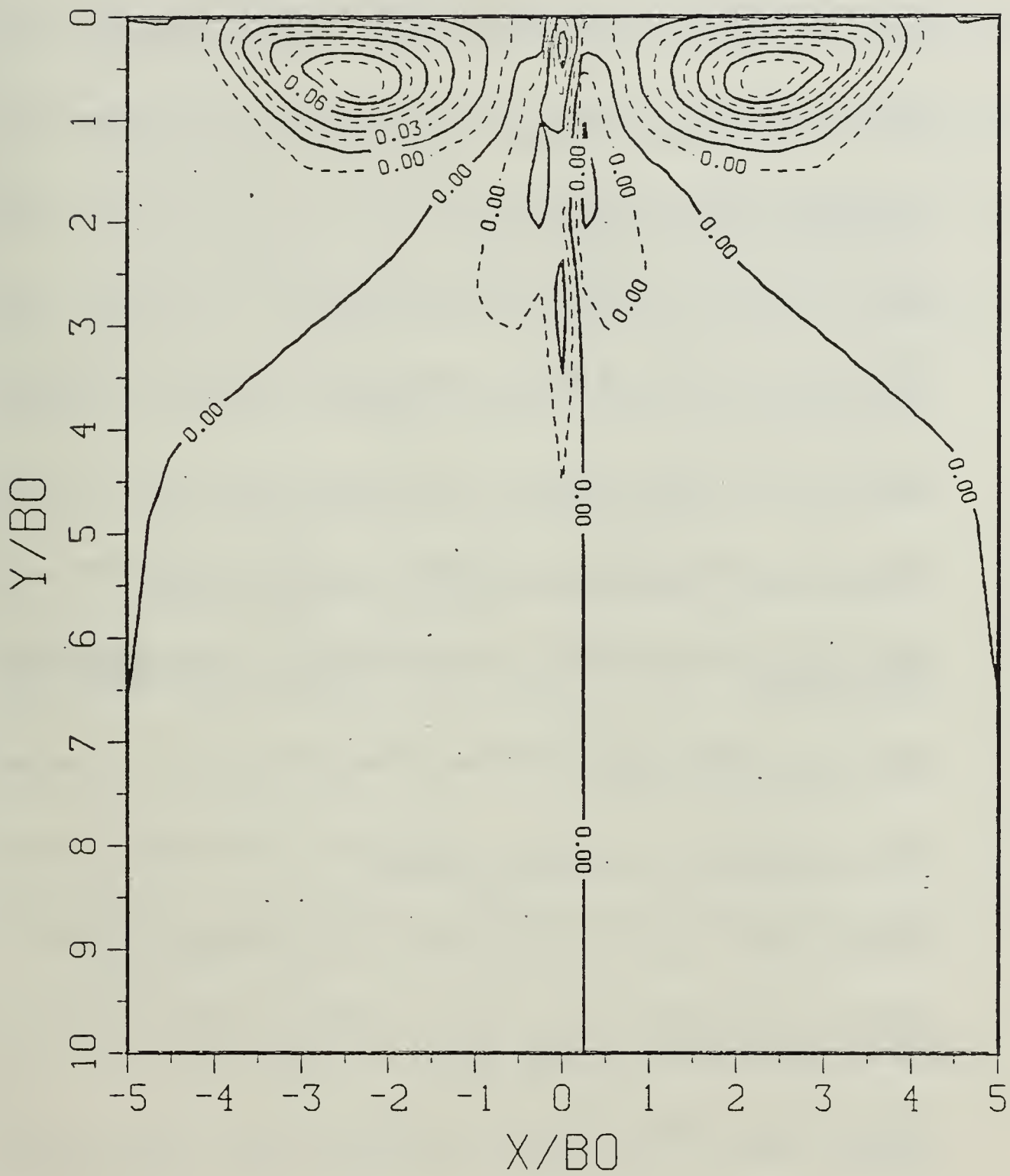


Figure B.52d Vorticity Field: SP = 0.50.

## LIST OF REFERENCES

1. Olsen, J.H., Golburg, A., and Rogers, M. (eds.). *Aircraft Wake Turbulence and Its Detection*. Plenum Press, New York, 1971.
2. Hallock, J.N. (ed.). *Proceedings of the Aircraft Wake Vortices Conference, 1977*. National Technical Information Services, Springfield, VA 22161.
3. Donaldson, C. duP. and Bilanin, A.J., *Vortex Wakes of Conventional Aircraft*, AGARDograph AGARD-AG-204, 1975.
4. Widnall, S.E., "The Structure and Dynamics of Vortex Filaments," *Annual Reviews of Fluid Mechanics*, Vol. 7, 1975, pp. 141-165.
5. Hallock, J.N. and Eberle, W.R. (eds.), *Aircraft Wake Vortices: A State-of-the-Art Review of the United States R&D Program*. Transportation Systems Center, Cambridge, MA, Report No. FAA-RD-77-23, 1977.
6. Sarpkaya, T., "Trailing Vortices in Homogeneous and Density-Stratified Media," *Journal of Fluid Mechanics*, Vol. 136, 1983, pp. 85-109.
7. Panton, R.L., Oberkampf, W.L., and Soskic, N., "Flight Measurements of a Wing Tip Vortex," *Journal of Aircraft*, Vol. 17, 1980, pp. 250-259.
8. Baker, G.R., Barker, S.J., Bofah, K.K. and Saffman, P.G., "Laser Anemometer Measurements of Trailing Vortices in Water," *Journal of Fluid Mechanics*, Vol. 65, pp. 325-336.
9. Crow, S.C., "Stability Theory for a Pair of Trailing Vortices," *AIAA Journal*, Vol. 8, 1970, pp. 2172-2179.
10. Peace, A.J. and Riley, N., "A Viscous Vortex Pair in Ground Effect," *Journal of Fluid Mechanics*, Vol. 129, 1983, pp. 409-426.
11. Barker, S.J. and Crow, S.C., "The Motion of a Two Dimensional Vortex Pair in Ground Effect," *Journal of Fluid Mechanics*, Vol. 82, 1977, pp. 659-671.
12. Tombach, I.H., "Transport of a Vortex in a Stably Stratified Atmosphere." *Aircraft Wake Turbulence and Its Detection*, Edited by J.H. Olsen et al., Plenum Press, New York, 1971, pp. 41-57.
13. Maxworthy, T., "Solitary Waves on Density Interfaces." *Waves on Fluid Interfaces*, Edited by R.E. Meyer, Academic Press, New York, 1983, pp. 201-220.
14. Naval Postgraduate School, Monterey, California. NPS-69-82-003, *Trailing Vortices in Stratified Fluids*, by T. Sarpkaya and S.K. Johnson, June 1982.

15. Johnson, S.K., *Trailing Vortices in Stratified Fluids*, M.S. Thesis, Naval Postgraduate School, Monterey, California, June 1982.
16. Turkmen, C., *Trailing Vortices in Stratified and Unstratified Fluids*, M.S. Thesis, Naval Postgraduate School, Monterey, California, December 1982.
17. Daly, J.J., *Effects of Ambient Turbulence and Stratification on the Demise of Trailing Vortices*, M.S. Thesis, Naval Postgraduate School, Monterey, California, 12 March 1986.
18. Sarpkaya, T. and Henderson, D.O., *Free surface Scars and Striations due to Trailing Vortices Generated by a Submerged Lifting Surface*, AIAA Paper No. AIAA-85-0445, January 1985.
19. Noble, W.D., *Characteristics of Vortices in Stratified Media*, M.S. Thesis, Naval Postgraduate School, Monterey, California, September 1986.
20. Chow, C.Y., *An Introduction to Computational Fluid Mechanics*, John Wiley & Sons, New York, 1979.

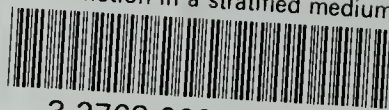
## INITIAL DISTRIBUTION LIST

		No. Copies
1.	Defense Technical Information Center Cameron Station Alexandria, Virginia 22304-6145	2
2.	Library, Code 0142 Naval Postgraduate School Monterey, California 93943-5002	2
3.	Department Chairman, Code 69 Department of Mechanical Engineering Naval Postgraduate School Monterey, California 93943-5000	1
4.	Prof. T. Sarpkaya, Code 69SL Department of Mechanical Engineering Naval Postgraduate School Monterey, California 93943-5000	10
5.	Lt. Brian S. L. Miller, USN 3937 Col. Ellis Ave. Alexandria, Virginia 22304	3

*pl* 17898 2

thesM58565

Vortex motion in a stratified medium.



3 2768 000 75932 8

DUDLEY KNOX LIBRARY